Safety Analysis Report

Docket Number 71-9287

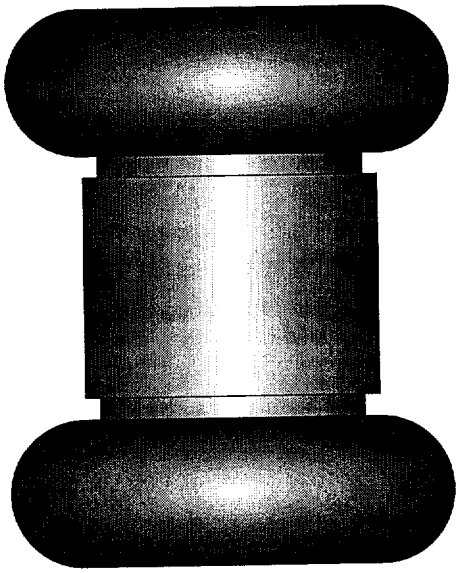

SteriGenics

Eagle

Cask

Rev 0
November 1998

prepared by:

PacTec
Packaging Technology, Inc.

4507-D Pacific Highway East
Tacoma WA 98424-2633

9812020248 981118
PDR ADOCK 07109287
B PDR

TABLE OF CONTENTS

1.0 GENERAL INFORMATION 1.1-1
1.1 INTRODUCTION 1.1-1
1.2 PACKAGE DESCRIPTION 1.2-1
1.2.1 Packaging 1.2-1
1.2.2 Operational Features 1.2-4
1.2.3 Contents of Packaging 1.2-4
1.3 APPENDICES 1.3-1
1.3.1 References 1.3-1
1.3.2 General Arrangement Drawings 1.3-2
2.0 STRUCTURAL EVALUATION 2.0-1
2.1 STRUCTURAL DESIGN 2.1-1
2.1.1 Discussion 2.1-1
2.1.2 Design Criteria 2.1-3
2.2 WEIGHTS AND CENTER OF GRAVITY 2.2-1
2.3 MECHANICAL PROPERTIES OF MATERIALS 2.3-1
2.3.1 Transportation Package 2.3-1
2.3.2 Impact Limiter Nonlinear Material Properties 2.3-5
2.4 GENERAL STANDARDS FOR ALL PACKAGES 2.4-1
2.4.1 Minimum Package Size 2.4-1
2.4.2 Tamper Indicating Device 2.4-1
2.4.3 Positive Closure 2.4-1
2.4.4 Chemical and Galvanic Reactions 2.4-1
2.4.5 Valves 2.4-1
2.4.6 Cask Design 2.4-1
2.4.7 External Temperatures 2.4-2
2.4.8 Venting 2.4-2
2.5 LIFTING AND TIEDOWN DEVICES 2.5-1
2.5.1 Lifting Devices 2.5-1
2.5.2 Tiedown Devices 2.5-1
2.6 NORMAL CONDITIONS OF TRANSPORT 2.6-1
2.6.1 Heat 2.6-1
2.6.2 Cold 2.6-5
2.6.3 Reduced External Pressure 2.6-8
2.6.4 Increased External Pressure 2.6-8
2.6.5 Vibration 2.6-9
2.6.6 Water Spray 2.6-11
2.6.7 Free Drop 2.6-11
2.6.8 Corner Drop 2.6-19
2.6.9 Compression 2.6-19
2.6.10 Penetration 2.6-19
2.7 HYPOTHETICAL ACCIDENT CONDITIONS 2.7-1
2.7.1 Free Drop 2.7-1
2.7.2 Crush 2.7-15
2.7.3 Puncture 2.7-15
2.7.4 Thermal 2.7-17
2.7.5 Immersion - Fissile 2.7-18
2.7.6 Immersion - All Packages 2.7-18
2.7.7 Summary of Damage 2.7-21

2.8 SPECIAL FORM CERTIFICATION 2.8-1
2.9 FUEL RODS 2.9-1
2.10 APPENDICES 2.10-1
2.10.1 References 2.10-1
2.10.2 Stress Analysis Finite Element Model Descriptions 2.10-1
2.10.3 Drop Analysis Finite Element Model Description 2.10-1
2.10.4 Closure Bolt Design Evaluation 2.10-1
2.10.5 Dynamic Test Results 2.10-1

3.0 THERMAL EVALUATION 3.1-1

3.1 DISCUSSION 3.1-1
3.1.1 Design Criteria 3.1-2
3.1.2 Overview of Thermal Design Features 3.1-3
3.2 SUMMARY OF THERMAL PROPERTIES OF MATERIALS 3.2-1
3.3 TECHNICAL SPECIFICATION OF COMPONENTS 3.3-1
3.3.1 Discussion of Temperature Sensitive Materials and Components 3.3-1
3.3.2 Thermal Loading from Cobalt-60 Source Capsules 3.3-2
3.3.3 Maximum Allowable Pressure 3.3-2
3.4 THERMAL EVALUATION FOR NORMAL CONDITIONS OF TRANSPORT 3.4-1
3.4.1 Thermal Models 3.4-1
3.4.2 Maximum Temperatures 3.4-4
3.4.3 Minimum Temperatures 3.4-4
3.4.4 Maximum Internal Pressures 3.4-4
3.4.5 Maximum Thermal Stresses 3.4-4
3.4.6 Evaluation of Package Performance for Normal Conditions of Transport 3.4-5
3.5 THERMAL EVALUATION FOR HYPOTHETICAL ACCIDENT CONDITIONS 3.5-1
3.5.1 Thermal Model 3.5-1
3.5.2 Package Conditions and Environment 3.5-1
3.5.3 Package Temperatures 3.5-2
3.5.4 Maximum Internal Pressures 3.5-3
3.5.5 Evaluation of Package Performance for Hypothetical Accident Thermal Conditions 3.5-3
3.6 APPENDICES 3.6-1
3.6.1 References 3.6-1
3.6.2 Convective Heat Transfer Coefficient Calculation 3.6-3
3.6.3 ANSYS Input Files 3.6-6

4.0 CONTAINMENT 4.1-1

5.0 SHIELDING EVALUATION 5.1-1

5.1 DISCUSSION AND RESULTS 5.1-1
5.2 SOURCE SPECIFICATION 5.2-1
5.2.1 Gamma Source 5.2-1
5.2.2 Neutron Source 5.2-1
5.3 MODEL SPECIFICATION 5.3-1
5.3.1 Description of Radial and Axial Shielding Configuration 5.3-1
5.3.2 Shield Regional Densities 5.3-9
5.4 SHIELDING EVALUATION 5.4-1
5.4.1 Dose Rates for Normal Transport Conditions 5.4-1
5.4.2 Dose Rates for Hypothetical Accident Conditions 5.4-3
5.5 APPENDICES 5.5-1
5.5.1 References 5.5-1
5.5.2 ORIGEN Input File 5.5-2

5.5.3 MCNP Input Files 5.5-3

6.0 CRITICALITY 6.1-1

7.0 OPERATING PROCEDURES 7.1-1

7.1 LOADING PROCEDURES 7.1-1
7.1.1 Loading the SEC in a Shielding Pool 7.1-1
7.1.2 Loading the SEC in a Dry Environment 7.1-3
7.2 PROCEDURES FOR UNLOADING THE PACKAGE 7.2-1
7.2.1 Unloading the SEC in a Shielding Pool 7.2-1
7.2.2 Unloading the SEC in a Dry Environment 7.2-2
7.3 PREPARING AN EMPTY PACKAGE FOR TRANSPORT 7.3-1
7.4 APPENDIX 7.4-1
7.4.1 References 7.4-1

8.0 ACCEPTANCE TESTS AND MAINTENANCE 8.1-1

8.1 ACCEPTANCE TESTS 8.1-1
8.1.1 Visual Inspection 8.1-1
8.1.2 Structural and Pressure Tests 8.1-1
8.1.3 Leak Tests 8.1-2
8.1.4 Component Tests 8.1-2
8.1.5 Tests for Shielding Integrity 8.1-2
8.1.6 Thermal Acceptance Tests 8.1-3
8.2 MAINTENANCE PROGRAM 8.2-1
8.2.1 Structural and Pressure Tests 8.2-1
8.2.2 Leak Tests 8.2-1
8.2.3 Subsystem Maintenance 8.2-1
8.2.4 Valves, Rupture Discs, and Gaskets on the Containment Vessel 8.2-2
8.2.5 Shielding 8.2-2
8.2.6 Thermal 8.2-2
8.3 APPENDIX 8.3-1
8.3.1 References 8.3-1

1.0 GENERAL INFORMATION

This section of the SteriGenics Eagle Cask (SEC) Safety Analysis Report (SAR) presents a general description of the package. The SEC, as configured and analyzed in subsequent sections, is utilized for off-site transport of Cobalt-60 source capsules which are classed as special form material in accordance with the requirements of 10 CFR 71 [1] and 49 CFR 173 [2]. General arrangement drawings of the packaging are provided in Appendix 1.3.2, *Packaging General Arrangement Drawings*.

1.1 Introduction

The SEC is a transportation system designed to transport special form Cobalt-60 source capsules. The packaging is designed to provide a safe means of transporting up to 72 of these source capsules. The design is optimized to provide maximum safety during the loading, transport, and unloading operations.

The packaging consists of a shielded cask body, a shielded cask closure lid, a payload basket with payload, and upper and lower impact limiters. The packaging is constructed primarily of ASTM Type 304 stainless steel.

Authorization is sought for shipment up to 72, Cobalt-60 source capsules as a Type B(U), special form material package per the definitions delineated in 10 CFR §71.4. The transport index for the package, determined in accordance with the definition of 10 CFR §71.4 is 6.0. The transport index is based on the radiation dose rate at 1 meter from the package side surface.

1.2 Package Description

The SEC is a stainless steel, welded vessel that provides a confinement barrier for the special form payload radioactive materials. The confinement boundary of the cask is composed of the inner shell, upper and lower end forgings, closure lid with bolts installed, and O-ring. The impact limiters are made from stainless steel toroids and are attached to each end of the outer cask to limit the consequences of normal and hypothetical accident events. Support for the payload is provided by a basket assembly which is inserted into the cask cavity. Lead shielding surrounds the payload and is contained within the stainless steel shells of the SEC.

General arrangement drawings are provided in Appendix 1.3.2, *Packaging General Arrangement Drawings*. An overall view of the SEC is provided in Figure 1.2-1.

1.2.1 Packaging

The SteriGenics Eagle Cask is described in this section. The general arrangement drawings on which the description is based are contained in Appendix 1.3.2, *Packaging General Arrangement Drawings*.

1.2.1.1 Gross Weight

The gross shipping weight of the SEC, including the cask body, payload and basket, and impact limiters, is 20,000 pounds. Although the SEC may be shipped with payloads ranging from 1 to 72 source capsules, the variation in gross weight is less than 50 pounds, so that 20,000 pounds is used for all calculations.

1.2.1.2 Materials of Construction, Dimensions, and Fabrication Methods

The SEC transportation cask consists of the internal basket and payload, a cask that provides confinement and acts as an environmental barrier, and energy absorbing toroidal impact limiters. The cask structural components are made of ASTM Type 304 austenitic stainless steel,. The shielding (which is completely enclosed by the structural components) is made of lead. The cask is protected at each end by energy absorbing impact limiters that consist of stainless steel toroids welded to an end cap. The impact limiters are attached to the cask using ball lock pins. These impact limiters also provide thermal shielding closure lid seal during the hypothetical fire transient event. The overall arrangement and design details of the various components of the SEC are presented in Appendix 1.3.2, *Packaging General Arrangement Drawings*. The SEC is described in more detail in the following sections.

1.2.1.2.1 Transportation Cask

The SEC is fabricated from stainless steel castings and plate. The SEC assembly is composed of upper and lower castings (which include the inner shell of the confinement boundary), outer shell, closure lid, closure bolts, O-ring seal, lead shielding, and two stainless steel heat shields which jacket the outer shell of the cask. The confinement boundary is defined as the inner shell, upper and lower castings, and closure lid with bolts installed.

The cask body consists of an inner stainless steel shell having an inner diameter of 10.75 inches, an outer stainless steel shell having an outer diameter of 35.5 inches and a thickness of 1 inch, upper and lower stainless steel castings[1], and lead shielding. The inner shell is cast integrally with the castings and has a minimum thickness of 1 inch at the axial center of the cask.

The payload cavity is defined by the inner shell, the shielded cask closure lid, and the bottom plate. The bottom plate of the payload cavity is 1 inch thick, and is cast integrally with the lower casting. The weld between the upper and lower castings, located at the center of the inner shell, is full penetration and radiograph inspected. The welds between the outer shell and the upper and lower castings, including an optional longitudinal girth weld, are full penetration welds, liquid penetrant inspected on the root and final passes. As shown in Appendix 1.3.2, *Packaging General Arrangement Drawings*, the bottom plate and lower casting are drilled with a ⅜ inch diameter drain passage which can be used to drain or flood the payload cavity with water. When the lid is installed, the payload cavity is 19 inches long.

A double thermal radiation shield is used to protect the cask from the hypothetical accident fire event, located outside the outer shell between the two impact limiters, and made of stainless steel. The inner shield is ¾ inches thick, and is radially separated from the outer shell by 12 gauge (0.105 inch thick) spacers at each end. The inner shield is attached to the lower end casting with a ⅜ inch groove weld, and is not attached to the upper casting. The outer shield is a sheet of 10 gauge (0.135 inch thick) material, welded to the castings at each end, and separated from the inner shield by a spiral wrap of 12 gauge (0.105 inch thick) wire.

The cask is lifted by threading lifting attachments into the upper casting. The attachment holes and the lid attachment bolt holes feature stainless steel threaded inserts.

The cask closure lid consists of a stainless steel shell enclosing lead shielding. The upper portion of the lid has a diameter of 19¾ inches and the lower portion of the lid has a diameter of 10¼ inches. The top surface of the lid is recessed 1/16 inch below the top end of the cask. The total axial thickness of lead in the cask lid is 13⅝ inches. The lid is penetrated by a ¾ inch diameter drain port and a ⅜ inch diameter vent port, each closed with a stainless steel plug. The closure lid drain port will also be used for access to the payload basket during in-plant use of the cask. A face-type O-ring seal is captured in the lid by means of a dovetail groove. This seal is designed to assist the confinement performance of the cask. Since the seal is not a containment boundary, it is not leak tested. The lid is attached to the cask using 12, ¾-10 UNC socket head cap screws made from ASTM A320, Grade L43, cadmium plated alloy steel.

The payload basket is capable of holding up to 72, Cobalt-60 source capsules in special form. It consists of four spacer disks for source capsule alignment, a bottom disk on which the capsules rest, and a center tube, all made of stainless steel.

[1] The upper and lower end structures are designated only as castings in the text, but may be alternately made from forged material.

1.2.1.2.2 Impact Limiters

Impact limiters are installed on either end of the cask to limit the consequences of normal and hypothetical accident events. The impact limiters are made from stainless steel toroids welded to end caps which enclose either end of the cask. The end caps are also constructed of stainless steel. The toroids are 20 inches in diameter and have a nominal wall thickness of ¾ inch. The major outside diameter of the limiters is 60 inches. Each cap is attached to the cask using 12, 1 inch diameter ball-lock pins oriented radially around the cap. These pins are inserted through the impact limiter cap into holes drilled around the periphery of the cask upper and lower castings. One shear pin on each limiter is installed with a lockwire to provide evidence of tampering. Details are provided in the general arrangement drawings in Appendix 1.3.2, *Packaging General Arrangement Drawings*.

1.2.1.2.3 Miscellaneous Features

A nameplate on the SEC provides the following information: model number, gross weight, and package identification number assigned by the Nuclear Regulatory Commission in accordance with 10 CFR §71.85(c). Package marking and labeling shall be in accordance with 10 CFR §71.5(a)(1)(ii).

1.2.1.4 Receptacles, Valves, Testing and Sampling Ports

The SEC design includes a closure lid drain port, a vent port, and a body drain port. The vent and drain ports permit venting of the cask cavity during loading and unloading of the package. There are no receptacles or valves utilized on the SEC.

1.2.1.5 Heat Dissipation

There are no active devices utilized on the SEC for the transfer or dissipation of heat. Heat dissipation from the package is entirely passive. Heat dissipation is achieved by convection and radiation from the exterior surfaces of the cask and impact limiters. White paint is used on the exterior surfaces of the cask and impact limiters to reduce the absorption of solar energy and to increase the rejection of internal heat. The package maximum heat dissipation is 5,082 watts (from 330,000 curies of Cobalt-60). A more detailed discussion of the package thermal characteristics is provided in Chapter 3.0.

1.2.1.6 Coolants

No coolants are utilized within the SEC.

1.2.1.7 Protrusions

There are no outer or inner protrusions on the SEC.

1.2.1.8 Lifting and Tiedown Devices

Other than the two threaded provisions in the cask body, there are no lifting or tiedown devices which are a structural part of the SEC. The SEC rests on a transport skid. A frame placed on the top of the upper impact limiter is tied to the transport trailer, thus capturing the package. The

transport skid also provides the means for lifting the package while assembled in its transport configuration.

1.2.1.9 Pressure Relief System

There is no pressure relief system in the SEC confinement boundary.

1.2.1.10 Shielding

The lead shielding around the sides of the cask (between the inner and outer shells) is cast in place, and has a maximum radial thickness of 10⅜ inches at the center. The axial thickness of lead in the cask lid is 13⅜ inches. In the cask bottom, the lead shielding is 11⅞ inches thick directly below the payload. Further details are provided in Chapter 5.0.

1.2.2 Operational Features

The SEC cask is not considered to be operationally complex and is similar to other transportation packages currently in use. All operational features are depicted on the drawings provided in Appendix 1.3.2, *Packaging General Arrangement Drawings*. Operating procedures are outlined in Chapter 7.0.

1.2.3 Contents of Packaging

The contents of the packaging described above are special form Cobalt-60 source capsules. Three types of capsules are included in this application as potential payloads. They are: (1) Nordion International, Inc. C-188 capsule, Types 1 through 12, (2) Puridec Capsule X.2089, and (3) Neutron Products, Inc. NPRP 450-10-B. All source capsules are be limited to a maximum of 18,333 curies each.

1.2.3.1 Radionuclide Inventory

The only payload condsidered is Cobalt-60 contained in special form source capsules. The Cobalt-60 is modeled primarily as a gamma source with a strength of 330,000 curies. These values are discussed in more detail in Chapter 5.0.

1.2.3.2 Maximum Payload Weight

The maximum payload weight is 50 pounds and includes the internal basket and a maximum of 72, Cobalt-60 source capsules. The details of the basket and payload weights are provided in Section 2.2.

1.2.3.3 Maximum Decay Heat

The maximum design basis decay heat load for the SEC is 5,082 watts.

1.2.3.4 Maximum Pressure Buildup

The SEC is designed for a maximum pressure of 50 psig. As discussed in Chapter 3.0, the maximum normal operating pressure (MNOP) and maximum hypothetical accident condition pressure is considerably less than this value.

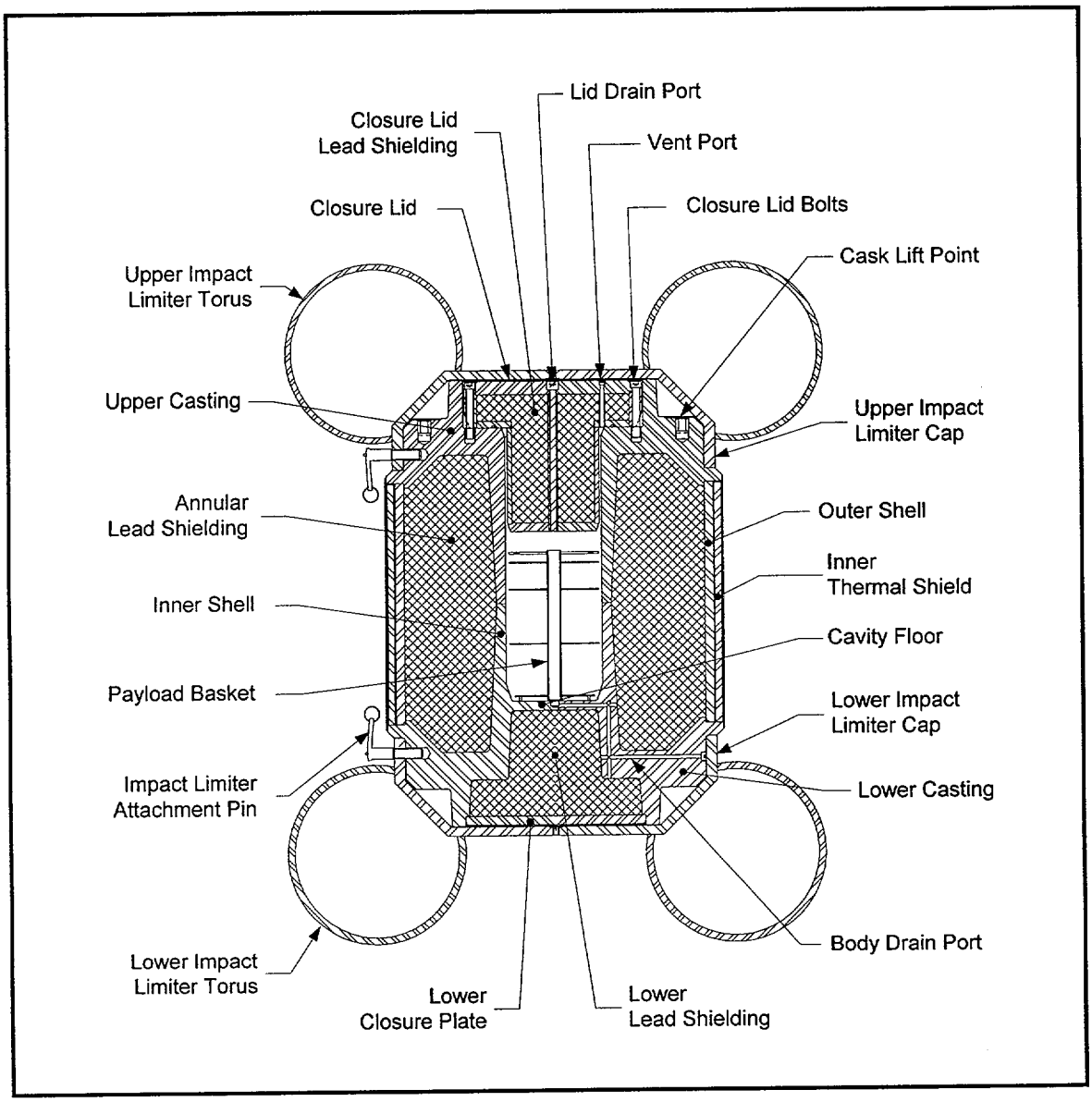

Figure 1.2-1 - SteriGenics Eagle Cask, Section View

1.3 Appendices

1.3.1 References

1. Title 10, Code of Federal Regulations, Part 71 (10 CFR 71), *Packaging and Transportation of Radioactive Materials*, United States Nuclear Regulatory Commission (USNRC), 1996.
2. Title 49, Code of Federal Regulations, Part 173 (49 CFR 173), *Shippers-General Requirements for Shipments and Packaging*, United States Department of Transportation (USDOT), 1995

1.3.2 General Arrangement Drawings

98003-SAR	1	0

REVISION HISTORY			
REV	DESCRIPTION	REL	DATE
0	INITIAL RELEASE	BH	11-16-98

NOTES, UNLESS OTHERWISE SPECIFIED:

1. INTERPRET DRAWING PER ANSI Y-14.5.
INTERPRET WELDS PER ANSI/AWS A2.4
2. THREADS PER ANSI B1.1.

[3] IDENTIFICATION: PACKAGE SHALL BE IDENTIFIED IN ACCORDANCE WITH THE REQUIREMENTS OF 10 CFR 71.85(c) ON THE OUTER THERMAL SHIELD OF THE CASK BODY WITH A SEAL WELDED STAINLESS STEEL NAMEPLATE.

4. PRIOR TO ASSEMBLY, ALL COMPONENTS SHALL BE CLEANED OF CUTTING OIL, MARKING DYES, WELD FLUX, SPATTER, SCALE, GRIME AND ALL OTHER FOREIGN MATERIAL. FINISHED ASSEMBLY AND ALL INTERIOR SURFACES SHALL BE CLEANED, AND VISUALLY OR WIPE TEST INSPECTED IN ACCORDANCE WITH ASTM-A380.

5. ALL WELDING PROCEDURES AND PERSONNEL SHALL BE QUALIFIED IN ACCORDANCE WITH ASME CODE, SECTION IX. WELD PROCEDURES AND WELDER QUALIFICATIONS SHALL BE AVAILABLE FOR AUDIT OR REVIEW.

6. ALL WELDS SHALL BE VISUALLY EXAMINED IN ACCORDANCE WITH AWS D1.1. VISUAL WELD INSPECTORS SHALL BE QUALIFIED PER AWS D1.1.

[7] INDICATED WELDS SHALL BE LIQUID PENETRANT INSPECTED ON ROOT AND FINAL PASSES IF A MULTIPASS WELD AND ON THE COMPLETED WELD IF A SINGLE PASS WELD IN ACCORDANCE WITH ASME CODE, SECTION III, DIVISION 1, SUBSECTION NB, ARTICLE NB-5000 AND SECTION V, ARTICLE 6.

[8] INDICATED WELDS SHALL BE RADIOGRAPH INSPECTED IN ACCORDANCE WITH ASME CODE SECTION III, DIVISION 1, SUBSECTION NB, ARTICLE NB-5000 AND SECTION V, ARTICLE 2.

[9] MATERIAL: CASTING, ASTM A-351, GRD CF8A
OPTIONAL MATERIAL: FORGED BILLET, ASTM A-182, GRD F304
MATERIAL SHALL BE ULTRASONIC OR RADIOGRAPHIC TEST INSPECTED IN ACCORDANCE WITH ASME CODE, SECTION III, DIVISION 1, SUBSECTION NB, ARTICLE NB-2500, AND SECTION V, ARTICLE 2.

10. DESIGN PRESSURE IS 50 PSIG. PAYLOAD CAVITY SHALL BE SUBJECTED TO AN INTERNAL TEST PRESSURE EQUAL TO A MINIMUM OF 150% OF THE DESIGN PRESSURE.

[11] IMPACT LIMITER TOROIDAL SHELLS SHALL BE FABRICATED FROM TYPE 304 STAINLESS STEEL HAVING A MINIMUM YIELD STRENGTH OF 34,000 PSI AND A MAXIMUM YIELD STRENGTH OF 38,000 PSI BASED ON 0.2% OFFSET. ALLOWABLE WALL THICKNESS SHALL BE 3/4 ±1/16.

[12] COAT THREADS WITH A LUBRICANT PRIOR TO ASSEMBLY.

[13] MATERIAL: ASTM A-240, TYPE 304 STAINLESS STEEL PLATE.

[14] TAMPER INDICATING SEALS SHALL BE INSTALLED AT ONE (1) ATTACHMENT PIN LOCATION ON BOTH UPPER & LOWER IMPACT LIMITER, AS SHOWN.

[15] PIPE PLUG MATERIAL: STAINLESS STEEL, TORQUE 1" NPT PLUGS TO 35-45 LB-FT AND 3/8 NPT PLUGS TO 100-120 LB-IN (LUBRICATED [12]).

[16] LABEL AS SHOWN USING 3/4 INCH MINIMUM HIGH CHARACTERS, COLOR: BLACK.

[17] IMPACT LIMITER LIFT ONLY; REMOVE IMPACT LIMITER TO EXPOSE CASK LIFTING HOLES.

[18] CLOSURE LID BOLT MATERIAL: ASTM A-320, GR L43, SOCKET HEAD CAP SCREW CADMIUM PLATED PER QQ-P-416E. TYPE II, CLASS 2. TORQUE TO 80-100 LB-FT (LUBRICATED [12]).

[19] LABEL AS SHOWN USING 1/2 INCH MINIMUM HIGH CHARACTERS, COLOR: BLACK.

[20] LEAD COMPOSITION SHALL BE PER FEDERAL SPECIFICATION QQ-L-171E, GR A OR C, OR ASTM B-29.

[21] OUTER SHELL FABRICATION SHALL COMPLY WITH THE TOLERANCE REQUIREMENTS OF ASME CODE SECTION III, DIVISION 1, SUBSECTION NE, ARTICLE NE-4220.

[22] LIFTING THREADS SHALL BE SUBJECTED TO A TEST LOAD EQUAL TO A MINIMUM OF 150% OF WORKING LOAD. INSPECT THREADS FOR DISTORTION AFTER TEST.

23. THERMAL ACCEPTANCE TEST SHALL BE PERFORMED ON A PROTOTYPE PACKAGE PER SAR SECTION 8.1.6.

24. REPAIR OF BASE MATERIAL:
FOR ALL INTERNAL CASK BODY AND LID SHELLS, REPAIR OF BASE MATERIAL SHALL BE IN ACCORDANCE WITH ASME CODE, SECTION III, DIVISION 1, SUBSECTION NB, ARTICLE NB-2539, OR ARTICLE NB-4131. MAXIMUM WELD REINFORCEMENT SHALL BE 3/32 INCH IN COMPLIANCE WITH ASME CODE, SECTION III, DIVISION 1, SUBSECTION NB, ARTICLE NB-4426, PARAGRAPH NB-4426.1.

FOR THE CASK BODY OUTER SHELL AND THERMAL SHIELDS, REPAIR OF BASE MATERIAL SHALL BE IN COMPLIANCE WITH ASME CODE, SECTION III, DIVISION 1, SUBSECTION NF, ARTICLE NF-4131, OR ARTICLE NF-2510 AND ASTM-A240. ALTERNATIVELY, REPAIRS MAY BE PERFORMED IN COMPLIANCE WITH ASME CODE, SECTION III, SUBSECTION NB-2538 AND NB-2539, OR ARTICLE NB-4131. MAXIMUM WELD REINFORCEMENT SHALL BE 3/32 INCH.

REMOVAL OF EXCESS WELD REINFORCEMENT FROM BASE MATERIAL REPAIR WELDS, TEMPORARY ATTACHMENT WELDS, ETC., SHALL BE UNIFORMLY BLENDED, i.e., SHALL HAVE A MAXIMUM WELD REINFORCEMENT AS STATED ABOVE AND HAVE A TAPERED TRANSITION TO THE BASE MATERIAL SURFACE.

DOCUMENTATION OF BASE MATERIAL REPAIRS SHALL BE IN COMPLIANCE WITH ASME CODE, SECTION III, DIVISION 1, SUBSECTION NB, ARTICLE NB-4132.

[25] SHIELDING INTEGRITY TEST PER SECTION 8.1.5 OF SAFETY ANALYSIS REPORT.

26. PAINT EXPOSED SURFACES (IN SHIPPING CONFIGURATION, EXCLUDING IMPACT LIMITER ATTACHMENT PINS) WITH A PRIMER COAT OF TNEMEC SERIES 66 (3-5 MILS DFT) AND A FINISH COAT OF TNEMEC SERIES 73 (3-5 MILS DFT) COLOR: WHITE.

APPROVED FOR CONSTRUCTION

ITEM	QTY	NEXT ASSY			
–	–	–	REL	B. Harris	11-16-98
–	–	–	APPD	[illegible]	11-12-98
–	–	–	APPD	[illegible]	11/12/98
–	–	–	APPD	[illegible]	11/12/98
–	–	–	ENGR	[illegible]	11/12/98
–	–	–	QA	[illegible]	11/13/98
–	–	–	CHECK	[illegible]	11/12/98
			DRAWN	T.WAAGAN	10/30/98

TOLERANCES, UNLESS OTHERWISE SPECIFIED:

LINEAL DIMENSION RANGE	DECIMAL			FRACTIONAL	ANGULAR
	3 PLACE	2 PLACE	1 PLACE		
0-6"	±0.020	±0.06	±0.2	±3/16	±2°
6"-24"	±0.030	±0.10	±0.3	±5/16	
> 24"	±0.050	±0.20	±0.5	±1/2	

PACTEC Packaging Technology, Inc. — TRANSNUCLEAR, INC.

STERIGENICS EAGLE CASK
GENERAL ARRANGEMENT DRAWING

SCALE: N/A | WT. N/A
REV: 0 | SHEET 1 OF 7
DWG SIZE: D | DWG NO. 98003-SAR
CADFILE: 98003SAR010.DWG

9812020248-01

FIGURE WITHHELD UNDER 10 CFR 2.390

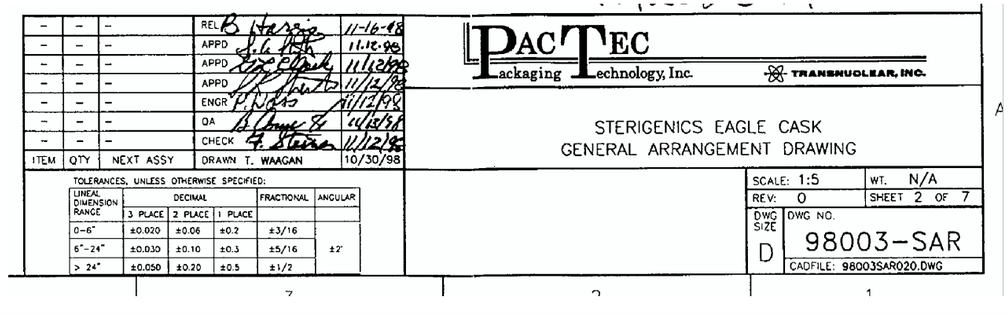

–	–	–	REL	B Waagan	11-16-98
–	–	–	APPD	J.L. Hoth	11.12.98
–	–	–	APPD	Lyn Eldridge	11/12/98
–	–	–	APPD	[illegible]	11/12/98
–	–	–	ENGR	P.N. Dale	11/12/98
–	–	–	QA	B Gray for	11/12/98
–	–	–	CHECK	T. Stevens	11/12/98
ITEM	QTY	NEXT ASSY	DRAWN	T. WAAGAN	10/30/98

TOLERANCES, UNLESS OTHERWISE SPECIFIED:

LINEAL DIMENSION RANGE	DECIMAL			FRACTIONAL	ANGULAR
	3 PLACE	2 PLACE	1 PLACE		
0–6"	±0.020	±0.06	±0.2	±3/16	±2°
6"–24"	±0.030	±0.10	±0.3	±5/16	
> 24"	±0.050	±0.20	±0.5	±1/2	

PACTEC Packaging Technology, Inc. — TRANSNUCLEAR, INC.

STERIGENICS EAGLE CASK
GENERAL ARRANGEMENT DRAWING

SCALE: 1:5 | WT. N/A
REV: 0 | SHEET 2 OF 7
DWG SIZE: D | DWG NO. 98003-SAR
CADFILE: 98003SAR020.DWG

FIGURE WITHHELD UNDER 10 CFR 2.390

–	–	–	REL	B. Hessie	11-16-98
–	–	–	APPD	J. G. Hoff	11-17-98
–	–	–	APPD	D.R. Shuck	11/12/98
–	–	–	APPD	R. Strout	11/12/98
–	–	–	ENGR	D. Wais	11/12/98
–	–	–	QA	M. Mayo G	11/3/98
–	–	–	CHECK	T. Stone	11/12/98
ITEM	QTY	NEXT ASSY	DRAWN T. WAAGIN		10/30/98

TOLERANCES, UNLESS OTHERWISE SPECIFIED:

LINEAL DIMENSION RANGE	DECIMAL			FRACTIONAL	ANGULAR
	3 PLACE	2 PLACE	1 PLACE		
0–6"	±0.020	±0.06	±0.2	±3/16	±2°
6"–24"	±0.030	±0.10	±0.3	±5/16	
> 24"	±0.050	±0.20	±0.5	±1/2	

PACTEC Packaging Technology, Inc. — TRANSNUCLEAR, INC.

STERIGENICS EAGLE CASK
GENERAL ARRANGEMENT DRAWING

SCALE: 1/4		WT. N/A	
REV: 0		SHEET 3 OF 7	
DWG SIZE D	DWG NO. 98003-SAR		
	CADFILE: 98003SAR030.DWG		

FIGURE WITHHELD UNDER 10 CFR 2.390

–	–	–	REL	B. Waagin	11-16-98
–	–	–	APPD	[illegible]	11-12-98
–	–	–	APPD	[illegible]	11/12/98
–	–	–	APPD	[illegible]	11/12/98
–	–	–	ENGR	[illegible]	11/12/98
–	–	–	QA	[illegible]	11/13/98
–	–	–	CHECK	[illegible]	11/12/98
ITEM	QTY	NEXT ASSY	DRAWN T. WAAGIN		10/30/98

TOLERANCES, UNLESS OTHERWISE SPECIFIED:

LINEAL DIMENSION RANGE	DECIMAL			FRACTIONAL	ANGULAR
	3 PLACE	2 PLACE	1 PLACE		
0–6"	±0.020	±0.05	±0.2	±1/16	±2°
6"–24"	±0.030	±0.10	±0.3	±5/16	
> 24"	±0.050	±0.20	±0.5	±1/2	

PACTEC Packaging Technology, Inc. — TRANSNUCLEAR, INC.

STERIGENICS EAGLE CASK
GENERAL ARRANGEMENT DRAWING

SCALE: 1/2	WT. N/A
REV: 0	SHEET 4 OF 7
DWG SIZE: D	DWG NO. 98003-SAR
	CADFILE: 98003SAR040.DWG

FIGURE WITHHELD UNDER 10 CFR 2.390

–	–	–	REL	11-16-98
–	–	–	APPD	11-12-98
–	–	–	APPD	11/12/98
–	–	–	APPD	11/12/98
–	–	–	ENGR	11/12/98
–	–	–	QA	11/12/98
–	–	–	CHECK	11/12/98
ITEM	QTY	NEXT ASSY	DRAWN T.WAAGIN	10/30/98

TOLERANCES, UNLESS OTHERWISE SPECIFIED:

LINEAL DIMENSION RANGE	DECIMAL			FRACTIONAL	ANGULAR
	3 PLACE	2 PLACE	1 PLACE		
0–6"	±0.020	±0.06	±0.2	±3/16	±2°
6"–24"	±0.030	±0.10	±0.3	±5/16	
> 24"	±0.050	±0.20	±0.5	±1/2	

PACTEC Packaging Technology, Inc. — TRANSNUCLEAR, INC.

STERIGENICS EAGLE CASK
GENERAL ARRANGEMENT DRAWING

SCALE: 1/5 | WT. N/A
REV: 0 | SHEET 5 OF 7
DWG SIZE: D | DWG NO. 98003-SAR
CADFILE: 98003SAR050.DWG

FIGURE WITHHELD UNDER 10 CFR 2.390

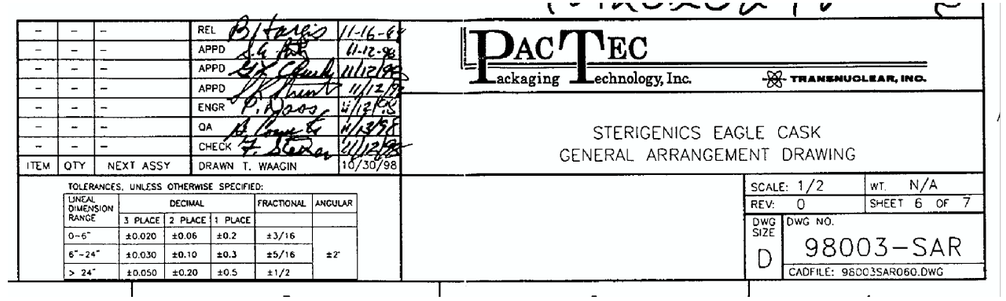

FIGURE WITHHELD UNDER 10 CFR 2.390

–	–	–	REL	B. Harris	11-16-98
–	–	–	APPD	S. A. Pitts	11-12-98
–	–	–	APPD	Eric O'Neill	11/12/98
–	–	–	APPD	K. Smith	11/12/98
–	–	–	ENGR	P. Ivans	11/12/98
–	–	–	QA	D. Cayer	11/13/98
–	–	–	CHECK	T. Stevens	11/12/98
ITEM	QTY	NEXT ASSY	DRAWN T. WAAGIN		10/30/98

TOLERANCES, UNLESS OTHERWISE SPECIFIED:

LINEAL DIMENSION RANGE	DECIMAL			FRACTIONAL	ANGULAR
	3 PLACE	2 PLACE	1 PLACE		
0–6"	±0.020	±0.06	±0.2	±3/16	±2°
6"–24"	±0.030	±0.10	±0.3	±5/16	
> 24"	±0.050	±0.20	±0.5	±1/2	

PACTEC Packaging Technology, Inc. — TRANSNUCLEAR, INC.

STERIGENICS EAGLE CASK
GENERAL ARRANGEMENT DRAWING

SCALE: 1/2	WT. N/A
REV: 0	SHEET 7 OF 7
DWG SIZE D	DWG NO. 98003-SAR
	CADFILE: 98003SAR070.DWG

2.0 STRUCTURAL EVALUATION

This chapter presents the structural design criteria, weights, mechanical properties of materials, and structural evaluations which demonstrate that the SteriGenics Eagle Cask (SEC) design meets all applicable structural criteria of 10 CFR 71 [1]. The adequacy of the design is demonstrated primarily by analysis, in accordance with Regulatory Guides 7.6 [2] and 7.8 [3]. Evaluation of the toroidal impact limiters is also performed by both static crush and free drop testing, and is documented in Appendix 2.10.5.

2.1 Structural Design

The SEC, with impact limiters installed, is shown in Figure 2.1-1. Each of the major subcomponents are discussed in the following paragraphs.

2.1.1 Discussion

The SEC is designed to safely transport special form Cobalt-60 source capsules. Since the payload is designated as special form, the SEC is defined as a confinement system. A section view of the cask is shown in Figure 2.1-2. As shown in the figure, the package consists of a shielded cask body, a shielded cask lid, a payload basket with payload, and upper and lower toroidal impact limiters. With the exception of fasteners, lead shielding, and miscellaneous parts, all of the material of the cask, including the toroidal impact limiters, is ASTM Austenitic Type 304 stainless steel. These components, shown in the Appendix 1.3.2, *Packaging General Arrangement Drawings* in are now discussed in detail.

The cask body consists of an inner stainless steel shell having an inner diameter of 10.75 inches and a minimum thickness of 1 inch, an outer stainless steel shell having an outer diameter of 35.5 inches and a thickness of 1 inch, relatively massive upper and lower stainless steel castings[1], and lead shielding. The inner shell is cast integrally with the castings as follows. The upper half of the inner shell is cast integrally with the upper casting, and the lower half of the inner shell is cast integrally with the lower casting. The upper and lower halves are joined at the axial center using a full penetration weld. As a feature of the casting method used, the inner shell possesses a 3° taper along each half-length, so that the upper and lower ends of the inner shell are slightly thicker than the minimum thickness of 1 inch at the axial center of the cask. The lead shielding around the sides of the cask (between the inner and outer shells) is cast in place, and has a maximum radial thickness of 10.38 inches at the center. In the cask bottom, the lead shielding is 11.88 inches thick directly below the payload, and 4.13 inches thick beneath the side lead shielding. The bottom lead shielding is then covered with a plate on the bottom of the cask having a thickness of 1 inch. All of the lead shielding in the cask is specified as ASTM B29, Chemical Lead.

The payload cavity consists of the inner shell, the shielded cask lid, and the bottom plate. The bottom plate of the payload cavity is 1 inch thick, and is cast integrally with the lower casting. A

[1] The upper and lower end structures are designated only as castings in the text, but may be alternately made from forged material.

transition taper of 3:1 is used at the bottom corner of the payload cavity. The weld between the upper and lower castings, located at the center of the inner shell, is full penetration and radiograph inspected. The welds between the outer shell and the upper and lower castings, including an optional longitudinal girth weld, are full penetration welds, liquid penetrant inspected on the root and final passes. As shown in Figure 2.1-2, the bottom cavity plate and lower casting are drilled with a ⅜ inch diameter drain passage which can be used to drain or flood the payload cavity with water. When the lid is installed, the payload cavity is 19 inches long.

A double thermal radiation shield is used to protect the cask from the hypothetical accident fire event, located outside the outer shell between the two impact limiters, and made of stainless steel. The inner shield is ¾ inches thick, and is radially separated from the outer shell by 12 gauge (0.105 inch thick) spacers at each end. The inner shield is attached to the lower casting with a ⅜ inch groove weld, and is not attached to the upper casting. The outer shield is a sheet of 10 gauge (0.135 inch thick) material, welded to the end castings at each end, and separated from the inner shield by a spiral wrap of 12 gauge (0.105 inch thick) wire. The cask is lifted by means of a lifting device mounted in two holes threaded into the upper casting. The cask lifting attachment holes and the lid lifting attachment holes feature stainless steel threaded inserts.

The cask lid consists of a stainless steel shell enclosing lead shielding. The upper portion of the lid has a diameter of 19¾ inches and a thickness of 5¼ inches, and the lower portion of the lid has a thickness of 11⅝ inches and a diameter of 10¼ inches. The top surface of the lid is recessed 1/16 inch below the top end of the cask. The top plate of the lid is 1½ inches thick, and the outer ring has a radial thickness of 1⅜ inches. The total axial thickness of lead in the cask lid is 14 5/16 inches. The lid is penetrated by a ¾ inch diameter drain port and a ⅜ inch diameter vent port, each closed with stainless steel NPT pipe plugs. A face-type O-ring seal, having an inner diameter of 13 inches and a cross-sectional diameter of 0.275 inches, is captured in the lid by means of a dovetail groove. This seal is designed to assist the confinement performance of the cask. Since the seal is not a containment boundary, it is not leak tested. The lid is attached to the cask using 12, ¾-10 UNC bolts made from ASTM A320, Grade L43, cadmium plated alloy steel.

Both upper and lower end impact limiters are metallic toroids. The toroidal structure is made from 20 inch outside diameter, ¾ inch wall thickness, stainless steel pipe elbows welded together using full penetration welds. The major outside diameter of the limiters is 60 inches. The toroid is welded to a cap structure which fits around the end of the cask. The cap structure is 1 inch thick and is also made of stainless steel. The impact limiters are attached to the cask by means of 12, one inch diameter shear pins oriented radially, equally spaced around the cap. The pins are of the ball-lock type, which are self-retaining and easy to use. One shear pin on each limiter is equipped with a lockwire to provide evidence of tampering.

The payload basket is capable of holding up to 72, Cobalt-60 source capsules in special form. It consists of four spacer disks for source capsule alignment, a bottom disk on which the source capsules rest, and a center tube, all of Type 304 stainless steel. No structural credit is taken for either the payload source capsules or the payload basket.

2.1.2 Design Criteria

2.1.2.1 Basic Design Criteria

The SEC is demonstrated to meet the requirements of 10 CFR 71 primarily by analysis, with confirmatory testing of the performance of the impact limiters. Allowable stresses are established in accordance with Regulatory Guide 7.6 as supplemented by the ASME B&PV Code [4]. These design criteria for the cask, in combination with the provisions of the special form payload, meet the following safety requirements of 10 CFR §71.51:

1. For normal conditions of transport, there shall be no loss or dispersal of radioactive contents, as demonstrated to a sensitivity of 10^{-6} A_2 per hour, no significant increase in external radiation levels, and no substantial reduction in the effectiveness of the package.
2. For hypothetical accident conditions, there shall be no escape of radioactive material exceeding a total amount A_2 in one week, and no external radiation dose rate exceeding one rem per hour at one meter from the external surface of the package.

The inner shell, lid, and end castings are classified as Section III, Subsection NB, Class 1 components. The outer shell is classified as a Subsection NF component support, but conservatively analyzed to the requirements of Subsection NB. The lead shielding is nonstructural, and is assumed incapable of supporting loads, unless the ability to support loads is unfavorable for the structural component under consideration. Material properties are taken from Section II, Part D, for Class 1 components of the ASME Code [5]. The buckling evaluations of the cask shells are performed in accordance with ASME Code Case N-284-1 [6]. The cask lid closure bolts are evaluated in accordance with the recommendations of NUREG/CR-6007 [7]. A summary of the design criteria used for all cask structures is provided in Table 2.1-1.

In addition, two other criteria are used in the design of the SEC:

Lifting. The allowable stresses for the lifting and handling components of the cask are based on the requirements of 10 CFR §71.45(a), i.e., minimum material yield strength with a load factor of 3.

Impact Limiters. Impact limiter components, including attachments, are allowed to exceed the material yield strength for all conditions. The acceptance criterion for impact limiters is that all of the kinetic energy associated with the free drop event be absorbed without contact of a relatively rigid cask component with the ground. The impact limiters must remain in place during impact to the extent that they remain capable of governing cask impact, including post-primary impacts.

Table 2.1-1 - Allowable Stress Limits

Stress Category	Normal Conditions	Accident Conditions
Cask Structure Stresses		
General Primary Membrane Stress Intensity	S_m	Lesser of: $2.4S_m$, $0.7S_u$
Local Primary Membrane Stress Intensity	$1.5S_m$	Lesser of: $3.6S_m$, S_u
Primary Membrane + Bending Stress Intensity	$1.5S_m$	Lesser of: $3.6S_m$, S_u
Range of Primary + Secondary Stress Intensity	$3.0S_m$	Not Applicable
Pure Shear Stress	$0.6S_m$	$0.42S_u$
Peak	Per Section 2.1.2.3.2	Not Applicable
Buckling	ASME Code Case N-284-1	
Cask Lid Fastener Stresses①		
Average Tensile Stress	S_m②	Lesser of: S_y, $0.7S_u$
Average Shear Stress	$0.6S_m$	Lesser of: $0.6S_y$, $0.42S_u$
Avg. Tensile + Avg. Shear	$R_t^2 + R_s^2 < 1$	$R_t^2 + R_s^2 < 1$
Avg. Tensile + Avg. Shear + Bending + Residual Torsion	$1.35S_m$ for $S_u > 100$ ksi	Not Applicable

Notes:

① Lid fastener stress limits are in accordance with NUREG/CR-6007.

② S_m is defined as $(2/3)S_y$ as recommended by NUREG/CR-6007.

2.1.2.2 Load Combinations

The SEC is evaluated for the load combinations shown in Table 2.1-2, which are in accordance with Regulatory Guide 7.8. Each normal condition of transport is applied separately. Each hypothetical accident condition is applied sequentially to determine the maximum cumulative damage in the following order: a 30 foot free drop, followed by a 40 inch drop onto a mild steel puncture bar, followed by exposure to a 30 minute, 1,475 °F thermal environment. As discussed in Section 2.7.2, the crush test is not applicable to the SEC.

Table 2.1-2 - Summary of Load Combinations for NCT and HAC

Condition	Applicable Initial Condition								
	Ambient Temperature		Insolation		Decay Heat		Internal Pressure		Fabrication Stresses
	100 °F	-20 °F	Max	Zero	Max	Zero	Max	Min	
Normal Conditions of Transport (Analyzed Separately)									
Hot Environment: 100 °F	×		×		×		×		×
Cold Environment: -40 °F				×		×		×	×
Increased External Pressure: 20 psia		×		×		×		×	×
Minimum External Pressure: 3.5 psia	×		×		×		×		×
Vibration and Shock:	×		×		×		×		×
		×		×		×		×	×
Free Drop: 1 foot drop	×		×		×		×		×
		×		×		×		×	×
Hypothetical Accident Conditions (Analyzed Sequentially)									
Free Drop: 30 foot drop	×		×		×		×		×
		×		×		×		×	×
Puncture: 40 inch drop	×		×		×		×		×
		×		×		×		×	×
Thermal: 1,475 °F fire	×			×①	×		×		×

Notes:

① The HAC fire event is analyzed with full insolation before and after the fire, and zero insolation during the fire, per 10 CFR §71.73(c)(4).

2.1.2.3 Miscellaneous Structural Failure Modes

2.1.2.3.1 Brittle Fracture

With the exception of the cask lid bolts, all of the structural components of the SEC are made from ASTM Type 304 austenitic stainless steel. This material does not undergo a ductile-to-brittle transformation in the temperature range of interest (i.e., as low as -20 °F), and thus does not need to be evaluated for brittle fracture. The lid closure bolts are made from ASTM A320, Grade L43 alloy steel bolting material, expressly designed for cold temperature service. Per Section 5 of NUREG/CR-1815 [8], bolts are generally not considered as fracture-critical components because multiple load paths exist and thus offer a redundant design. Thus, brittle fracture of the SEC structural materials is not of concern.

2.1.2.3.2 Fatigue

2.1.2.3.2.1 Normal Operating Cycles

Normal operating cycles do not represent a fatigue concern for the SEC. The full amplitude of stress under normal conditions does not exceed the value of S_a for the specified number of load cycles taken from Table I-9.1 of the ASME B&PV Code [9]. This is demonstrated by the following fatigue analysis of the cask structural components and of the closure bolts.

The maximum number of cycles for the SEC is based on a 40 year design life and a round trip of approximately once per week, 50 weeks per year. Each round trip is conservatively assumed to represent transport of a full, maximum heat payload in each direction, for two maximum stress cycles per round trip[2]. The maximum number of cycles for the SEC is therefore

$$n = 40 \times 50 \times 2 = 4{,}000$$

From Table I-9.1 (for Figure I-9.2.1, for austenitic steels) of the ASME B&PV Code, the maximum allowable alternating stress intensity $S_a = 80{,}653$ psi for 4,000 cycles. For a maximum bounding temperature of 525 °F (conservatively greater than the maximum temperature of the cask body under NCT), the value of S_a is reduced as follows:

$$S_a = 80{,}653 \frac{25.675(10^6)}{28.3(10^6)} = 73{,}172 \text{ psi}$$

where $25.675(10^6)$ psi is the modulus of elasticity at the bounding temperature of 525 °F and $28.3(10^6)$ psi is the modulus used to create Figure I-9.2.1. This value is the fatigue stress for normal operating cycles for Type 304 stainless steel.

From Section 2.6.1, the maximum stress in the cask body due to NCT maximum temperature loadings, including the maximum internal design pressure of 50 psi and thermal differential expansion stresses associated with the lead gamma shielding, is 27,267 psi, located on the lower face of the upper casting near the intersection with the top of the inner shell (i.e., the upper inside corner of the annular lead cavity)[3]. This stress is primarily due to the thermal loading, and represents a peak stress due to its location at a corner. It is also primarily a bending stress, since the inner shell, which is warmer than the outer shell, expands more than the outer shell. This differential expansion results in a rotation of the upper casting, consistent with the inner shell of the cask expanding more than the outer shell. The sense of the rotation is such that the direction of the stress in the upper inside corner of the annular lead cavity is compressive. Since the stress varies from zero (room temperature case) to compressive (NCT maximum temperature case), and since fatigue crack growth requires varying tensile stresses, the compressive stress cannot cause fatigue failure. However, since the stress is primarily bending, a corresponding tensile region of stress must occur on the inside of the inner shell, essentially balancing the compressive stress on the inside of the inner shell, and is equal to 26,669 psi, as shown in Figure 2.6-3. Since this

[2] This is conservative since not all payloads have the maximum heat load.

[3] Due to cask and thermal loading symmetry, this discussion also applies to the lower end of the cask, however, the upper end governs.

tensile stress is not located in proximity to a geometric discontinuity, no factor for stress concentration is required. The margin of safety on fatigue for normal operating cycles for the cask body therefore is

$$MS = \frac{73{,}172}{26{,}669} - 1 = \underline{+1.74}$$

The lid closure bolts are replaced after a total of 150 cycles, or, since the lid is installed twice for each round trip of the cask, a total of 75 cask round trips. The maximum allowable alternating stress intensity S_a is taken from Table I-9.1 (for Figure I-9.4, for high strength steel bolting material) of the ASME Code. The following equation, provided in note 2 of ASME B&PV Code Table I-9.1, may be solved for the allowable alternating stress corresponding to 150 cycles.

$$\frac{N}{N_i} = \left(\frac{N_j}{N_i}\right)^{\log\left(\frac{S_i}{S_a}\right)/\log\left(\frac{S_i}{S_j}\right)}$$

where N is 150 cycles and S_a is the corresponding maximum allowable alternating stress intensity. The other parameters are the cycles and allowable stresses which bound the desired result, and have the following values: $N_i = 100$ cycles, $S_i = 320$ ksi, $N_j = 200$ cycles, and $S_j = 225$ ksi. The solution of this equation yields a value for $S_a = 260.4$ ksi at 150 cycles. For a maximum bolt temperature of 350 °F under NCT, the value of S_a is reduced as follows:

$$S_a = 260{,}400\frac{26.4(10^6)}{30.0(10^6)} = 229{,}152 \text{ psi}$$

where $26.4(10^6)$ psi is the modulus of elasticity at the bolting temperature of 350 °F and $30.0(10^6)$ psi is the modulus used to create Figure I-9.4. This value is the fatigue stress for normal operating cycles for the cask lid closure bolts.

The maximum stress developed in the lid closure bolts during normal operations (given in Section 2.10.4) is 52,129 psi. This stress includes normal pressure and vibration loads, thermal stresses, and a conservative inclusion of 50% of the applied preload torque as a residual torsional stress. Including a factor of 4 to conservatively account for the stress concentration associated with the bolt threads, the maximum fatigue-related stress is 52,129 × 4 = 208,516 psi. The margin of safety on fatigue for normal operating cycles for the cask lid closure bolts is

$$MS = \frac{229{,}152}{208{,}516} - 1 = \underline{+0.10}$$

Therefore, fatigue due to normal operating cycles is not of concern.

2.1.2.3.2.2 Normal Vibration in Transport

Fatigue due to the vibration associated with normal transport is discussed in Section 2.6.5.

2.1.2.3.3 Buckling

Regulatory Guide 7.6 states that buckling is an unacceptable failure mode for the analytic assessment of containment vessels. The intent of this provision is to preclude large deformations

which would compromise the validity of linear analysis assumptions and quasi-linear stress allowables, as given in Paragraph C.6 of Regulatory Guide 7.6.

Buckling investigations contained herein consider the outer shell of the SEC. The outer and inner shells of the cask are closely connected through the relatively rigid end castings, thus, the two shells act to strengthen each other. One shell cannot buckle independently of the other. However, the strength of the inner shell for buckling considerations is conservatively ignored.

The shell buckling analysis is performed in subsequent normal conditions of transport and hypothetical accident condition subsections in accordance with the ASME Code Case N-284-1. The nomenclature is strictly followed in order to preclude the need for a full description of the analysis within this report. The basic steps involved in determining are summarized as follows.

1. Theoretical elastic buckling stresses are determined for hoop, axial compression, and in-plane shear loadings using classical theory.
2. Capacity reduction factors are applied which account for the difference between classical theory and predicted instability stresses for fabricated shells.
3. Plasticity reduction factors are applied for those cases where elastically determined buckling stresses are above the proportional limit.
4. Elastic and inelastic buckling checks which employ appropriate factors of safety and appropriate interaction equations are made using worst case applied compressive and in-plane shear stresses.

Buckling evaluations are performed in Sections 2.6.7 (Free Drop, NCT), 2.7.1 (Free Drop, HAC), and 2.7.4 (Immersion).

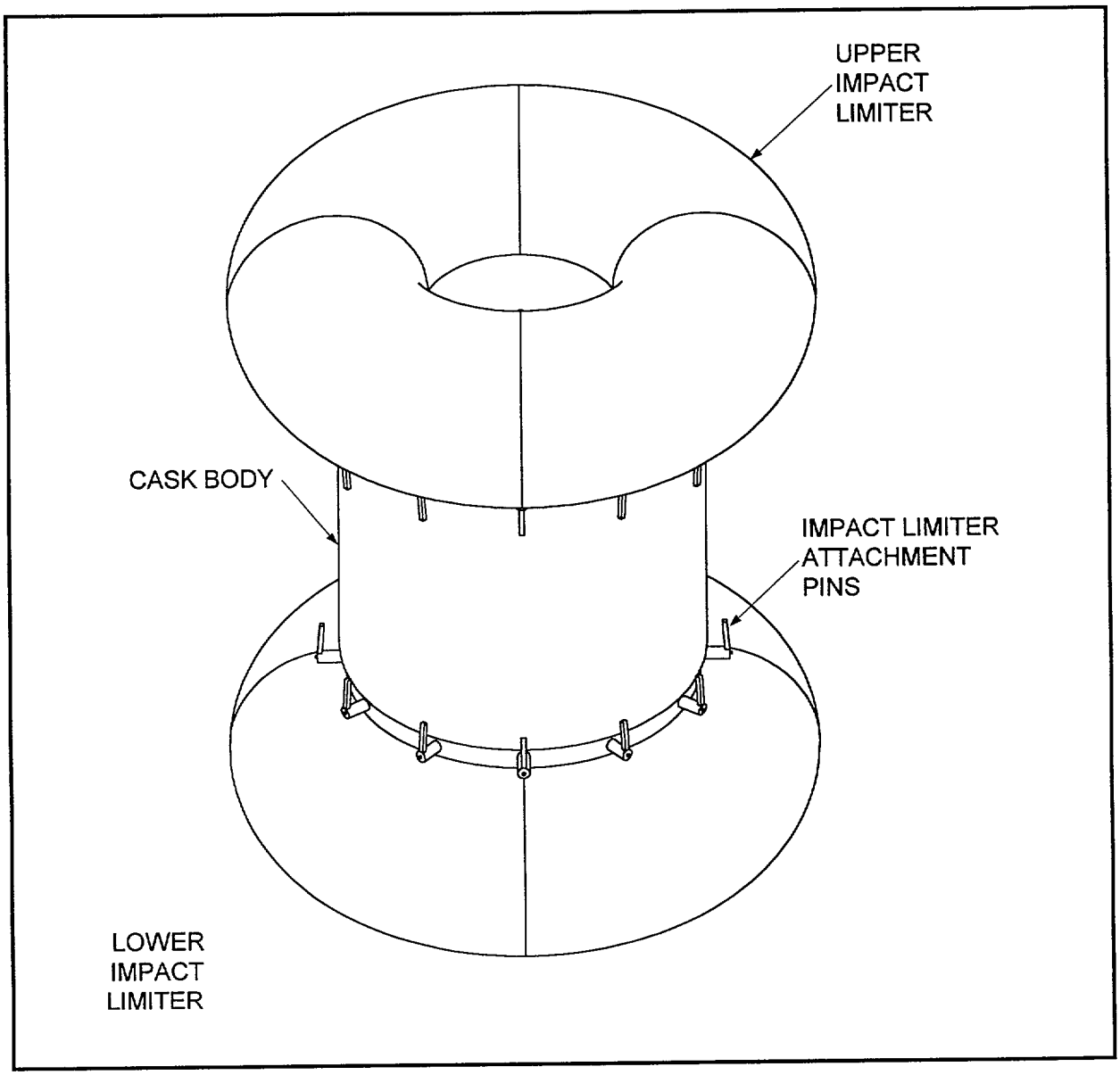

Figure 2.1-1 - SteriGenics Eagle Cask (Assembled)

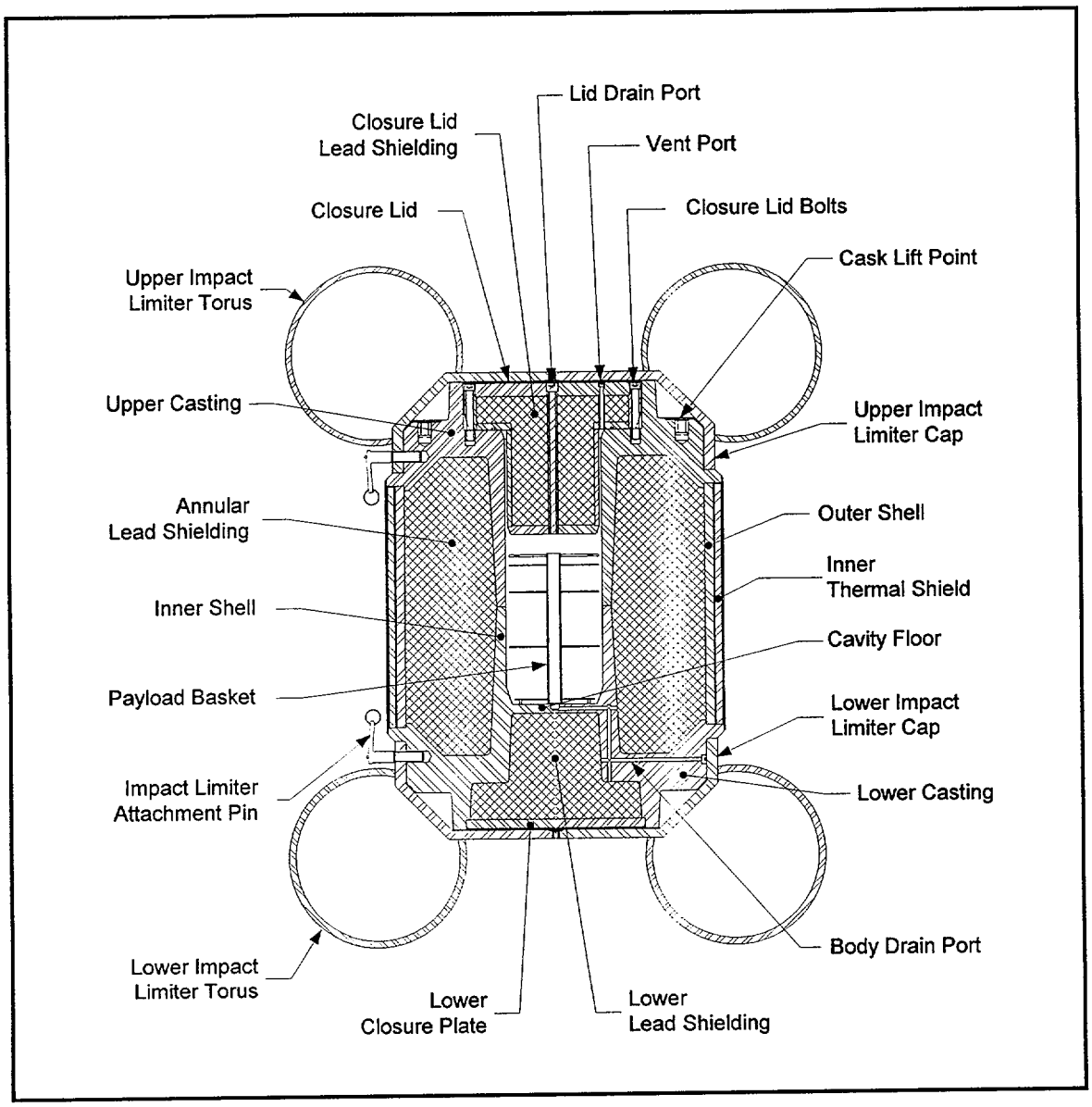

Figure 2.1-2 - SteriGenics Eagle Cask (Section View)

2.2 Weights and Center of Gravity

SEC component weight and total weight is given in Table 2.2-1. The reference point for center of gravity calculations is the bottom surface of the cask. The radial position of the center of gravity is on the cask centerline. The mass moment of inertia of the cask about a transverse axis through its center of gravity is 19,626 in-lb-s^2.

Table 2.2-1 - SEC Weights

Component	Weight (lb)	C.G. (inches)
Cask body①	15,100	24.0
Cask lid	900	43.8
Impact limiters (pair)	3,950	23.1
Payload (incl. basket)	50	24.4
TOTAL (including payload):		
without impact limiters	16,050	25.1
with impact limiters	20,000	24.7

Notes:

① The cask body consists of the upper casting, the lower casting, the outer shell, the lead shielding, and the dual thermal shield.

2.3 Mechanical Properties of Materials

2.3.1 Transportation Package

Mechanical properties for the materials used for the structural components of the SEC are given in this section. Temperature dependent material properties for structural components are obtained from Section II, Part D, of the ASME B&PV Code [5]. Nonlinear material properties used in impact limiter analyses are described in Section 2.3.2.

The SEC is made from several different materials. The cask body components, including the inner shell, outer shell, end castings, thermal shield, payload basket, and lid are fabricated from ASTM Type 304 stainless steel. The closure lid and threaded lifting holes are fitted with thread inserts made from austenitic stainless steel. The impact limiters are made entirely of Type 304 stainless steel. The lead shielding is ASTM B29 Chemical Lead. The NPT pipe plugs used in the body drain port, and the lid drain and vent ports are made from 300 series stainless steel. The lid closure bolts are made from ASTM A320, Grade L43, cadmium plated alloy steel. The ball lock pins, which retain the impact limiters, are made from alloy steel with aluminum handles. The closure lid O-ring dust seal is made from fluorocarbon elastomer rubber.

The cask drawings presented in Appendix 1.3.2, *Packaging General Arrangement Drawings*, identify these materials and their use. Tables 2.3-1 and 2.3-2 present the properties of the structural materials used in the cask. Table 2.3-3 and Figure 2.3-1 present the properties of the lead shielding. Material properties are linearly interpolated or extrapolated from these values as necessary.

Table 2.3-1 - Type 304 Stainless Steel Material Properties

Material Specification	Temperature, °F	Yield Strength① (S_y), psi	Ultimate Strength② (S_u), psi	Design Stress Intensity③ (S_m), psi	Elastic Modulus④, $\times 10^6$ psi	Coefficient of Thermal Expansion⑤, $\times 10^{-6}$ in/in/°F
ASTM A240 ASTM A276 Type 304	-40	**30,000**	**75,000**	**20,000**	**28.8**	**8.21**
	-20	30,000	75,000	20,000	**28.7**	**8.26**
	70	30,000	75,000	20,000	28.3	---
	100	30,000	75,000	20,000	**28.1**	8.55
	200	25,000	71,000	20,000	27.6	8.79
	300	22,500	66,000	20,000	27.0	9.00
	400	20,700	64,400	18,700	26.5	9.19
	500	19,400	63,500	17,500	25.8	9.37
	600	18,200	63,500	16,400	25.3	9.53
	700	17,700	63,500	16,000	24.8	9.69

Notes:

① ASME B&PV Code, Section II, Part D, Table Y-1.

② ASME B&PV Code, Section II, Part D, Table U.

③ ASME B&PV Code, Section II, Part D, Table 2A.

④ ASME B&PV Code, Section II, Part D, Table TM-1, Material Group G.

⑤ ASME B&PV Code, Section II, Part D, Table TE-1, 18Cr-8Ni, Coefficient B (mean from 70 °F).

⑥ When necessary, values are linearly interpolated or extrapolated and given in **bold** text.

⑦ The weight density and Poisson's ratio for stainless steel are 0.290 lb/in^3 and 0.3, respectively.

Table 2.3-2 - ASTM A320, Grade L43, Bolting Material Properties

Material Specification	Temperature, °F	Yield Strength① (S_y), psi	Ultimate Strength② (S_u), psi	Design Stress Intensity③ (S_m), psi	Elastic Modulus④, $\times 10^6$ psi	Coefficient of Thermal Expansion⑤, $\times 10^{-6}$ in/in/°F
ASTM A320, L43	-40	**105,000**	**125,000**	**35,000**	**28.3**	**5.89**
	-20	105,000	**125,000**	35,000	**28.2**	**5.95**
	70	105,000	**125,000**	35,000	27.8	---
	100	105,000	125,000	35,000	**27.6**	6.27
	200	99,000	125,000	33,000	27.1	6.54
	300	95,700	125,000	31,900	26.7	6.78
	400	91,800	125,000	30,600	26.1	6.98
	500	88,500	125,000	29,500	25.7	7.16
	600	84,300	125,000	28,100	25.2	7.32
	700	79,200	125,000	26,400	24.6	7.47

Notes:

① ASME B&PV Code, Section II, Part D, Table Y-1.

② ASME B&PV Code, Section III, Code Case N-249, Table 5, for Specification No. SA-354, Grade BC, bolting material, the temperature-dependent ultimate tensile strength values, S_u, for AISI 4340 bolting material, the material composition of ASTM A320, Grade L43, bolts.

③ ASME B&PV Code, Section II, Part D, Table 4.

④ ASME B&PV Code, Section II, Part D, Table TM-1, Material Group B.

⑤ ASME B&PV Code, Section II, Part D, Table TE-1, Material Group E, 1¾Ni-¾Cr-¼Mo, Coefficient B (mean from 70 °F).

⑥ When necessary, values are linearly interpolated or extrapolated and given in **bold** text.

⑦ The weight density and Poisson's ratio for carbon steel are 0.283 lb/in^3 and 0.3, respectively.

Table 2.3-3 - Mechanical Properties of Lead Shielding

Material Specification	Temperature, °F	Yield Strength① (S_y), psi	Ultimate Strength② (S_u), psi	Design Stress Intensity③ (S_m), psi	Elastic Modulus④, $\times 10^6$ psi	Coefficient of Thermal Expansion⑤, $\times 10^{-6}$ in/in/°F
ASTM B29 Chemical Lead	-99	---	---	---	2.50	15.28
	70	---	---	---	2.34	16.07
	100	584	1,570	276	2.30	16.21
	175	509	1,162	293	2.20	16.58
	250	498	844	277	2.09	16.95
	325	311	642	189	1.96	17.54
	440	---	---	---	1.74	18.50
	620	---	---	---	1.36	20.39

Notes:

① WADC Technical Report 57-695, ASTIA Document No. 151165, "Determination of the Mechanical Properties of a High Purity Lead and a 0.05% Copper-Lead Alloy," April 1958, by Thomas Tietz, Stanford Research Center, pp. 21,26.

② NUREG/CR-0481, SAND77-1872, "An Assessment of Stress-Strain Data Suitable for Finite Element Elastic-Plastic Analysis of Shipping Containers," H. J. Rack and G. A. Knorovsky, Sept. 1978, p. 66.

③ The weight density and Poisson's ratio for lead are 0.41 lb/in^3 and 0.45, respectively.

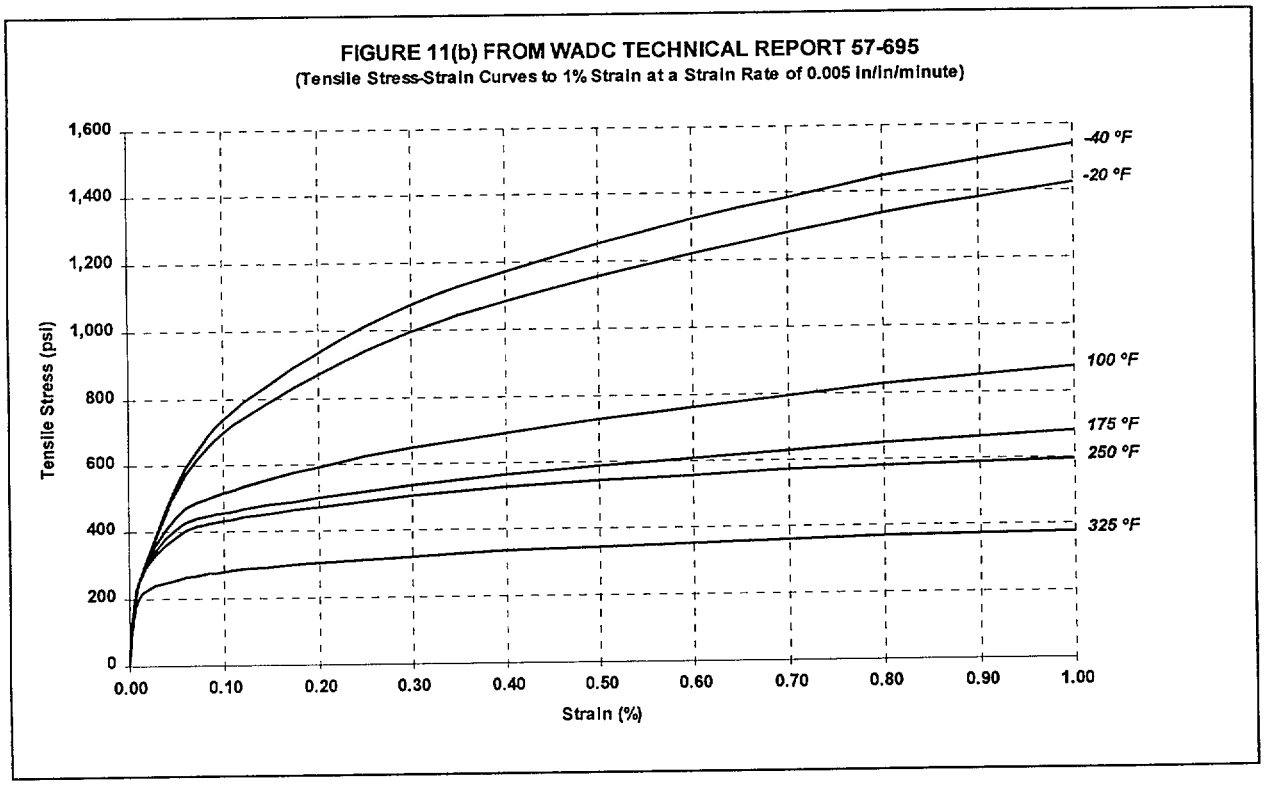

Figure 2.3-1 - Tensile Stress-Strain Curves for Lead Shielding [10]

2.3.2 Impact Limiter Nonlinear Material Properties

The SEC impact limiters are constructed in the form of toroids, made from Type 304 stainless steel. The impact loads experienced by the cask in the NCT and HAC free drop events are a function of the material nonlinear stress-strain behavior. The analysis of impact forces is discussed in Sections 2.6.7 and 2.7. The impact limiters are analyzed using the explicit dynamic finite element code, LS-DYNA, described in Section 2.10.3. Since the impact behavior of the impact limiters is highly nonlinear, material properties in the form of true stress-strain curves are required in order to evaluate the impact response. Material properties are developed for the lower bound strength, maximum deflection case and for the upper bound strength, maximum impact force case. In both cases, stress-strain properties are used in analysis which maximize the worst case behavior. The parameters of both types of material definitions are developed in the following paragraphs.

Variation in the impact behavior of the limiters is modest, and is the result of small variations in the Type 304 material properties as a result of temperature as well as the possible range of annealed material properties. The properties of interest are the yield point and the tangent modulus. Both of these properties vary inversely with temperature. Therefore, the minimum impact loads can be expected from the minimum strength, warmest material, and the maximum impact loads from the maximum strength, coldest material. The minimum temperature of interest for the free drop is -20 °F, and the maximum temperature of the impact limiter toroidal shell for Normal Conditions of Transport is bounded by 200 °F.

The minimum yield strength corresponds to both a temperature of 200 °F as well as to the minimum strength material which could be used to fabricate the toroids. The temperature effect on yield strength for temperatures above room temperature is obtained from Figure 2.7.1.1.1(a) of MIL-HDBK-5F [24]. According to the figure, the tensile strength of Type 304 stainless steel at 200 °F is 14% lower than it is at 70 °F. As shown on the drawings in Section 1.3.2, the material used to fabricate the impact limiter toroids is specified to have a room temperature yield strength no less than 34,000 psi. The minimum yield strength at 200 °F is therefore 0.86 × 34,000 = 29,240 psi. A minimum tensile yield strength of at 200 °F of 29,000 psi is conservatively used.

The maximum yield strength corresponds to both a temperature of -20 °F as well as to the maximum strength material which could be used to fabricate the toroids. The temperature effect on yield strength for temperatures below room temperature is again obtained from Figure 2.7.1.1.1(a) of MIL-HDBK-5F. According to the figure, the tensile yield strength of Type 304 stainless steel at -20 °F is 9% higher than it is at 70 °F. As shown on the drawings in Appendix 1.3.2, *Packaging General Arrangement Drawings*, the material used to fabricate the impact limiters is specified to have a room temperature yield strength no greater than 38,000 psi. The maximum yield strength at -20 °F is therefore 1.09 × 38,000 = 41,420 psi. A maximum tensile yield strength at -20 °F of 42,000 psi is conservatively used.

The tangent modulus is defined as the slope of the true stress strain curve between the material yield point and the ultimate breaking strength, given as

$$E_t = \frac{S_u - S_y}{\varepsilon_u - 0.002}$$

where S_u is the ultimate strength, S_y is the yield strength, ε_u is the ultimate elongation or strain, and the elongation or strain at the yield point is defined as 0.2%, or 0.002. Data is taken from NUREG/CR-0481 [11], Table IV for Type 304 material. Since the data in this table is in the form of engineering stress-strain data, it must first be converted to true stress-strain data before use in the equation above. This conversion can be performed using the following relations from Reference [12]:

$$\sigma_{true} = \sigma_{eng}\left(1 + e_{eng}\right)$$

$$\varepsilon_{true} = \ln\left(1 + e_{eng}\right)$$

where σ_{eng} is the engineering stress value, and e_{eng} is the elongation (as a decimal value, percent divided by 100). As an example, the data for 100 °C from Table IV of Reference [11] is first converted from engineering to true stress-strain and then used to calculate the tangent modulus. First, the true ultimate tensile strength is

$$S_u = \sigma_{eng}\left(1 + e_{eng}\right) = 109{,}050 \text{ psi}$$

where σ_{eng} is 68,800 psi and e_{eng} is 58.8%. Similarly, the true yield strength is

$$S_y = \sigma_{eng}(1 + 0.002) = 24{,}250 \text{ psi}$$

$S_y = \sigma_{eng}(1 + 0.002) = 24{,}250$ psi, where σ_{eng} is the stress at 0.2% strain of 24,200 psi. The true ultimate strain is

$$\varepsilon_u = \ln\left(1 + e_{eng}\right) = 0.461$$

The tangent modulus at 100 °C is therefore

$$E_t = \frac{S_u - S_y}{\varepsilon_u - 0.002} = 184{,}750 \text{ psi}$$

This operation is performed on the data in Table IV of Reference 10 from -50 °C to 100 °C, and the results interpolated for -20 °F and 200 °F, resulting in tangent moduli of 446,300 psi and 188,300 psi, respectively. The larger the tangent modulus, the greater is the impact force; therefore the low temperature value of 446,300 psi is conservatively bounded by a value of 450,000 psi at -20 °F. Conversely, the high temperature value is conservatively bounded by rounding the value of 188,300 psi down to 185,000 psi at 200 °F.

To better characterize the behavior of the impact limiters in service, quarter scale engineering tests were performed at room temperature for side, end, and c.g.-over-corner orientations. These quasi-static tests consisted of crushing prototypic impact limiter specimens in a test machine, forming a force-deflection curve. Next, a tensile test of the material used for the quarter scale test specimens provided a stress-strain curve for use in a corresponding analytical prediction of test results. A yield point of 38,000 psi, an ultimate strength of 92,650 psi, and a tangent modulus of 240,000 psi were calculated for the test specimen material using the method described above. Analytical force-deflection curves were generated using these material properties and the LS-DYNA analysis models described in Section 2.10.3, and compared to the force-deflection curves obtained from the quarter scale test. These comparisons are shown in Figures 2.3-2 to 2.3-4. Each figure contains three curves: the long, smooth curve represents the static test data; the lower unsmoothed line represents the analysis model prediction using the bi-linear stress-strain curve obtained for the test material; and the upper unsmoothed line represents an analysis prediction using a multi-linear stress-strain curve.

As shown, the prediction resulting from the use of a multi-linear stress-strain curve provides a very good match with the test results. The multi-linear curve was obtained as follows. Starting with the bi-linear curve, the curve was then given an arbitrary "bulge", convex upward, until the analytical prediction matched the test result. The resulting curve is shown in Figure 2.3-5, along with the basic bi-linear curve. (The basic bi-linear curve for the test conditions was found above as having a yield point of 38,000 psi and a tangent modulus of 240,000 psi.) The same multi-linear curve provides a good match to test data in each of the three orientation cases as shown in Figures 2.3-2 to 2.3-4. Therefore, in analytically predicting the test force-deflection results, the use of the multi-linear stress-strain curve gives superior results to the basic, bi-linear stress-strain curve.

To ensure that the maximum impacts are not underpredicted in the NCT and HAC free drop impact analyses described in Section 2.7.1, a multi-linear stress-strain curve is used instead of a bi-linear curve in all cold free drop analysis cases. The cold, -20 °F bi-linear stress-strain curve is adjusted proportionately the same as the room temperature test curve. As an example,

consider the adjustment of stress at a plastic strain level of 0.3. Referring to Figure 2.3-5, which shows the room temperature curves developed from the quasi-static quarter scale test, the adjustment factor is

$$SF = \frac{\sigma_m}{\sigma_b} = 1.136$$

where SF is the stress adjustment factor for a plastic strain level of 0.3, σ_m = 125,000 psi is the stress from the multi-linear curve, and σ_b = 110,000 psi is the stress from the bi-linear curve. The stress at a temperature of -20 °F and a plastic strain of 0.3 is therefore

$$\sigma_{cm} = (SF)\sigma_{cb}$$

where σ_{cb} is the stress at -20 °F from the bi-linear stress strain curve developed above, and σ_{cm} is the corresponding multi-linear curve stress value. This same procedure is carried out at five different plastic strain levels, namely strains of 0.0, 0.05, 0.1, 0.3, and 0.6. Note that the adjustment is always to a higher level of stress, which leads to a higher impact and a more conservative result. Also note that this adjustment is not carried out for the stress-strain curves used for warm impact. In that case, the bi-linear stress-strain curve leads to conservatively higher impact limiter deformations. Therefore, the lower-bound bi-linear stress-strain curve is used for warm condition impact analyses.

Impact limiter material impact properties are summarized in Tables 2.3-4 and 2.3-5, and both curves are plotted in Figure 2.3-7.

Table 2.3-4 - Bi-linear Stress-Strain Curve for Maximum Deflection (Warm) Cases

Condition	Yield Strength, S_y, psi	Elastic Modulus, E_e, psi	Tangent Modulus, E_t, psi
Warm, 200 °F, Minimum Properties	29,000	$27.6(10^6)$	185,000

Table 2.3-5 - Multi-Linear Stress-Strain Curve for Maximum Impact (Cold) Cases

Condition	Plastic Strain① (in/in)	Stress Adjustment Factor (SF)	Multi-Linear Stress (σ_{cm}, psi)
Cold, -20 °F, Maximum Properties	0.0	1.0	42,000
	0.05	1.140	73,530
	0.10	1.177	102,400
	0.30	1.136	201,100
	0.60	1.0	312,000

Notes:

① Values shown are True-Strain and True-Stress. The elastic modulus for the multi-linear material properties is $28.7(10^6)$ psi.

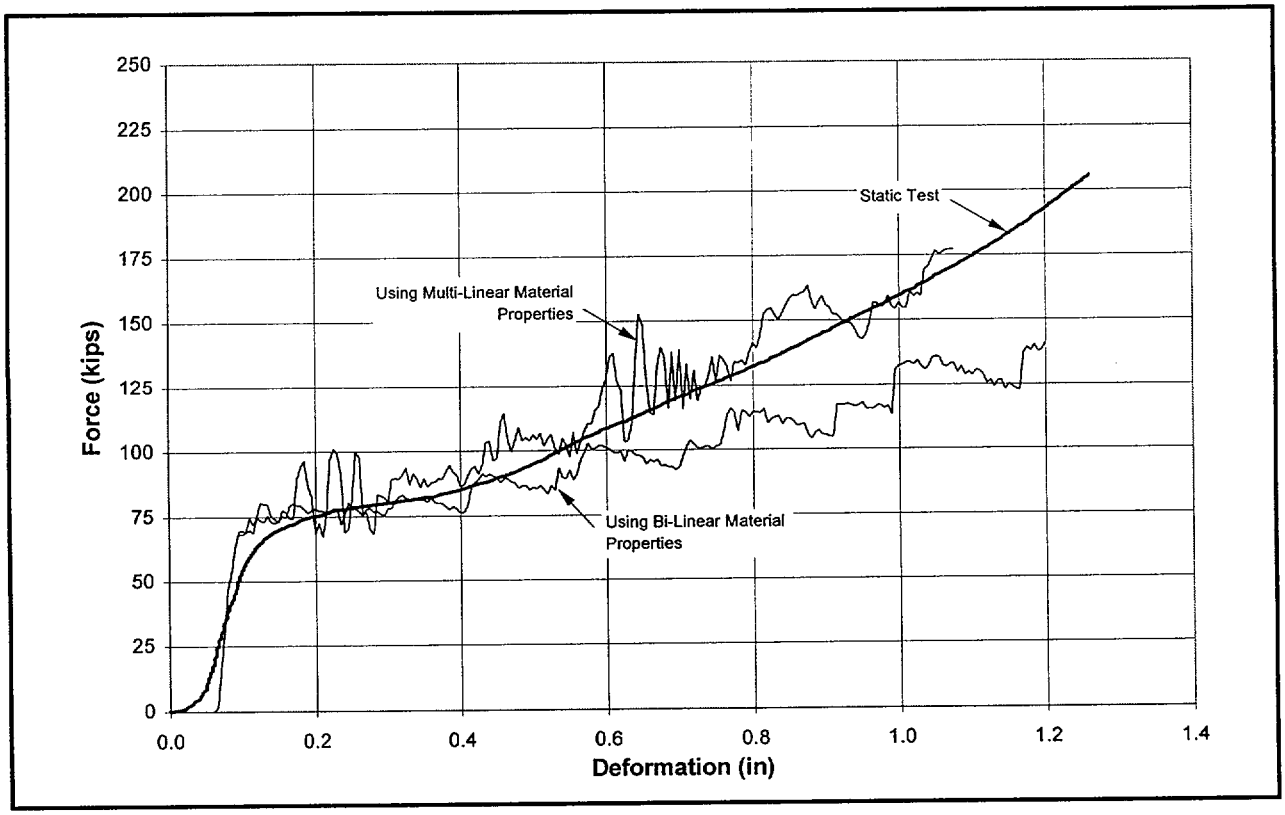

Figure 2.3-2 - Quarter Scale Force-Deflection Curve, End Orientation

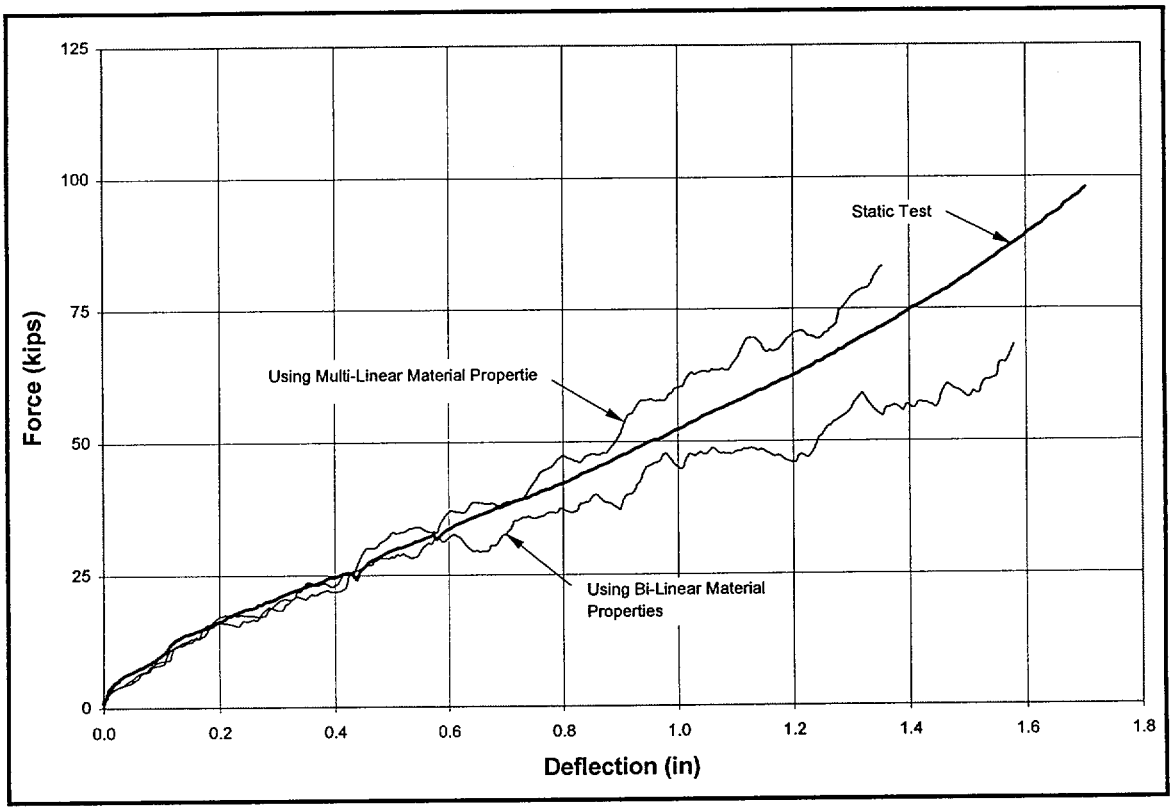

Figure 2.3-3 - Quarter Scale Force-Deflection Curve, Side Orientation

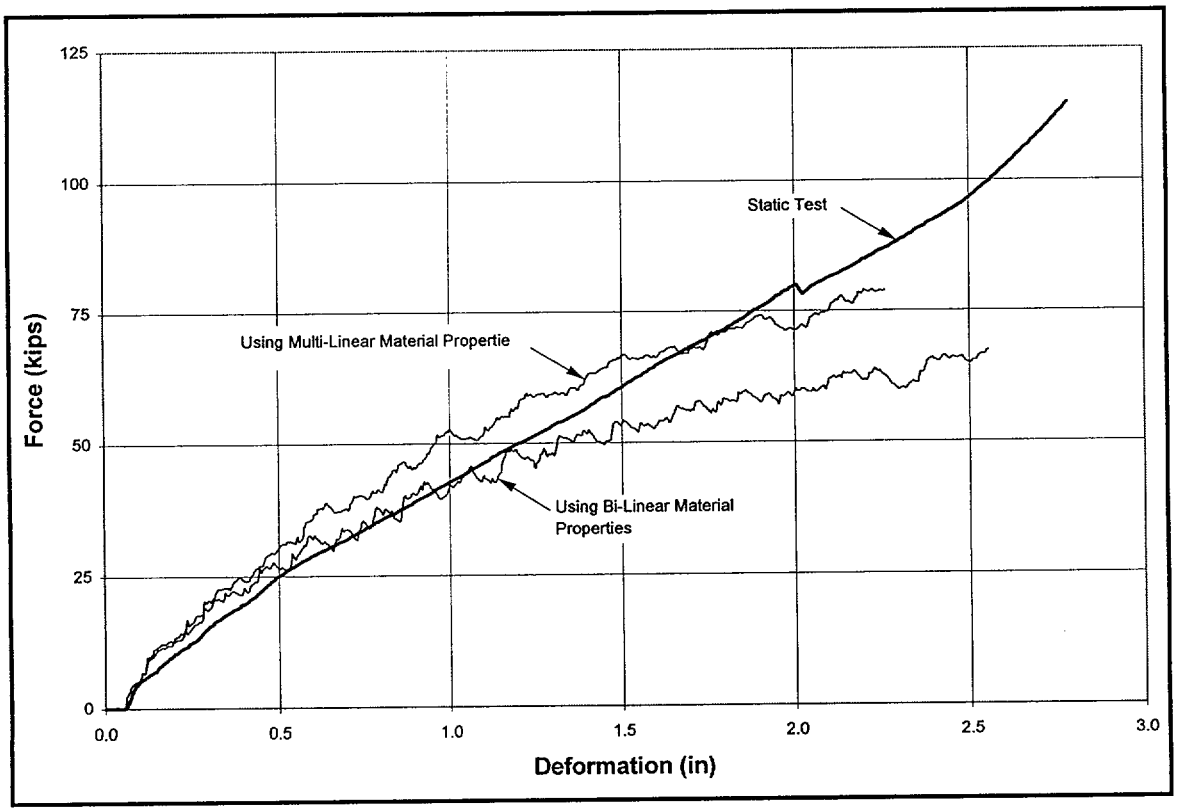

Figure 2.3-4 - Quarter Scale Force-Deflection Curve, C.G. Over Corner Orientation

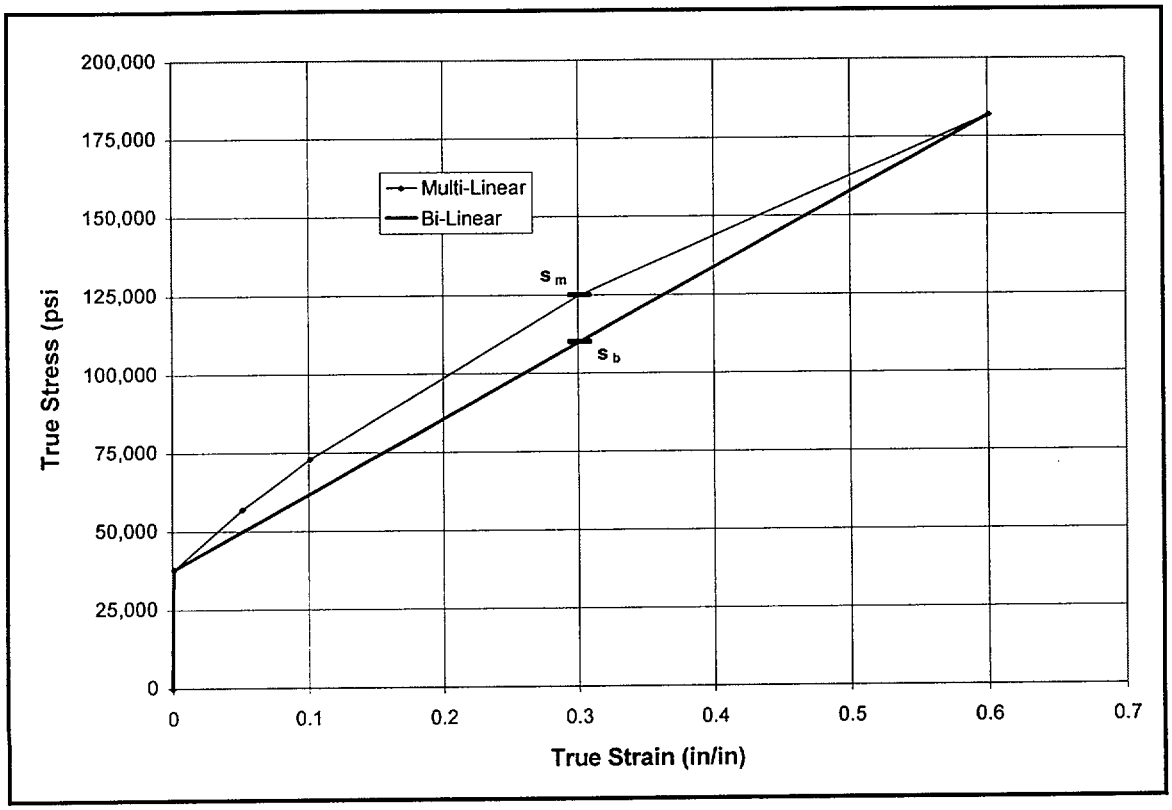

Figure 2.3-5 - True Stress-Strain Curves for Engineering Test

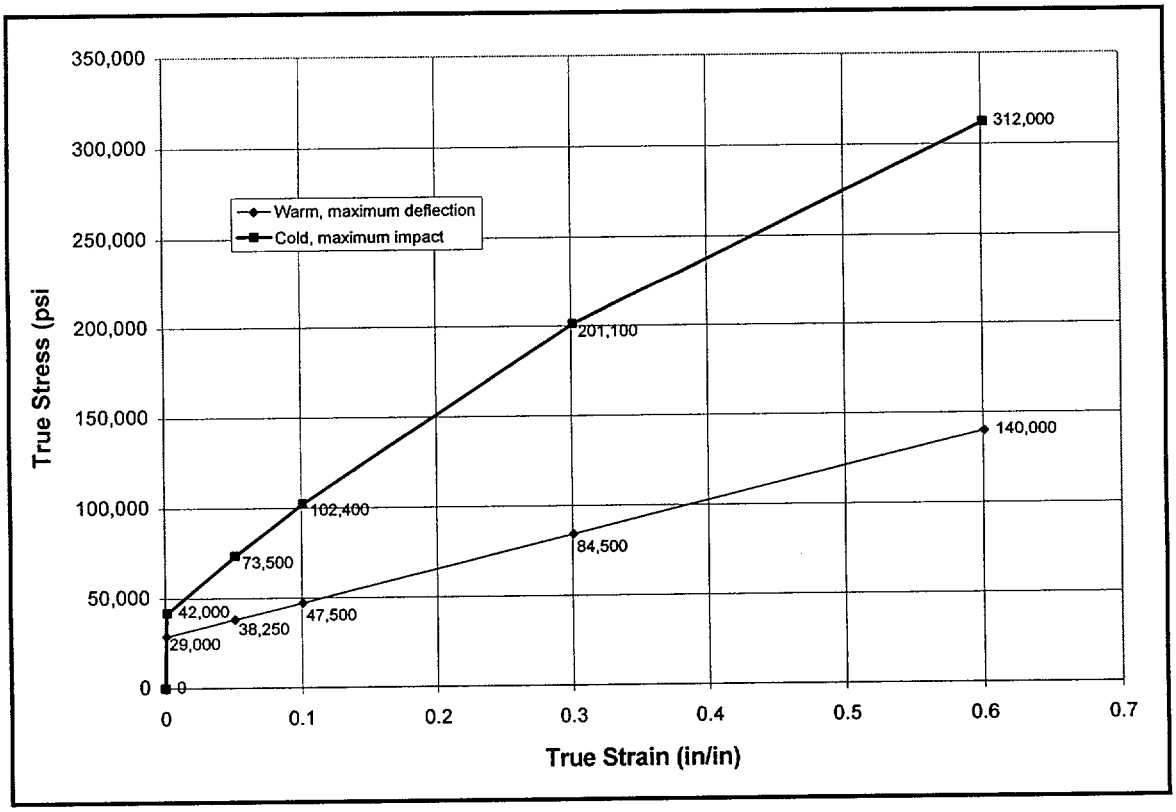

Figure 2.3-6 - Bounding Stress-Strain Curves Used in Impact Analysis

2.4 General Standards for All Packages

The SEC has been evaluated with respect to the general standards for all packaging specified in 10 CFR §71.43 [1]. Results of the evaluations are discussed in the following sections.

2.4.1 Minimum Package Size

The smallest overall dimension of the package is the diameter of the cask body, equal to 37.6875 inches. This is significantly greater than the 10 CFR §71.43(a) minimum allowable dimension of 4 inches.

2.4.2 Tamper Indicating Device

Tamper indicating seals are attached to the ball-lock pins that attach the limiters to the cask body, one seal on each limiter. Since the impact limiters must be removed to gain access to the cask cavity and the drain/vent ports, an intact seal is evidence that the package has not been opened. Thus, the requirement of 10 CFR §71.43(b) is satisfied.

2.4.3 Positive Closure

The SEC cannot be opened inadvertently. Positive closure of the cask is provided by a single lid secured by twelve, ¾-10 UNC-2A x 7.5 inch long, ASTM A320, Grade L43, alloy steel bolts. When assembled for transport, the lid and vent/drain ports are covered by the impact limiters, which prevents accidental removal or loosening. Thus, the requirement of 10 CFR §71.43(c) is satisfied.

2.4.4 Chemical and Galvanic Reactions

The materials of construction used in the SEC will not have significant reactions with the payload, with air, or with water. All of these materials have been used previously in radioactive materials packaging without incident related to corrosion. The only components of the package which are not made from austenitic stainless steel are made from lead and alloy steel bolting material. The lead is sealed within an airtight cavity. The bolts are made of alloy steel with cadmium plating, which is corrosion resistant. Thus, the requirement of 10 CFR §71.43(d) is satisfied.

2.4.5 Valves

The SEC is defined as a confinement system designed to transport radioactive material in special form. Therefore, radioactive contents cannot escape through valves or openings during transport. Nevertheless, all openings in the SEC are plugged securely during transport. Thus, the requirement of 10 CFR §71.43(e) is satisfied.

2.4.6 Cask Design

As shown in Sections 2.6, 3.4, and 5.4, the SEC design satisfies the requirements of 10 CFR §71.71. Thus, the requirements of 10 CFR §71.43(f) are met.

2.4.7 External Temperatures

The SEC is an exclusive use package designed for use in a 100 °F environment. During transport, a personnel barrier and shipping pallets prevent access to any region of the package where surface temperatures exceed 185 °F. Thus, the requirements of 10CFR §71.43(g) are met.

2.4.8 Venting

The package does not incorporate any feature that would permit continuous venting during transport. Thus, the requirement of 10 CFR §71.43(h) is met.

2.5 Lifting and Tiedown Devices

2.5.1 Lifting Devices

The SEC is lifted from two threaded lift points. Lifting devices are installed in thread inserts made from ASTM 302 stainless steel. The failure mode of the lifting device is via shear tearout of the device from the inserts.

Since the cask weight distribution is axisymmetric, per Section 2.2, the lifting load is evenly distributed between the two lifting devices. Although normal operating procedures call for the cask to be lifted without the lower impact limiter, it is conservatively assumed for the purpose of this analysis that it is in place during lifting. Since the upper impact limiter must be removed prior to installation of the lifting devices, lifting the cask with the upper limiter in place is impossible. The weight of the loaded cask with bottom impact limiter is bounded by 18,000 lb. Since the weight will be evenly distributed between the two lifting devices, the load per side is F = 18,000/2 = 9,000 lb.

The outer threads of the threaded insert are 1⅜-12 UNF, and the minimum shear area for the insert is taken from the manufacturer's data for a length of 1.5 inches as $A_o = 3.7929$ in^2. The shear stress in the outer threads is

$$\tau_o = \frac{F}{A_o} = 2{,}373 \text{ psi}$$

The governing shear area for the inner threads is that of the insert, which is 1-8 UNC-3B, or from Reference [13], $A_i = 2.3989$ in^2/in. The shear stress in the inner threads is

$$\tau_i = \frac{F}{A_i L} = 2{,}501 \text{ psi}$$

where L = 1.50 inches. Therefore, the inner thread shear stress is governing. The Type 302 stainless steel insert has properties similar to Type 304 stainless steel, and at a bounding temperature of 400 °F, the yield strength from Table 2.3-1 is 20,800 psi. The margin of safety is

$$MS = \frac{20{,}800(0.6)}{2{,}501(3)} - 1 = +0.66$$

where the factor of 0.6 in the numerator accounts for the shear failure mode and the factor of 3 in the denominator ensures that a minimum factor of safety of 3 is present. In the case of lifting overload, the device will strip out of the threaded insert without damage to the cask. Therefore, the requirements of 10 CFR §71.45(a) [1] are met.

2.5.2 Tiedown Devices

During transport, the SEC rests on a steel pallet, and is held down to the pallet by means of a steel frame which rests on top of the upper impact limiter. This frame is attached by four wire ropes or equivalent to the conveyance, so that a nominal downward load is applied to keep the SEC in place. In this configuration, the SEC contacts only the pallet on the bottom and the steel

frame on the top, and therefore has no integral tiedown devices which are a part of the package. Therefore, per 10 CFR §71.45(b)(1), no analysis of tiedown devices is required.

2.6 Normal Conditions of Transport

When subjected to normal conditions of transport (NCT) as specified in 10 CFR §71.71 [1], the SEC transportation cask meets the performance requirements specified in Subpart E of 10 CFR 71. This is demonstrated in the following subsections where each NCT condition is addressed and shown to meet the applicable design criteria. A summary of load combinations used herein, consistent with Regulatory Guide 7.8 [3], is provided in Section 2.1.2.2.

2.6.1 Heat

The cask thermal evaluation for the normal heat condition is presented in Chapter 3.0. The normal heat condition is evaluated by applying a 100 °F ambient temperature, maximum insolation, and maximum decay heat per Regulatory Guide 7.8 and 10 CFR §71.71(c)(1).

2.6.1.1 Summary of Pressures and Temperatures

Maximum NCT cask temperatures are presented in Figure 2.6-1. The figure shows a temperature output plot, generated from the finite element thermal model described in Section 3.4. Except for details relating specifically to thermal analysis, the model is the same one used to calculate stress and deformation, and is described in detail in Section 2.10.2.1. The maximum heat condition corresponds to the maximum 330,000 Ci payload, 100 °F ambient environment, and maximum insolation. The maximum temperature anywhere in the cask is 518 °F, located at the center of the payload cavity floor. The maximum temperature of the inner shell is 500 °F, located at the inside center of the inner shell. The maximum temperature of the end castings, lid[1], and outer shell is 400 °F. The inner shell temperature of 500 °F is a peak temperature at the warmest part of the shell, and the majority of the inner shell has temperatures well below this value. Thus, for all normal conditions of transport mechanical loads, the payload floor design temperature is bounded by 520 °F, the inner shell design temperature is bounded by 510 °F, and the end castings, lid, and outer structural shell design temperature is bounded by 410 °F. The resulting design allowable stress intensities, per the discussions of Sections 2.1.2 and 2.3, are summarized in Table 2.6-1. In the analyses which follow, the temperature distribution shown in Figure 2.6-1 is used to determine differential thermal expansion and thermal stresses of cask components.

Table 2.6-1 - Summary of Allowable Stresses for NCT

Parameter	Payload Floor	Inner Shell	Outer Shell, End Castings
Temperature, °F	520	510	410
Design Stress, S_m, psi	17,280	17,390	18,580
Ultimate Stress, S_u, psi	63,500	63,500	64,310

[1] The lowest part of the lid experiences temperatures in excess of 400 °F, but in areas subsequently analyzed, lid temperatures are below 400 °F.

The initial pressure in the cask at assembly is ambient, i.e., 14.7 psia. As determined in Section 3.4.4, the Maximum Normal Operating Pressure (MNOP) is conservatively determined to be 23.9 psig. The cask has a design pressure of 50 psig, which is significantly higher than the MNOP. The 50 psig design pressure and the thermal gradients discussed above are used in the analyses discussed in Sections 2.6.1.3 and 2.6.1.4.

2.6.1.2 Differential Thermal Expansion

Under NCT heat conditions, both the closure lid and the payload maintain positive clearances to the cask body. The minimum room temperature clearance between the cask upper casting and the lid is found on the upper, larger portion of the lid. The opening in the casting is 20.0 inches in diameter, and the upper portion of the lid is 19.75 inches in diameter, for a radial clearance of 0.125 inches. As shown by Figure 2.6-1, the maximum temperature of the outer ring of the upper portion of the lid is bounded by 350 °F, and the minimum temperature of the upper opening in the cask is bounded by 285 °F. The minimum radial clearance between the lid and the cask at NCT maximum temperatures therefore is

$$\text{Clr} = 0.125 - [19.75\alpha_{350}(350 - 70) - 20.0\alpha_{285}(285 - 70)] = 0.113 \text{ inches}$$

where, from Table 2.3-1, $\alpha_{350} = 9.10(10^{-6})$ in/in/°F and $\alpha_{285} = 8.97(10^{-6})$ in/in/°F. The minimum diametrical clearance is twice this value, or 0.226 inches, which is only slightly less than the initial clearance. Thus, the closure lid retains a positive clearance to the cask body under NCT maximum temperatures.

The payload cavity is 10.75 inches in diameter and 19 inches long. The payload basket has a maximum diameter of 10 inches and a length of 18 inches, yielding a radial clearance of 0.375 inches and an axial clearance of 1 inch. Due to these large initial clearances over the payload basket, differential thermal expansion is not of concern.

Due to different thermal expansion coefficients, as well as to a temperature gradient, the lead gamma shielding creates a stress in the inner shell under NCT heat conditions. An upper bound interface pressure between the lead and the inner shell is now determined, and applied as a pressure load to the finite element model. First, note that the lead and the cask inner and outer shells are all in contact, and are stress-free, at the point of solidification of the lead at 620 °F. As the cask and lead cool, the lead contracts more than the stainless steel, and an interface pressure develops between the lead and the inner shell. This interface pressure is a function of the amount of interference between the lead and inner shell, and of the yield point of the lead at the NCT temperature. Due to the effects of material creep, the interface pressure will diminish over a relatively short period of time, thus reducing the resulting inner shell stresses. Conservatively, the effects of lead creep are neglected. The amount of interference between the lead and the inner shell depends upon the free state radii of these components, both at their respective NCT temperatures. The free state radii of the inner shell are

$$r_{ioh} = r_{io}[1 + \alpha_{sh}(T_{sh} - 70)] = 6.401 \text{ inches}$$

$$r_{iih} = r_{ii}[1 + \alpha_{sh}(T_{sh} - 70)] = 5.397 \text{ inches}$$

where r_{ioh} is the outer free state radius[2] of the inner shell and r_{iih} is the inner free state radius of the inner shell, both at the maximum NCT temperature of the inner shell of T_{sh} = 510 °F. The other parameters used in the equations in this section are given in Table 2.6-2.

Table 2.6-2 - Parameters for Lead Differential Expansion Calculations (Warm)

Name	Variable	Value, inches①	Name	Variable	Value, in/in/°F
Inner shell inner radius	r_{ii}	5.375	TEC②, inner shell, 510 °F	α_{sh}	$9.39(10^{-6})$
Inner shell outer radius③	r_{io}	6.375	TEC②, inner shell, 620 °F	α_{s620}	$9.56(10^{-6})$
Outer shell inner radius	r_{oi}	16.75	TEC②, lead, 427 °F	α_{Lh}	$18.39(10^{-6})$
Outer shell outer radius	r_{oo}	17.75	TEC②, lead, 620 °F	α_{L620}	$20.39(10^{-6})$

Notes:

① At room temperature, approximately 70 °F.

② Thermal Expansion Coefficient.

③ Minimum diameter.

To determine the free state radii of the lead under NCT temperatures, it is necessary to start with the radii of the steel shells at the lead solidification point at 620 °F, at which point all of the components are in stress free contact. The radii of the lead/steel interfaces at 620 °F are

$$r_{Li620} = r_{io620} = r_{io}\left[1 + \alpha_{s620}(620 - 70)\right] = 6.409 \text{ inches}$$

$$r_{Lo620} = r_{oi620} = r_{oi}\left[1 + \alpha_{s620}(620 - 70)\right] = 16.838 \text{ inches}$$

where r_{Li620}/r_{io620} represent the inner lead/steel interface radius, and r_{Lo620}/r_{oi620} represents the outer lead/steel interface radius at 620 °F. These values are then used to find the free state lead dimensions at the NCT bulk average temperature of lead of T_{Lh} = 427 °F as follows. Note that two thermal expansion terms are used (first contracting the lead from 620 °F to 70 °F, then expanding it from 70 °F to T_{Lh}), since the thermal expansion coefficients given in Section 2.3 are based on 70 °F.

[2] The inner shell possesses a 3° taper on its outer surface as a consequence of the casting process. The minimum diameter of 6.375 inches is conservatively used in this analysis.

$$r_{Lih} = r_{Li620}\left[1 - \alpha_{L620}(620 - 70) + \alpha_{Lh}(T_{Lh} - 70)\right] = 6.379 \text{ inches}$$

$$r_{Loh} = r_{Lo620}\left[1 - \alpha_{L620}(620 - 70) + \alpha_{Lh}(T_{Lh} - 70)\right] = 16.760 \text{ inches}$$

where r_{Lih} is the inner radius of the lead, and r_{Loh} is the outer radius, at NCT. Since the lead has a relatively low yield stress, the interface pressure between the inner shell and the lead will be governed by the lead yield stress, which in turn depends on the location of the lead stress state on the lead stress-strain curve. The hoop strain in the lead is equal to u/r, where u represents the radial displacement of the inner surface, and r is the inner radius, of the lead. The interface pressure can be conservatively maximized by assuming that the inner shell is rigid, and that therefore all of the radial interference is taken by the lead. The radial interference is

$$u = r_{ioh} - r_{Lih} = 0.022 \text{ inches}$$

The maximum lead strain is then

$$\varepsilon_{Lh} = \frac{u}{r_{Lih}}(100) = 0.345\%$$

Stress-strain curves for lead at various temperatures are published in Reference [10] and reproduced in Figure 2.3-1. From the curve representing a lead temperature of 325 °F (conservatively below the actual bulk average temperature of the lead of 427 °F), the maximum lead stress corresponding to a strain of 0.345% is bounded by σ_{Lh} = 350 psi. At the actual temperature of 427 °F, the yield stress would be even lower. The maximum sustainable interface pressure can be backed out of the equation for hoop stress in a thick walled cylinder, Reference [14], Table 32, Case 1a, as

$$p_h = \frac{\sigma_{Lh}}{\dfrac{r_{Loh}^2 + r_{Lih}^2}{r_{Loh}^2 - r_{Lih}^2}} = 261 \text{ psi}$$

In the finite element thermal stress analysis discussed in Section 2.6.1.3.2, a conservative upper bound external pressure of 300 psi is applied to the inner shell to represent the worst case lead contraction loading.

2.6.1.3 Stress Calculations

2.6.1.3.1 Stresses Due to Pressure Loading

The finite element model described in Section 2.10.2 is loaded with the internal maximum design pressure of 50 psi, without thermal loading, and gives the result shown in Figure 2.6-2. The maximum primary stress intensity is 289 psi, located on the meridian of the inner shell, at the point of minimum thickness of the inner shell. The maximum primary plus bending stress is 686 psi, and is located on the lower surface of the payload cavity floor on the cask central axis.

2.6.1.3.2 Stresses Due to Thermal Gradients

The same finite element model is loaded with 50 psi internal pressure (as in Section 2.6.1.3.1), as well as with the structural temperatures shown in Figure 2.6-1 and the lead contraction pressure determined in Section 2.6.1.2, and gives the result shown in Figure 2.6-3. The maximum stress intensity due to pressure and thermal gradient loading is 27,267 psi and occurs on the lower face of the upper casting, near the intersection with the inner shell (i.e., in the upper inside corner of the annular lead cavity).

2.6.1.4 Comparison with Allowable Stresses

From Table 2.1-1, the limit on primary membrane stress is S_m. At the bounding temperature of the inner shell of 510 °F given in Section 2.6.1.1, the value of S_m for Type 304 is 17,390 psi. For the primary stress intensity of 289 psi given in Section 2.6.1.3.1, the margin of safety is

$$MS = \frac{17,390}{289} - 1 = \underline{+ 59.2}$$

From Table 2.1-1, the limit on primary membrane plus bending stress is $1.5S_m$. At the bounding temperature of the payload cavity floor of 520 °F given in Section 2.6.1.1, the value of $1.5S_m$ for Type 304 is equal to $1.5 \times 17,280 = 25,920$ psi. For the primary plus bending stress intensity of 686 psi given in Section 2.6.1.3.1, the margin of safety is

$$MS = \frac{25,920}{686} - 1 = \underline{+ 36.8}$$

From Table 2.1-1, the limit on the range of primary plus secondary stress intensity is $3S_m$, which is $3.0 \times 17,390 = 52,170$ psi, where the design temperature of 510 °F applies. For the primary stress intensity of 27,621 psi given in Section 2.6.1.3.2, the margin of safety is

$$MS = \frac{52,170}{27,267} - 1 = \underline{+ 0.91}$$

As shown, all margins of safety for the NCT warm condition are positive.

2.6.1.5 Closure Lid Bolt Stress

The closure lid bolt stress is calculated in Section 2.10.4, per the recommendations of NUREG/CR 6007 [7]. The maximum NCT stress occurs during the NCT warm operating condition. The resulting tensile stress, accounting for initial preload, differential thermal expansion, and cask design pressure, is 47,283 psi. Adding residual torsion from preloading, the total maximum stress intensity in the bolt is 52,129 psi. The corresponding maximum combined stress ratio, which must be less than unity, is 0.76. Details of this analysis are provided in Section 2.10.4.

2.6.2 Cold

For the cold condition, a -40 °F steady state ambient temperature is utilized per Regulatory Guide 7.8 [3], with zero insolation and zero decay heat. This results in a uniform temperature of -40 °F throughout the cask. The materials of construction for the SEC transportation cask are not

adversely affected by the -40 °F condition, including brittle fracture, which is evaluated in Section 2.1.2.3.1.

In Section 2.6.1.2, the interface pressure between the cask inner shell and the lead gamma shielding was evaluated at the NCT maximum temperature. Since the lead will contract further at lower temperatures, that analysis is now repeated for the NCT cold condition. As discussed in Section 2.6.1.2, the lead and the cask inner and outer shells are all in contact, and stress free, at the point of solidification of the lead at 620 °F. As the cask and lead cool, the lead contracts more than the stainless steel, and an interface pressure develops between the lead and the inner shell. This interface pressure is a function of the amount of interference between the lead and inner shell, and of the yield point of the lead at the cold temperature. As stated in Section 2.6.1.2, material creep in the lead will reduce the interface pressure over time, but the effect is conservatively neglected. The amount of interference between the lead and the inner shell depends upon the free state radii of these components, both at -40 °F. The cold free state radii of the inner shell are

$$r_{ioc} = r_{io}[1 + \alpha_{sc}(-40 - 70)] = 6.369 \text{ inches}$$

$$r_{iic} = r_{ii}[1 + \alpha_{sc}(-40 - 70)] = 5.370 \text{ inches}$$

where r_{ioc} is the outer free state radius of the inner shell and r_{iic} is the inner free state radius of the inner shell, at -40 °F. The other parameters used in the equations in this section are given in Table 2.6-3.

Table 2.6-3 - Parameters for Lead Differential Expansion Calculations (Cold)

Name	Variable	Value, inches①	Name	Variable	Value, in/in/°F
Inner shell inner radius	r_{ii}	5.375	TEC②, inner shell, -40 °F	α_{sc}	$8.21(10^{-6})$
Inner shell outer radius③	r_{io}	6.375	TEC②, lead, -40 °F	α_{Lc}	$15.56(10^{-6})$
Average inner shell radius	r_{avg}	5.875	TEC②, lead, 620 °F	α_{L620}	$20.39(10^{-6})$

Notes:

① At room temperature, approximately 70 °F.

② Thermal Expansion Coefficient.

③ Minimum diameter.

To determine the free state radii of the lead at -40 °F, it is necessary to start with the radii of the steel shells at the lead solidification point at 620 °F, at which point all of the components are in stress free contact. The radii of the lead/steel interfaces at 620 °F were found in Section 2.6.1.2. The value r_{Li620} = 6.409 inches represents the inner radius of the lead and r_{Lo620} = 16.838 inches

represents the outer lead radius. These values are then used to find the free state lead dimensions at the cold temperature of -40 °F as follows. Note that two thermal expansion terms are used (first contracting the lead from 620 °F to 70 °F, then contracting it further from 70 °F to -40 °F), since the thermal expansion coefficients given in Section 2.3 are based on 70 °F.

$$r_{Lic} = r_{Li620}\left[1 - \alpha_{L620}(620 - 70) + \alpha_{Lc}(-40 - 70)\right] = 6.326 \text{ inches}$$

$$r_{Loc} = r_{Lo620}\left[1 - \alpha_{L620}(620 - 70) + \alpha_{Lc}(-40 - 70)\right] = 16.620 \text{ inches}$$

where r_{Lic} is the inner radius of the lead, and r_{Loc} is the outer radius, at -40 °F. Since the lead has a relatively low yield stress, the interface pressure between the inner shell and the lead will be governed by the lead yield stress, which in turn depends on the location of the lead stress state on the lead stress-strain curve. The hoop strain in the lead is equal to u/r, where u represents the radial displacement of the inner surface, and r is the inner radius of the lead. The interface pressure can be conservatively maximized by assuming that the inner shell is rigid, and therefore all of the radial interference is taken by the lead. The radial interference is

$$u = r_{ioc} - r_{Lic} = 0.043 \text{ inches}$$

The maximum lead strain is then

$$\varepsilon_{Lh} = \frac{u}{r_{Lic}}(100) = 0.68\%$$

Stress-strain curves for lead at various temperatures are published in Reference [10] and reproduced in Figure 2.3-1. From the curve representing a lead temperature of -40 °F, the maximum lead stress corresponding to a strain of 0.68% is bounded by σ_{Lc} = 1,400 psi. The maximum sustainable interface pressure can be backed out of the equation for hoop stress in a thick walled cylinder, Reference [14], Table 32, Case 1a, as

$$p_c = \frac{\sigma_{Lc}}{\dfrac{r_{Loc}^2 + r_{Lic}^2}{r_{Loc}^2 - r_{Lic}^2}} = 1{,}046 \text{ psi}$$

Using this external pressure, the inner shell membrane stress is

$$\sigma_i = \frac{p_c r_{avg}}{t} = 6{,}145 \text{ psi}$$

where r_{avg} is the minimum average inner shell radius, 5.875 inches, and t is the minimum wall thickness of 1 inch. From Table 2.3-1, the allowable primary membrane stress intensity (S_m) is 20,000 psi. The margin of safety is

$$MS = \frac{20{,}000}{6{,}145} - 1 = \underline{+ 2.25}$$

Therefore, the NCT cold condition is not of concern.

2.6.3 Reduced External Pressure

The effect of reduced external pressure of 3.5 psia, per 10 CFR §71.71(c)(3), is considered negligible for the SEC transportation cask compared to other design loadings. This conclusion is based on the NCT structural analyses presented in Section 2.6.1 demonstrating the structural integrity for a 50 psig internal design pressure. Based on the Maximum Normal Operating Pressure (MNOP) of 23.9 psig, the reduced external pressure conditions would cause a pressure of 35.1 psig. Therefore, the 50 psig internal design pressure analysis is conservatively bounding for the reduced external pressure case.

2.6.4 Increased External Pressure

The effect of an increased external pressure of 20 psia, per 10 CFR §7171(c)(4), is considered negligible for the SEC compared to other design loadings, based on the relatively high shell thickness-to-shell radius ratio for both inner and outer shells of the cask. Consistent with Regulatory Guide 7.8, this loading corresponds to an ambient temperature of -20 °F, no insolation, no decay heat, and minimum internal pressure. Since the cask is closed under ambient conditions, the internal pressure in the cask at a temperature of -20 °F is

$$p_i = p_{amb} \frac{(-20 + 460)}{(70 + 460)} = 12.2 \text{ psia}$$

where p_{amb} is 14.7 psia. The net differential pressure p_o is therefore 20 - 12.2 = 7.8 psi. The hoop stress, σ_θ, axial stress, σ_ϕ, and in-plane shear stress, $\sigma_{\phi\theta}$, are found from:

$$\sigma_\theta = \frac{p_o r}{t} \qquad \sigma_\phi = \frac{p_o r}{2t} \qquad \sigma_{\phi\theta} = \frac{p_o r}{4t}$$

where p_o is the applied differential pressure, r is the mean radius (5.875 inches for the inner shell and 17.25 inches for the outer shell), and t is the shell thickness (a minimum of one inch for both shells). These stresses are summarized in Table 2.6-4 for both inner and outer shells. In light of the small magnitude of all of these stress components, and of the relatively stiff proportions of the cask shells, buckling of the cask shells due to the increased external pressure condition is not of concern.

Table 2.6-4 - Shell Stress for 7.8 psi Differential Pressure

Inner Shell		Outer Shell	
Axial Stress, σ_ϕ	22.9 psi	Axial Stress, σ_ϕ	67.3 psi
Hoop Stress, σ_θ	45.8 psi	Hoop Stress, σ_θ	134.6 psi
Shear Stress, $\sigma_{\phi\theta}$	11.5 psi	Shear Stress, $\sigma_{\phi\theta}$	33.6 psi

2.6.5 Vibration

The effects of vibration normally incident to transport are shown to be insignificant. Draft ANSI N14.23 [15] identifies peak truck trailer vibration inputs. Table 2 of ANSI N14.23 shows peak vibration accelerations of a trailer bed as a function of package and tiedown system natural frequency. For the frequency range 0 to 5 Hz, and conservatively assuming a light package, Table 2 gives peak accelerations (99% level) of $2g$ in the vertical direction, and $0.1g$ in both the lateral and longitudinal directions. All other frequency ranges give significantly lower acceleration levels. Due to cask symmetry, the vertical load of $\pm 2g$ governs the $\pm 0.1g$ in the lateral and longitudinal directions.

Fatigue assessments consider the effects on a structural component over a range of loading between maximum and minimum load levels. These assessments require that stress concentration factors be applied to calculated stresses in order to account for stress increases in the region of any local structural discontinuities. Regulatory Guide 7.6 [2] states that, in the region of discontinuities, a stress concentration factor of four should be used where the factor is unknown. Therefore, a concentration factor of four is used in the assessment of fatigue stresses.

Design fatigue curves are taken from Figure I-9.2.1 and Table I-9.2.2 of the ASME B&PV Code [9], Section III, Appendix I for the Type 304 stainless steel cask material, from which the allowable amplitude, S_a, of the alternating stress component (1/2 of the alternating stress range) as a function of number of loading cycles may be obtained. Table I-9.2.2 extends the fatigue allowable data to the endurance limit, which is used in the fatigue assessment of transportation vibration. The allowable amplitude, S_a, from Table I-9.2.2 for Type 304 stainless steel cask material at 10^{11} cycles is 13,600 psi. This value is adjusted based on the ratio of room temperature elastic modulus of $28.3(10)^6$ psi, which is the basis for Table I-9.2.2, and the elastic modulus at NCT maximum temperature, as follows:

$$S_a = 13{,}600\left[\frac{25.7(10^6)}{28.3(10^6)}\right] = 12{,}351 \text{ psi}$$

where 25.7 (10^6) psi is the elastic modulus at the bounding temperature of all cask components of 520 °F from Table 2.3-1.

The SEC transportation cask is shipped vertically. The first fatigue assessment is performed for the plate which covers the lower lead cavity, and which is located on the lower end of the cask, as shown in Figure 2.6-4. This plate is a circular disk, welded on its perimeter to the lower

casting of the cask, and it supports the lower lead gamma shielding. The alternating stress in the plate weld is calculated using the weight of the lower lead shield and the self weight of the plate. Due to the thickness and rigidity of the lead and of the plate, the weld is loaded in essentially pure shear. The alternating stresses are conservatively assumed to completely reverse about zero, instead of alternating about a mean load of one half of the inertia load. The weight of the lead is bounded by 800 lb, and the weight of the lower plate is 91 lb, for a sum of 800 + 91 = 891 lb. A value of W = 900 lb is conservatively used. The shear area of the ½ inch groove weld is

$$A = \pi dt = 31.42 \text{ in}^2$$

where the plate diameter d = 20 inches and the width of the weld, t = 0.5 inches. The weld stress for one g is

$$\tau_1 = \frac{W}{A} = 28.6 \text{ psi}$$

For a vibration level of g = 2, and a stress concentration factor of SCF = 4, the stress is

$$\tau = \tau_1(g)(SCF) = 228.8 \text{ psi}$$

The margin of safety against transportation vibration fatigue is

$$MS = \frac{12{,}351}{228.8} - 1 = \underline{+53.0}$$

This margin of safety reflects conservative assumptions regarding the vibration magnitude and the stress concentration factor.

The second fatigue assessment is performed for the weld which attaches the lower, smaller diameter portion of the closure lid to the upper, larger diameter portion, as shown in Figure 2.6-5. The weld is loaded in tension by the weight of the lead gamma shielding in the lid. As in the first assessment, the load on the weld is conservatively assumed to be completely reversing about zero. The same vibration level and stress concentration factors are used. The area of weld supporting the load is calculated based on a full penetration weld, conservatively ignoring the added support of the drain port tube. The area is

$$A = \frac{\pi}{4}\left(10.25^2 - 9.25^2\right) = 15.3 \text{ in}^2$$

The combined weight of the lead, the lower steel cylinder, and the lower steel plate of the closure lid is conservatively bounded by W = 700 lb. The weld stress for one g is

$$\sigma_1 = \frac{W}{A} = 45.8 \text{ psi}$$

For a vibration level of g = 2, and a stress concentration factor of SCF = 4, the stress is

$$\sigma = \sigma_1(g)(SCF) = 366.4 \text{ psi}$$

The margin of safety is

$$MS = \frac{12{,}375}{366.4} - 1 = \underline{+ 32.8}$$

Therefore, fatigue of the SEC due to transportation vibration is not of concern.

2.6.6 Water Spray

The materials of construction used in the SEC are not affected by the water spray test identified in 10 CFR §71.71(c)(6).

2.6.7 Free Drop

Section 10 CFR §71.71(c)(7) includes a NCT free drop from a height of 3 ft for a package having a weight of 11,000 to 22,000 lb. Since the drop orientation must include the orientation for which maximum damage is expected, the governing drops of end, side, c.g. over corner, and side slapdown drops, discussed in greater detail in Section 2.7.1.1, are analyzed for the NCT free drop event. Impact forces and structural response for the SEC are calculated using the implicit finite element code LS-DYNA. The LS-DYNA model is described in Section 2.10.3. Resulting impacts for the NCT 3 ft drops are given in Table 2.7-1 and repeated in Table 2.6-5 below. A discussion of impact forces and deformations applicable to NCT free drops is given in Section 2.7.1.1.

Table 2.6-5 - NCT Free Drop Maximum Impacts

Orientation	Cold Impact①, g	Warm Impact①, g
End (vertical, 90°)	78	57
Side (horizontal, 0°)	43	30
C.G. over Corner (54.5°)	29	21
Slapdown, Primary (15°)	21	15
Slapdown, Secondary (0°)	24	17

Notes:

① Measured at the cask center of gravity.

The SEC stresses are analyzed for the NCT free drop using a finite element model which is loaded by a global, quasi-static acceleration field. The magnitude of the field is determined from the impact response of the cask during the 3 ft free drop events as summarized in Table 2.6-5. The cask stress analysis for NCT is identical with the analysis for HAC, with the following exceptions:

- Thermal stresses are included in the NCT stress analyses
- The applied quasi-static acceleration fields are lower, corresponding to the lower drop height

- Allowable stresses are lower, in accordance with Regulatory Guide 7.6 recommendations.

As discussed in Section 2.7.1.4, cask stresses are governed by those resulting from the end and side drop orientations. The stress analyses for NCT for the end drop and the side drop are given in Sections 2.6.7.1 and 2.6.7.2.

2.6.7.1 NCT End Drop

As shown in Table 2.6-5, the maximum impact level during the NCT end drop is 78g. For the end drop stress analysis of the SEC, therefore, a global acceleration field of 80g is conservatively applied to the ANSYS® [17] finite element model. The construction of the end drop stress analysis model is described in Section 2.10.2.1. The temperatures shown in Figure 2.6-1 are applied to the model as described below. Both bottom-down and top-down orientations are considered. Five analyses are performed:

- Cask body stress
- Closure lid bolt stress
- Closure lid weld stress
- Lower closure plate stress
- End drop buckling evaluation

Cask body stress. In the bottom-down orientation, the cask is considered fixed at its lowest extremity, and since the lower impact limiter is supporting the cask, the mass of the lower impact limiter need not be considered. The mass of the closure lid is conservatively considered to be concentrated at the inner diameter of the cask-to-lid interface, thus maximizing its contribution to the overall response, and the mass of the upper impact limiter is concentrated at the upper extremity of the cask. The mass of the lower end lead shield is applied as a pressure to the lower one inch thick plate, and the mass of the annular lead shield is applied as a hydrostatic pressure load as described in Section 2.10.2.1. The resulting stresses, including thermal stress, are shown in Figure 2.6-6. The maximum stress is located on the lower face of the upper casting, near the intersection with the inner shell (i.e., in the upper inside corner of the annular lead cavity), and represents a maximum membrane plus bending plus secondary stress ($P_L + P_b + Q$) of 31,600 psi. Since there is no stress at this point in the room temperature, static condition, this represents the range of primary plus secondary stress intensity, which, according to Table 2.1-1, has a limit of $3.0S_m$. From Table 2.6-1, for Type 304 stainless steel at a bounding temperature of 410 °F for the end casting, this is equal to 55,740 psi. The margin of safety on the range of primary plus secondary stress in the bottom-down end drop case is therefore

$$(P_L + P_b + Q): \quad MS = \frac{55{,}740}{31{,}600} - 1 = \underline{+0.76}$$

The stresses which obtain in the absence of thermal stress are shown in Figure 2.6-7. The maximum stress occurs in the lower part of the outer shell. Stresses are linearized along path 1 as shown in detail in Figure 2.6-8. The maximum primary membrane stress (P_m) is 14,170 psi. Again, a bounding temperature of the inner shell of 410 °F for the outer shell is used. From Table 2.1-1, the allowable stress under NCT is S_m, which for Type 304 stainless steel at a

temperature of 410 °F, from Table 2.6-1, is 18,580 psi. The margin of safety on primary membrane stress in the bottom-down end drop case is therefore

$$(P_m):\ MS = \frac{18{,}580}{14{,}170} - 1 = \underline{+0.31}$$

The maximum membrane plus bending stress ($P_L + P_b$) is 17,830 psi[3]. From Table 2.1-1, the allowable stress under NCT is $1.5S_m$, which for Type 304 stainless steel at a temperature of 410 °F, from Table 2.6-1, is 27,870 psi. The margin of safety on membrane plus bending stress in the bottom-down end drop case is therefore

$$(P_L + P_b):\ MS = \frac{27{,}870}{17{,}830} - 1 = \underline{+0.56}$$

In the top-down orientation, the cask is considered fixed at its upper extremity, and since the upper impact limiter is supporting the cask, the mass of the upper impact limiter need not be considered. The mass of the closure lid, supported by the lid bolts in this orientation, is applied at a diameter equivalent to the lid bolt circle. The mass of the lower impact limiter is considered concentrated at the lowest cask extremity. The mass of the lower end lead shield is conservatively considered to be concentrated at the inside edge of the inner shell, thus maximizing its contribution to overall response, and the mass of the annular lead shield is applied as a hydrostatic pressure load as described in Section 2.10.2.1. The resulting stresses, including thermal stress, are shown in Figure 2.6-9. The maximum stress is located near the upper end of the inner shell, and represents a maximum membrane plus bending plus secondary stress ($P_L + P_b + Q$) of 36,329 psi. Since there is no stress at this point in the room temperature, static condition, this represents the range of primary plus secondary stress intensity, which, according to Table 2.1-1, has a limit of $3.0S_m$. From Table 2.6-1, for Type 304 stainless steel at a bounding temperature of 510 °F for the inner shell, this is equal to 52,170 psi. The margin of safety on the range of primary plus secondary stress in the top-down end drop case is therefore

$$(P_L + P_b + Q):\ MS = \frac{52{,}170}{36{,}329} - 1 = \underline{+0.44}$$

The stresses which occur in the absence of thermal stress are shown in Figure 2.6-10. Stresses are linearized along path 1, and shown in detail in Figure 2.6-11. The maximum primary membrane stress (P_m) is 14,260 psi. A bounding temperature of the outer shell of 410 °F is used. From Table 2.1-1, the allowable stress under NCT is S_m, which for Type 304 stainless steel at a temperature of 410 °F, from Table 2.6-1, is 18,580 psi. The margin of safety on primary membrane stress in the top-down end drop case is therefore

$$(P_m):\ MS = \frac{18{,}580}{14{,}260} - 1 = \underline{+0.30}$$

The maximum membrane plus bending stress ($P_L + P_b$) is 18,120 psi. From Table 2.1-1, the allowable stress under NCT is $1.5S_m$, which for Type 304 stainless steel at a temperature of

[3] Since membrane and membrane plus bending stresses are linearized, the values given in this section may differ slightly from the maximum values shown in the figures.

410 °F, from Table 2.6-1, is 27,870 psi. The margin of safety on membrane plus bending stress in the top-down end drop case is therefore

$$(P_L + P_b): \quad MS = \frac{27,870}{18,120} - 1 = \underline{+0.54}$$

Therefore, the allowable stresses as established in Section 2.1 have been met for the cask structure in the end drop.

Closure lid bolt stress. The lid bolt stresses are determined in Section 2.10.4 per NUREG/CR-6007. The maximum bolt stress occurs during the top-down drop, in the warm case. The resulting tensile stress, which is a result of preload, residual torsion, thermal loading, and free drop loading of 80g, is 52,129 psi. The corresponding maximum combined stress ratio, which must be less than unity, is 0.74. The analysis of the closure lid attachment bolts in the top-down drop is discussed in Section 2.10.4.

Closure lid weld stress. In a bottom-down end drop, the weld attaching the lower, smaller diameter portion of the closure lid to the upper, larger diameter portion will experience a stress. This weld was analyzed in connection with transportation vibration in Section 2.6.5, where the weld stress for one g was found to be $\sigma_1 = 45.8$ psi. The stress in the weld is therefore

$$\sigma = \sigma_1(80) = 3,664 \text{ psi}$$

This stress is classified as a primary membrane stress, and the allowable stress is S_m, found above to be equal to 17,390 psi, where a temperature of 410 °F is conservatively assumed for this portion of the closure lid. The margin of safety is

$$MS = \frac{18,580}{3,664} - 1 = \underline{+4.07}$$

Lower closure plate stress. Also in a bottom-down end drop, the lower plate which covers the lower lead cavity is subject to stress. The weld attaching this plate to the cask governs, and was analyzed in Section 2.6.5, where the weld stress for one g was found to be $\tau_1 = 28.6$ psi. The impact load is again bounded by 80g. The stress in the weld is

$$\tau = \tau_1(80) = 2,288 \text{ psi}$$

This stress is classified as a primary membrane stress, and the allowable stress is S_m, found above to be equal to 17,390 psi, where a temperature of 510 °F is conservatively assumed for the lower plate weld. The margin of safety is (with an added factor of 0.6 to account for pure shear)

$$MS = \frac{18,580(0.6)}{2,288} - 1 = \underline{+3.87}$$

NCT end drop buckling evaluation. The SEC is evaluated for buckling due to the NCT end drop inertia load using ASME Code Case N-284-1. Axial stresses are developed due to the weight of the material loading the shells in the NCT end drop. To simplify the analysis, the outer shell is considered to act alone, conservatively supporting the entire buckling load, without assistance from the inner shell. The supported weight is the sum of the upper impact limiter, the upper casting, the closure lid, the inner and outer shells, and the thermal shields. The annular

lead shield supports itself in simple compression on its lower face. The lower casting, the lower end lead, and the lower impact limiter are supported by the ground. Conservatively, the thermal axial stress, which is tensile, is not considered to reduce the compressive stress arising from the end drop. In the buckling evaluation, there is no difference between top-down and bottom-down orientations. Consistent with Regulatory Guide 7.6 philosophy, a factor of safety of 2.0, corresponding to ASME Code, Level A service conditions is applied, as specified in Code Case N-284-1.

The weight of the components which contribute to the end drop buckling load are listed in Table 2.6-8. Each weight is conservatively upper-bounded. The total weight of these components is W = 6,375 lb.

Table 2.6-8 - End Drop Buckling Weight

Component Name	Weight, lb
Upper Impact Limiter	2,000
Upper Casting & Inner Shell	1,725
Closure Lid	900
Outer Shell	850
Thermal Shields	900
Total	6,375

The loading of the outer shell is based on this weight, as well as on the end drop impact level of the upper casting, and the area of the outer shell, which is

$$A = \pi \left(r_o^2 - r_i^2 \right) = 108.4 \text{ in}^2$$

where the outer radius of the outer shell, r_o = 17.75 inches, and the inner radius, r_i = 16.75 inches. The axial stress is therefore

$$\sigma_\phi = \frac{W}{A} g = 4{,}705 \text{ psi}$$

where the NCT end drop impact level is again bounded by g = 80. Maximum impact response from the cold, -20 °F case is conservatively combined with warm allowables corresponding to maximum NCT temperature, which is bounded by 410 °F for the outer shell.

Buckling analysis parameters are given in Table 2.6-9, and results in Table 2.6-10. As shown, all interaction check parameters are less than 1.0, as required. Therefore, the SEC transportation cask does not experience buckling in the NCT end drop.

Table 2.6-9 - Cask Buckling Geometry Parameters

Geometry, Temperature, and Material Input	
	Outer Shell
Outside Diameter, inches	35.5
Inside Diameter, inches	33.5
Length, inches	26.0
Geometry Output (nomenclature consistent with ASME Code Case N-284)	
R =	17.25
t =	1.00
R/t =	17.25
ℓ_ϕ =	26.0
ℓ_θ =	108.38
M_ϕ =	6.26
M_θ =	26.10
M =	6.26

Table 2.6-10 - Cask Buckling Summary for NCT, End Drop Impact

Condition	Outer Shell	Remarks
Capacity Reduction Factors (-1511)		
$\alpha_{\phi L}$ =	0.2748	
$\alpha_{\theta L}$ =	0.8000	
$\alpha_{\phi\theta L}$ =	0.8000	
Plasticity Reduction Factors (-1610)		
$\eta_{\phi L}$ =	0.0811	
$\eta_{\theta L}$ =	0.0523	
$\eta_{\phi\theta L}$ =	0.0837	
Theoretical Buckling Values (-1712.1.1)		
C_{ϕ} =	0.6050	
$\sigma_{\phi eL}$ =	926,965 psi	
$C_{\theta r}$ =	0.1807	
$\sigma_{\theta eL} = \sigma_{reL}$ =	276,932 psi	
$C_{\theta h}$ =	0.1636	
$\sigma_{\theta eL} = \sigma_{heL}$ =	250,637 psi	
$C_{\phi\theta}$ =	0.3222	
$\sigma_{\phi\theta eL}$ =	493,697 psi	
Elastic Interaction Equations (-1713.1.1)		
σ_{xa} =	127,370 psi	
σ_{ha} =	100,255 psi	
σ_{ra} =	110,773 psi	
$\sigma_{\tau a}$ =	197,479 psi	
Axial + Hoop ⇨ Check (a):	*N/A*	
Axial + Hoop ⇨ Check (b):	*N/A*	
Axial + Shear ⇨ Check (c):	*0.0369*	<1 ∴ OK
Hoop + Shear ⇨ Check (d):	*0.0000*	<1 ∴ OK
Axial + Hoop + Shear ⇨ Check (e,a):	*N/A*	
Axial + Hoop + Shear ⇨ Check (e,b):	*N/A*	
Inelastic Interaction Equations (-1713.2.1)		
σ_{xc} =	10,330 psi	
σ_{rc} =	5,794 psi	
$\sigma_{\tau c}$ =	16,528 psi	
Axial + Hoop ⇨ Check (a):	*0.4555*	<1 ∴ OK
Axial + Shear ⇨ Check (b):	*0.4555*	<1 ∴ OK
Hoop + Shear ⇨ Check (c):	*0.0000*	<1 ∴ OK

2.6.7.2 NCT Side Drop

As shown in Table 2.6-5, the maximum impact level during the NCT side drop is 43g. For the side drop stress analysis of the SEC, therefore, a global acceleration field of 50g is conservatively applied to the ANSYS® finite element model. The temperatures shown in Figure 2.6-1 are applied to the model as described below. The construction of the side drop stress analysis model is described in Section 2.10.2.2. Two analyses are performed:

- Cask body stress
- Closure lid bolt stress in the side-slapdown free drop event

Cask body stress. The cask is modeled in three dimensions and is half-symmetry, the plane of symmetry being the plane of the side drop. The load applied by the impact limiters is modeled as a pressure extending over the length of the cask-to-limiter interface, and extends circumferentially 30° in half-symmetry. The lower end lead and closure lid inertia loads are likewise applied to the respective interior portions of the model as pressures over 30°. The weight of the annular lead is distributed to the inner and outer shells as described in Section 2.10.2.2. The resulting stresses are shown in Figure 2.6-12. The maximum stress is located on the upper face of the lower casting near the lower end of the inner shell (i.e., in the lower inside corner of the annular lead cavity) and represents a maximum membrane plus bending plus secondary stress ($P_L + P_b + Q$) of 36,975 psi. Since there is no stress at this point for the room temperature, static condition, this represents the range of primary plus secondary stress intensity, which, according to Table 2.1-1, has a limit of $3.0S_m$. From Table 2.6-1, for Type 304 stainless steel at a bounding temperature of 410 °F, this is equal to 55,740 psi. The margin of safety on the range of primary plus secondary stress in the bottom-down end drop case is therefore

$$(P_L + P_b + Q): \quad MS = \frac{55{,}740}{36{,}975} - 1 = \underline{+0.51}$$

The stresses which occur in the absence of thermal stress are shown in Figure 2.6-13. Stresses are linearized along paths 1 and 2, shown in detail in Figure 2.6-14. The maximum primary membrane stress (P_m) occurs along path 2, and equals 5,977 psi. A bounding temperature of the outer shell of 410 °F is used. From Table 2.1-1, the allowable stress under NCT is S_m, which for Type 304 stainless steel at a temperature of 410 °F, from Table 2.6-1, is 18,580 psi. The margin of safety on primary membrane stress in the bottom-down end drop case is therefore

$$(P_m): \quad MS = \frac{18{,}580}{5{,}977} - 1 = \underline{+2.11}$$

The maximum membrane plus bending stress ($P_L + P_b$) occurs along path 1 and equals 9,549 psi. From Table 2.1-1, the allowable stress under NCT is $1.5S_m$, which for Type 304 stainless steel at a temperature of the end casting of 410 °F, from Table 2.6-1, is 27,870 psi. The margin of safety on membrane plus bending stress in the bottom-down end drop case is therefore

$$(P_L + P_b): \quad MS = \frac{27{,}870}{9{,}549} - 1 = \underline{+1.92}$$

Therefore, the allowable stresses as established in Section 2.1 are met for the cask in the side drop.

Lateral forces on the closure lid in the slapdown free drop event. In Section 2.7.1.4, it is determined that the lateral impact on the closure lid center of gravity is 1.962 times the magnitude of impact at the cask c.g. for the case of the slapdown free drop. From Table 2.6-5, the impact at the cask c.g. during the secondary impact of the slapdown events are bounding, equal to 24 g (cold) and 17g (warm). The maximum lateral impact accelerations applied to the closure lid c.g. in the NCT slapdown events are therefore

$$G = g_{c.g,cold.}(1.962) = 49g$$

$$G = g_{c.g,warm.}(1.962) = 39g$$

where $g_{c.g.,\,cold} = 25g$ and $g_{c.g.,\,warm} = 20g$, conservatively rounded up from the values given for the secondary impact in the slapdown events in Table 2.6-5. When these values are applied to the lid in the closure bolt analysis described in Section 2.10.4, the resulting combined stresses, which are a result of preload, residual torsion, thermal loading, are bounded by the warm case having a stress of 61,558 psi. The combined stress ratio, which must be less than unity, is 0.79. Therefore, closure bolts are adequate for the worst case loading in the slapdown event.

2.6.8 Corner Drop

The SEC is not required to be evaluated for the corner drop condition on the basis that 10 CFR §71.71(c)(8) applies only to rectangular fiberboard or wood packages weighing less than 110 lb or to cylindrical fiberboard or wood packages weighing less than 220 lb. The SEC weighs much more than these limits and therefore does not need to be evaluated for the NCT corner drop.

2.6.9 Compression

The SEC is not required to be evaluated for the compression condition on the basis that 10 CFR §71.71(c)(9) applies only to packages weighing less than 11,000 lb. The SEC weighs much more than this and therefore does not need to be evaluated for compression.

2.6.10 Penetration

The impact of a 1.25 inch diameter, hemispherically ended, 13 lb steel bar, per 10 CFR §71.71(c)(10), dropped vertically from a height of 40 inches, has no significant effect on the SEC transportation cask. Slight denting of the thermal shield on the outside of the cask can occur, but the bar cannot penetrate or rip into the shield, and cannot harm the impact limiters. Further, there are no protuberances which could be affected by this drop. Therefore, this test has no significant effect on the package.

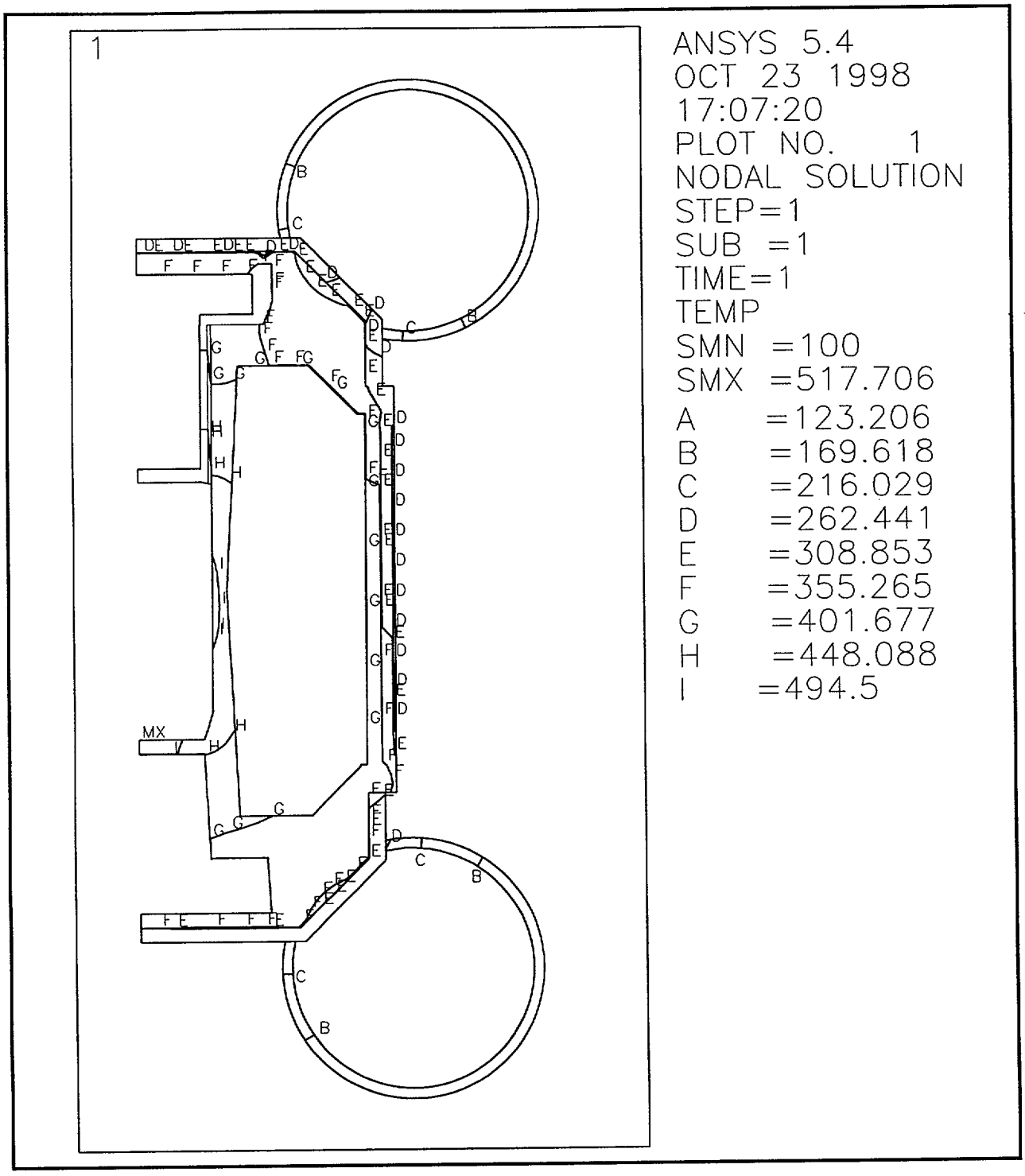

Figure 2.6-1 - NCT Maximum Cask Temperatures

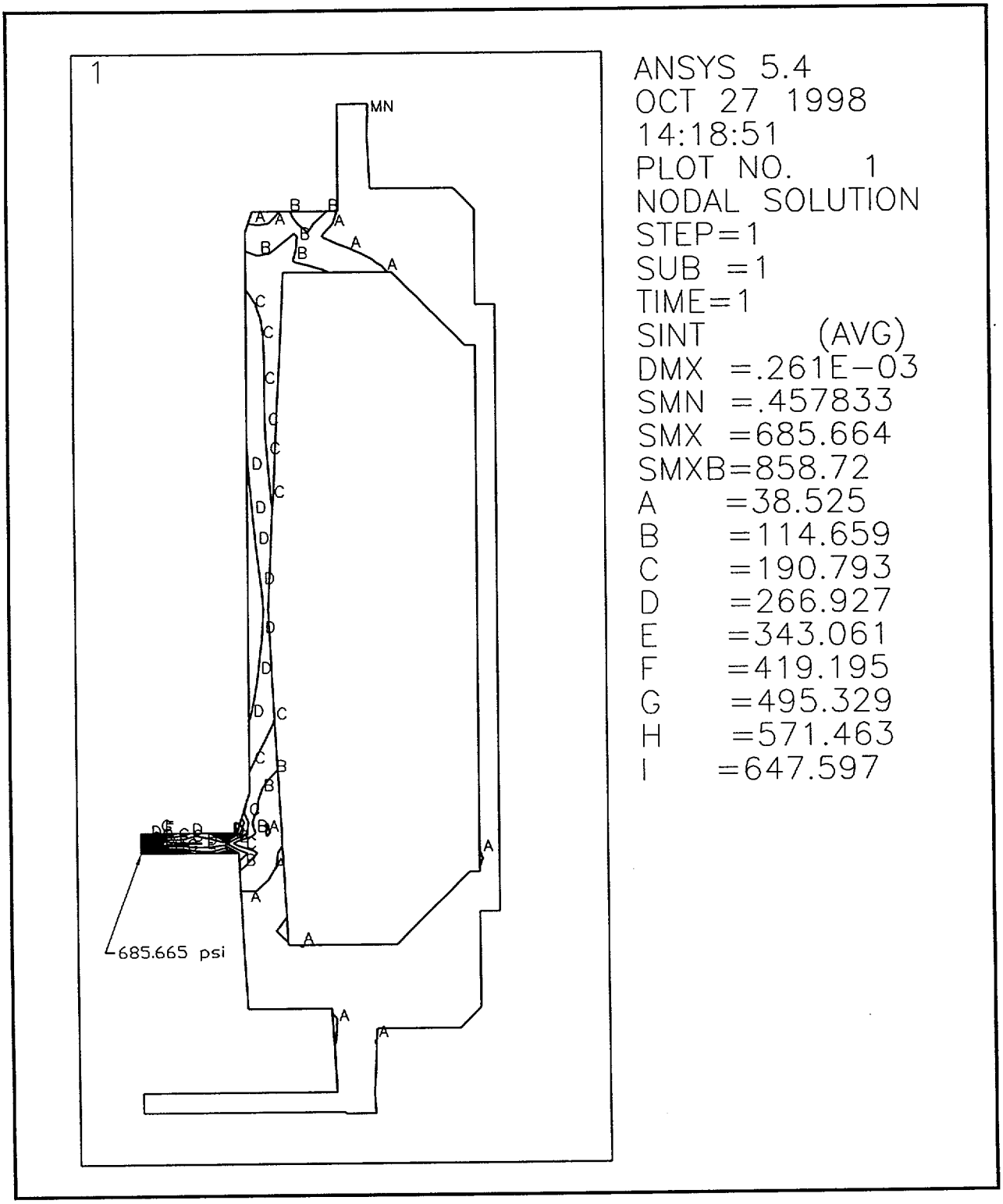

Figure 2.6-2 - NCT Internal Pressure Only Cask Stress Contours

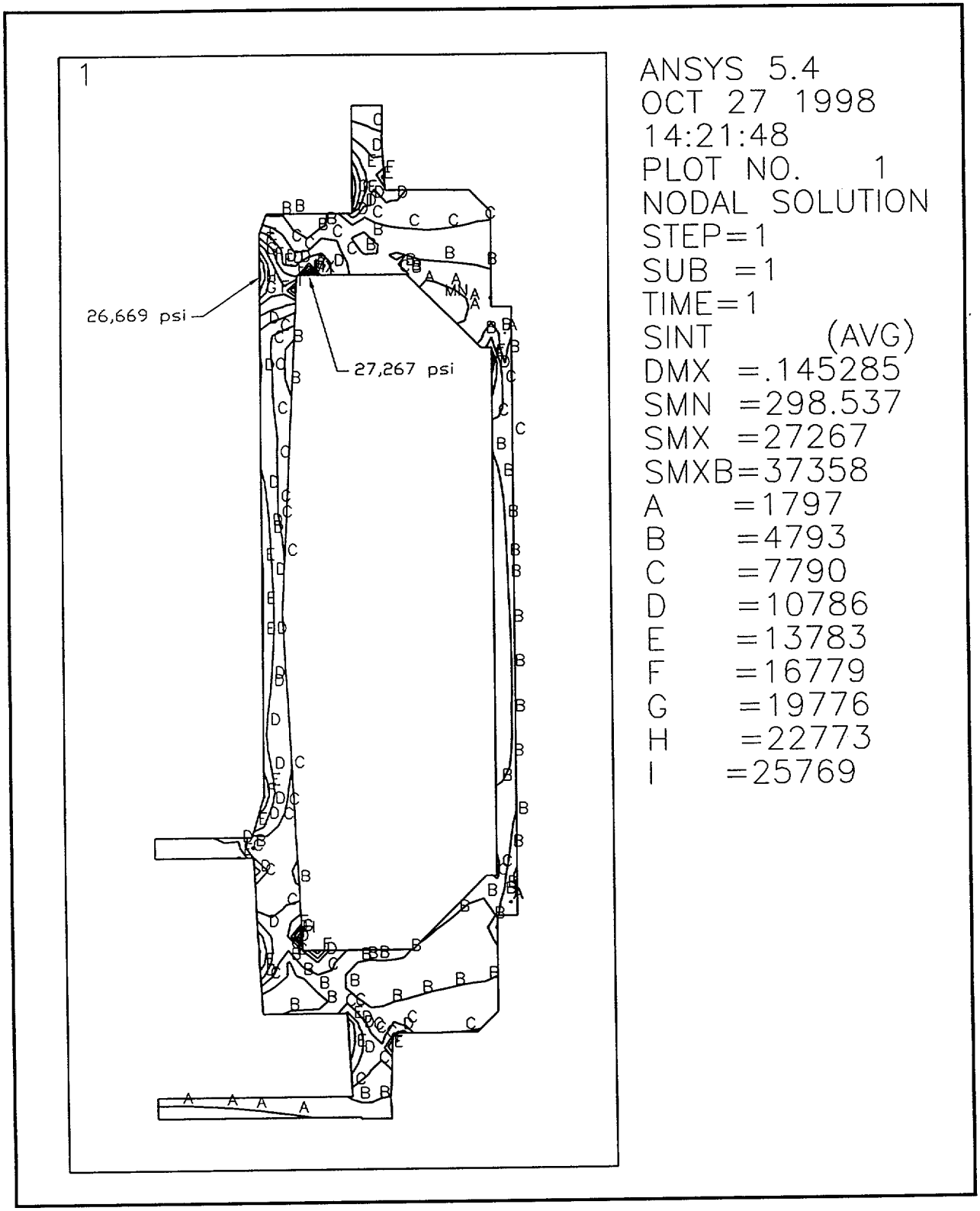

Figure 2.6-3 - NCT Internal Pressure plus Thermal Stress Contours

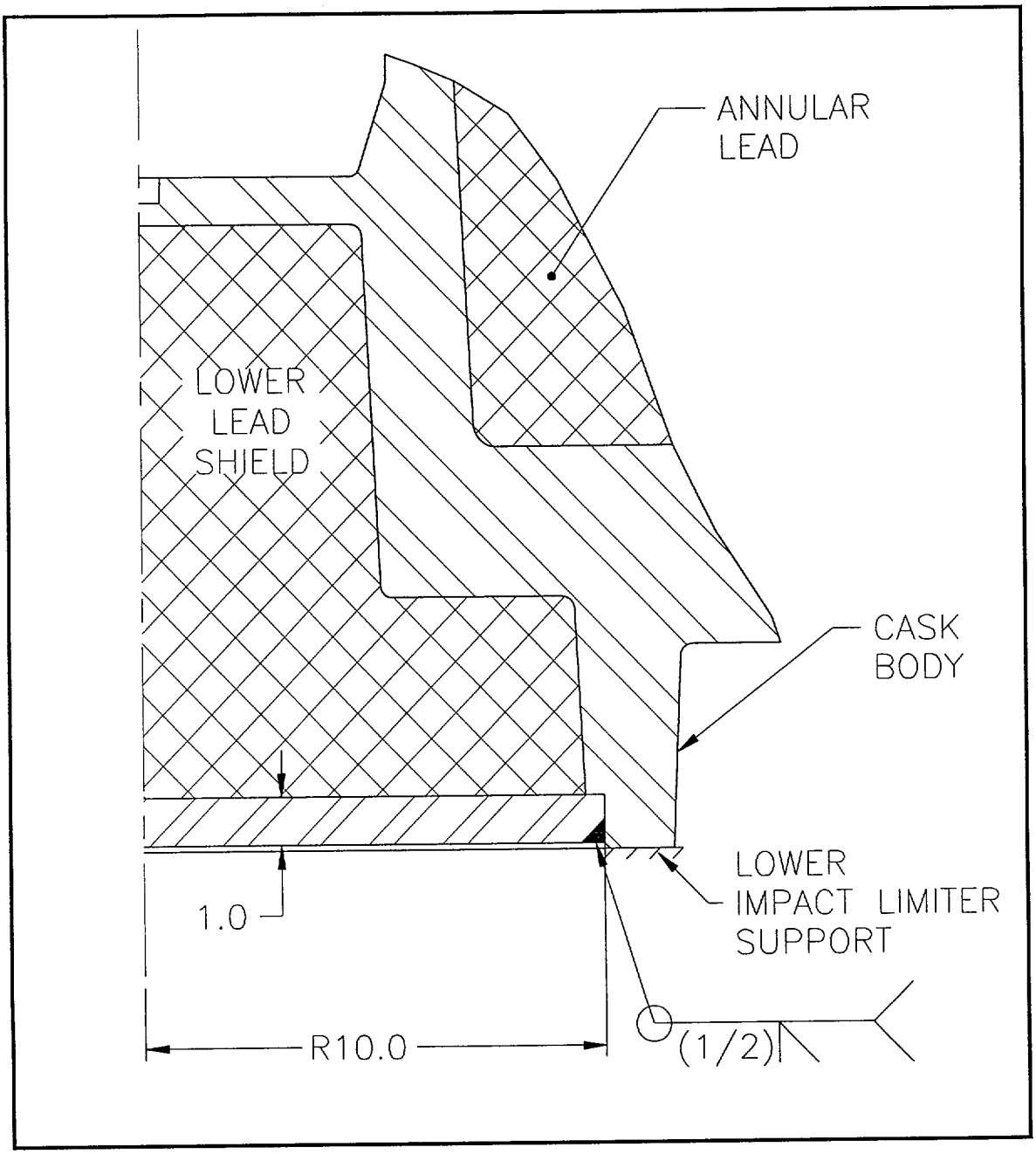

Figure 2.6-4 - Detail of Attachment of Lower Cover Plate

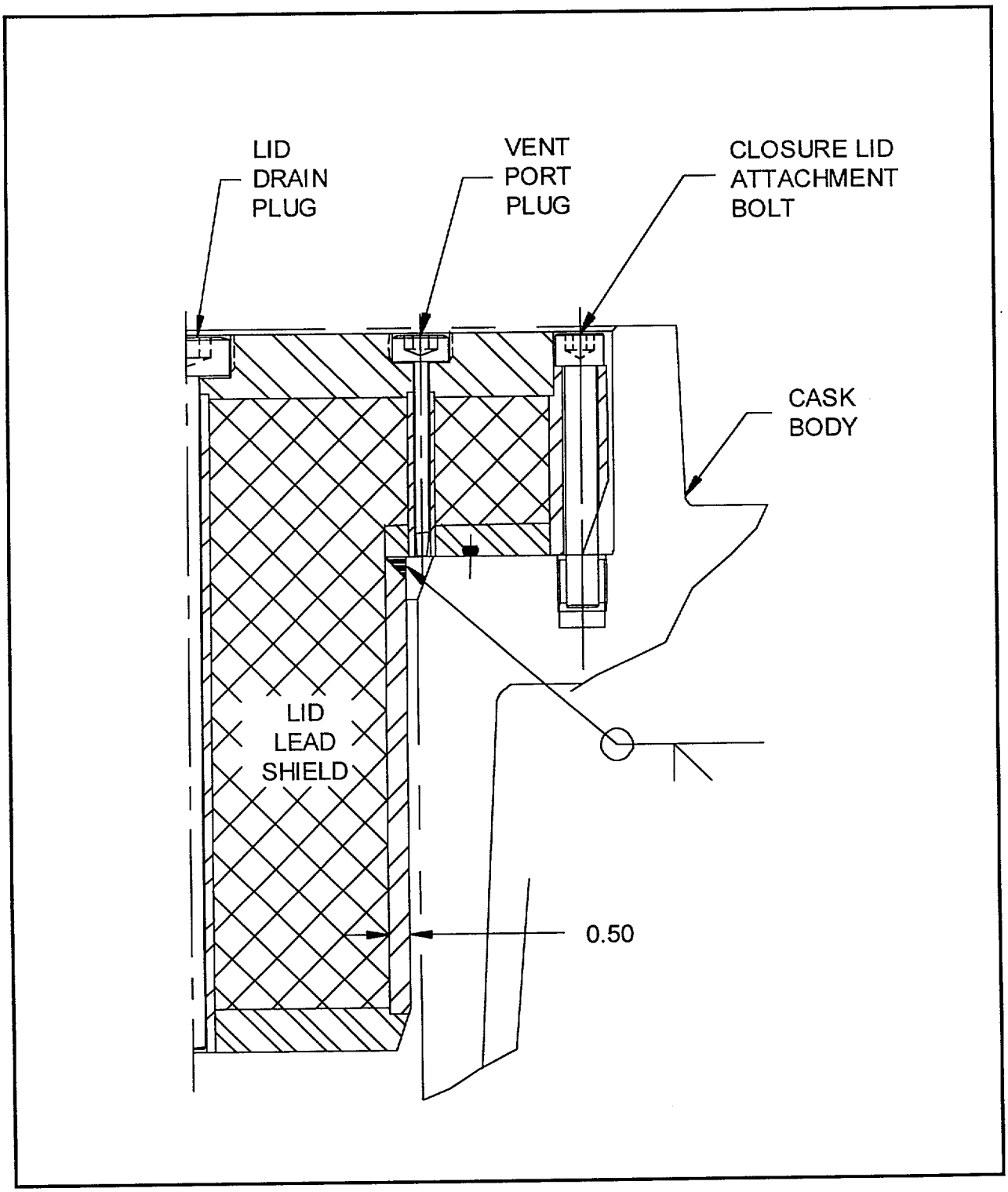

Figure 2.6-5 - Detail of Closure Lid Construction

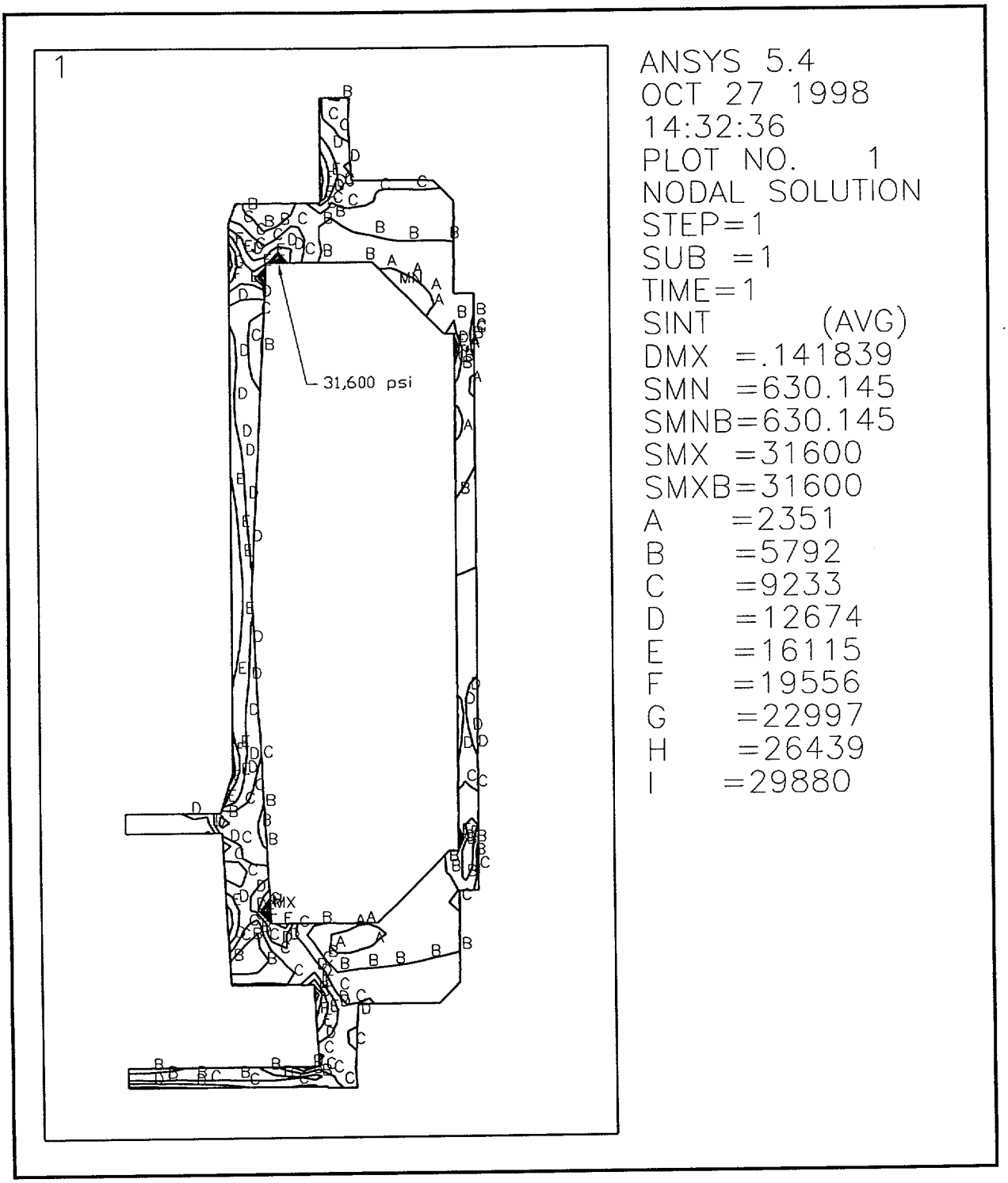

Figure 2.6-6 - NCT Bottom Down End Drop Stress Contours, Including Thermal Stress

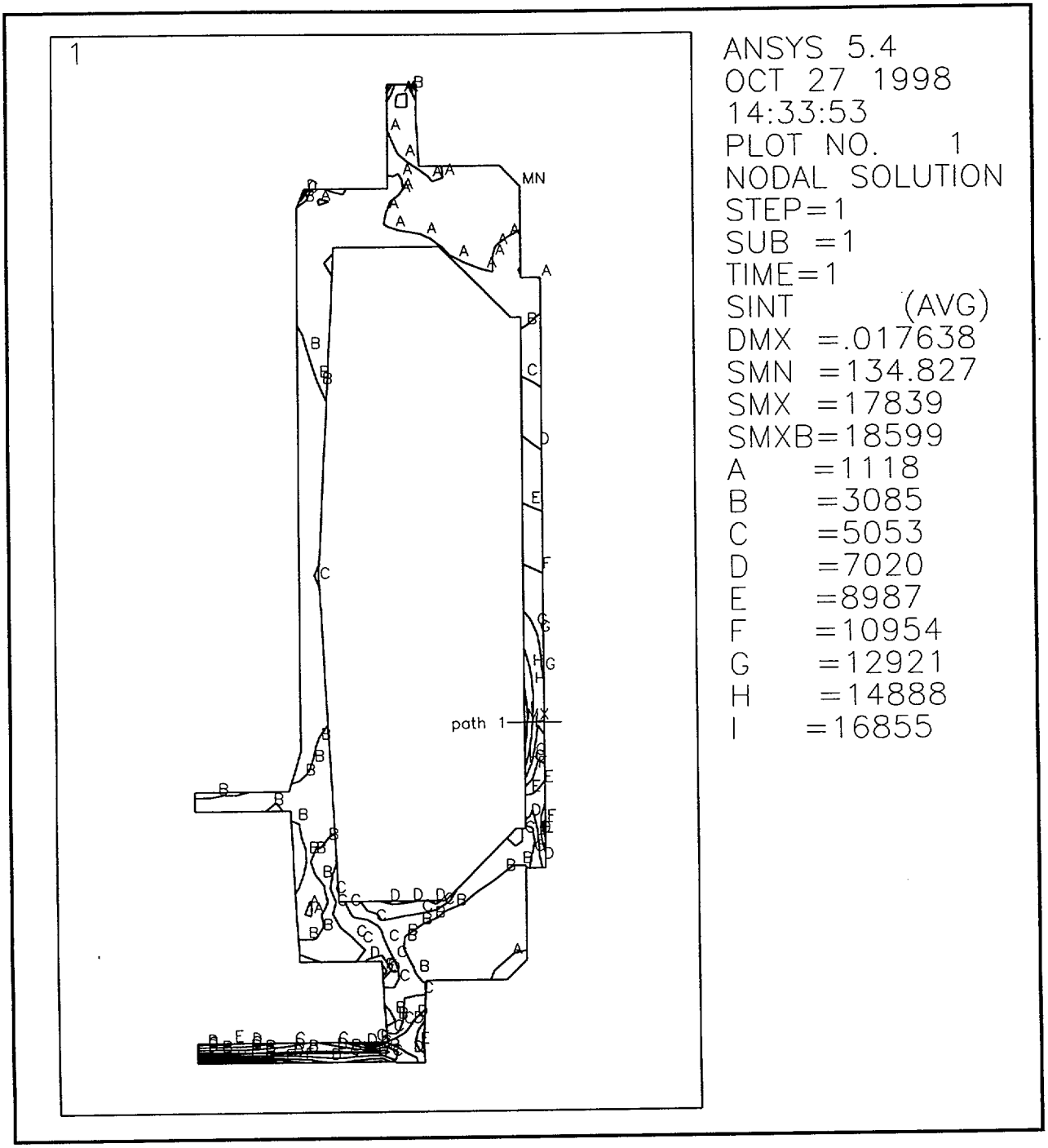

Figure 2.6-7 - NCT Bottom Down End Drop Stress Contours, Without Thermal Stress

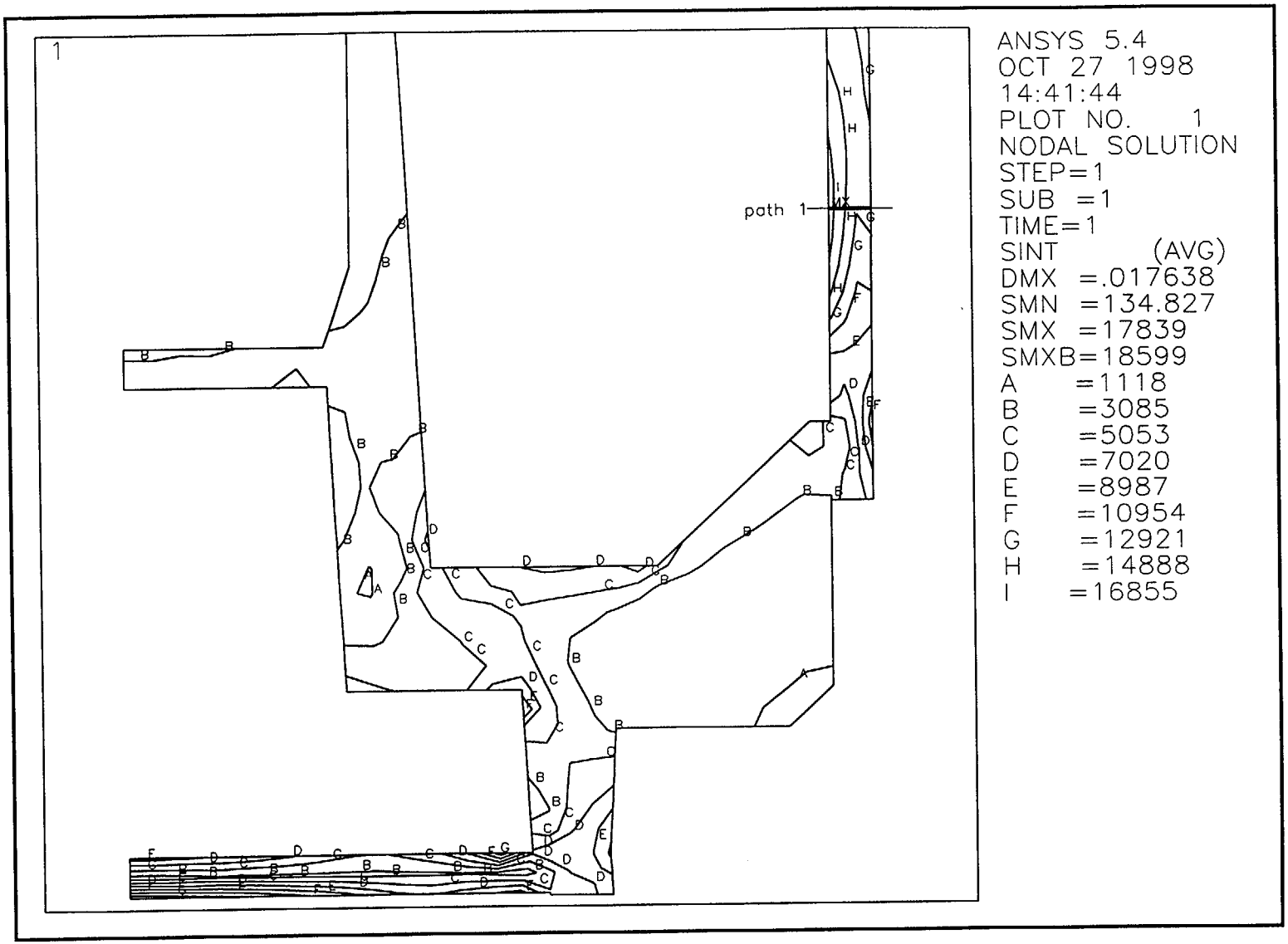

Figure 2.6-8 - NCT Bottom Down End Drop Stress Contours, Without Thermal Stress, Detail of Path 1

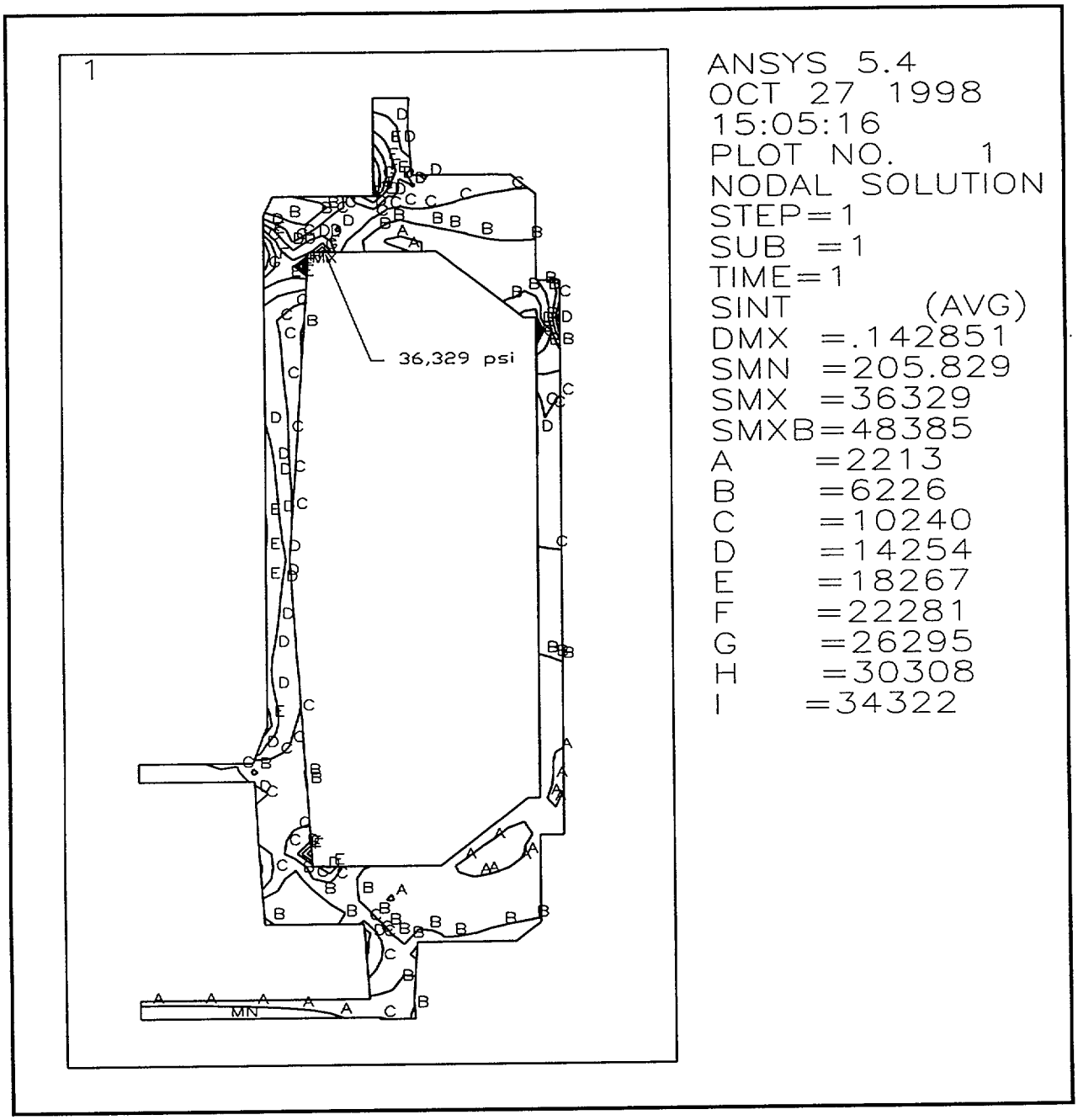

Figure 2.6-9 - NCT Top Down End Drop Stress Contours, Including Thermal Stress

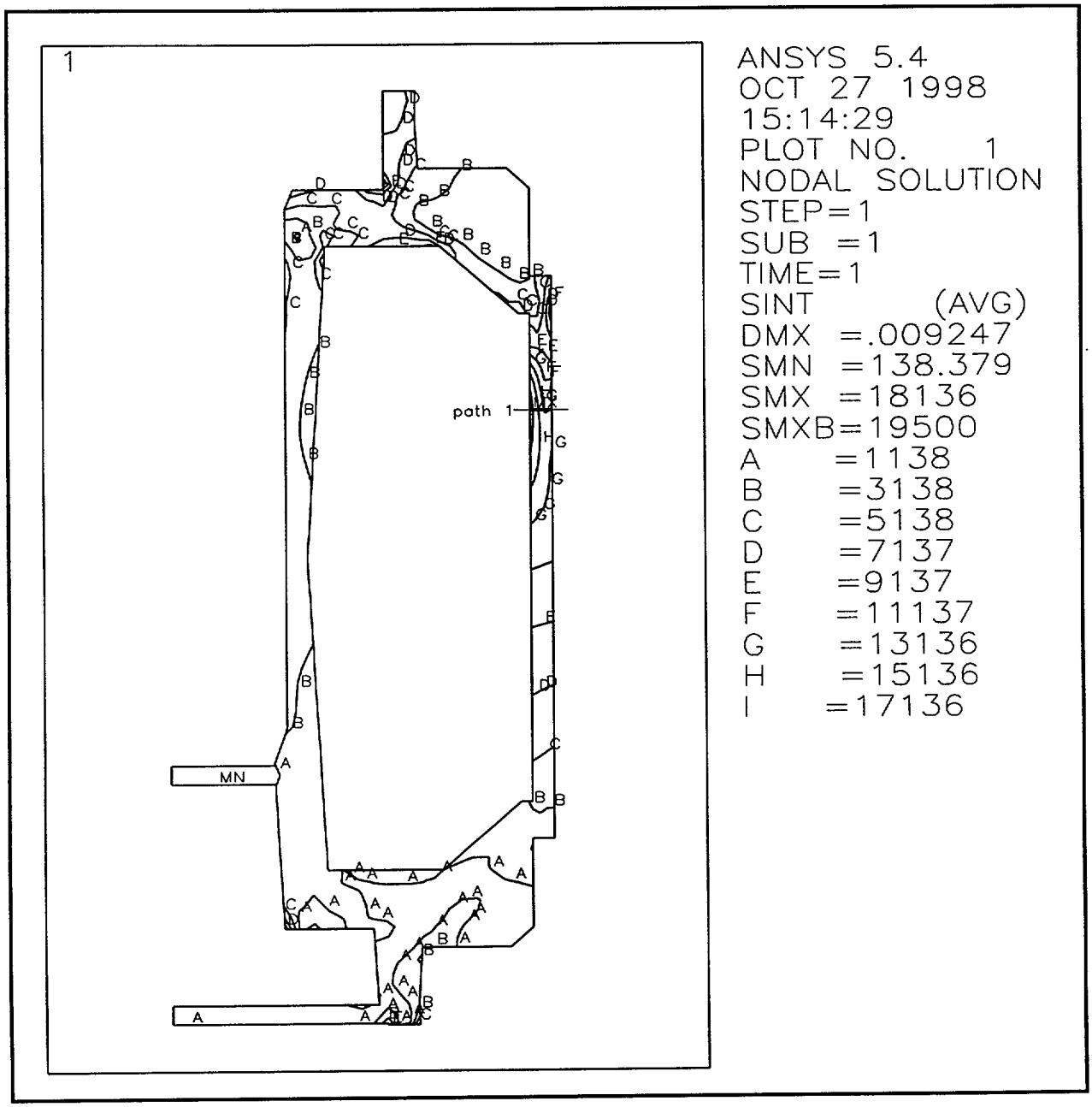

Figure 2.6-10 - NCT Top Down End Drop Stress Contours, Without Thermal Stress

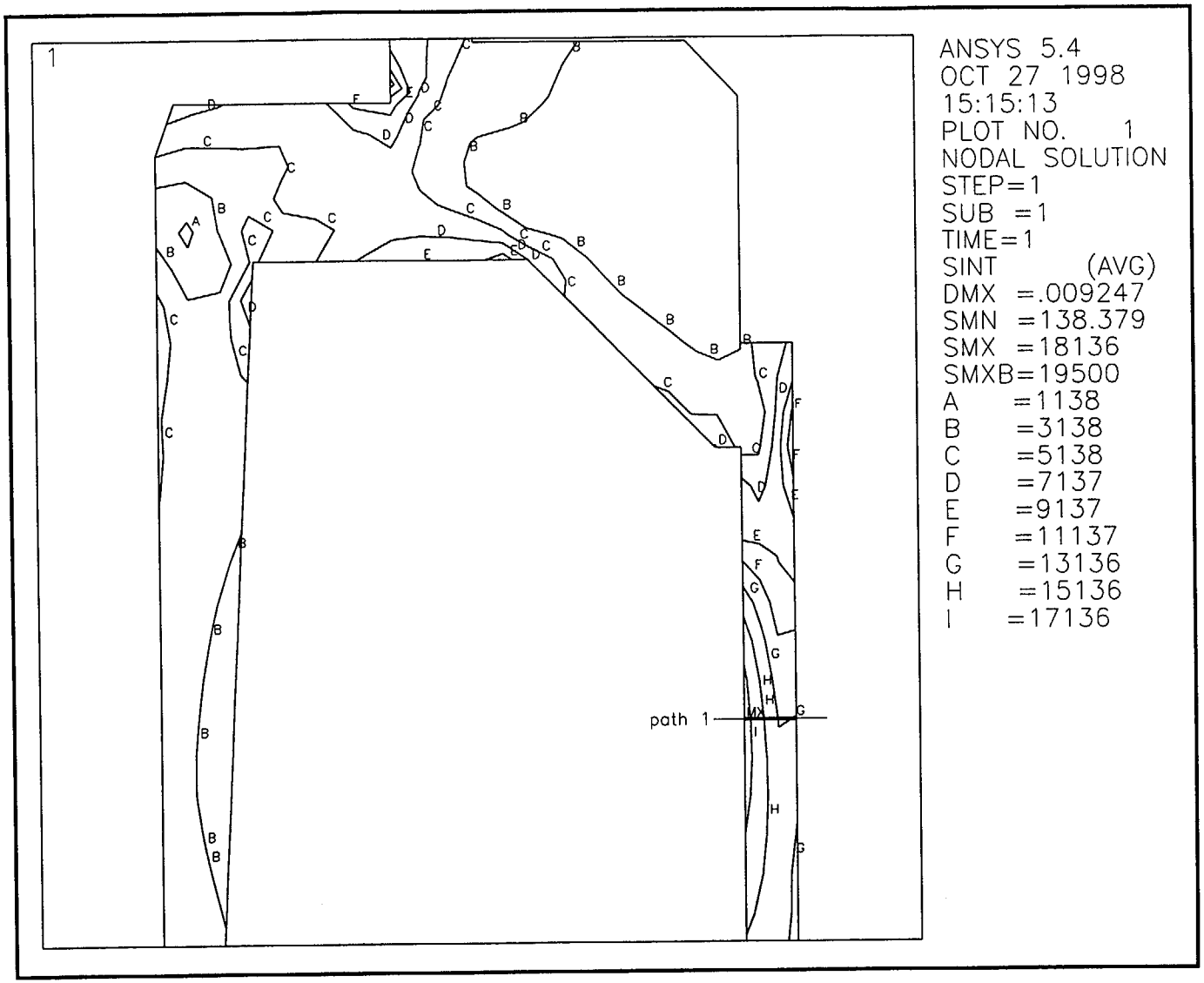

Figure 2.6-11 - NCT Top Down End Drop Stress Contours, Without Thermal Stress, Detail of Path 1

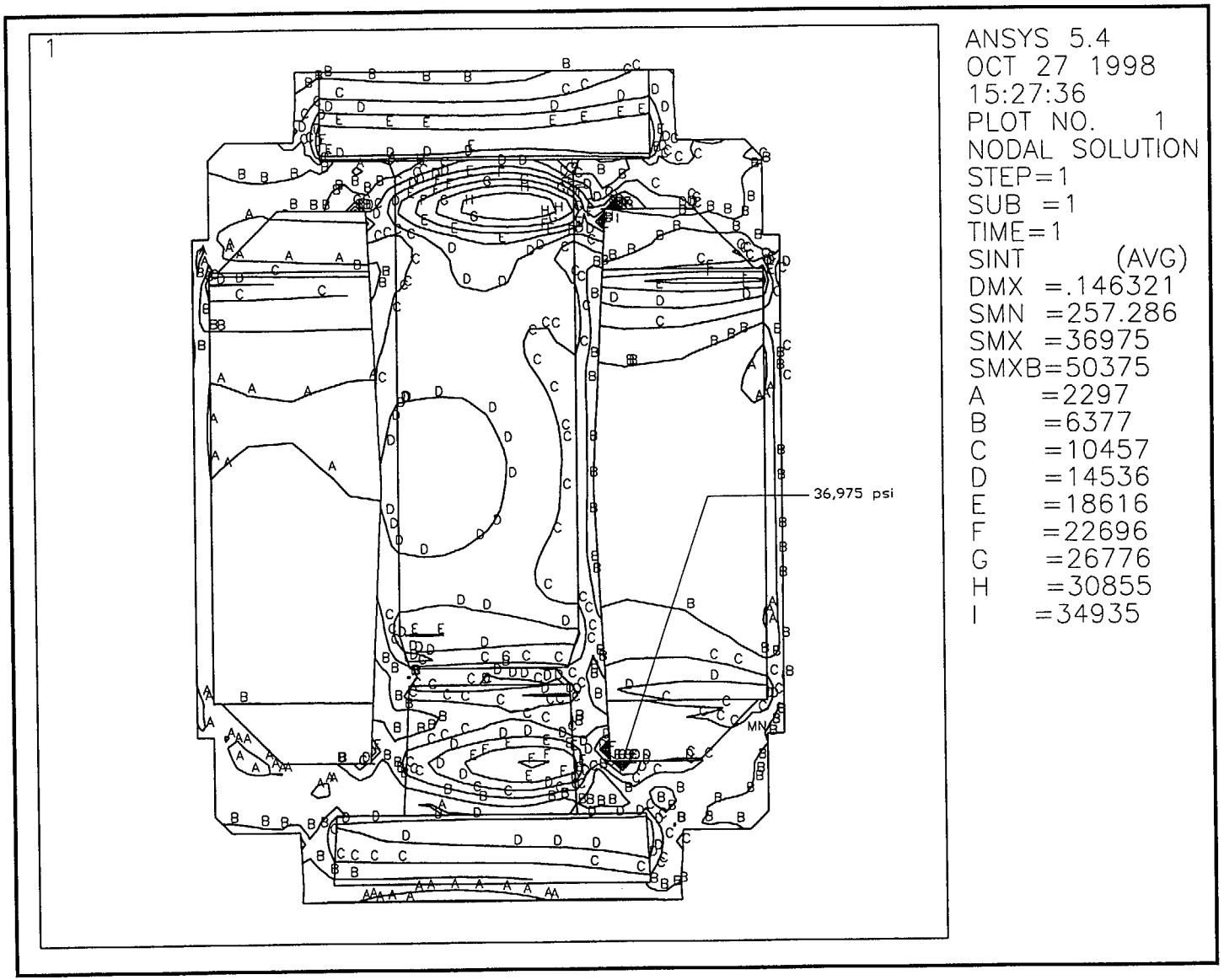

Figure 2.6-12 - NCT Side Drop Stress Contours, Including Thermal Stress

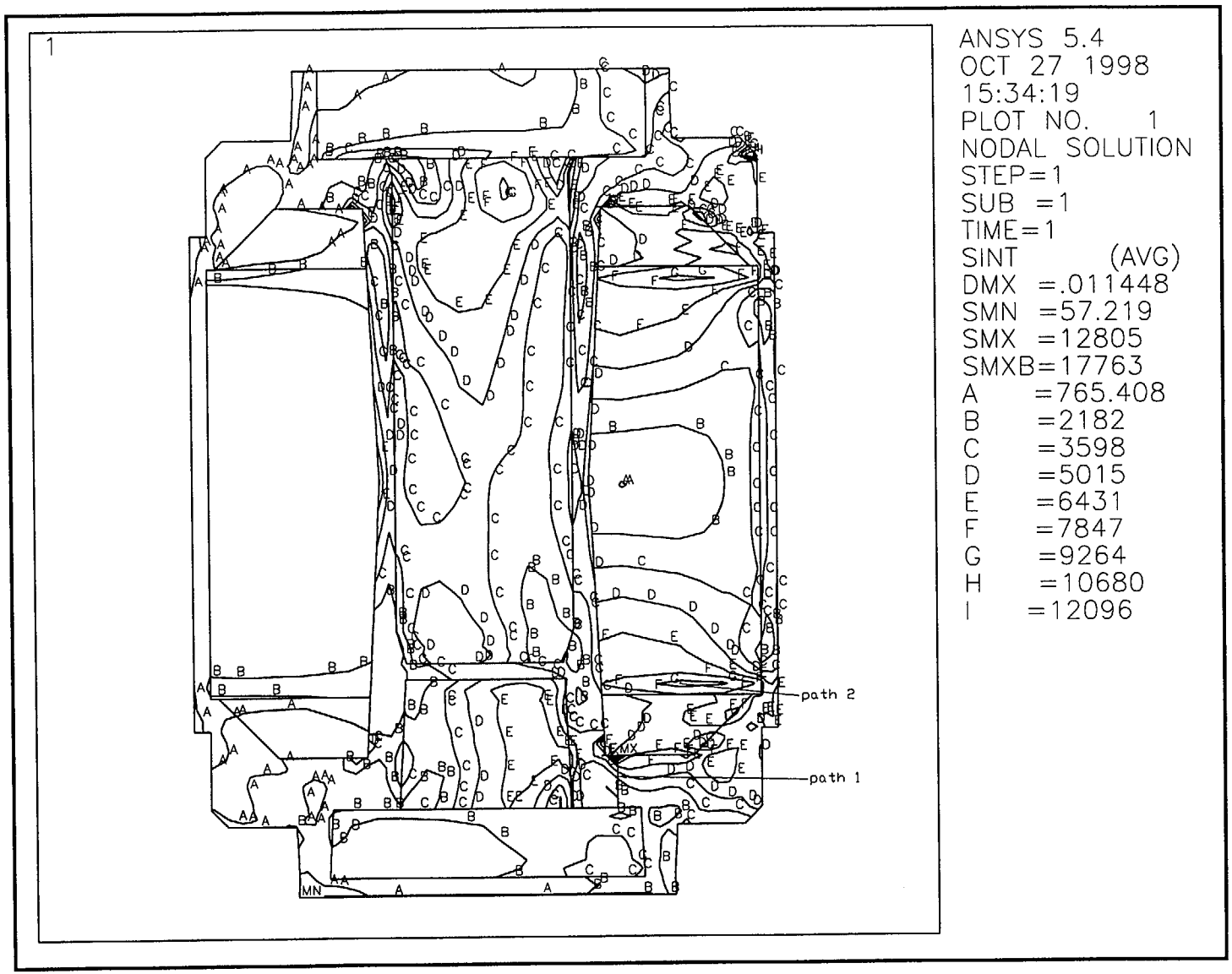

Figure 2.6-13 - NCT Side Drop Stress Contours, Without Thermal Stress

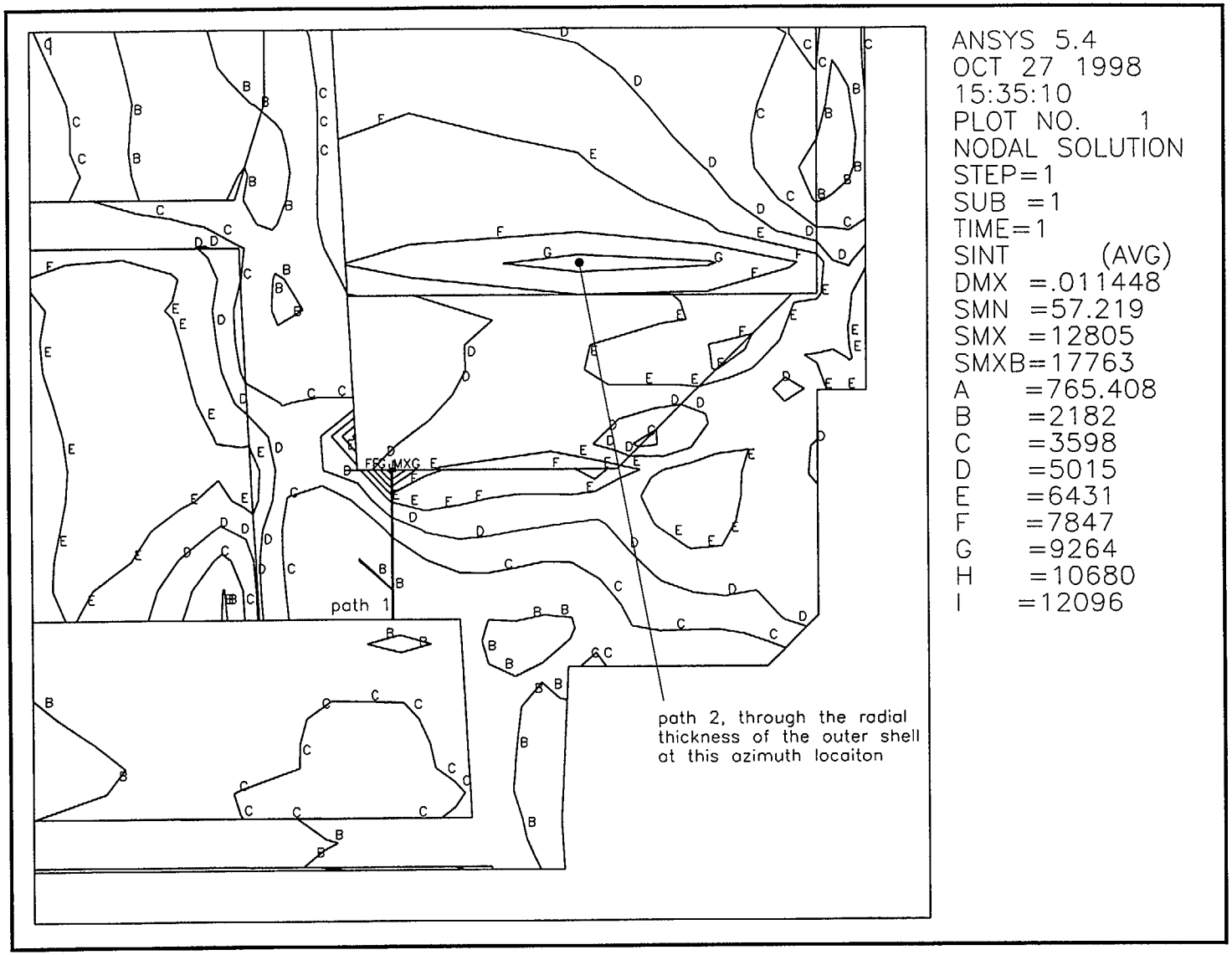

Figure 2.6-14 - NCT Side Drop Stress Contours, Without Thermal Stress, Detail of Paths 1 and 2

2.7 Hypothetical Accident Conditions

When subjected to the hypothetical accident conditions (HAC) as specified in 10 CFR §71.73 [1], the SEC meets the performance requirements specified in Subpart E of 10 CFR 71. This is demonstrated in the following subsections, where each accident condition is addressed and the cask shown to meet the applicable design criteria. The method of demonstration is primarily by analysis. The loads specified in 10 CFR §71.73 are applied sequentially, per Regulatory Guide 7.8 [3]. Resulting stresses are maintained below the limits established by Regulatory Guide 7.6 [2]. Dynamic testing of the performance of the impact limiters is discussed in Section 2.10.5. Lid closure bolt analyses for HAC events is presented in Section 2.10.4.

2.7.1 Free Drop

Subpart F of 10 CFR 71 requires that a 30 ft free drop be considered for the SEC. The free drop is to occur onto a flat, essentially unyielding, horizontal surface, and the cask is to strike the surface in an orientation for which maximum damage is expected. Several impact orientations and bounding ambient environments are considered. Since the payload amounts to only approximately ¼ of one percent of the total package weight, it may be neglected, and the weight of the package assumed invariant. In order to minimize the number of specific analyses that must be performed, the worst case maximum cold drop impact loads are conservatively applied to the cask using material properties and allowables corresponding to maximum (warm) Normal Conditions of Transport (NCT) temperatures.

2.7.1.1 Impact Forces and Deformations

The SEC free drop impact is attenuated by means of metallic, hollow toroidal impact limiters, placed on the top and the bottom of the cask, as shown in Figures 2.1-1 and 2.1-2. These structures are made from Type 304 stainless steel pipe elbows. Dissipation of the energy associated with the HAC free drops is accomplished primarily by plastic bending deformation of the walls of the pipes which compose the limiters. The material properties which govern the deformation load generated by the limiters are controlled as described in Section 2.3.2, with the result that impact loads and deformations vary relatively little over the range of temperatures to which the limiters may be exposed.

Impact forces, deformations, and impact limiter attachment forces are calculated using the LS-DYNA explicit finite element code [16]. LS-DYNA finite element models are described in Section 2.10.3. The end drop orientation uses a quarter-symmetry model, and the side, c.g. over corner, and slapdown cases use a half-symmetry model. Other than the differences relating to symmetry, the two models are identical. The impact limiter material stress-strain curve has a significant effect on the calculated level of impact. As described in Section 2.3.2, the stress-strain curve used for cold, maximum impact cases is given an upper bound to ensure that maximum impacts are conservatively evaluated. Conversely, the stress-strain curve used for warm, maximum deflection cases is given a lower bound to ensure that maximum impact limiter deflections are conservatively evaluated.

Impact analysis for the SEC is performed for four governing orientations: end (axis vertical), side (axis horizontal), center of gravity-over-corner (axis 54.5° from the horizontal), and a side

slapdown (axis 15° to the horizontal). For the slapdown case, the lid end of the cask strikes the ground second, and provides the greatest lateral impact on the closure lid. The slapdown case also applies the greatest forces to the impact limiter attachments. The adequacy of the attachments is discussed in Section 2.7.1.5.

Results are generated for both the HAC, 30 ft free drop and the NCT, 3 ft free drop and reported in Table 2.7-1. The effect of rotation in the slapdown events is discussed in Section 2.7.1.4. Final deformed shape plots of the impact limiters and impact acceleration time histories are provided in Figures 2.7-1 to 2.7-16, indexed according to Table 2.7-2. These results represent the global, rigid body impact of the cask with the ground.

Table 2.7-1 - Summary of Impact Analysis Results for HAC and NCT

Orientation	HAC			
	Maximum Impact (Cold)		Minimum Impact (Warm)	
	Impact① (g)	Deformation (in.)	Impact① (g)	Deformation② (in.)
End	166	3.59	100	5.67
Side	135	4.98	81	7.69
C.G.-over-Corner	66	8.74	48	12.85
Slapdown, Primary	64	4.71	38	7.06
Slapdown, Secondary	70	5.08	42	7.58
Orientation	**NCT**			
	Maximum Impact (Cold)		Minimum Impact (Warm)	
	Impact① (g)	Deformation (in.)	Impact① (g)	Deformation (in.)
End	78	0.70	57	0.97
Side	43	1.46	30	1.95
C.G.-over-Corner	29	2.12	21	2.12
Slapdown, Primary	21	1.48	15	1.78
Slapdown, Secondary	24	1.29	17	2.06

Notes:

① Impact acceleration given at cask c.g.

② The HAC warm case defines governing deformations. Minimum remaining clearance is discussed in Section 2.7.1.4.

To evaluate stresses in the cask structure, the implicit finite element program ANSYS®, Version 5.4, is used [17]. The ANSYS® finite element code is used for the stress analysis due to shorter solution times than the explicit LS-DYNA code, as well as the ready availability of advanced

features such as stress linearization. The LS-DYNA code is therefore used to evaluate the dynamic impact forces and deflections, and the ANSYS® code is used for the subsequent quasi-static stress evaluations. The cask stresses are evaluated by applying the maximum rigid body impact from the relevant impact time history to the ANSYS® cask model as a global acceleration field. A detailed stress analysis is performed for the two orientations which govern cask stresses: the end drop (both top-down and bottom-down) and the horizontal side drop. For the end drop, an axisymmetric model is used, described in detail in Section 2.10.2.1, and for the horizontal side drop, a half-symmetry side drop model is used, described in Section 2.10.2.2. In both models, only the load carrying steel structure is explicitly modeled. The lid, the lead shielding, the outer thermal shields, and the impact limiters are included in the stress models as either point masses or applied pressures, as appropriate. Results of the end drop analyses are presented in Section 2.7.1.2, and of the side drop in Section 2.7.1.3. Oblique drops are discussed in Section 2.7.1.4. The c.g.-over-corner drop orientation is important only for the evaluation of maximum impact limiter deformation, discussed in Section 2.7.1.4.

Table 2.7-2 - Index to Impact Analysis Plots

	Figure Number			
	NCT		HAC	
Orientation	Deformed Shape Plot①	Impact Time History②	Deformed Shape Plot①	Impact Time History②
End	2.7-1	2.7-5	2.7-9	2.7-13
Side	2.7-2	2.7-6	2.7-10	2.7-14
C.G.-over-corner	2.7-3	2.7-7	2.7-11	2.7-15
Slapdown	2.7-4	2.7-8	2.7-12	2.7-16

Notes:

① All deformed shape plots correspond to maximum deflection, warm conditions. Deflected shapes for maximum impact, cold conditions are not governing in any case.

② All impact time history plots correspond to maximum impact, cold conditions. Impact time histories for maximum deflection, warm conditions are not governing in any case.

2.7.1.2 HAC End Drop

As shown in Table 2.7-1, the maximum impact acceleration during the HAC end drop is 166g. For the end drop stress analysis of the SEC, therefore, a global acceleration field of 175g is conservatively applied to the ANSYS® finite element model. The construction of the end drop stress analysis model is described in Section 2.10.2.1. Both bottom-down and top-down orientations are considered. Five analyses are performed:

- Cask body stress
- Closure lid bolt stress
- Closure lid weld stress
- Lower closure plate stress

- End drop buckling evaluation

Cask body stress. In the bottom-down orientation, the cask is considered fixed at its lowest extremity, and since the lower impact limiter is supporting the cask, the mass of the lower impact limiter need not be considered. The mass of the closure lid is conservatively considered to be concentrated at the inner diameter of the cask-to-lid interface, thus maximizing its contribution to the overall response, and the mass of the upper impact limiter is concentrated at the upper extremity of the cask. The mass of the lower end lead shield is applied as a pressure to the lower one inch thick plate, and the mass of the annular lead shield is applied as a hydrostatic pressure. The resulting stresses are shown in Figure 2.7-17. Stresses are linearized along paths 1 and 2 in order to obtain the maximum membrane and membrane plus bending stresses. The maximum primary membrane stress (P_m) is located on path 1, and is equal to 31,670 psi[1]. Since this stress is located in the outer shell, the maximum temperature of the outer shell of 410 °F is used. From Table 2.1-1, the allowable stress under HAC is the lesser of $2.4S_m$ or $0.7S_u$, which for Type 304 stainless steel at a temperature of 410 °F, from Table 2.6-1, is 44,592 psi. The margin of safety on primary membrane stress in the bottom-down end drop case is therefore

$$(P_m):\ MS = \frac{44,592}{31,670} - 1 = \underline{+0.41}$$

The maximum membrane plus bending stress ($P_L + P_b$) is 39,010 psi, located on path 2. From Table 2.1-1, the allowable stress under HAC is the lesser of $3.6S_m$ or S_u, which for Type 304 stainless steel at a temperature of 410 °F, from Table 2.6-1, is 64,310 psi. The margin of safety on membrane plus bending stress in the bottom-down end drop case is therefore

$$(P_L + P_b):\ MS = \frac{64,310}{39,010} - 1 = \underline{+0.65}$$

In the top-down orientation, the cask is considered fixed at its upper extremity, and since the upper impact limiter is supporting the cask, the mass of the upper impact limiter need not be considered. The mass of the closure lid is applied at a diameter equivalent to the lid bolt circle. The mass of the lower impact limiter is considered concentrated at the lowest cask extremity. The mass of the lower end lead shield is conservatively considered to be concentrated at the inside edge of the inner shell, thus maximizing its contribution to overall response, and the mass of the annular lead shield is treated as above. The resulting stresses are shown in Figure 2.7-18. Stresses are linearized along paths 1 and 2 in order to obtain the maximum membrane and membrane plus bending stresses. The maximum primary membrane stress (P_m) is located on path 1, and is equal to 32,100 psi. Since this stress is located in the outer shell, the maximum temperature of the outer shell of 410 °F is used. From Table 2.1-1, the allowable stress under HAC is the lesser of $2.4S_m$ or $0.7S_u$, which for Type 304 stainless steel at a temperature of 410 °F, from Table 2.6-1, is 44,592 psi. The margin of safety on primary membrane stress in the bottom-down end drop case is therefore

[1] Since membrane and membrane plus bending stresses are linearized, the values given in this section may differ slightly from the maximum values shown in the figures.

$$(P_m):\ MS = \frac{44,592}{32,100} - 1 = \underline{+0.39}$$

The maximum membrane plus bending stress ($P_L + P_b$) is 39,660 psi, located on path 2. From Table 2.1-1, the allowable stress under HAC is the lesser of $3.6S_m$ or S_u, which for Type 304 stainless steel at a temperature of 410 °F, from Table 2.6-1, is 64,310 psi. The margin of safety on membrane plus bending stress in the bottom-down end drop case is therefore

$$(P_L + P_b):\ MS = \frac{64,310}{39,660} - 1 = \underline{+0.62}$$

Therefore, the allowable stresses as established in Section 2.1 have been met for the cask structure in the end drop.

Closure lid bolt stress. The lid bolt stresses are determined in Section 2.10.4 per NUREG/CR-6007 [7]. The maximum stress occurs during the top-down drop in the cold case. The resulting tensile stress, which is a result of preload and free drop loading of 175g, is 55,431 psi. The corresponding maximum combined stress factor, which must be less than unity, is 0.63. The analysis of the closure lid attachment bolts in the top-down drop is discussed in Section 2.10.4.

Closure lid weld stress. In a bottom-down end drop, the weld attaching the lower, smaller diameter portion of the closure lid to the upper, larger diameter portion will experience a stress. This weld was analyzed in connection with transportation vibration in Section 2.6.5, where the weld stress for one g was found to be $\sigma_1 = 45.8$ psi. An impact load of 175g is conservatively applied along the axis of the lid. The stress in the weld is therefore

$$\sigma = \sigma_1(175) = 8,015 \text{ psi}$$

This stress is classified as a primary membrane stress, and the allowable stress is $2.4S_m$, found above to be equal to 44,592 psi, where a temperature of 410 °F is conservatively assumed for this portion of the closure lid. The margin of safety is

$$MS = \frac{44,592}{8,015} - 1 = \underline{+4.56}$$

Lower closure plate stress. Also in a bottom-down end drop, the lower plate which covers the lower lead cavity is subject to stress. The weld attaching this plate to the cask governs, and was analyzed in Section 2.6.5, where the weld stress for one g was found to be $\sigma_1 = 28.6$ psi. An impact load of 175g is again applied along the axis of the cask. The stress in the weld is

$$\sigma = \sigma_1(175) = 5,005 \text{ psi}$$

This stress is classified as a primary membrane stress, and the allowable stress is $2.4S_m$, found above to be equal to 44,592 psi, where a temperature of 410 °F is conservatively assumed for the lower plate weld. The margin of safety is (with an added factor of 0.6 to account for pure shear)

$$MS = \frac{44,592(0.6)}{5,005} - 1 = \underline{+4.35}$$

HAC end drop buckling evaluation. The SEC is evaluated for buckling due to the HAC end drop inertia load using ASME Code Case N-284-1 [6]. Axial stresses are developed due to the weight of the material loading the shells in the HAC end drop. To simplify the analysis, the outer shell is considered to act alone, conservatively supporting the entire buckling load, without assistance from the inner shell. The supported weight is the sum of the upper impact limiter, the upper casting, the closure lid, the inner and outer shells, and the thermal shields. The annular lead shield supports itself in simple compression on its lower face. The lower casting, the lower center lead, and the lower impact limiter are supported by the ground. Conservatively, the thermal axial stress, which is tensile, is not considered to reduce the compressive stress arising from the end drop. In the buckling evaluation, there is no difference between top-down and bottom-down orientations. Consistent with Regulatory Guide 7.6 philosophy, a factor of safety of 1.34, corresponding to ASME Code, Level D service conditions is applied, as specified in Code Case N-284-1.

The weight of the components which contribute to the end drop buckling load are listed in Table 2.7-3. Each weight is conservatively upper-bounded. The total weight of these components is W = 6,375 lb.

Table 2.7-3 - End Drop Buckling Weight

Component Name	Weight, lb
Upper Impact Limiter	2,000
Upper Casting & Inner Shell	1,725
Closure Lid	900
Outer Shell	850
Thermal Shields	900
Total	6,375

The loading of the outer shell is based on this weight, the end drop impact response of the upper casting, and the area of the outer shell, which is

$$A = \pi\left(r_o^2 - r_i^2\right) = 108.4\ in^2$$

where the outer radius of the outer shell, r_o = 17.75 inches, and the inner radius, r_i = 16.75 inches. The axial stress is therefore

$$\sigma_\phi = \frac{W}{A} g = 10{,}292 \text{ psi}$$

where the end drop impact level is g = 175, conservatively rounded up from the value given in Table 2.7-1. Maximum impact response from the cold, -20 °F case is conservatively combined with warm allowables corresponding to maximum NCT temperature, which is bounded by 410 °F for the outer shell.

Buckling analysis parameters are given in Table 2.7-4, and results in Table 2.7-5. As shown, all interaction check parameters are less than 1.0, as required. Therefore, the SEC does not experience buckling in the HAC end drop.

Table 2.7-4 - Cask Buckling Geometry Parameters

Geometry, Temperature, and Material Input	
	Outer Shell
Outside Diameter, inches	35.5
Inside Diameter, inches	33.5
Length, inches	26.0
Geometry Output (nomenclature consistent with ASME Code Case N-284)	
R =	17.25
t =	1.00
R/t =	17.25
ℓ_ϕ =	26.0
ℓ_θ =	108.38
M_ϕ =	6.26
M_θ =	26.10
M =	6.26

Table 2.7-5 - Cask Buckling Summary for HAC, End Drop Impact

Condition	Outer Shell	Remarks
Capacity Reduction Factors (-1511)		
$\alpha_{\phi L}$ =	0.2748	
$\alpha_{\theta L}$ =	0.8000	
$\alpha_{\phi\theta L}$ =	0.8000	
Plasticity Reduction Factors (-1610)		
$\eta_{\phi L}$ =	0.0811	
$\eta_{\theta L}$ =	0.0523	
$\eta_{\phi\theta L}$ =	0.0837	
Theoretical Buckling Values (-1712.1.1)		
C_{ϕ} =	0.6050	
$\sigma_{\phi eL}$ =	926,965 psi	
$C_{\theta r}$ =	0.1807	
$\sigma_{\theta eL} = \sigma_{reL}$ =	276,932 psi	
$C_{\theta h}$ =	0.1636	
$\sigma_{\theta eL} = \sigma_{heL}$ =	250,637 psi	
$C_{\phi\theta}$ =	0.3222	
$\sigma_{\phi\theta eL}$ =	493,697 psi	
Elastic Interaction Equations (-1713.1.1)		
σ_{xa} =	190,104 psi	
σ_{ha} =	149,634 psi	
σ_{ra} =	165,332 psi	
$\sigma_{\tau a}$ =	294,745 psi	
Axial + Hoop ⇨ Check (a):	*N/A*	
Axial + Hoop ⇨ Check (b):	*N/A*	
Axial + Shear ⇨ Check (c):	*0.0541*	<1 ∴ OK
Hoop + Shear ⇨ Check (d):	*0.0000*	<1 ∴ OK
Axial + Hoop + Shear ⇨ Check (e,a):	*N/A*	
Axial + Hoop + Shear ⇨ Check (e,b):	*N/A*	
Inelastic Interaction Equations (-1713.2.1)		
σ_{xc} =	15,418 psi	
σ_{rc} =	8,648 psi	
$\sigma_{\tau c}$ =	24,669 psi	
Axial + Hoop ⇨ Check (a):	*0.6675*	<1 ∴ OK
Axial + Shear ⇨ Check (b):	*0.6675*	<1 ∴ OK
Hoop + Shear ⇨ Check (c):	*0.0000*	<1 ∴ OK

2.7.1.3 HAC Side Drop

As shown in Table 2.7-1, the maximum impact acceleration during the HAC side drop is 135g. For the side drop stress analysis of the SEC, therefore, a global acceleration field of 145g is conservatively applied to the ANSYS® finite element model [17]. The construction of the side drop stress analysis model is described in Section 2.10.2.2. The cask is modeled in three dimensions and is half-symmetry, the plane of symmetry being the plane of the side drop. The load applied by the impact limiters is modeled as a pressure extending over the length of the cask-to-limiter interface, and extends circumferentially 30° in half-symmetry. The lower end lead and the lid inertia loads are likewise applied as pressures over 30°. The weight of the annular lead is distributed to the inner and outer shells as described in Section 2.10.2.2. The resulting stresses are shown in Figure 2.7-19. Stresses are linearized along paths 1 and 2 in order to obtain the maximum membrane and membrane plus bending stresses. The maximum primary membrane stress (P_m) is located on path 2, and is equal to 17,280 psi. Since this stress is located in the end casting, the maximum temperature of the end casting of 410 °F is used. From Table 2.1-1, the allowable stress under HAC is the lesser of $2.4S_m$ or $0.7S_u$, which for Type 304 stainless steel at a temperature of 410 °F, from Table 2.6-1, is 44,592 psi. The margin of safety on primary membrane stress in the side drop case is therefore

$$(P_m):\ MS = \frac{44{,}592}{17{,}280} - 1 = \underline{+1.58}$$

The maximum membrane plus bending stress ($P_L + P_b$) is 27,640 psi, located on path 1, through the outer shell. From Table 2.1-1, the allowable stress under HAC is the lesser of $3.6S_m$ or S_u, which for Type 304 stainless steel at a temperature of 410 °F, from Table 2.6-1, is 64,310 psi. The margin of safety on membrane plus bending stress in the side drop case is therefore

$$(P_L + P_b):\ MS = \frac{64{,}310}{27{,}640} - 1 = \underline{+1.33}$$

Therefore, the allowable stresses as established in Section 2.1 have been met for the cask structure in the side drop. The impact level on the cask lid is governed by the side-slapdown drop, and is discussed in Section 2.7.1.4.

2.7.1.4 Oblique Drop

For the HAC free drop, the SEC can strike the ground in any primary orientation. As shown in the following discussion, the cask stresses for all oblique drop orientations are conservatively bounded by the side drop (horizontal) orientation. This evaluation is based on the axial, shear, and moment forces in the cask shells as derived in NUREG/CR-3966 [18]. It is shown that, for the specific impact forces developed in the HAC oblique free drops, the cask shell stress intensity is governed by the side drop case. The inertia load experienced by the cask lid is discussed later in this section.

In Section 2.2 of reference [18], the maximum axial force, R, shear force, V, and bending moment, M, in the cask shells are given for the primary oblique impact as:

$$R_p = F_p \sin(\theta)$$

$$V_p = F_p\cos(\theta)$$

$$M_p = (4/27)\, F_p L\cos(\theta)$$

where the subscript p indicates the primary impact event, L is the overall length of the cask, θ is the primary impact angle with respect to the horizontal, and F_p is the maximum primary impact limiter force. For the subsequent secondary (slapdown) impact, the maximum values of the above parameters are:

$$R_s = 0$$

$$V_s = F_s$$

$$M_s = (4/27)\, F_s L$$

where the subscript s indicates the secondary impact event, and F_s is the maximum secondary impact limiter force. In the horizontal side drop impact, the maximum values of the above parameters are:

$$R_h = 0$$

$$V_h = F_h$$

$$M_h = (1/4)\, F_h L$$

where the subscript h indicates the horizontal case, and F_h is the maximum impact limiter force in the side drop. The cask shell stresses resulting from these applied forces and moments can be calculated as follows:

$$\sigma_a = \frac{R_i}{A}$$

$$\tau = \frac{V_i}{A}$$

$$\sigma_b = \frac{M_i c}{I}$$

where σ_a is the axial stress, τ the shear stress, and σ_b the bending stress in the cask shells, and where A is the cross sectional area of the cask shells, and I is the moment of inertia. The maximum stress intensity in the cask shells is determined by combining the component stresses using Mohr's circle as follows:

$$\text{S.I.} = \frac{\sigma_a + \sigma_b}{2} \pm \sqrt{\left(\frac{\sigma_a + \sigma_b}{2}\right)^2 + \tau^2}$$

For purposes of comparison, it is only necessary to consider one shell, for example, the inner shell. The cross sectional area of the inner shell is

$$A = (\pi/4)\left(d_o^2 - d_i^2\right) = 36.9 \text{ in}^2$$

and the moment of inertia is

$$I = (\pi/64)\left(d_o^4 - d_i^4\right) = 641.7 \text{ in}^4$$

where d_o = 12.75 inches and d_i = 10.75 inches. The parameter c = 12.75/2 = 6.375 inches, and the length L = 56 inches.

The maximum force on a single impact limiter in the HAC 30 ft, horizontal side drop is determined from the impact value given in Table 2.7-1 and an overall cask weight of W = 20,000 lb as follows:

$$F_h = \frac{Wg_h}{2} = 1.35(10^6)\,lb$$

where $g_h = 135$[2] from Table 2.7-1, and the denominator of 2 yields the value for one of the two limiters. The worst case oblique free drop is the shallow-angle side slapdown orientation at a primary impact angle of 15 degrees. The primary and secondary impact limiter forces are found as follows:

$$F_p = Wg_p = 1.28(10^6)\,lb$$

$$F_s = Wg_s = 1.40(10^6)\,lb$$

where g_p = 64 and g_s = 70 from Table 2.7-1. The resulting cask shell forces and resulting maximum combined stress intensities are shown in Table 2.7-6. Since only the inner shell properties are used, the stress intensity is relative, and is used for comparison between the different cases only. The stress values in the table therefore do not represent actual inner shell stress intensity. As shown, the stress intensity is greatest in the horizontal side drop case. Therefore, the side drop stress analyses, detailed in Section 2.7.1.4, are enveloping for all oblique drop orientations.

Table 2.7-6 - Cask Shell Force and Stress Comparison

Case	Impact Limiter Force, lb	Axial Force, R, lb	Shear Force, V, lb	Bending Moment, M, in-lb	Relative① Stress Intensity, psi
Side Drop	$1.35(10^6)$	0	$1.35(10^6)$	$18.900(10^6)$	194,640
15°, Primary	$1.28(10^6)$	331,288	$1.24(10^6)$	$10.257(10^6)$	120,216
15°, Secondary	$1.40(10^6)$	0	$1.40(10^6)$	$11.615(10^6)$	126,747

Notes:

① Stress for comparison purposes; not actual inner shell stress.

Lateral forces on the closure lid. While the maximum cask shell stresses are enveloped by the horizontal side drop orientation, the maximum side impact experienced by the cask lid occurs in

[2] In other analyses in this section, upper-bound impacts are used. In this case, however, the best comparison is obtained by using the impact accelerations as calculated.

the slapdown event where the lid end of the cask is at the secondary end of the cask. The acceleration of any point along the cask axis in the slapdown event is

$$G = g_{c.g.} + \alpha L$$

where $g_{c.g.}$ is the acceleration of the cask center of gravity, α is the angular acceleration, and L the distance from the center of gravity to the point of interest, in this case, the mass center of the lid. The angular acceleration is

$$\alpha = \frac{F_s L}{I}$$

where F_s is the maximum secondary impact limiter force and I is the mass moment of inertia of the cask about its center of gravity, and which is based on the familiar expression, Torque = $I\alpha$. The value of $g_{c.g.}$, which is given in Table 2.7-1, is formed from

$$g_{c.g.} = \frac{F_s}{W}$$

where W is the cask weight, and this can be rearranged to give $F_s = g_{c.g.}W$. Substituting the expressions for α and for F_s into the first equation gives

$$G = g_{c.g.}\left(1 + \frac{WL^2}{Ig}\right)$$

where g is the gravitational constant, and G has the units of gravity. For a distance between the cask center of gravity and the lid center of gravity of L = 19.1 inches (determined using values in Table 2.2-1), for a cask weight of W = 20,000 lb, and for a mass moment of inertia of the cask of I = 19,626 in-lb-s^2, the value for G at the lid mass center is

$$G = g_{c.g.}(1.962) = 147g$$

where $g_{c.g.}$ = 75, conservatively rounded up from the value given for the secondary impact in the cold case slapdown event in Table 2.7-1. When this value is applied to the lid in the closure bolt analysis described in Section 2.10.4, the resulting tensile and shear stresses are 25,685 psi and 32,919 psi, respectively, and the combined stress ratio, which must be less than unity, is 0.69. Therefore, closure bolts are adequate for the worst case loading in the slapdown event.

Minimum impact limiter clearance. In order to completely attenuate drop energy, the impact limiter must not deform more that the amount available. The maximum allowable deformation is that deformation which can take place along the line of crush before "hard" contact occurs. From Table 2.7-1, the greatest deformations occur in the HAC, warm case, in the end, side, and c.g.-over-corner orientations. The maximum deformation occurs in the minimum stiffness, c.g.-over-corner case. At an orientation of 54.5° to the horizontal, the distance along the vertical crush line between the inside of the torus and the nearest edge of the rigid cap structure is 15.52 inches. As shown in Table 2.7-1, the maximum impact limiter deflection in this case is 12.85 inches. The Minimum Remaining Clearance (MRC) is

$$MRC = 15.52 - 12.85 = 2.67 \text{ inches}$$

Therefore, the impact limiter is adequate to prevent bottom-out in the worst case. Remaining clearance for the three cases discussed above are given in Table 2.7-7.

Table 2.7-7 - Minimum Remaining Impact Limiter Clearance

Orientation (HAC, Warm Cases)	Minimum Available Distance, inches	Maximum Deformation, inches	Minimum Remaining Clearance, inches
End	11.25	5.67	5.58
Side	11.25	7.69	3.56
C.G.-Over-Corner	15.52	12.85	2.67

2.7.1.5 Impact Limiter Retention

Each impact limiter is retained to the cask using twelve, one inch diameter quick release ball lock pins. As shown in Figure 2.1-2, the pins are oriented radially to the cask axis, and pass through the impact limiter attachment skirt and into the massive end castings. In end impact and for most other impact orientations, the impact force vector developed by the crush of the toroid passes through the cask body. In such cases, the limiter is supported completely by the cask body, and no moment of force is generated between the limiter and the cask. For near horizontal impacts, however, the force vector may not pass through the cask body, and a moment may develop. The maximum moment is associated with the maximum moment arm, measured between the impact force vector and the lower support point between the limiter and the cask body, which occurs for a horizontal (side drop) orientation, as shown in Figure 2.7-20. As shown, the maximum moment arm of the impact force is $a_{if} = 8.125$ inches. Since the impact limiter cap (the part of the impact limiter which is the interface between the cask and the toroid) is a rigid structure and closely fits the cask, the load on the attachment pins is single shear.

From Table 2.7-1, the maximum impact force on an impact limiter in a horizontal orientation occurs in the secondary impact of the 15° slapdown, cold HAC free drop, and is $F = (70)W = 1.4(10^6)$ lb, where $W = 20{,}000$ lb from Table 2.2-1. In this analysis, the maximum force is conservatively bounded by $F = 1.5(10^6)$ lb. As shown in Figure 2.7-20, a friction force exists between the cask body and the impact limiter near the lower support point. The moment arm for the friction force is equal to the cask interface diameter, $a_{ff} = 33.5$ inches. The coefficient of friction may be lower bounded by $\mu = 0.05$, based on Table 3.2.1 of reference [21] for lubricated mild steel on mild steel[3]. The frictional moment opposes the applied moment, and the maximum net moment is therefore

$$M = F(a_{if}) - F(\mu)(a_{ff}) = 9{,}675{,}000 \text{ in} - \text{lb}$$

[3] The actual materials of construction for both parts of the interface are Type 304 stainless steel, which has greater friction with itself than mild steel. Due to the relatively high normal operating temperatures, any unintentional lubrication between the surfaces is not effective. However, the surfaces are conservatively assumed to be lubricated.

where the first term is the impact moment and the second term is the resisting frictional moment. The load distribution in the attachment pins is a function of the distance of each pin from the upper support point shown in Figure 2.7-20. The distribution is shown schematically in Figure 2.7-21a. The shear force in each pin is linearly proportional to the maximum pin force as follows:

$$F_i = F_{max}\left(\frac{d_i}{D}\right)$$

where F_i is the shear force in a typical pin, d_i is the distance from the upper support point to the pin, F_{max} is the shear force on the pin nearest the ground, and D is the distance from the upper support point to the pin nearest the ground, or 33.5 inches. The moment contribution of each pin is

$$M_i = F_i d_i = \left(\frac{F_{max}}{D}\right) d_i^2$$

The total moment is the sum of contributions of all the pins, which is

$$M = \frac{F_{max}}{D}\sum d_i^2$$

This can be rearranged to solve for F_{max} as follows:

$$F_{max} = \frac{MD}{\sum d_i^2}$$

A typical distance d_i for an attachment pin is calculated with the aid of Figure 2.7-21b. For 12 pins, the angle between them is 30°. For the typical pin shown in the figure, the distance d_i is equal to

$$d = \frac{D}{2}(1 + \sin 30) = 25.125 \text{ inches}$$

The value Σd_i^2 for all 12 pins is equal to 5,050 in^2. The maximum attachment pin shear force is therefore

$$F_{max} = \frac{MD}{\sum d_i^2} = 64{,}181 \text{ lb}$$

From the manufacturer's catalog, the pins have a double shear strength, with a factor of safety of 2, of 73,500 lb. The actual capacity in single shear and with a factor of safety of 1 is also 73,500 lb, since the double shear factor of 2 cancels out the factor of safety of 2. This capacity is the load which could be repeatedly applied to the pin without damage, and therefore, its use as a maximum allowable load in the hypothetical accident is conservative. The margin of safety is

$$MS = \frac{73{,}500}{64{,}181} - 1 = \underline{+0.15}$$

The hole in the impact limiter skirt is D = 1½ inches in diameter and is located d = 1 11/16 in from the edge. Using the 40° tearout method from Faupel and Fisher [19], the distance in the direction of shear is

$$L=d-0.383D=1.293 \text{ inches}$$

The shear tearout is double shear. The shear area is

$$A=2Lt=3.168 \text{ inches}$$

where t, the thickness of the impact limiter skirt, is 1.225 inches. The shear stress at the location of the most highly loaded pin is

$$\tau=\frac{F_{max}}{A}=20{,}259 \text{ psi}$$

The stress in the skirt is a primary shear stress. From Table 2.1-1, the allowable stress is $0.42S_u$ for accident conditions. From Table 2.3-1, the S_u of the skirt material (Type 304) at a temperature of 350 °F is 65,200 psi. The margin of safety is

$$MS=\frac{(0.42)65{,}200}{\tau}-1=+0.35$$

Therefore, the impact limiters remain in place throughout the worst case impact event.

2.7.2 Crush

The crush test specified in 10 CFR §71.73(c)(2) is required only when the specimen has a mass not greater than 1,100 lb, an overall density not greater than 62.4 lb/ft^3, and radioactive contents greater than 1,000 A_2, not as special form. Since none of these parameters are satisfied by the SEC, no crush test is required.

2.7.3 Puncture

The SEC is evaluated for puncture resistance under HAC as defined in 10 CFR §71.73(c)(3). The puncture event is defined as the ability to withstand a 40 inch drop onto a vertical, cylindrical mild steel bar, 6 inches in diameter, in an orientation and at a location on the cask for which maximum damage is expected. The cask is evaluated for the following three critical puncture drops:

1) Direct puncture onto the cask closure lid, with the axis of the bar oriented to pass through the center of gravity of the package. This orientation imparts all of the puncture potential energy through the cask lid for the greatest damage, imparting only negligible energy to cask rotation. Conservatively, the one inch thick impact limiter cover plate, which completely covers the cask lid during transport, is neglected. Since the cask lid is slightly recessed below the edge of the top casting and there are no features on the lid or top casting which could be damaged by an oblique or sliding impact of the puncture bar, an oblique puncture orientation is not necessary.
2) Direct puncture onto the cask bottom cover plate, with the axis of the bar oriented to pass through the center of gravity of the package. This orientation imparts all of the puncture

potential energy through the cask bottom structures for the greatest damage, imparting only negligible energy to cask rotation. Conservatively, the one inch thick impact limiter cover plate, which completely covers the cask bottom during transport, is neglected. As discussed above for the cask lid, no oblique puncture impact on the cask bottom is necessary.

3) Direct puncture onto the cask outer shell, with the bar oriented to pass through the cask center of gravity. This orientation imparts all of the puncture potential energy through the cask side structures for the greatest damage, imparting only negligible energy to cask rotation. Since the puncture bar has an edge radius of 0.25 inches, it cannot gouge or rip the thermal shield on the outside of the cask, since it is 0.135 inches thick. Therefore, no oblique impact on the cask side is necessary.

Since all punctures are normal to a Type 304 stainless steel plate which is backed by lead, puncture analyses must satisfy Nelms' equation [20].

Cask Lid (1). The outer plate of the cask lid is 1.5 inches thick. For a bounding temperature of 350 °F, the ultimate strength of Type 304 material is S_u = 65,200 psi. The bounding weight of the cask, including impact limiters, is W = 20,000 lb. The required thickness is

$$t=\left(\frac{W}{S_u}\right)^{0.71}=0.432 \text{ inches}$$

The margin of safety on cask lid outer plate thickness is

$$MS=\frac{1.5}{0.432}-1=\underline{+2.47}$$

Therefore, puncture of the cask lid is not of concern.

Cask Bottom (2). The lower plate of the cask is one inch thick. For a bounding temperature of 400 °F, the ultimate strength of Type 304 material is S_u = 64,400 psi. The required thickness is

$$t=\left(\frac{W}{S_u}\right)^{0.71}=0.436 \text{ inches}$$

The margin of safety on the lower plate thickness is

$$MS=\frac{1.0}{0.436}-1=\underline{+1.29}$$

Therefore, puncture of the cask lower plate is not of concern.

Cask Outer Shell (3). The cask outer shell is 1.0 inches thick. The bounding temperature is 400 °F, and therefore the required thickness is again 0.436 inches. The margin of safety on cask outer shell thickness is

$$MS=\frac{1.0}{0.436}-1=\underline{+1.29}$$

Therefore, puncture of the cask outer shell is not of concern.

2.7.4 Thermal

The SEC thermal evaluation for HAC is presented in Section 3.5. The SEC is designed to withstand the HAC, 30 minute, fully engulfing pool fire of 1,475 °F as required by 10 CFR §71.73(c)(4).

2.7.4.1 Summary of Pressures and Temperatures

As shown in Section 3.4.4, the Maximum Normal Operating Pressure (MNOP) under normal conditions of transport is 23.9 psig. As shown in Section 3.5, the maximum internal cask pressure during or after the HAC fire event is 26.5 psig. The cask has a design pressure of 50 psig, which is significantly higher than this maximum value. Therefore, the 50 psig design pressure is bounding. Cask component stresses for an internal pressure of 50 psig are calculated in Section 2.6.1 and are compared to allowable stresses at the higher HAC fire event material temperatures in Section 2.7.4.2.

As a result of the HAC fire event, the maximum temperature of the cask inner shell, outer shell, end castings, or lid is bounded by 630 °F. This temperature is used for all components made of Type 304 stainless steel for HAC internal pressure loading during or after the HAC fire event. At this temperature, the values of S_m and S_u for Type 304 are 16,280 psi and 63,500 psi, respectively.

2.7.4.2 Stress Calculations

Cask stresses due to an internal pressure of 50 psig are presented in Section 2.6.1.3.1, where the maximum membrane stress is found to be 289 psi. Since a pressure of 50 psig bounds the pressure for the HAC fire event (including post-fire conditions), the margin of safety may be calculated using this value of stress and the allowables determined in Section 2.7.4.1. From Regulatory Guide 7.6, the limit on primary membrane stress is the lesser of $2.4S_m$ or $0.7S_u$, which from Section 2.7.4.1 is $2.4S_m = 39{,}072$ psi. The margin of safety therefore is

$$MS = \frac{39{,}072}{289} - 1 = \underline{+134}$$

The stress analysis of the lid closure bolts is performed in Section 2.10.4, and all stress ratios are less than unity, as required. Therefore, the HAC fire event is not of concern.

Per Regulatory Guide 7.6, paragraph C.7, the extreme range of stress must be considered. Of all the various allowable stresses corresponding to the different conditions evaluated (including fabrication stresses and normal conditions of transport), the largest allowable stress is equal to the material ultimate strength, S_u. It is therefore conservative to assume that S_u bounds all stresses actually developed in the structure. For Type 304 stainless steel, $S_u = 75{,}000$ psi at 70 °F. The maximum possible stress intensity range is twice this value, or 150,000 psi. Applying a factor of four to account for possible stress concentrations at structural discontinuities gives a total stress range of 600,000 psi. The alternating component is one-half of this value, or 300,000 psi. To account for temperature effects, this value of alternating stress is factored by the ratio of modulus of elasticity. This ratio is formed between the modulus of elasticity at room temperature (at which the test data applies directly) and the modulus of elasticity at the

maximum temperature, conservatively bounded by the lead melt temperature of 620 °F for any structural part of the package. The adjusted stress is

$$S_{alt} = 300{,}000 \frac{E_{70°F}}{E_{620°F}} = 336{,}905 \text{ psi}$$

where $E_{70°F} = 28.3(10^6)$ psi and $E_{620°F} = 25.2(10^6)$ psi. Per Figure I-9.2.1 and Table I-9.1 of the ASME Code [9], the allowable value for S_{alt} at 10 cycles is 708,000 psi. The margin of safety is

$$MS = \frac{708{,}000}{336{,}905} - 1 = \underline{+1.10}$$

Considering the significant conservatism used in the underlying assumptions (e.g., use of allowable stress rather than smaller actual stresses, assuming worst case stresses are fully reversing, use of the maximum factor of stress concentration), it is apparent that the actual margin of safety is larger than 1.10. Thus, the requirement of paragraph C.7 of Regulatory Guide 7.6 is met.

2.7.5 Immersion - Fissile

The SEC does not carry any fissile material, and therefore, this section does not apply.

2.7.6 Immersion - All Packages

The effect of immersion of the package in 50 ft of water (equivalent to 21.7 psig) per 10 CFR §71.73(c)(6), is considered negligible for the SEC compared to other design loadings, based on results of analysis utilizing ASME Code Case N-284-1. Consistent with Regulatory Guide 7.6 philosophy, a factor of safety of 1.34, corresponding to ASME Code, Level D service conditions is applied, as specified in Code Case N-284-1. Although the design pressure is 50 psi, a minimum internal pressure corresponding to ambient is conservatively used. The pressure differential across the cask confinement boundary is therefore 21.7 - 0 = 21.7 psi.

Buckling analysis geometry parameters are provided in Table 2.7-8, and loading parameters are given in Table 2.7-9. The buckling analysis conservatively uses inner and outer shell temperatures consistent with Section 2.6.1, i.e., 510 °F for the inner shell and 410 °F for the outer shell. The hoop stress, σ_θ, axial stress, σ_ϕ, and in-plane shear stress, $\sigma_{\phi\theta}$, are found from:

$$\sigma_\theta = \frac{p_o r}{t} \qquad \sigma_\phi = \frac{p_o r}{2t} \qquad \sigma_{\phi\theta} = \frac{p_o r}{4t}$$

where p_o is the applied pressure of 21.7 psi, r is the mean radius, and t is the shell thickness. As shown in Table 2.7-10, all the interaction check parameters are less than 1.0, as required. Therefore, buckling of the cask shells under immersion conditions is not of concern.

Table 2.7-8 - Cask Buckling Geometry Parameters

Geometry, Temperature, and Material Input		
	Inner Shell	**Outer Shell**
Outside Diameter, inch	12.75	35.5
Inside Diameter, inch	10.75	33.5
Length, inch	33.25	26.0
Geometry Output (nomenclature consistent with ASME Code Case N-284)		
R =	5.875	17.25
t =	1.00	1.00
R/t =	5.88	17.25
ℓ_ϕ =	33.25	26.0
ℓ_θ =	36.91	108.38
M_ϕ =	13.72	6.26
M_θ =	15.23	26.10
M =	13.72	6.26

Table 2.7-9 - Shell Stress for 21.7 psi Differential Pressure

Inner Shell		**Outer Shell**	
Axial Stress, σ_ϕ	63.8 psi	Axial Stress, σ_ϕ	187.2 psi
Hoop Stress, σ_θ	127.5 psi	Hoop Stress, σ_θ	374.3 psi
Shear Stress, $\sigma_{\phi\theta}$	31.9 psi	Shear Stress, $\sigma_{\phi\theta}$	93.6 psi

Table 2.7-10 - Cask Immersion N-284-1 Summary

Condition	Inner Shell	Outer Shell	Remarks
Capacity Reduction Factors (-1511)			
$\alpha_{\phi L}$ =	0.2217	0.2748	
$\alpha_{\theta L}$ =	0.8000	0.8000	
$\alpha_{\phi\theta L}$ =	0.8000	0.8000	
Plasticity Reduction Factors (-1610)			
$\eta_{\phi L}$ =	0.0328	0.0811	
$\eta_{\theta L}$ =	0.0935	0.0523	
$\eta_{\phi\theta L}$ =	0.0163	0.0837	
Theoretical Buckling Values (-1712.1.1)			
C_{ϕ} =	0.6050	0.6050	
$\sigma_{\phi cL}$ =	2,651,702 psi	926,965 psi	
$C_{\theta r}$ =	0.0588	0.1807	
$\sigma_{\theta cL} = \sigma_{reL}$ =	257,867 psi	276,932 psi	
$C_{\theta h}$ =	0.0588	0.1636	
$\sigma_{\theta cL} = \sigma_{hcL}$ =	257,867 psi	250,637 psi	
$C_{\phi\theta}$ =	0.2028	0.3222	
$\sigma_{\phi\theta cL}$ =	888,920 psi	493,697 psi	
Elastic Interaction Equations (-1713.1.1)			
σ_{xa} =	438,793 psi	190,104 psi	
σ_{ha} =	153,950 psi	149,634 psi	
σ_{ra} =	153,950 psi	165,332 psi	
$\sigma_{\tau a}$ =	530,699 psi	294,745 psi	
Axial + Hoop ⇨ Check (a):	*N/A*	*N/A*	
Axial + Hoop ⇨ Check (b):	*N/A*	*N/A*	
Axial + Shear ⇨ Check (c):	*0.0001*	*0.0010*	<1 ∴ OK
Hoop + Shear ⇨ Check (d):	*0.0008*	*0.0023*	<1 ∴ OK
Axial + Hoop + Shear ⇨ Check (e,a):	*N/A*	*N/A*	
Axial + Hoop + Shear ⇨ Check (e,b):	*N/A*	*N/A*	
Inelastic Interaction Equations (-1713.2.1)			
σ_{xc} =	14,396 psi	15,418 psi	
σ_{rc} =	14,396 psi	8,648 psi	
$\sigma_{\tau c}$ =	8,637 psi	24,669 psi	
Axial + Hoop ⇨ Check (a):	*0.0089*	*0.0433*	<1 ∴ OK
Axial + Shear ⇨ Check (b):	*0.0044*	*0.0122*	<1 ∴ OK
Hoop + Shear ⇨ Check (c):	*0.0008*	*0.0023*	<1 ∴ OK

2.7.7 Summary of Damage

From the analyses presented in Section 2.7.1 through 2.7.6, it is shown that the hypothetical accident sequence does not result in any significant structural damage to the SEC, and that all stress criteria established for hypothetical accident conditions in Section 2.1.2 are satisfied. Most permanent damage occurs in the impact limiters in the free drop and puncture events, and is acceptable. Damage to the package surface also occurs due to the puncture event described in Section 2.7.3. However, it is shown that the outer shell is not perforated, and deformation is limited to an area approximately the size of the puncture bar diameter. The thermal consequences of puncture damage to both the impact limiters and to the package surface are discussed in Section 3.5.

A dynamic test of the impact limiters was performed as discussed in Section 2.10.5. Three 30 ft free drops and three 40 inch puncture drops were performed. The 30 ft free drop testing was performed in the end (vertical), side (horizontal), and c.g. over corner orientations, and demonstrated the ability of the finite element impact analysis to accurately predict bounding values of impact acceleration and deformation. The 40 inch puncture drop testing was performed in three different orientations which included a drop on the impact limiter, with the puncture bar axis aligned with the c.g. of the package. Only minor denting of the limiter toroid resulted, having no effect on thermal or structural analysis assumptions.

The dynamic testing also demonstrated the ability of the impact limiter attachments to withstand dynamic forces. As discussed in Section 2.7.1.5, the side drop orientation places the maximum free drop load on the impact limiter attachments. In the test 30 ft side drop, no significant damage to the attachment ball-lock pins occurred. In addition, one of the three puncture drop tests was oriented to apply a worst-case loading to the impact limiter attachments. Although four of the attachment pins sheared off, the limiter remained attached to the test cask after the drop. Also of note is that the test article had only eight attachment pins, whereas the SEC will feature 12 pins. Therefore, retention of the impact limiter in free drops or puncture drops is assured.

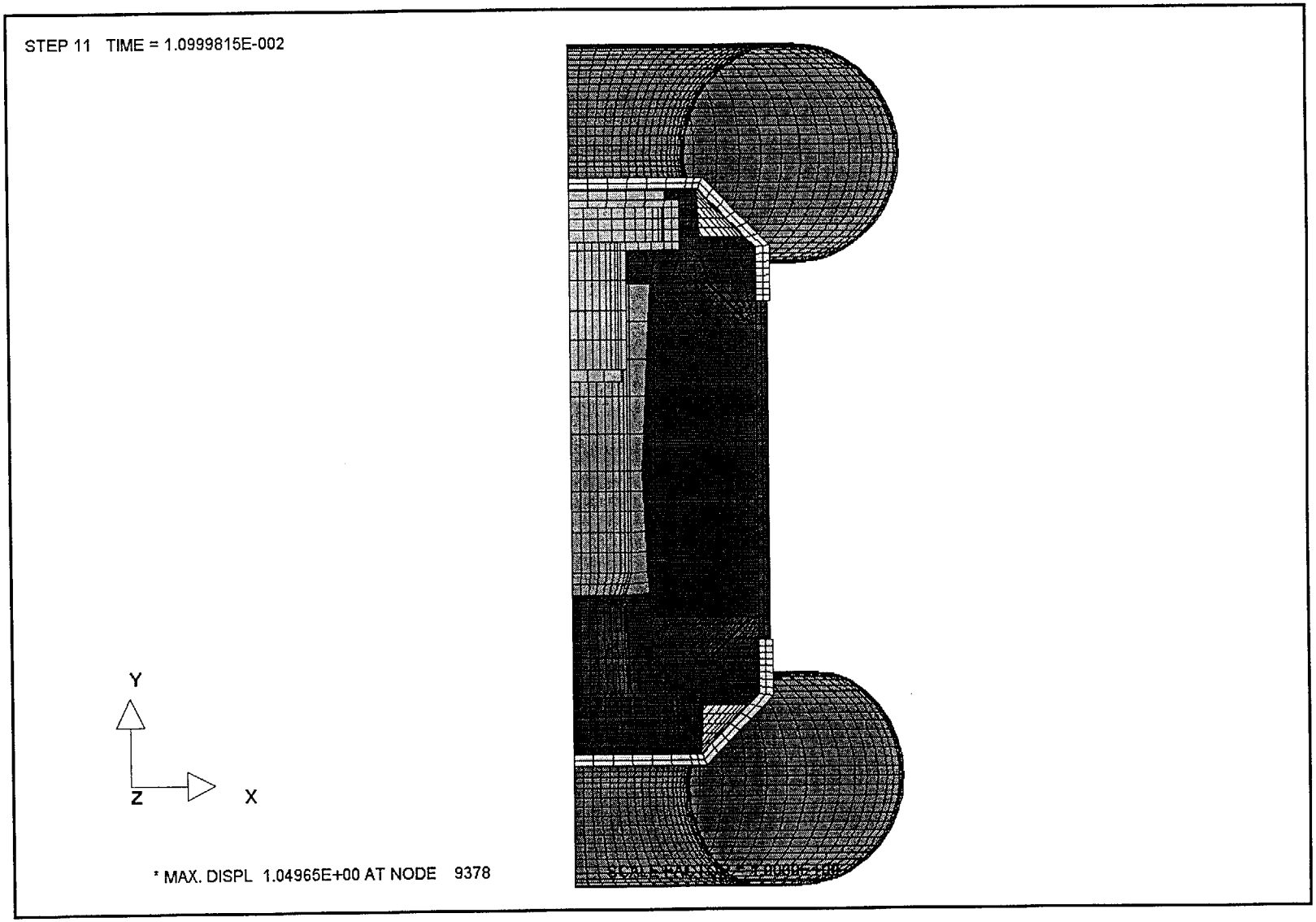

Figure 2.7-1 - Impact Limiter Deformed Shape, Warm NCT End Drop

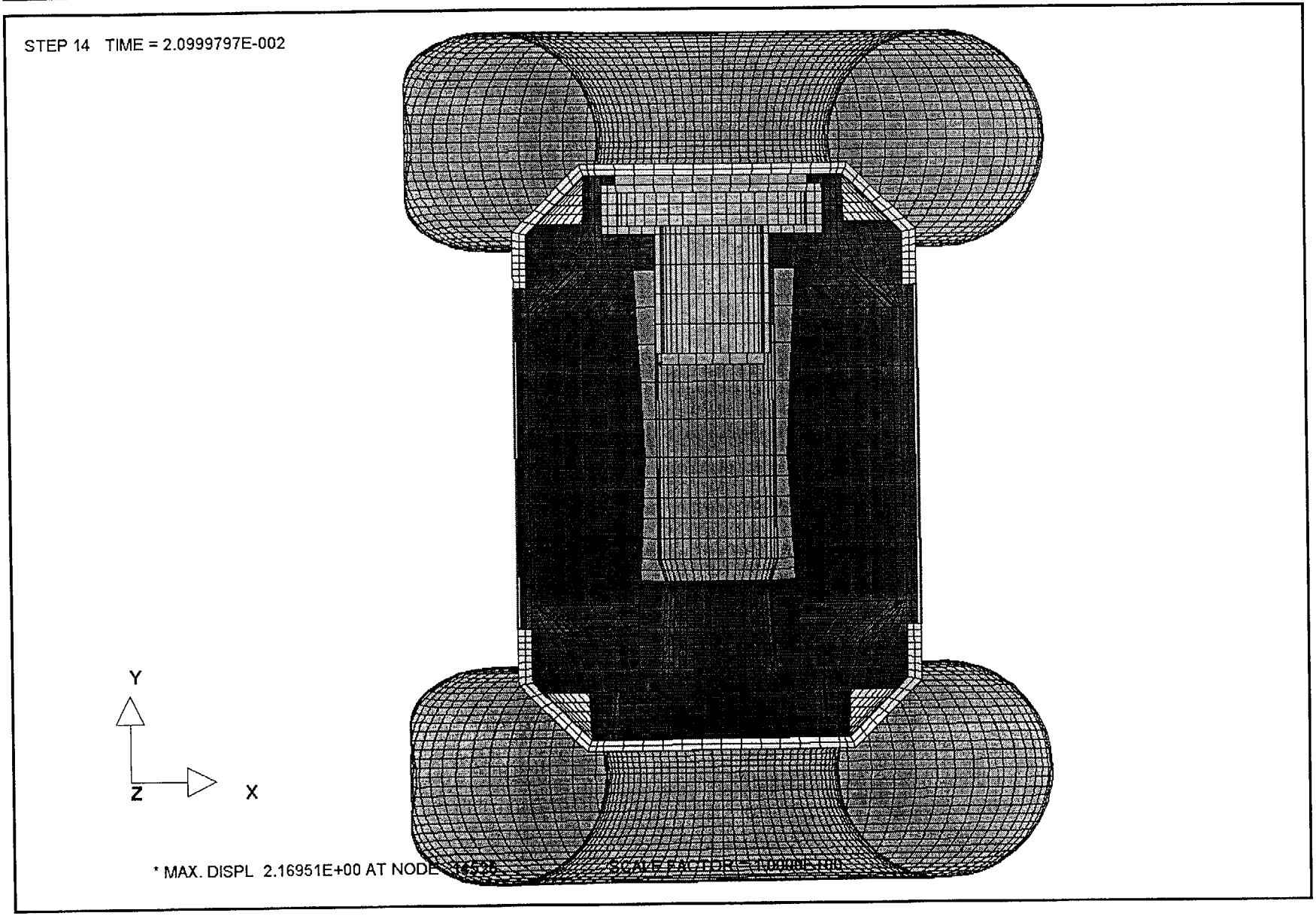

Figure 2.7-2 - Impact Limiter Deformed Shape, Warm NCT Side Drop

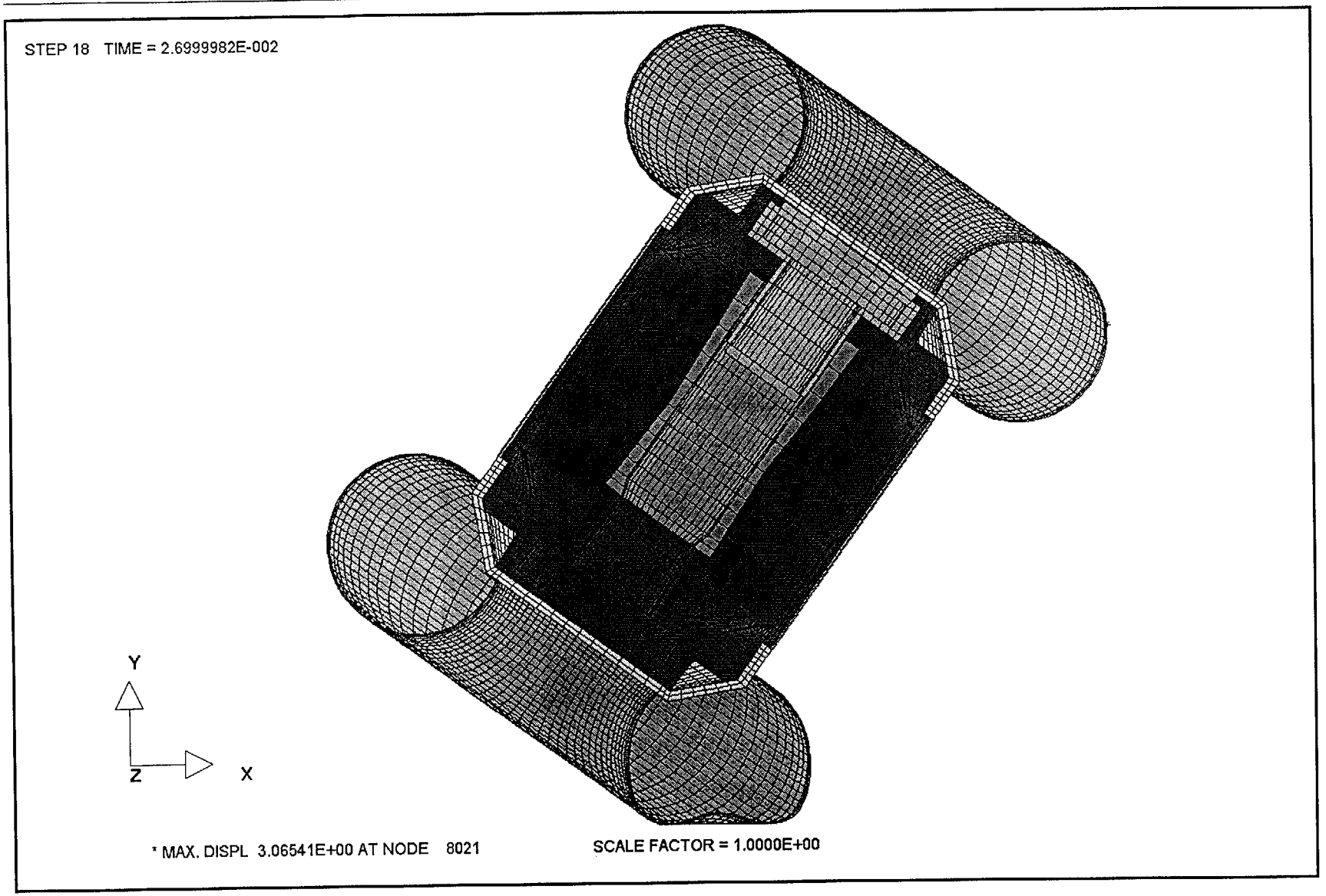

Figure 2.7-3 - Impact Limiter Deformed Shape, Warm NCT C.G.-Over-Corner Drop

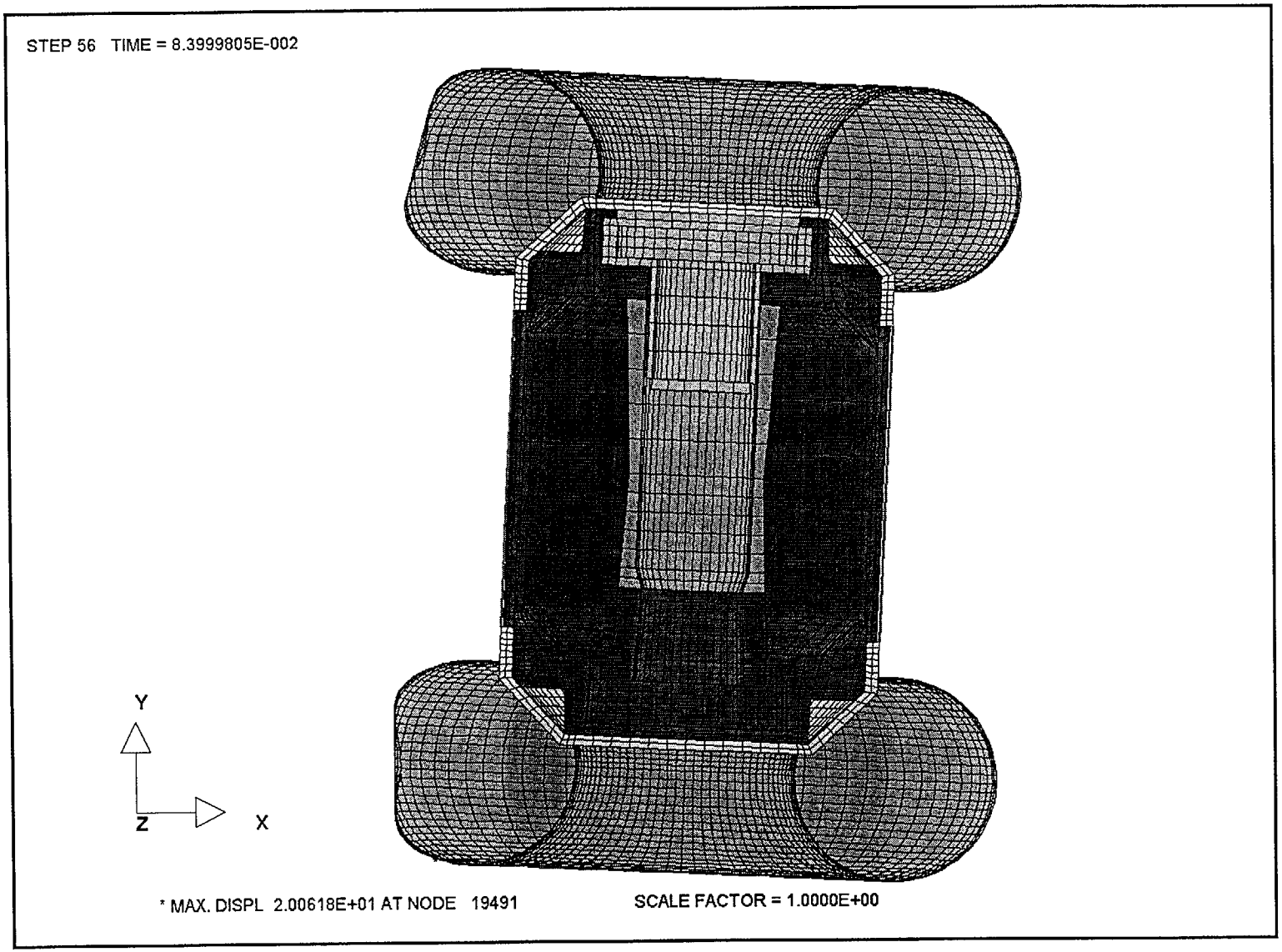

Figure 2.7-4 - Impact Limiter Deformed Shape, Warm NCT Slapdown Drop

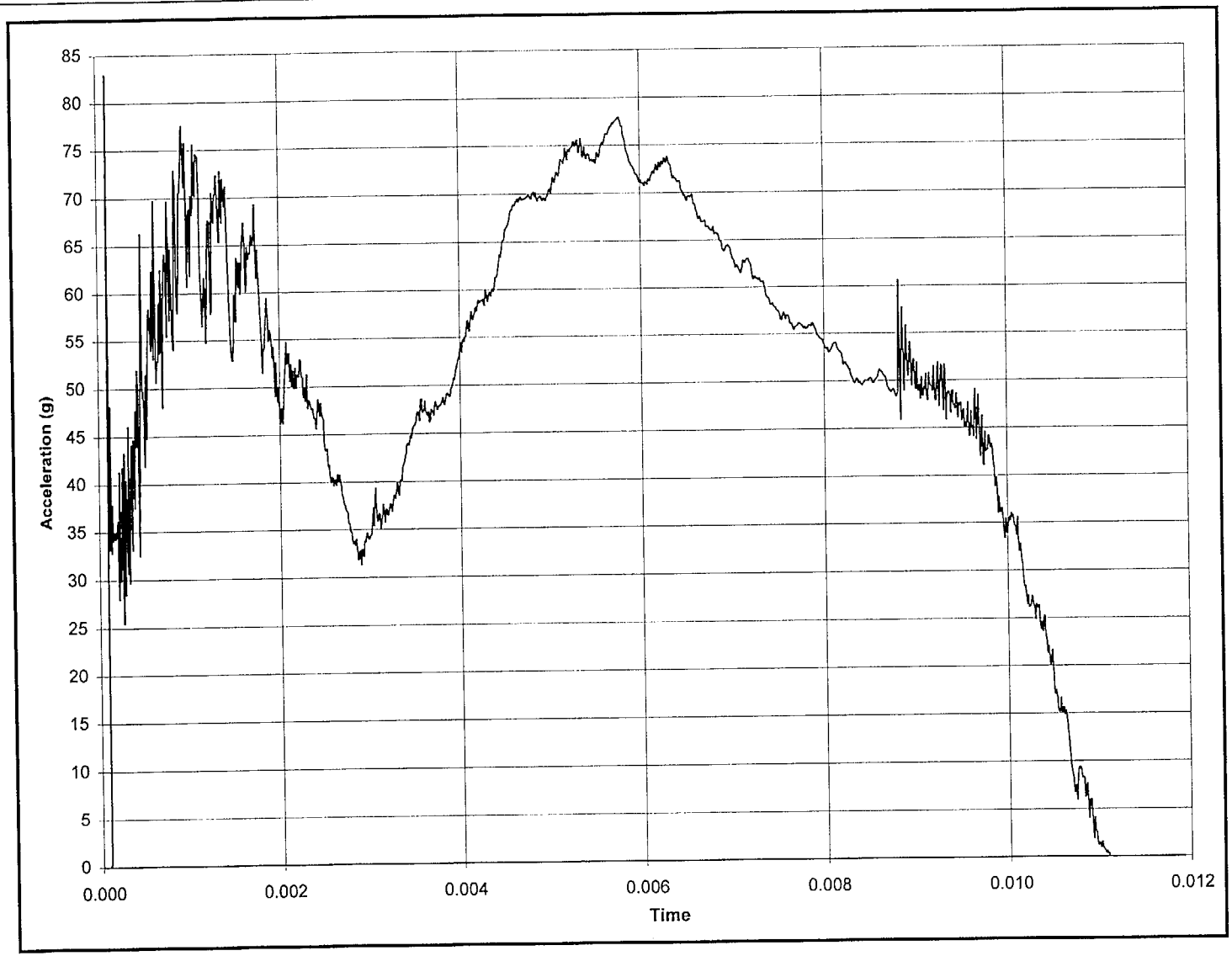

Figure 2.7-5 - Impact Time History, Cold NCT End Drop

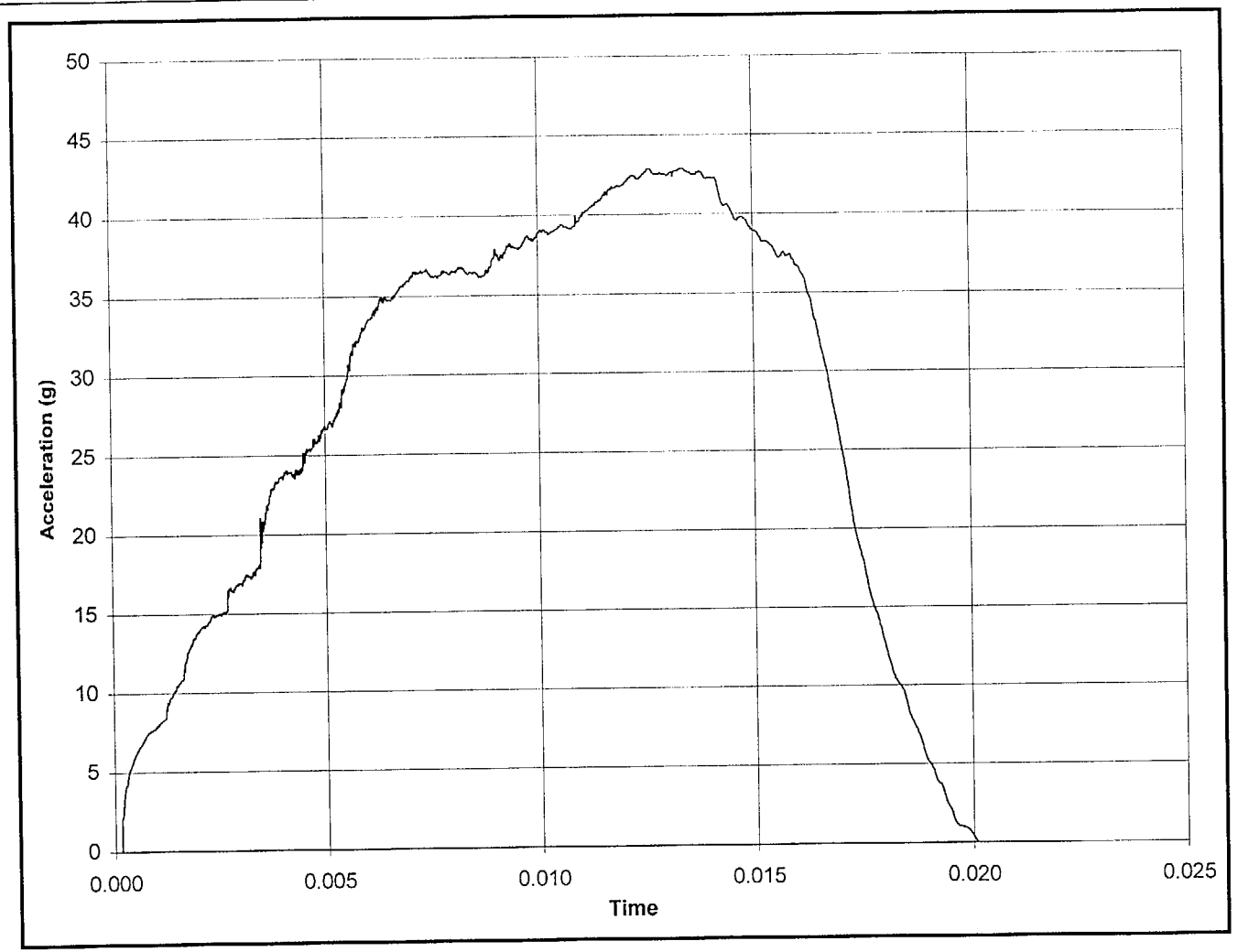

Figure 2.7-6 - Impact Time History, Cold NCT Side Drop

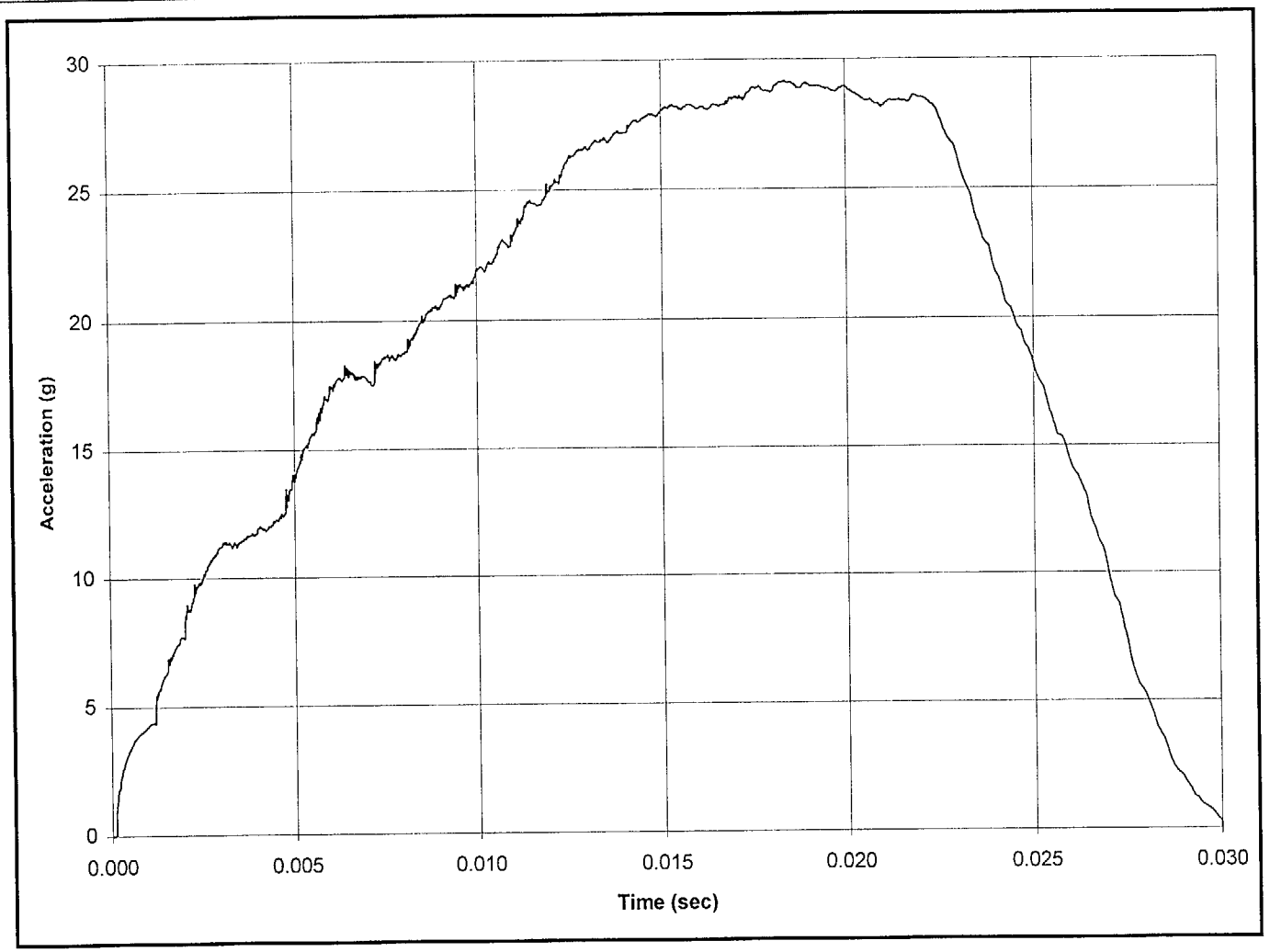

Figure 2.7-7 - Impact Time History, Cold NCT C.G.-Over-Corner Drop

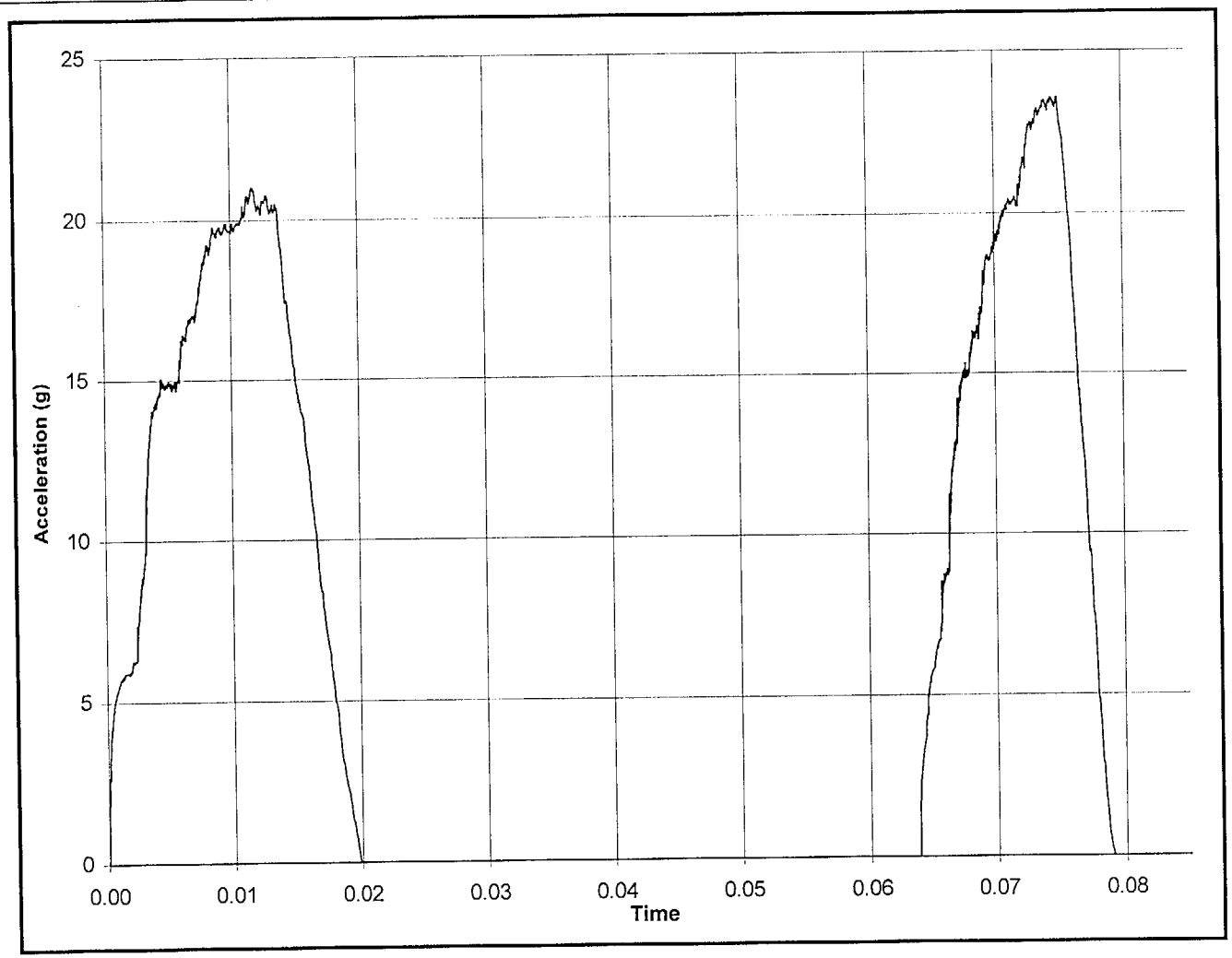

Figure 2.7-8 - Impact Time History, Cold NCT Slapdown Drop

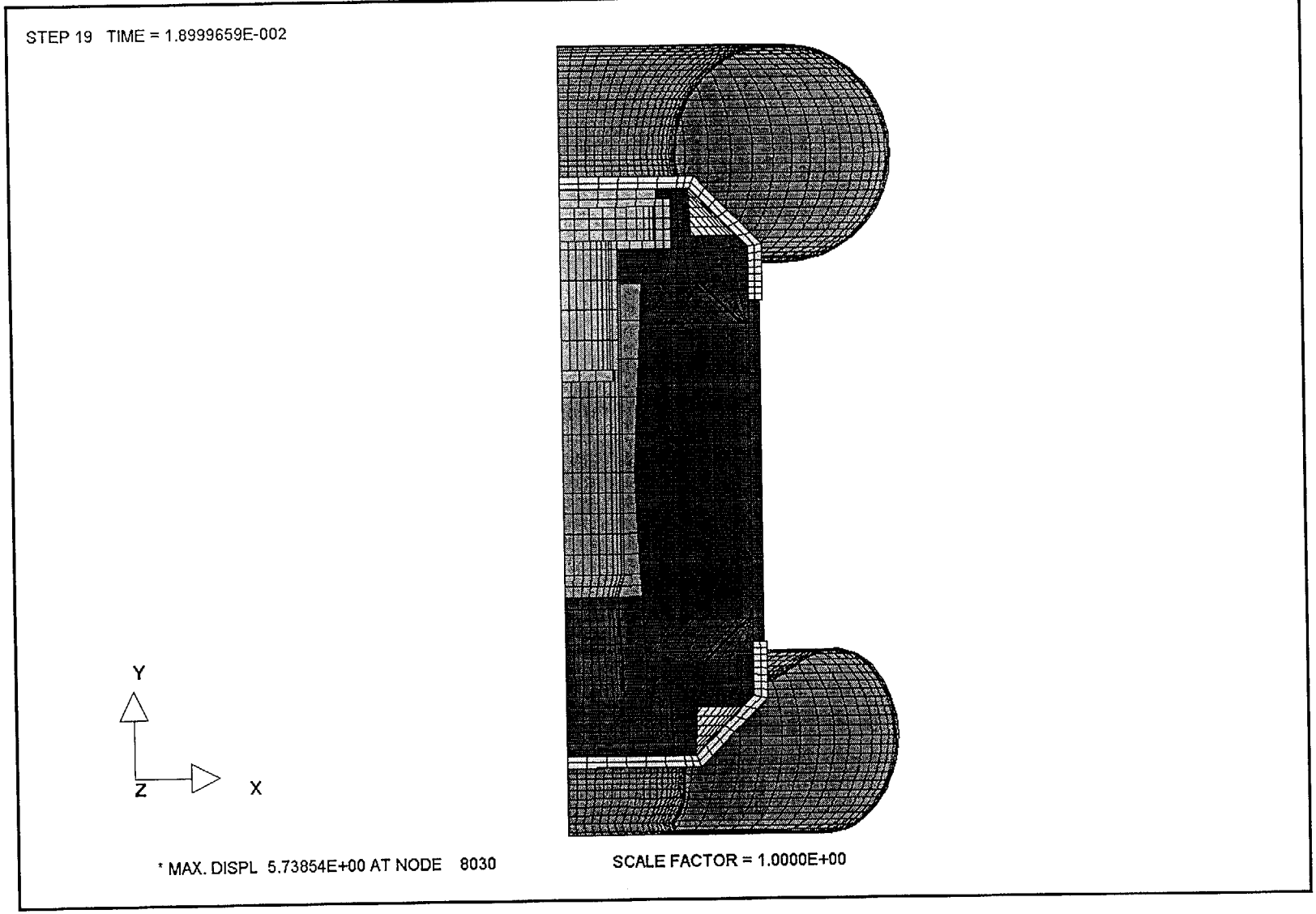

Figure 2.7-9 - Impact Limiter Deformed Shape, Warm HAC End Drop

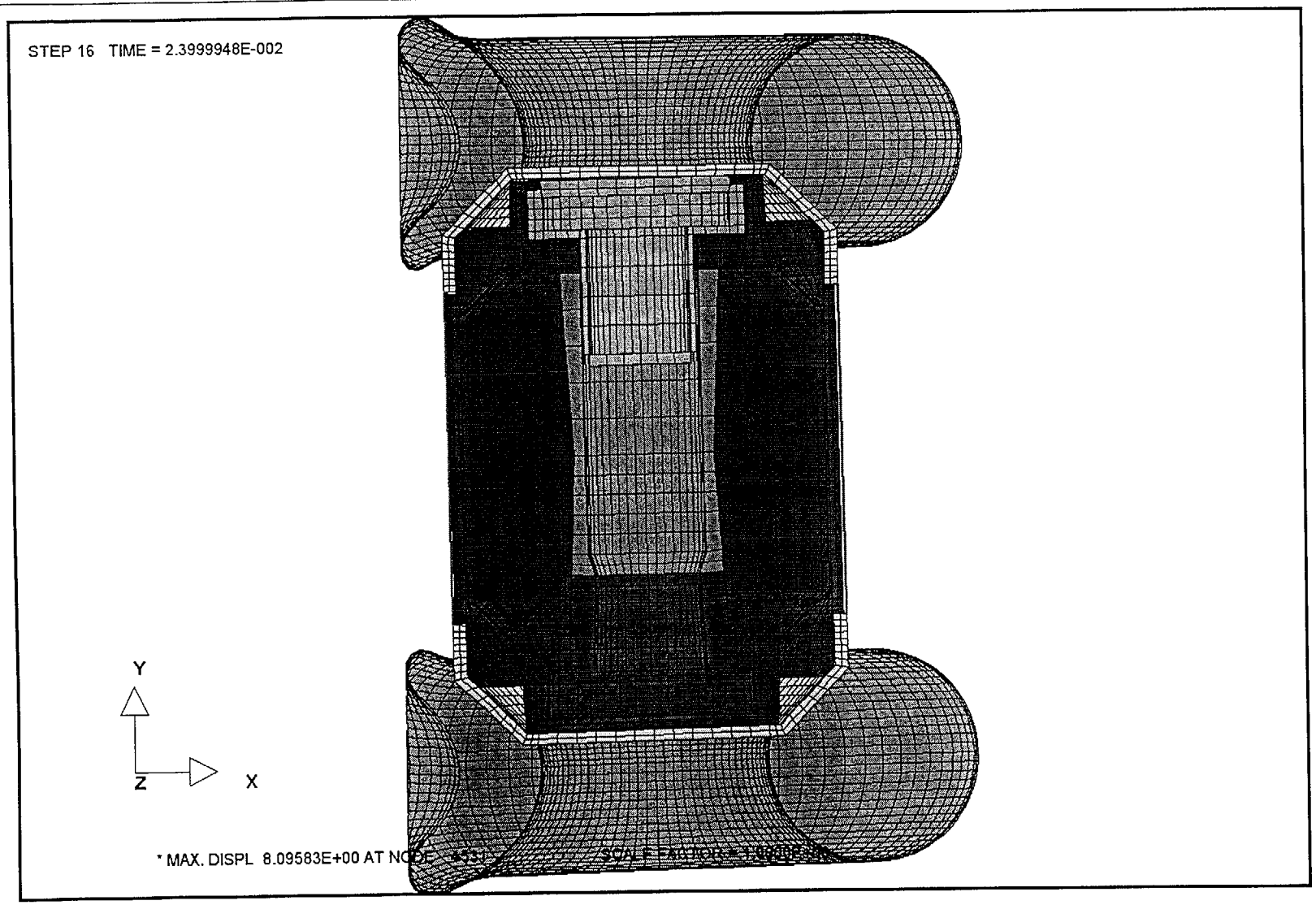

Figure 2.7-10 - Impact Limiter Deformed Shape, Warm HAC Side Drop

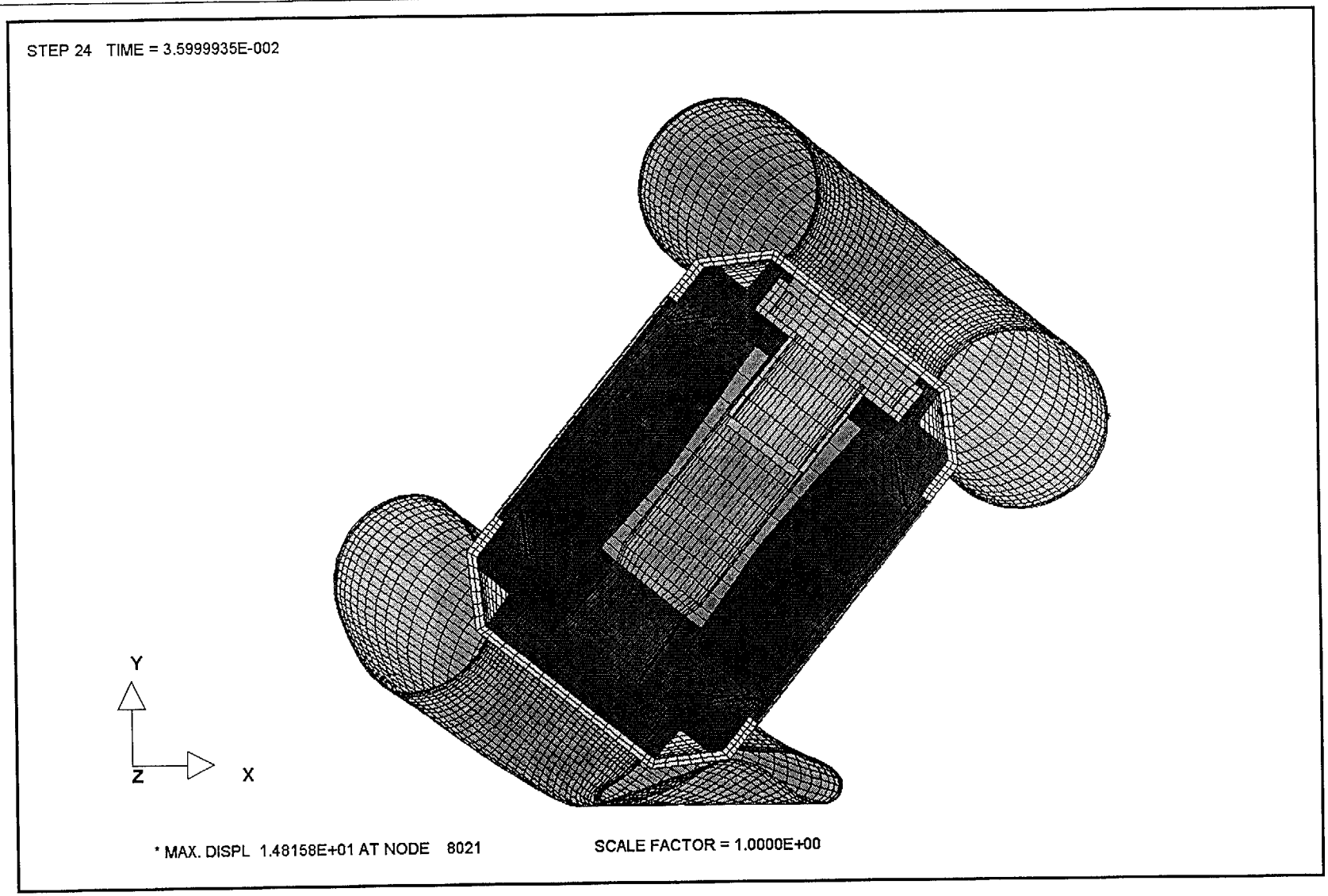

Figure 2.7-11 - Impact Limiter Deformed Shape, Warm HAC C.G.-Over-Corner Drop

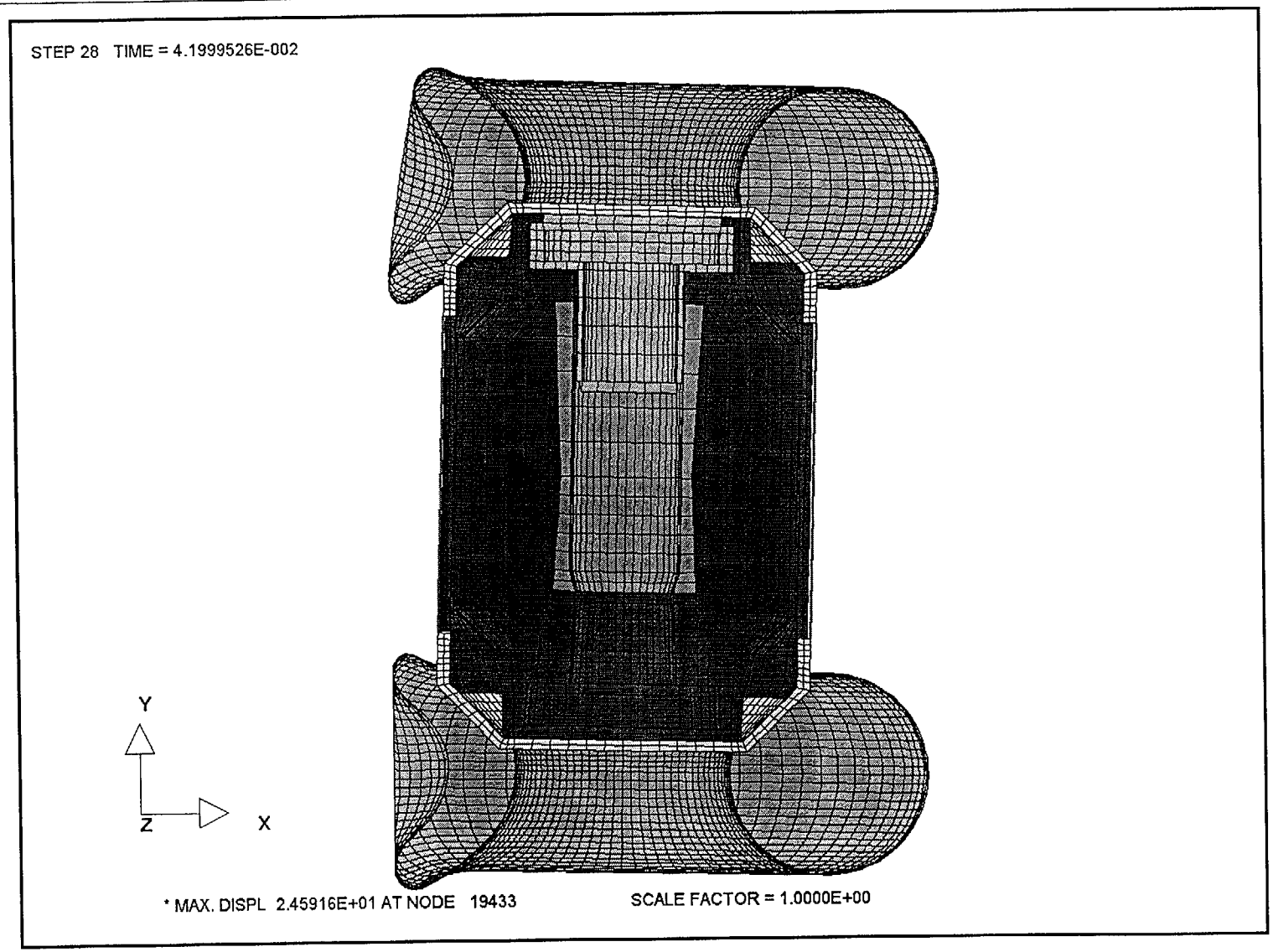

Figure 2.7-12 - Impact Limiter Deformed Shape, Warm HAC Slapdown Drop

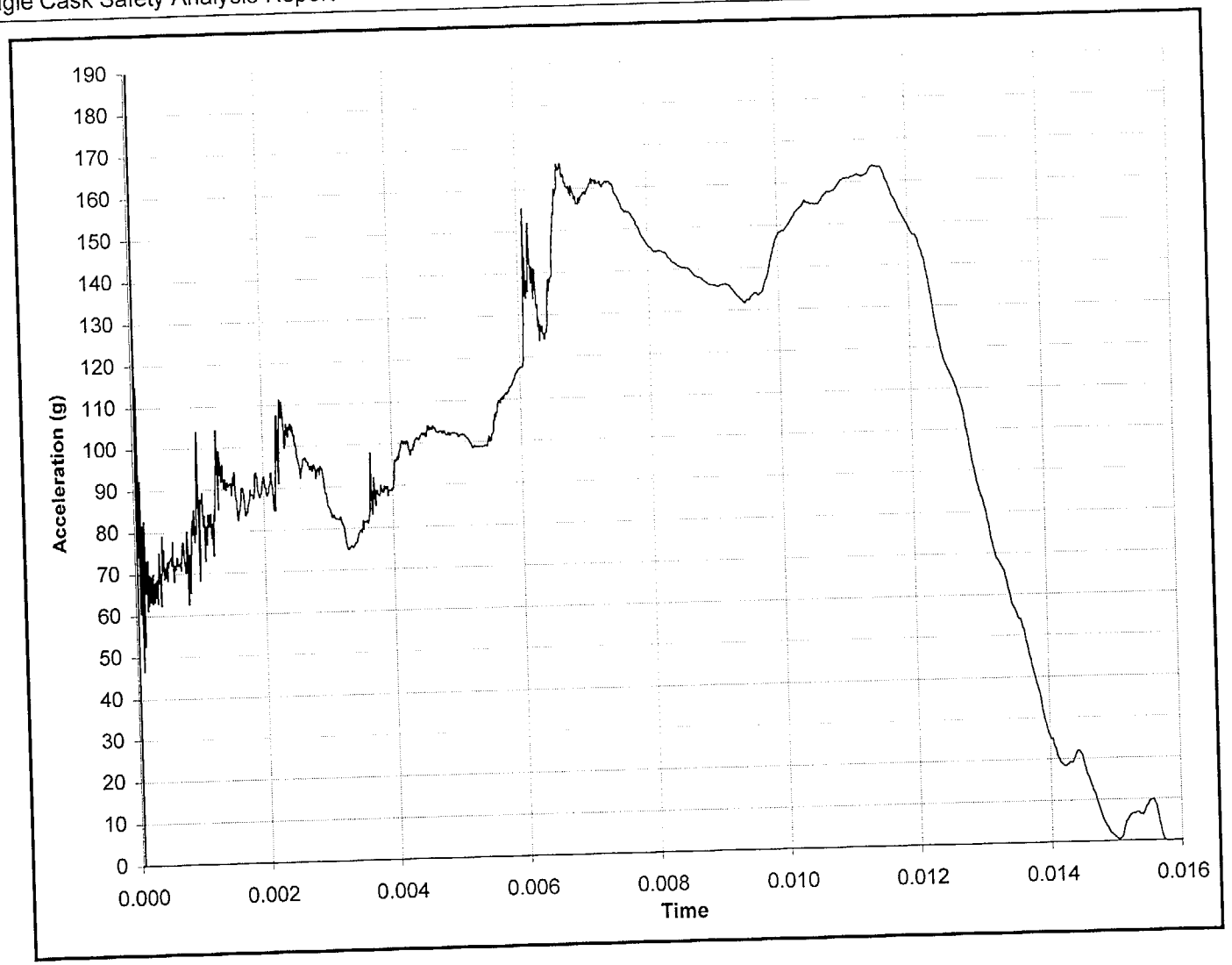

Figure 2.7-13 - Impact Time History, Cold HAC End Drop

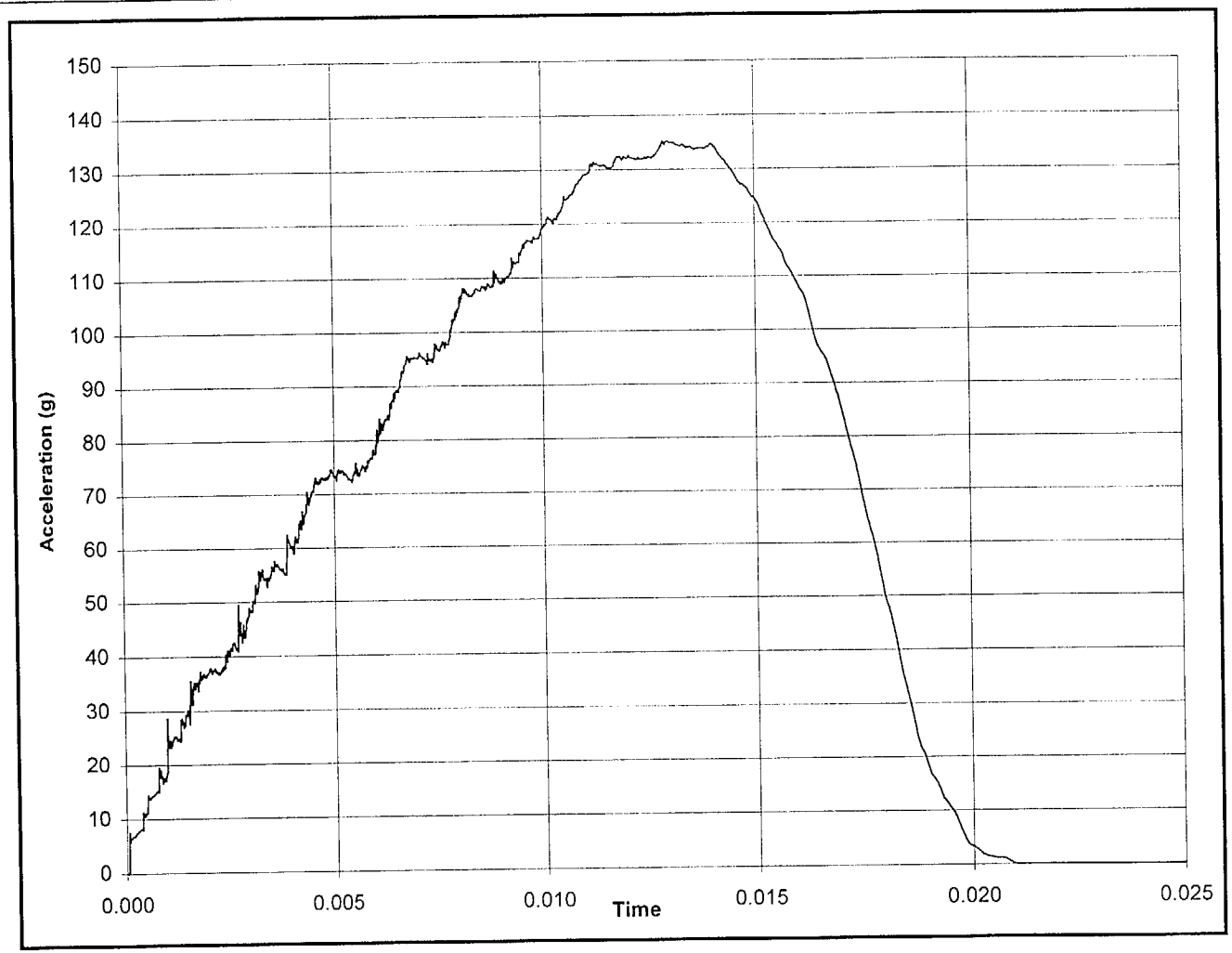

Figure 2.7-14 - Impact Time History, Cold HAC Side Drop

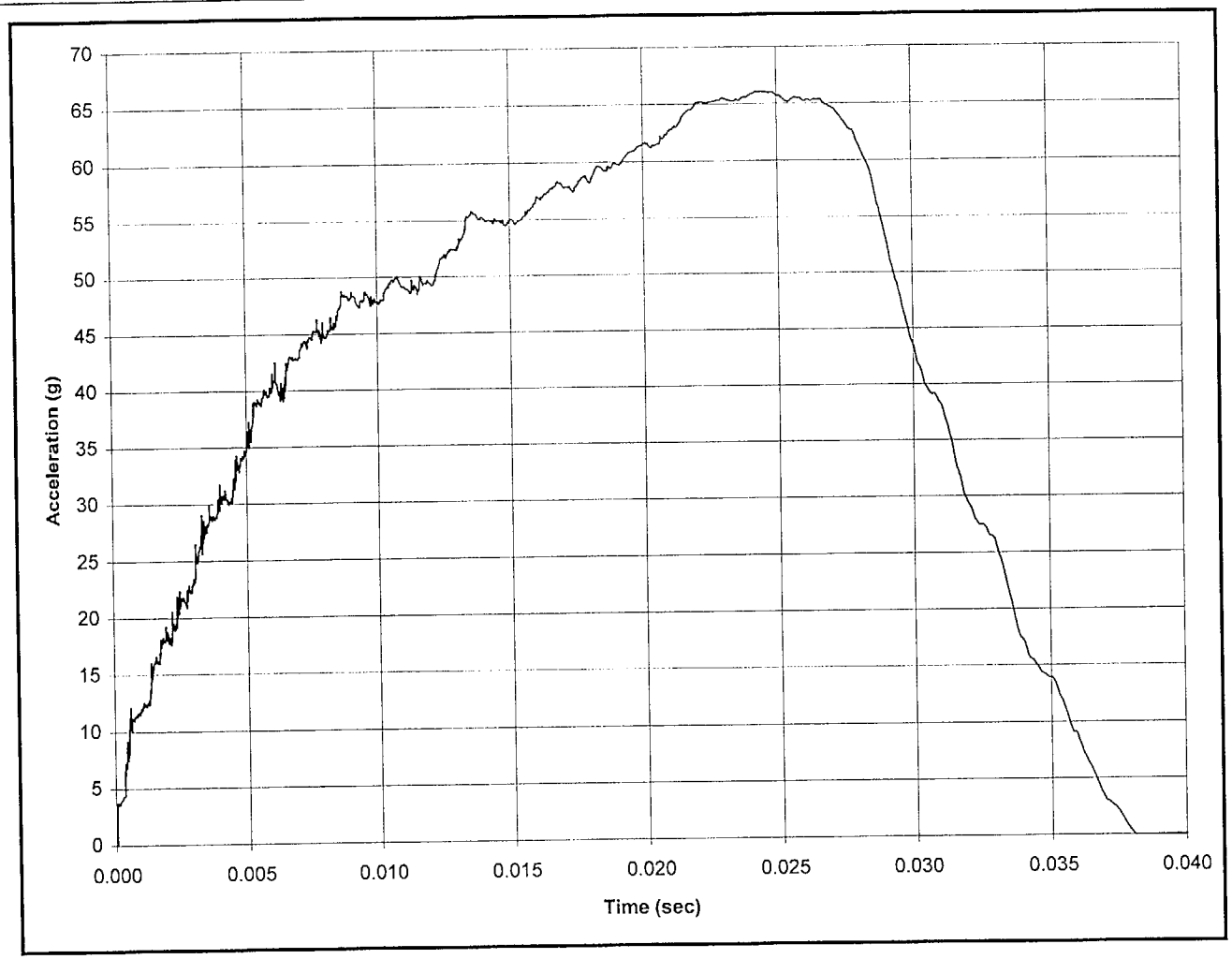

Figure 2.7-15 - Impact Time History, Cold HAC C.G.-Over-Corner Drop

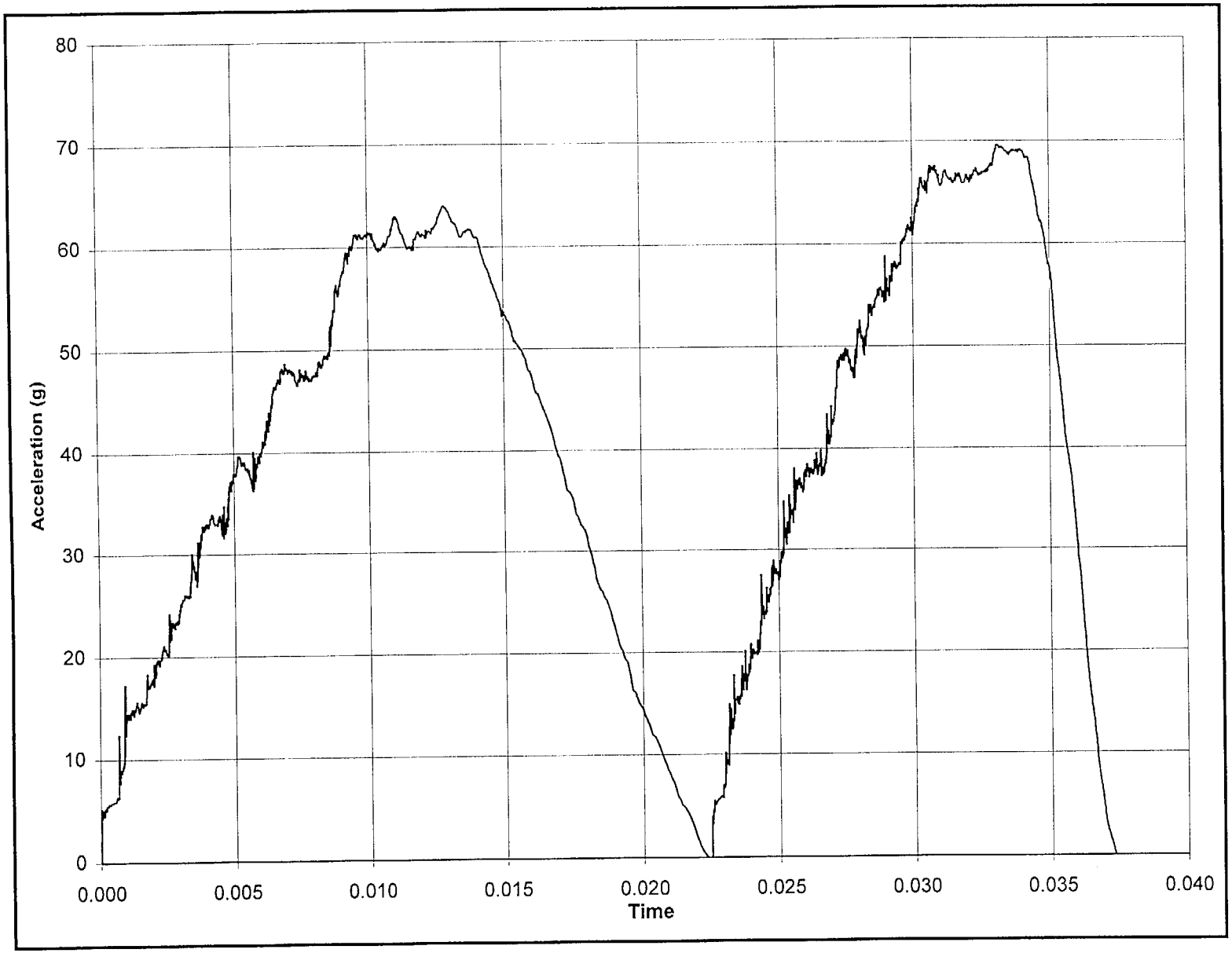

Figure 2.7-16 - Impact Time History, Cold HAC Slapdown Drop

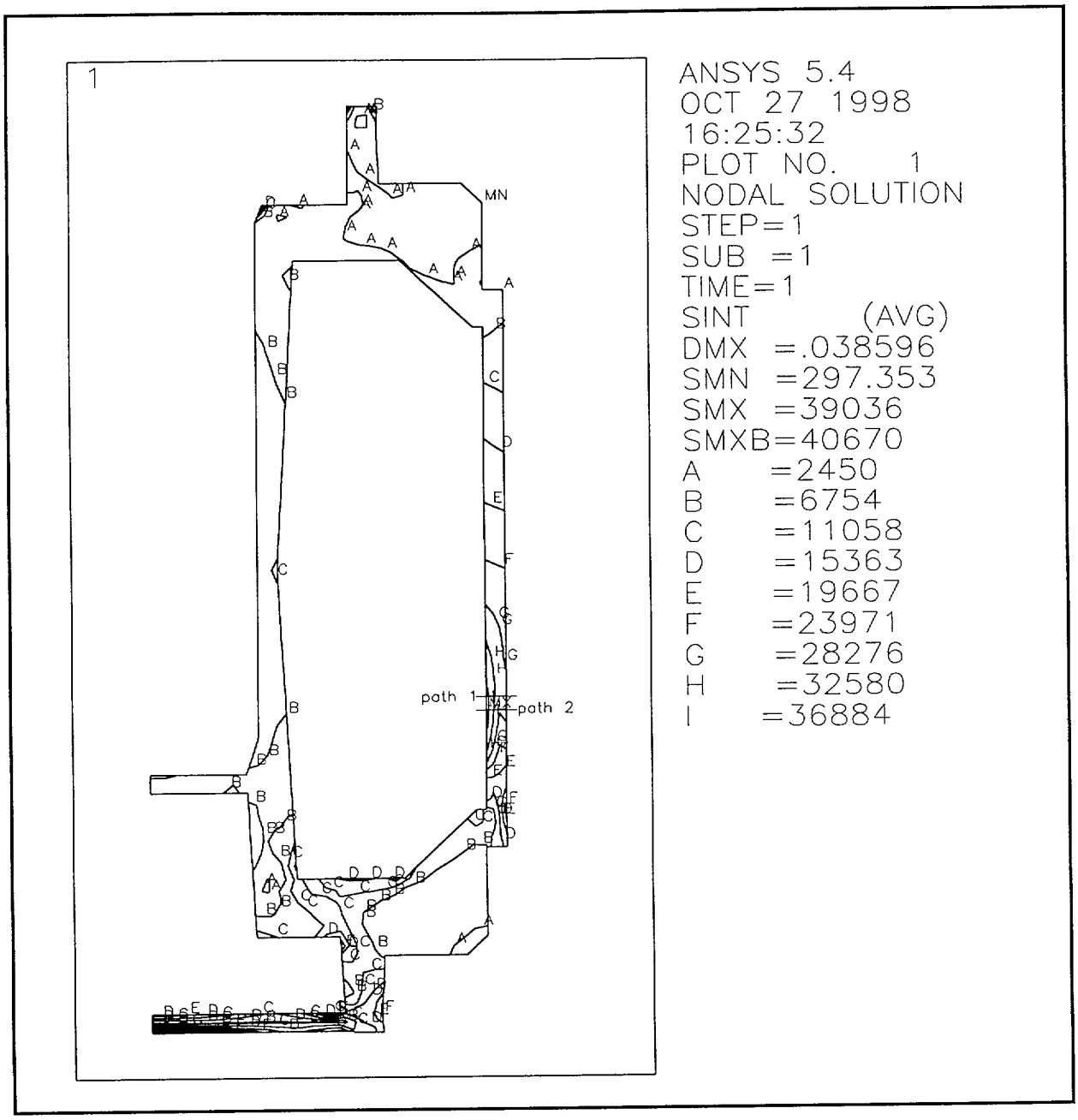

Figure 2.7-17 - HAC Bottom-Down End Drop Stress Contours

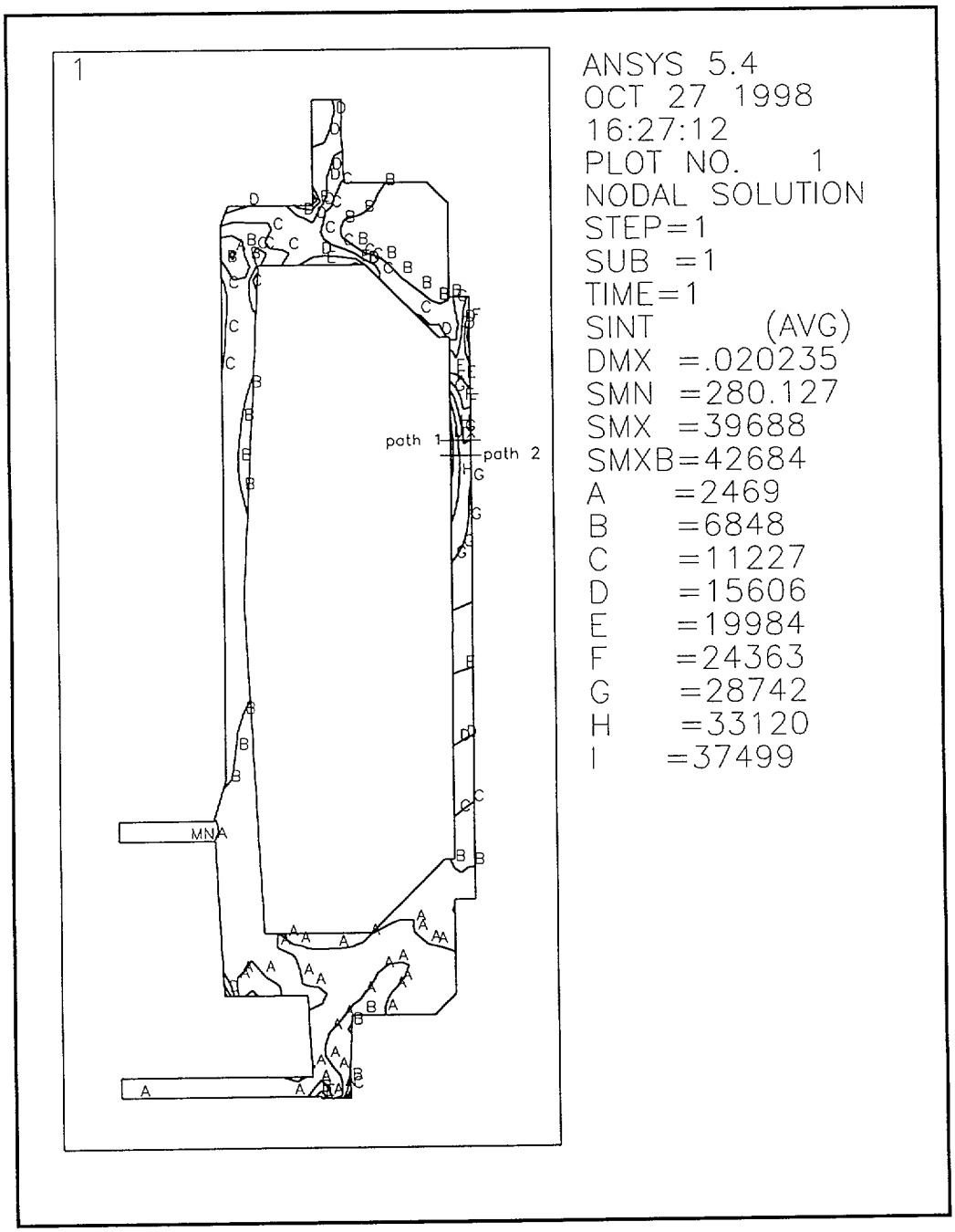

Figure 2.7-18 - HAC Top-Down End Drop Stress Contours

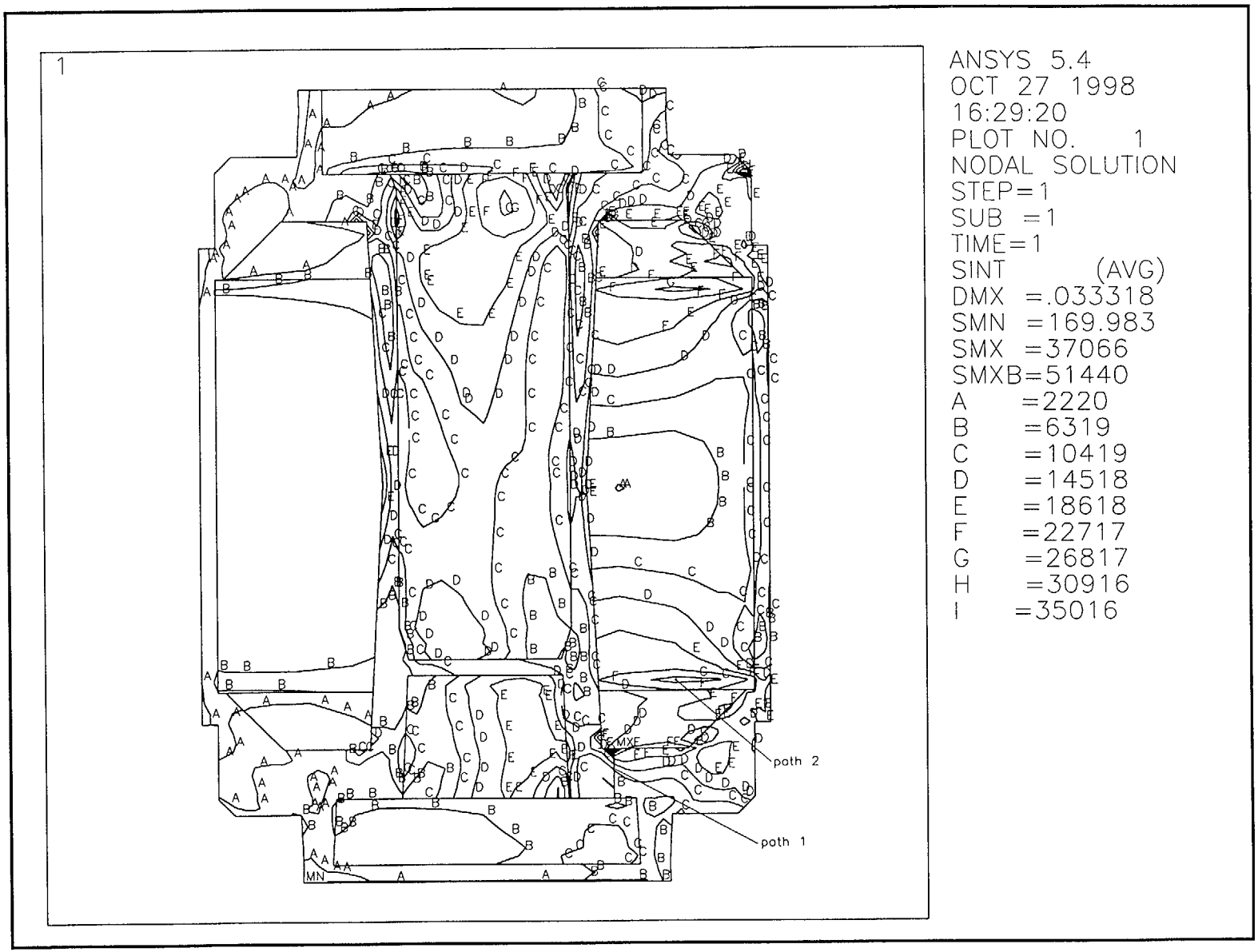

Figure 2.7-19 - HAC Side Drop Stress Contours

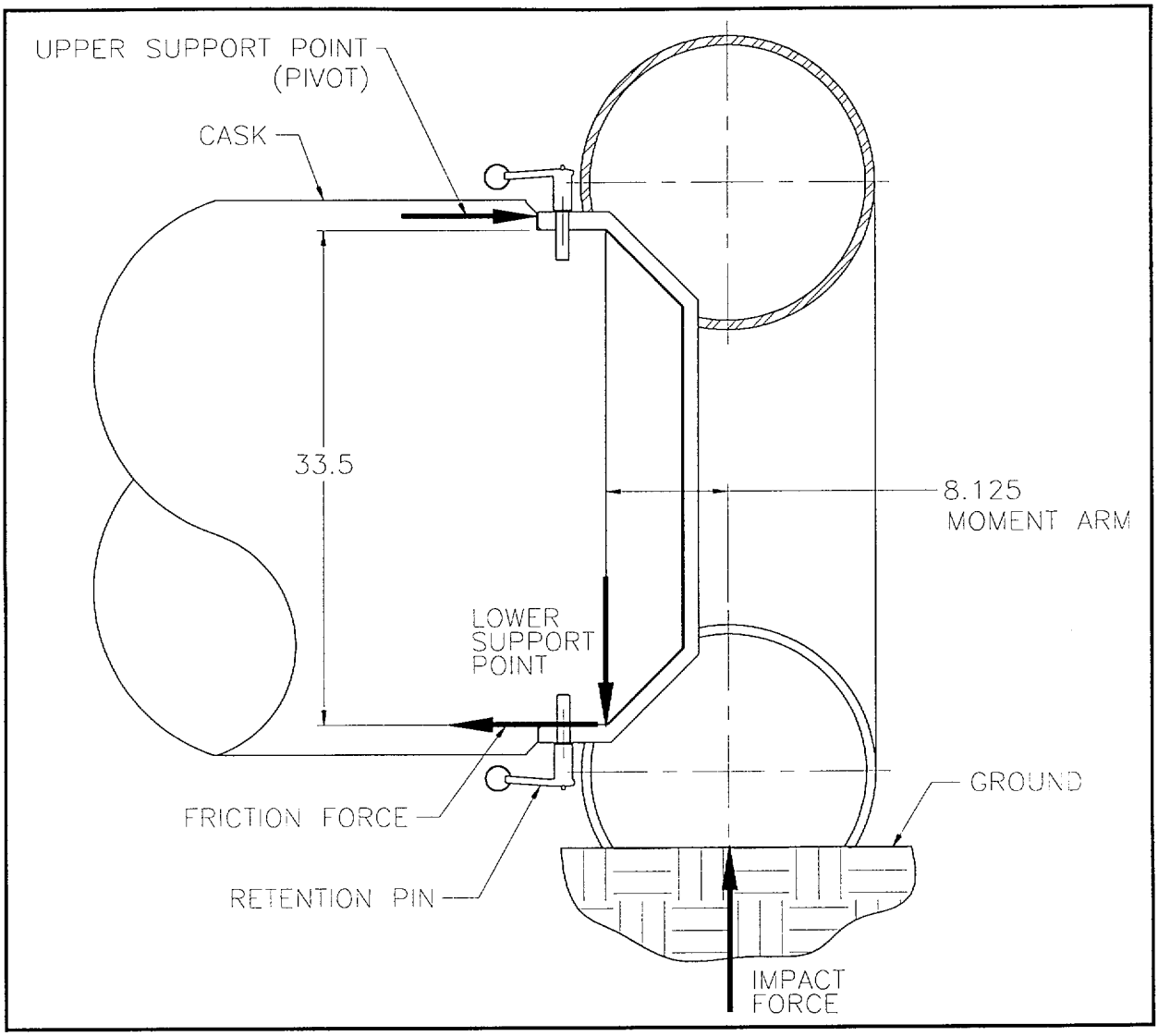

Figure 2.7-20 - Impact Limiter Attachment Pins - Force Diagram

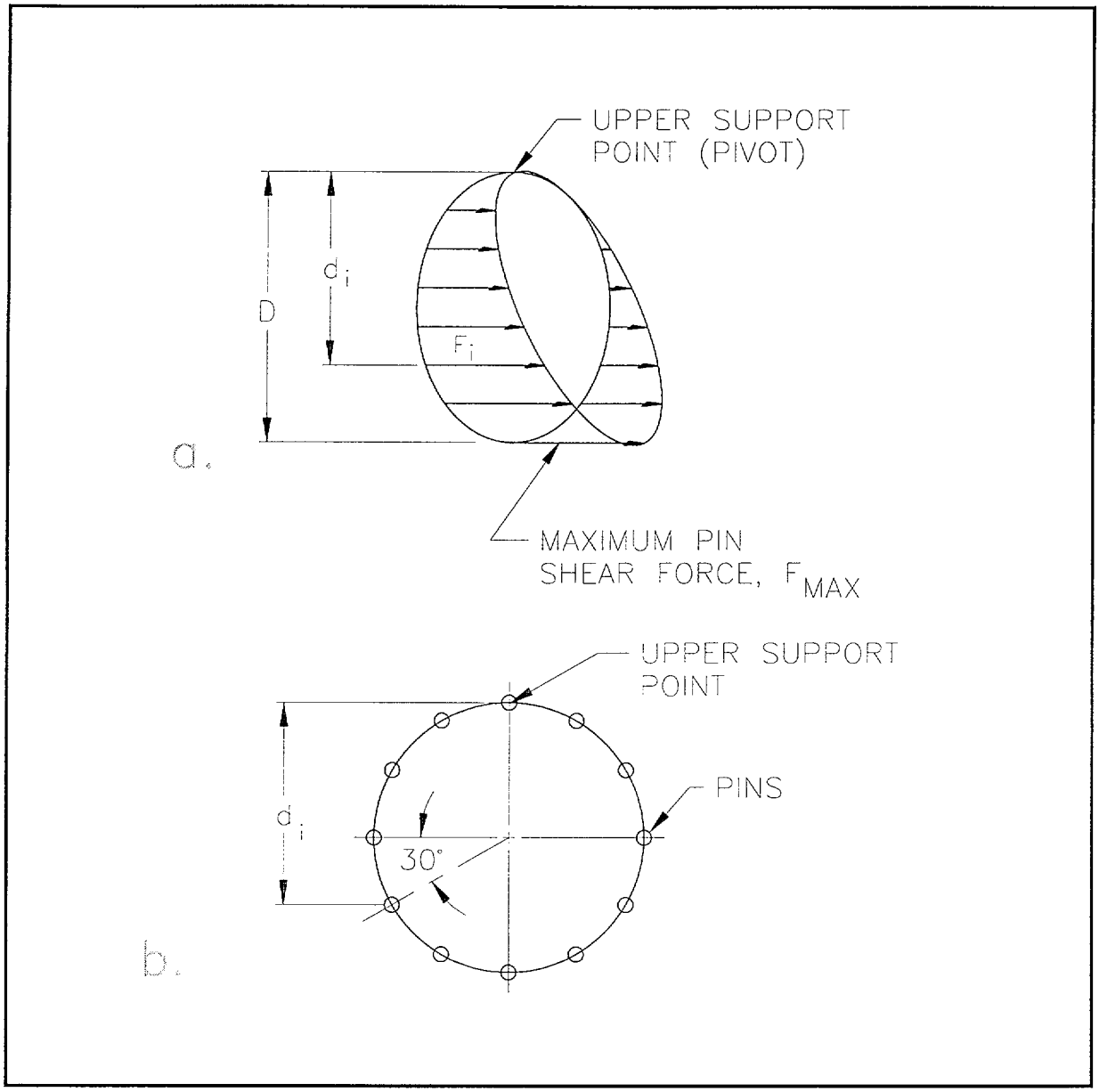

Figure 2.7-21 - Impact Limiter Attachment Pin Load Distribution

2.8 Special Form Certification

The contents of the SteriGenics Eagle Cask (SEC) are special form Cobalt-60 source capsules. Three types of capsules are included in this application as potential payloads. They are manufactured by: (1) Nordion International, Inc., (2) Puridec, and (3) Neutron Products, Inc.. All source capsules are limited to a maximum of 18,333 Curies each. The special form certifications for the above capsules are as follows:

Manufacturer	**Model Number**	**Certification Number**
Nordion International, Inc.	C-188 capsule, Types 1 through 12	CDN/0010/S-85
Puridec	X.2089	GB/343/S-85
Neutron Products, Inc.	NPRP 450-10-B	USA/0458/S

2.9 Fuel Rods

This section does not apply, since fuel rods are not shipped in the SEC.

2.10 Appendices

2.10.1 References

1. Title 10, Code of Federal Regulations, Part 71 (10 CFR 71), *Packaging and Transportation of Radioactive Material*, 1-1-98 Edition.
2. U. S. Nuclear Regulatory Commission, Regulatory Guide 7.6, *Design Criteria for the Structural Analysis of Shipping Cask Containment Vessels*, Revision 1, March 1978.
3. U. S. Nuclear Regulatory Commission, Regulatory Guide 7.8, *Load Combinations for the Structural Analysis of Shipping Casks for Radioactive Material*, Revision 1, March 1978.
4. American Society of Mechanical Engineers (ASME) Boiler and Pressure Vessel Code, Section III, *Rules for Construction of Nuclear Power Plant Components*, 1995 Edition, 1997 Addenda.
5. American Society of Mechanical Engineers (ASME) Boiler and Pressure Vessel Code, Section II, *Materials*, Part D, *Properties*, 1995 Edition, 1997 Addenda.
6. American Society of Mechanical Engineers (ASME) Boiler and Pressure Vessel Code, Section III, *Rules for Construction of Nuclear Power Plant Components*, Division 1, Class MC, Code Case N-284-1, *Metal Containment Shell Buckling Design Methods*, 1995 Edition, 1997 Addenda.
7. G. C. Mok, L. E. Fischer, S. T. Hsu, *Stress Analysis of Closure Bolts for Shipping Casks*, NUREG/CR-6007, UCRL-ID-110637, U. S. Nuclear Regulatory Commission, 1992.
8. W. R. Holman, R. T. Langland, *Recommendations for Protecting Against Failure by Brittle Fracture in Ferritic Steel Shipping Containers Up to Four Inches Thick*, NUREG/CR-1815, URCL-53013, U. S. Nuclear Regulatory Commission, August 1981.
9. American Society of Mechanical Engineers (ASME) Boiler and Pressure Vessel Code, Section III, *Rules for Construction of Nuclear Power Plant Components*, Appendix I, *Design Stress Intensity Values, Allowable Stresses, Material Properties, and Design Fatigue Curves*, 1995 Edition, 1997 Addenda.
10. WADC Technical Report 57-695, ASTIA Document No. 151165, *"Determination of the Mechanical Properties of a High Purity Lead and a 0.05% Copper-Lead Alloy,"* April 1958, by Thomas Tietz, Stanford Research Center.
11. Henry J. Rack, Gerald A. Knorovsky, *An Assessment of Stress-Strain Data Suitable for Finite-Element Elastic-Plastic Analysis of Shipping Containers*, NUREG/CR-0481, SAND77-1872, R-7, September 1978.
12. W. Johnson, P. B. Mellor, *Engineering Plasticity*, Halstead Press/Wiley and Sons, New York, 1983.
13. Boucher, R. C., *Strength of Threads*, Product Engineering, November 27, 1961.
14. Warren C. Young, *Roark's Formulas for Stress and Strain*, Sixth Edition, McGraw-Hill, Inc., New York, 1989.

15. ANSI N14.23, *Design Basis for Resistance to Shock and Vibration of Radioactive Material Packages Greater Than One Ton in Truck Transport* (Draft), 1980, American National Standards Institute, Inc., New York.

16. Livermore Software Technology Corporation, LS-DYNA User's Manual, Report 1082, June 1, 1997, Version 940.

17. ANSYS®, Inc., ANSYS Engineering Analysis System User's Manual for ANSYS® Revision 5.4, Canonsburg, PA.

18. T. A. Nelson, R. C. Chun, *Methods for Impact Analysis of Shipping Containers*, NUREG/CR-3966, URCL-20639, U. S. Nuclear Regulatory Commission, 1987.

19. J. H. Faupel, F. E. Fisher, *Engineering Design*, Second Edition, Wiley-Interscience, New York, 1981.

20. A. Nelms, *Structural Analysis of Shipping Casks, Effect of Jacket Physical Properties and Curvature on Puncture Resistance*, ORNL-TM-1312, Vol. 3, Oak Ridge National Laboratory, 1968.

21. E. A. Avallone, T. Baumeister III, *Mark's Standard Handbook for Mechanical Engineers*, Ninth Edition, McGraw-Hill, 1986.

22. Livermore Software Technology Corporation, FEMB User's Manual, Version 26, September 5, 1996.

23. *Keenserts Inserts and Studs*, Tridair Inserts, Rexnord Corporation, 1987.

24. Department of Defense, *Metallic Materials and Elements for Aerospace Vehicle Structures*, MIL-HDBK-5F, 1 November 1990.

2.10.2 Stress Analysis Finite Element Model Descriptions

The quasi-static free drop structural evaluation of the SEC is performed using the finite element models described in this section. The end drop analysis uses an axisymmetric representation, and is described in Section 2.10.2.1. The side drop analysis uses a half-symmetric, three-dimensional representation, and is described in Section 2.10.2.2. The geometry, loading, boundary conditions, and other aspects of the models are described in the following subsections. Note, the dynamic impact event analysis finite element model is discussed in Appendix 2.10.3.

2.10.2.1 Axisymmetric End Drop Finite Element Model Description

The model is generated with ANSYS® Revision 5.4 [17] using PLANE42, 2-D structural solid elements in an axisymmetric configuration, and is shown in Figures 2.10.2-1 and 2.10.2-2. As shown, only those parts of the cask are modeled which require evaluation for stress in the NCT and HAC free drop event in the end orientation. Therefore, the impact limiters, payload, and lead shielding are not modeled structurally. The cask lid is evaluated using classical methods, and is therefore also not included in the finite element model. The weight of these structures, however, is included in the model. The manner of inclusion depends on whether the specific drop event is top-down or bottom-down, as discussed below.

Bottom-Down Drop. Details are shown in Figure 2.10.2-1. The weight of the lid is modeled as a point mass, element MASS21, conservatively considered to be concentrated at the top of the inner edge of the payload cavity. The actual loading of the lid would tend to be distributed along the top surface of the lid/cask interface. Concentrating the weight of the lid at the inner edge of the payload cavity increases its effect on total deformation and stress response. The weight used for the cask lid is 900 lb. The weight of the upper impact limiter is modeled as two MASS21 point masses, located at the two places where the impact limiter contacts the cask. One mass element is located on the uppermost annular surface of the cask, and one at the step in the end casting near the impact limiter attachment pins. Each mass element is equal to 1,000 lb for a conservative total impact limiter weight of 2,000 lb. Since the cask is supported by the lower impact limiter, the weight of the lower limiter is not modeled. The inner and outer thermal shields are not structural parts of the cask, and are therefore not explicitly modeled. The weight of the thermal shields, a total of 900 lb, is included in the end castings. Half of the weight is in the upper casting, and half in the lower casting. The added weight is located as shown in Figure 2.10.2-1, and is achieved by an increase in the density of the indicated area. The lead shielding is conservatively assumed to have no structural strength. The weight of the annular lead shield is modeled as a hydrostatic pressure whose magnitude is a function of the distance from the top of the lead annulus. The pressure is found from

$$p = \rho g y$$

where ρ is the density of lead (0.41 lb/in^3), g is the impact level in units of gravity, and y is the distance from the top of the lead. The total height of the annular lead column is 33.25 inches. The resulting varying pressure is applied on the sides (inner and outer shells) and on the bottom of the annular cavity. The weight of the lower end lead is modeled as a distributed pressure load over the upper surface of the lower closure plate. The magnitude of the pressure is found from

$$p = \frac{W_L}{A} g$$

where W_L = 750 lb, A = 298.6 in^2, based on a maximum radius of the lower lead of 9.75 inches, and g is the impact level in units of gravity. The weight of the payload is much less than 1% of the modeled weight, and is therefore neglected.

The bottom-down model is supported against the applied loading by means of a pressure applied on the lowermost annular surface of the cask as shown in Figure 2.10.2-1. In addition, a single node is constrained in the axial direction. The applied support pressure is adjusted until the reaction force at this node is negligibly small.

Top-Down Drop. Details are shown in Figure 2.10.2-2. The weight of the lid is modeled as a point mass (MASS21) located at the lid bolt circle, which represents the lid as suspended by the bolts in a top-down orientation. The weight of the lower impact limiter is modeled using two point masses, in the same manner as described above for the upper impact limiter in the bottom-down orientation. Since the cask is supported by the upper impact limiter, the weight of the upper limiter is not modeled. The weight of the lower lead is conservatively considered to be concentrated at a point (MASS21) located at the lower inside corner of the inner shell. The weight of the lower lead would normally load the structure in a distributed manner, and thus its concentration at a point conservatively increases deformation and stress response. The weight of the annular lead, the thermal shields, and the payload are treated the same as for the bottom-down orientation.

The top-down model is supported against the applied loading by means of a pressure applied on the uppermost annular surface of the cask as shown in Figure 2.10.2-2. In addition, a single node is constrained in the axial direction. As before, the applied support pressure is adjusted until the reaction force at this node is negligibly small.

Common Boundary Conditions. All nodes on the center axis of the cask are restrained from motion in the radial direction. A pressure of 50 psi, equal to the design pressure, is applied to all surfaces in the payload cavity. The payload cavity extends from the center axis at the payload floor up to the location of the O-ring in the closure lid. This pressure leads to a net axial force, and to counter this force, an axial force of the same magnitude is applied in the opposite direction to a node on the lid interface corresponding to the closure lid bolt circle. Inertia loads from impact events are applied as a global acceleration field in the axial direction.

Nodal temperatures from the thermal analysis, representing maximum NCT temperatures, are read into all runs. In cases where thermal stress is not desired (such as all HAC cases and certain NCT cases as discussed in Section 2.6), thermal expansion coefficients are set to zero.

A special condition is that of the NCT heat case, described in Section 2.6.1.3.2. In that case, no acceleration field is applied, and the annular lead is modeled as a pressure of 300 psi on the outside of the inner shell, arising from the contraction of the lead material as discussed in Section 2.6.1.2. The design pressure of 50 psi and the thermal stresses are also applied to this case.

Input files used to build the model and to perform all of the axisymmetric analyses discussed in Sections 2.6 and 2.7 are available within Report ED-034.

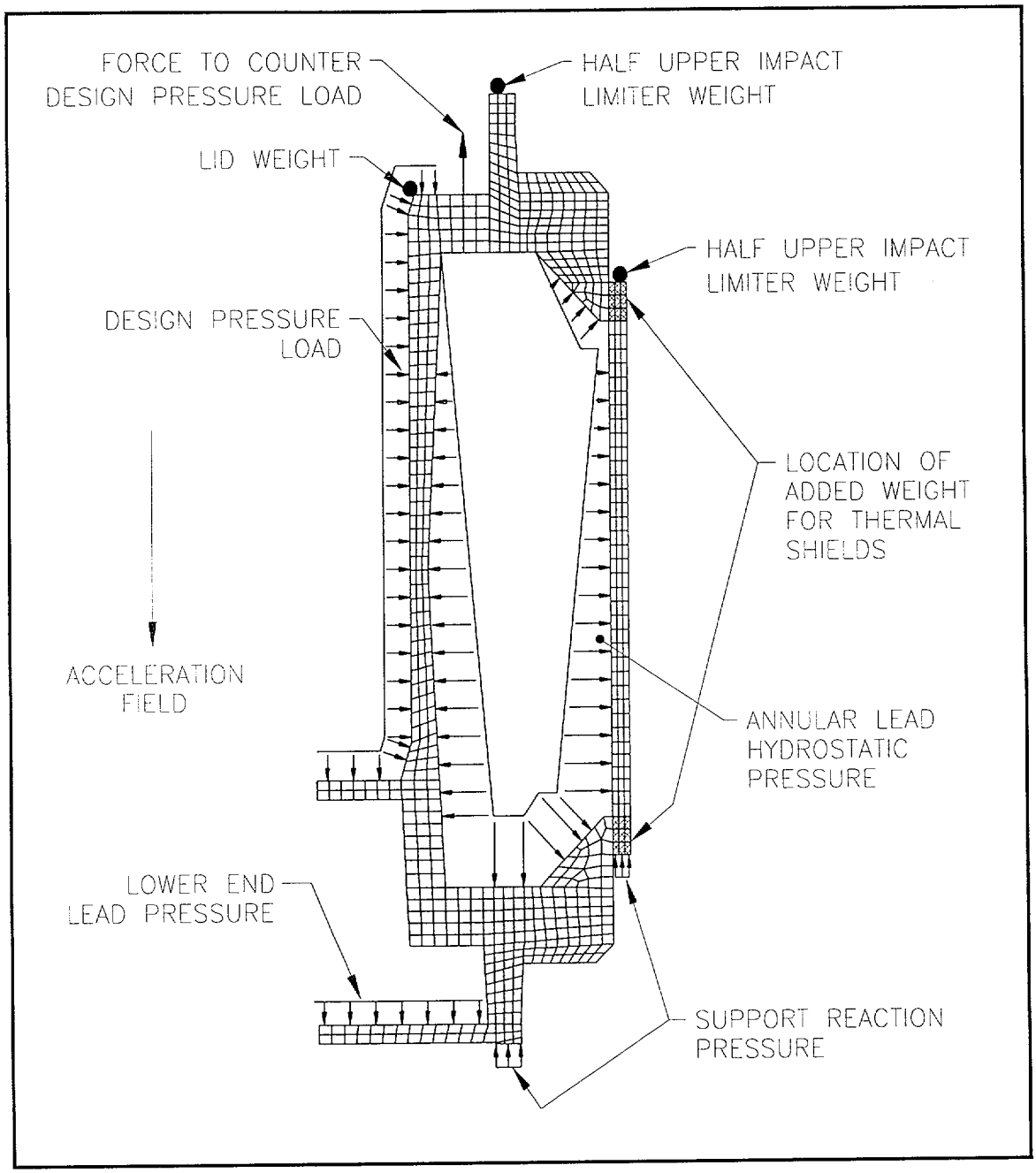

Figure 2.10.2-1 - Bottom-Down End Drop Axisymmetric Finite Element Model

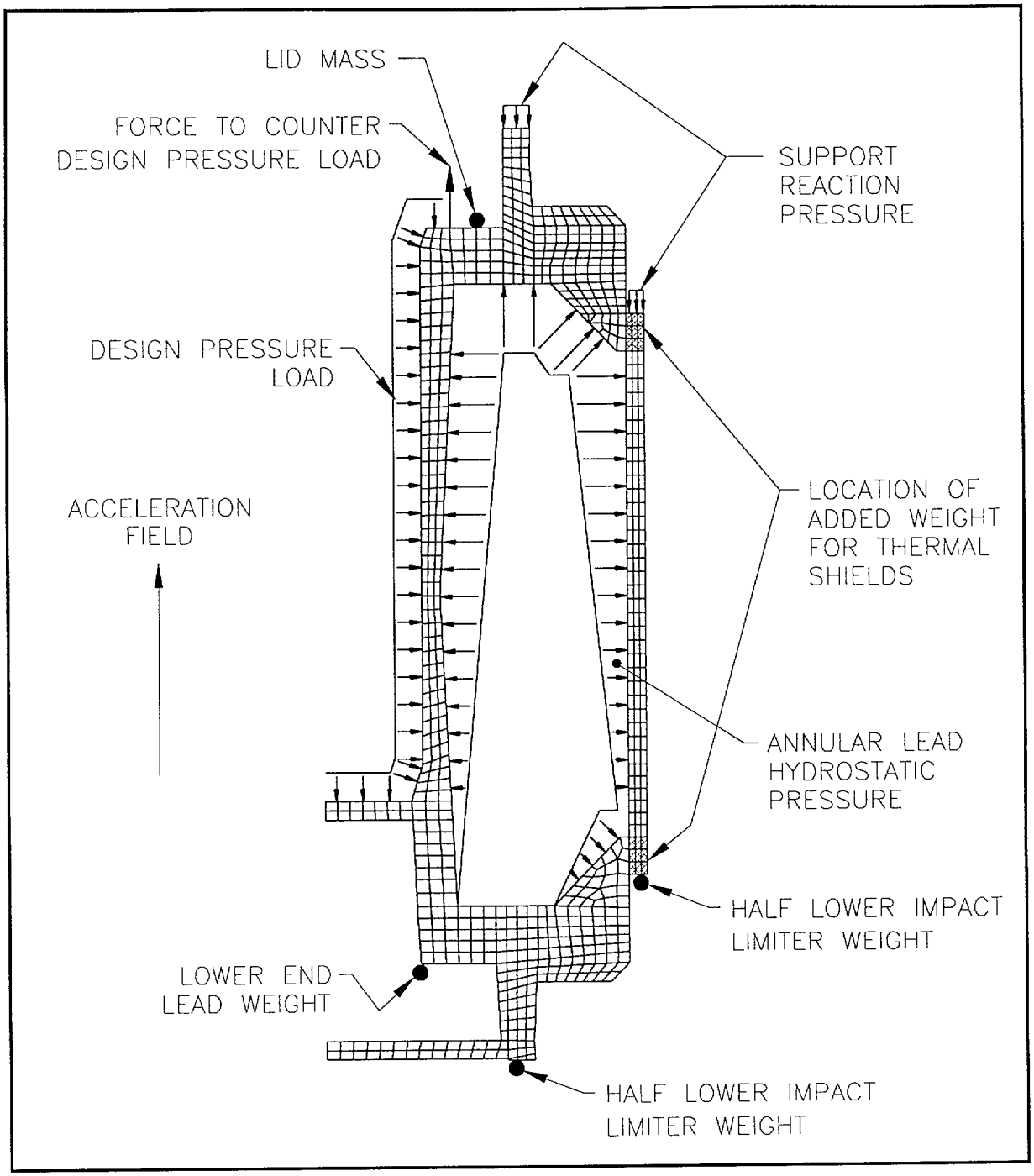

Figure 2.10.2-2 - Top-Down End Drop Axisymmetric Finite Element Model

2.10.2.2 Half-Symmetry Side Drop Finite Element Model Description

The model is generated with ANSYS® Revision 5.4 using SOLID45, 3-D structural elements in a three dimensional, half-symmetry configuration as shown in Figure 2.10.2-3. Again, only those parts of the cask are modeled which require evaluation for stress in the NCT and HAC free drop

event in the side orientation. The weight of all structures which are not explicitly modeled is included as discussed below.

The model is generated by sweeping the axisymmetric model (described in Section 2.10.2.1) around 180° and changing the element type to SOLID45. The weight of the thermal shield is included in the same way as in the case of the axisymmetric model described above. The weight of the lid and of the lower end lead are applied as a pressures as shown in Figure 2.10.2-4. In half-symmetry, half of the weight is applied in each case, and the pressure extends over an included angle of 30°, which represents the circumferential extent of contact. The annular lead shield is conservatively assumed to have no structural strength and is therefore applied as an increase in density of the cask shells. Half of the weight of the annular lead (one quarter, in the half-symmetric model) is applied to the upper half of the inner shell (quarter shell, in the half-symmetric model), and the other half of the weight of the annular lead (quarter) is applied to the lower half (quarter) of the outer shell. The weight is applied as an increase of the density of the material above that of steel alone.

The model is supported by applied pressures over the cylindrical contact region between the cask and impact limiters as shown in Figure 2.10.2-4. In addition, one node at the top and one at the bottom of these support areas are restrained from motion, and the pressures are adjusted until the reaction forces at these nodes are negligible. The model is constrained against deformation across the symmetry plane, and from axial motion by the constraint of a single node at the cask bottom. Inertia loads from impact events are applied as a global acceleration field in the radial direction, parallel to the plane of symmetry.

As for the axisymmetric case, an internal design pressure and the equivalent lid force loads are applied to the payload cavity of the model. Nodal temperatures from the thermal analysis, representing maximum NCT temperatures, are read into all runs. In cases where thermal stress is not desired (such as all HAC cases and certain NCT cases as discussed in Section 2.6), thermal expansion coefficients are set to zero.

Input files used to build the model and to perform all of the half-symmetry analyses discussed in Sections 2.6 and 2.7 are available within Report ED-034.

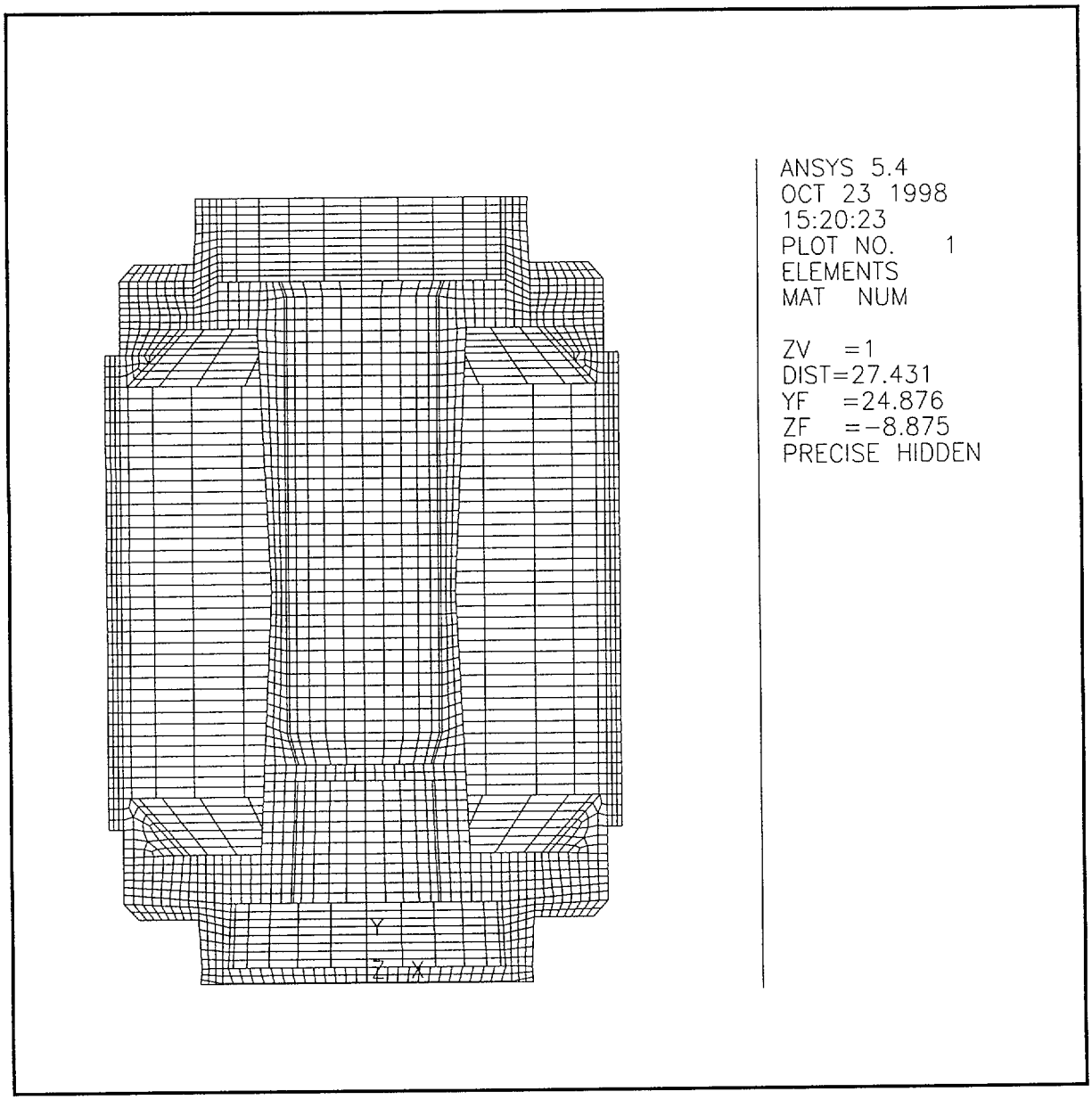

Figure 2.10.2-3 - Half-symmetry Finite Element Model, Elements

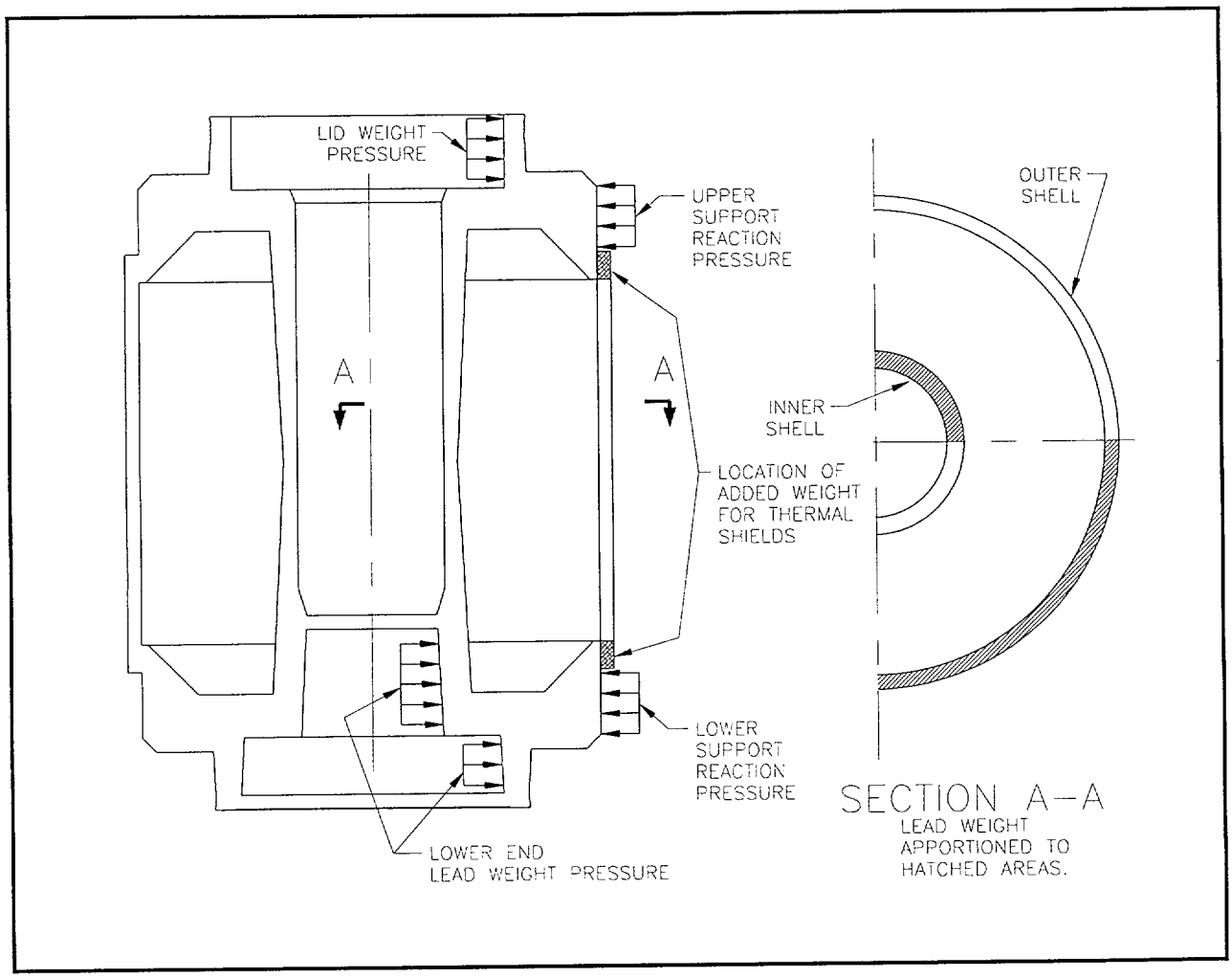

Figure 2.10.2-4 - Half-symmetry Finite Element Model Boundary Conditions

2.10.3 Drop Analysis Finite Element Model Description

The evaluation of the SEC toroidal impact limiter is performed using the dynamic finite element models described in this section. The geometry, loading, boundary conditions, and other aspects of the models are described in the following subsections. The results of the free drop analysis are described in Section 2.7.

2.10.3.1 Finite Element Model Description

The toroidal impact limiters are analyzed for the normal conditions of transport (NCT), 3 ft free drop and the hypothetical accident conditions (HAC), 30 ft free drop as defined in 10 CFR 71. The models described herein are used to determine the impact response of the toroidal impact limiters and define the inputs to the cask structural analyses.

The analyses are performed using LS-DYNA [16], version 940.1a. Pre- and post- processing of the models is performed using the FEMB, version 26.3d pre/post processor [22]. Two basic models are used; a quarter-symmetric and a half-symmetric. The quarter-symmetric model (shown in Figure 2.10.3-1) is used to analyze the end drop orientation. Symmetry constraints are applied to the X-Y and Y-Z planes. The half-symmetric model (shown in Figure 2.10.3-2) is used for the side (horizontal), c.g.-over-corner (54.5° to horizontal) and slapdown (15° to horizontal) orientations. The half-symmetric model is created by symmetry reflection of the quarter-symmetric model and is geometrically equivalent. Symmetry constraints are applied only to the X-Y plane of the half-symmetric model. The only loads applied are initial velocity definitions at each node of the models. The initial velocity is set to 527.5 in/s, corresponding to a 30 ft free drop for HAC, and 166.8 in/s, corresponding to a 3 ft free drop for NCT. The same half-symmetry model serves for all of the listed cases by merely changing the angle of orientation to the ground. To model impact, the cask strikes a rigid wall structure, modeled using a 'rigid-wall' contact type. The results of the model consist of the time history of force between the cask and the wall.

The cask is composed of rigid brick elements (solid element formulation 1, 8-node constant stress solid), and serves only to create the correct mass, mass moment of inertia, and geometry for the analysis of the energy absorption of the impact limiters. The entire model, including impact limiters, weighs 20,035 lb and has a mass moment of inertia of 19,996 in-lb-s^2. Both of these values differ only negligibly from the values listed in Section 2.2.

The impact limiter cap (the plate structure which forms the interface between the cask and the toroid) is modeled using elastic brick elements (solid element formulation 1, 8-node constant stress solid). For side, slapdown and corner analyses, the limiter is constrained to the cask using three dimensional rigid beam elements (beam element formulation 2, Belytschko-Schwer)[1]. The beams run from one limiter to the other and are attached to the bottom of each limiter at the 0°, 90°, and 180° azimuth locations and merely keep the limiter in its proper position during the

[1] These elements are not designed to directly represent the impact limiter attachment pins. Loads on the pins are evaluated using a classical approach in Section 2.7.1.5.

analyses. Both the solid and beam elements exhibit three degrees of freedom at each node; displacements in the x, y, and z directions.

The hollow toroids are modeled using 3-D shell elements (shell element formulation 10, Belytschko-Wong-Chiang) located at the mid-fiber of the toroid, and have a thickness of 0.75 inches. The shell element exhibits six degrees of freedom at each of the 4 nodes; displacements in the x, y, and z directions, and rotations about the x, y, and z axes. Five integration points through the thickness of the shell are used. Hourglassing control is set to type 5 (stiffness form) with a default hourglass coefficient of 0.10.

Two contact types are defined. Contact between the cask and the impact limiter cap is modeled using the 'CONTACT_AUTOMATIC_SINGLE_SURFACE' option, which automatically models contact between any one element with any other element. The toroid to impact surface contact is modeled using a 'RIGIDWALL_PLANAR', which models an infinitely rigid impact target. No friction is used in any of the contacts.

A sample input file is contained in Section 2.10.3.3. In this sample file, certain types of information, such as the node definition, element definition, and constraint information, are presented for only a few representative nodes (or elements) for brevity. All of the input and output files are available within Report ED-035.

2.10.3.2 Material Properties

Two different stress-strain curves are used depending on the type of analysis performed, as detailed in Section 2.3.2. For warm, maximum deflection cases, the stress-strain properties of the material are lower-bounded by the use of a bi-linear stress-strain curve, material law 3, plastic-kinematic. The yield point is 29,000 psi, the elastic modulus is $27.6(10^6)$ psi, and the tangent modulus is 185,000 psi. For cold, maximum impact cases, the stress-strain properties are upper-bounded by the use of a multi-linear stress strain curve, material law 24, piecewise linear plasticity. The stress-strain points for the cold case are given in Table 2.10.3-1. Poisson's ratio in all cases is 0.3. Further discussion of the development of material properties for use in impact analysis is provided in Section 2.3.2.

Table 2.10.3-1 - Multi-Linear Stress-Strain Curve for Maximum Impact (Cold) Cases

Condition	Plastic Strain (in/in)	Stress Adjustment Factor (SF)	Multi-Linear Stress① (σ_{cm}, psi)
Cold, -20 °F, Maximum Properties	0.0	1.0	42,000
	0.05	1.140	73,530
	0.10	1.177	102,400
	0.30	1.136	201,100
	0.60	1.0	312,000

Notes:

① Values shown are True-Strain and True-Stress.

② The elastic modulus for the multi-linear material properties is $28.7(10^6)$ psi.

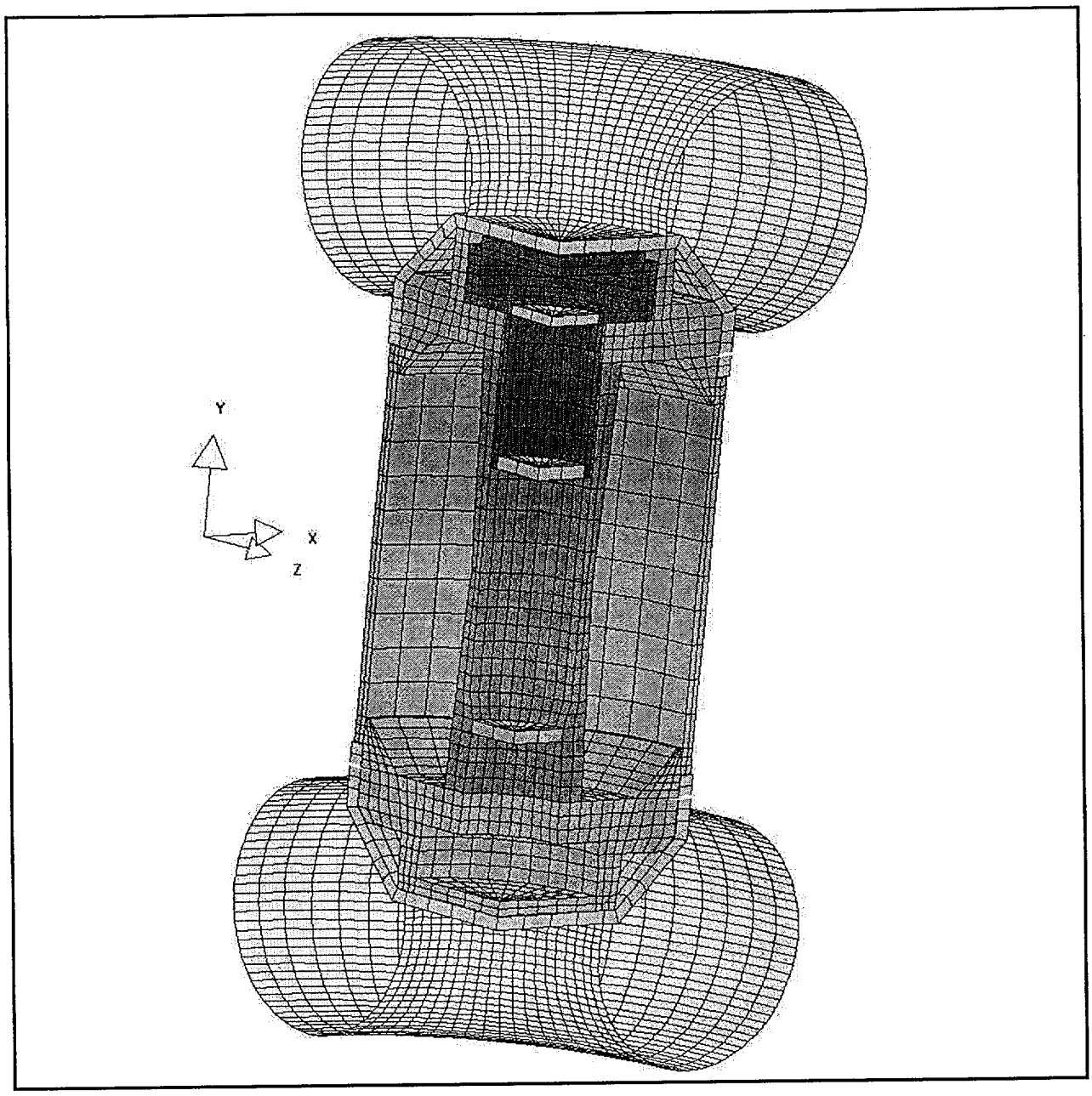

Figure 2.10.3-1 - LS-DYNA Model, End Drop

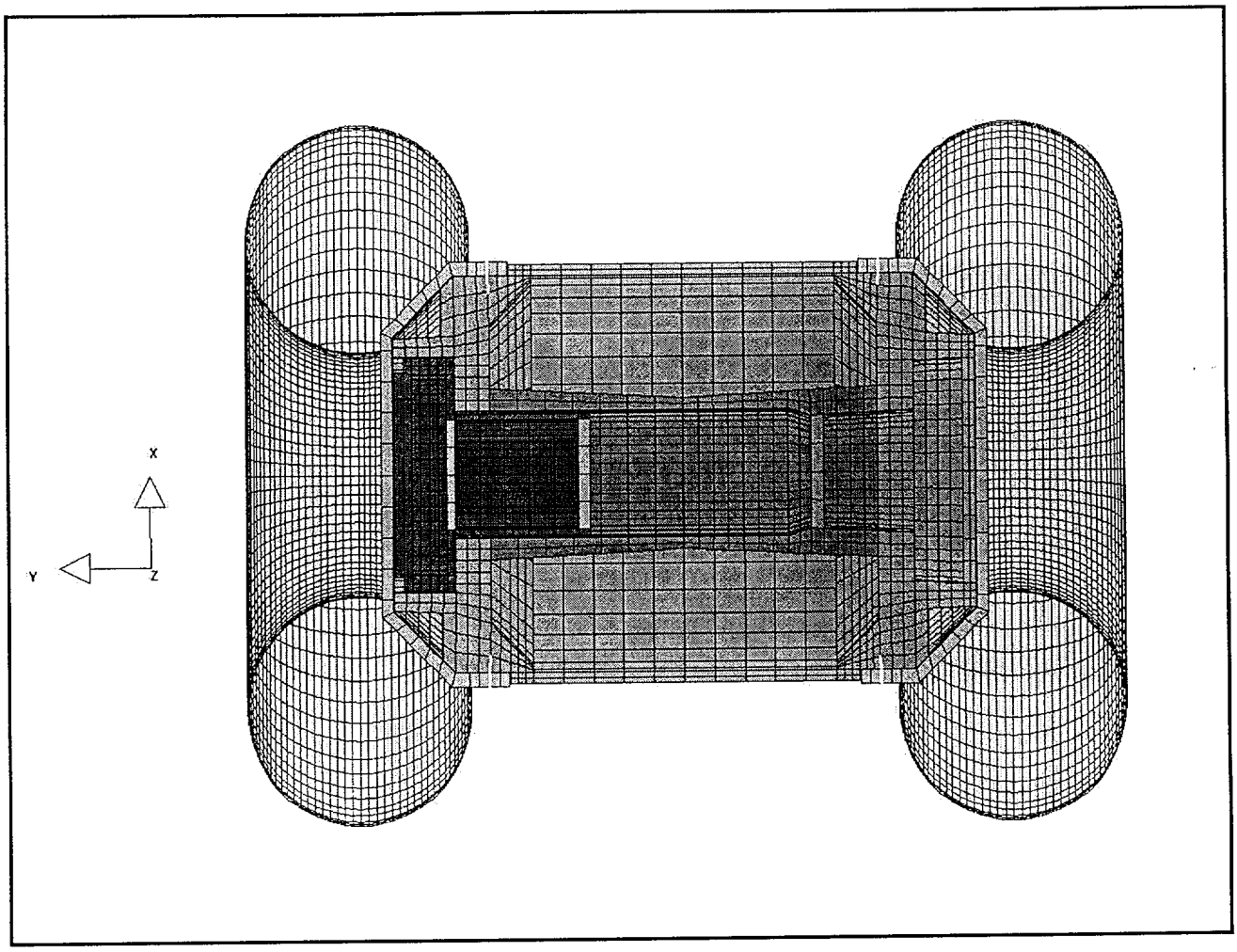

Figure 2.10.3-2 - LS-DYNA Model, Side, Corner and Slapdown Drop

2.10.3.3 Sample Input File

```
*KEYWORD
$---+----1----+----2----+----3----+----4----+----5----+----6----+----7----+----8
$                    (1) TITLE CARD.
$---+----1----+----2----+----3----+----4----+----5----+----6----+----7----+----8
*TITLE
HAC_COLD_END
$---+----1----+----2----+----3----+----4----+----5----+----6----+----7----+----8
$                    (2) CONTROL CARDS.
$---+----1----+----2----+----3----+----4----+----5----+----6----+----7----+----8
*CONTROL_TERMINATION
$    ENDTIM    ENDCYC     DTMIN    ENDNEG    ENDMAS
  .250E-01         0      .000      .000      .000
*CONTROL_TIMESTEP
$    DTINIT      SCFT      ISDO    TSLIMT      DTMS      LCTM     ERODE     MS1ST
      .000      .900         0
*CONTROL_HOURGLASS
$       IHQ        QH
          5      .100
*CONTROL_BULK_VISCOSITY
$        Q2        Q1
     1.500      .060
*CONTROL_SHELL
$    WRPANG     ITRIST      IRNXX     ISTUPD     THEORY        BWC      MITER
    20.000          2         -1          0         10          1          1
*CONTROL_CONTACT
$    SLSFAC     RWPNAL     ISLCHK     SHLTHK     PENOPT     THKCHG      ORIEN
      .070
$    USRSTR     USRFAC      NSBCS     INTERM      XPENE
         0          0         10          0      4.000
*CONTROL_ENERGY
$      HGEN       RWEN     SLNTEN      RYLEN
         1          2          1          1
*CONTROL_DAMPING
$    NRCYCK      DRTOL     DRFCTR     DRTERM     TSSFDR     IRELAL      EDTTL     IDRFLG
       250       .001       .995
*CONTROL_OUTPUT
$     NPOPT     NEECHO     NREFUP     IACCOP      OPIFS     IPNINT     IKEDIT
         0          0          0          0       .000          0        100
$---+----1----+----2----+----3----+----4----+----5----+----6----+----7----+----8
$                    (3) DATABASE CONTROL CARDS - ASCII HISTORY FILE
$---+----1----+----2----+----3----+----4----+----5----+----6----+----7----+----8
$*DATABASE_HISTORY_OPTION
$       ID1        ID2        ID3        ID4        ID5        ID6        ID7        ID8
$
$OPTION : BEAM    BEAM_SET   NODE   NODE_SET
$         SHELL   SHELL_SET  SOLID  SOLID_SET
$         TSHELL  TSHELL_SET
$---+----1----+----2----+----3----+----4----+----5----+----6----+----7----+----8
$                    (4) DATABASE CONTROL CARDS FOR ASCII FILE
$---+----1----+----2----+----3----+----4----+----5----+----6----+----7----+----8
*DATABASE_RWFORC
  .100E-04
*DATABASE_NODOUT
  .100E-05
```

```
*DATABASE_HISTORY_NODE
      3311       8248       3089       8014       4291       4406       2479
      7441
*DATABASE_ELOUT
  .500E-05
*DATABASE_HISTORY_BEAM
$---+----1----+----2----+----3----+----4----+----5----+----6----+----7----+----8
      3136       3137       3138       3139       3140       3141       3142
      3143       6249       6250       6253       6254
$---+----1----+----2----+----3----+----4----+----5----+----6----+----7----+----8
$                    (5) DATABASE CONTROL CARDS FOR BINARY FILE
$---+----1----+----2----+----3----+----4----+----5----+----6----+----7----+----8
*DATABASE_BINARY_D3PLOT
$  DT/CYCL      LCDT    NOBEAM
  .125E-02
*DATABASE_BINARY_D3THDT
$  DT/CYCL      LCDT    NOBEAM
  .125E-02
$*DATABASE_BINARY_OPTION
$  DT/CYCL      LCDT    NOBEAM
$
$OPTION : D3DRFL D3DUMP RUNRSF INTFOR
$---+----1----+----2----+----3----+----4----+----5----+----6----+----7----+----8
*DATABASE_EXTENT_BINARY
         0          0          3          0          1          1          1          1
         0          0          0          0          0          0
$---+----1----+----2----+----3----+----4----+----5----+----6----+----7----+----8
$                    (6) DEFINE PARTS CARDS
$---+----1----+----2----+----3----+----4----+----5----+----6----+----7----+----8
*PART
$HEADING
 PART PID =         7 PART NAME :LID
$       PID       SID       MID     EOSID      HGID      GRAV    ADPOPT      TMID
         7         7         6
*PART
$HEADING
 PART PID =         8 PART NAME :CASK
$       PID       SID       MID     EOSID      HGID      GRAV    ADPOPT      TMID
         8         9         7
*PART
$HEADING
 PART PID =        10 PART NAME :LIDHAT
$       PID       SID       MID     EOSID      HGID      GRAV    ADPOPT      TMID
        10         9         1
*PART
$HEADING
 PART PID =        11 PART NAME :TOROID
$       PID       SID       MID     EOSID      HGID      GRAV    ADPOPT      TMID
        11        12         1
*PART
$HEADING
 PART PID =        13 PART NAME :PB1.P
$       PID       SID       MID     EOSID      HGID      GRAV    ADPOPT      TMID
        13         9         2
*PART
$HEADING
 PART PID =        15 PART NAME :PB2.P
$       PID       SID       MID     EOSID      HGID      GRAV    ADPOPT      TMID
        15         9         3
```

```
*PART
$HEADING
 PART PID =        16 PART NAME :TPB1.P
$       PID       SID       MID     EOSID      HGID      GRAV    ADPOPT      TMID
        16          9         4
*PART
$HEADING
 PART PID =        17 PART NAME :TPB2.P
$       PID       SID       MID     EOSID      HGID      GRAV    ADPOPT      TMID
        17          9         5
*PART
$HEADING
 PART PID =        18 PART NAME :PIN
$       PID       SID       MID     EOSID      HGID      GRAV    ADPOPT      TMID
        18         19         6
$---+----1----+----2----+----3----+----4----+----5----+----6----+----7----+----8
$                    (7) MATERIAL CARDS
*MAT_PIECEWISE_LINEAR_PLASTICITY
$MATERIAL NAME:304EP
$       MID        RO         E        PR      SIGY      ETAN      EPPF      TDEL
          1 7.400E-04 2.870E+07 2.900E-01 4.200E+04 0.000E+00 0.000E+00 0.000E+00
$         C         P      LCSS      LCSR
  .000E+00  .000E+00  .000E+00  .000E+00
$      EPS1      EPS2      EPS3      EPS4      EPS5      EPS6      EPS7      EPS8
 0.000E+00     0.050     0.010      0.30      0.60
$       ES1       ES2       ES3       ES4       ES5       ES6       ES7       ES8
 4.200E+04 7.353E+04 1.024E+05 2.011E+05 3.120E+05
*MAT_ELASTIC
$MATERIAL NAME:pb1
$       MID        RO         E        PR        DA        DB         K
          2 1.339E-02 2.870E+07 2.900E-01 0.000E+00 0.000E+00 0.000E+00
*MAT_ELASTIC
$MATERIAL NAME:pb3
$       MID        RO         E        PR        DA        DB         K
          3 7.600E-03 2.870E+07 2.900E-01 0.000E+00 0.000E+00 0.000E+00
*MAT_ELASTIC
$MATERIAL NAME:tpb1
$       MID        RO         E        PR        DA        DB         K
          4 4.980E-03 2.870E+07 2.900E-01 0.000E+00 0.000E+00 0.000E+00
*MAT_ELASTIC
$MATERIAL NAME:tpb2
$       MID        RO         E        PR        DA        DB         K
          5 1.202E-02 2.870E+07 2.900E-01 0.000E+00 0.000E+00 0.000E+00
*MAT_ELASTIC
$MATERIAL NAME:PIN
$       MID        RO         E        PR        DA        DB         K
          6 7.400E-04 2.870E+07 2.900E-01 0.000E+00 0.000E+00 0.000E+00
*MAT_ELASTIC
$MATERIAL NAME:Cask
$       MID        RO         E        PR        DA        DB         K
          7 1.065E-03 2.870E+07 2.900E-01 0.000E+00 0.000E+00 0.000E+00
$---+----1----+----2----+----3----+----4----+----5----+----6----+----7----+----8
$                    (7.1) SECTION CARDS
$---+----1----+----2----+----3----+----4----+----5----+----6----+----7----+----8
*SECTION_SOLID
$       SID    ELFORM
          7
*SECTION_SOLID
$PROPERTY NAME:SOLID
```

```
$       SID     ELFORM
          9          1
*SECTION_SHELL
$PROPERTY NAME:TOROID
$       SID     ELFORM      SHRF       NIP      PROPT    QR/IRID      ICOMP
         12         10  .833E+00       5.0        1.0         .0
$        T1         T2         T3         T4      NLOC
 7.500E-01 7.500E-01 7.500E-01 7.500E-01
*SECTION_BEAM
$PROPERTY NAME:PIN
$       SID     ELFORM      SHRF    QR/IRID       CST
         19          2
$         A        ISS        ITT        IRR        SA
 7.850E-01 4.910E-02 4.910E-02 7.820E-02 7.850E-01
$---+----1----+----2----+----3----+----4----+----5----+----6----+----7----+----8
$                    (8) NODAL POINT CARDS
$---+----1----+----2----+----3----+----4----+----5----+----6----+----7----+----8
*NODE
$   NODE               X               Y               Z      TC      RC
       1  .735016200E+01  .520037600E+02 -.735006300E+01
       2  .739504200E+01  .515070900E+02 -.739494400E+01
       3  .743992300E+01  .510104000E+02 -.743982500E+01
       4  .787981600E+01  .520037600E+02 -.672991600E+01
       .          .              .               .
       .          .              .               .
       .          .              .               .
10319  .289374900E+01  .653678100E+01 -.182698400E+02
   10320  .144692000E+01  .653678100E+01 -.183837100E+02
   10321  .912376400E-04  .653678100E+01 -.184975700E+02
$---+----1----+----2----+----3----+----4----+----5----+----6----+----7----+----8
$                    (9) SOLID ELEMENT CARDS
$---+----1----+----2----+----3----+----4----+----5----+----6----+----7----+----8
*ELEMENT_SOLID
$    EID     PID      N1      N2      N3      N4      N5      N6      N7      N8
     776      10    1267    1266    1311    1312    1268    1268    1313    1313
     777      10    1268    1266    1311    1313    1269    1269    1314    1314
     778      10    1269    1266    1311    1314    1270    1270    1315    1315
     779      10    1270    1266    1311    1315    1271    1271    1316    1316
       .       .       .       .       .       .       .       .       .       .
       .       .       .       .       .       .       .       .       .       .
       .       .       .       .       .       .       .       .       .       .
    5486      10    9490    9492    9491    9489    9512    9514    9513    9511
    5487      10    9492    9494    9493    9491    9514    9516    9515    9513
    5488      10    9494    9496    9495    9493    9516    9518    9517    9515
$---+----1----+----2----+----3----+----4----+----5----+----6----+----7----+----8
$                    (10) BEAM ELEMENT CARDS
$---+----1----+----2----+----3----+----4----+----5----+----6----+----7----+----8
*ELEMENT_BEAM
$    EID     PID      N1      N2      N3
    3136      18    2592    1641    1685
    3137      18    1641    1640    1684
    3138      18    2597    1621    1665
    3139      18    1621    1620    1664
    3140      18    3989    5032    5054
    3141      18    5032    5031    5053
    3142      18    3984    5014    5036
    3143      18    5014    5011    5033
    6249      18    7604    7279    7301
    6250      18    7279    7278    7300
```

```
    6253       18     8683     9473     9495
    6254       18     9473     9474     9496
$---+----1----+----2----+----3----+----4----+----5----+----6----+----7----+----8
$                    (11) SHELL ELEMENT CARDS
$---+----1----+----2----+----3----+----4----+----5----+----6----+----7----+----8
*ELEMENT_SHELL
$     EID      PID       N1       N2       N3       N4
        1       11        1        4        5        2
        2       11        2        5        6        3
        3       11        4        7        8        5
        .        .        .        .        .        .
        .        .        .        .        .        .
        .        .        .        .        .        .
    6246       11     9424     9426     9425     9423
    6247       11     9426     9428     9427     9425
    6248       11     9428     9430     9429     9427
$---+----1----+----2----+----3----+----4----+----5----+----6----+----7----+----8
$                    (16) BOUNDARY CONDITION CARDS
$---+----1----+----2----+----3----+----4----+----5----+----6----+----7----+----8
*BOUNDARY_SPC_NODE
$ NID/NSID        CID       DOFX       DOFY       DOFZ      DOFRX      DOFRY      DOFRZ
        31          0          0          0          1          1          1          0
        32          0          0          0          1          1          1          0
        33          0          0          0          1          1          1          0
        64          0          0          0          1          1          1          0
         .          .          .          .          .          .          .          .
         .          .          .          .          .          .          .          .
         .          .          .          .          .          .          .          .
$---+----1----+----2----+----3----+----4----+----5----+----6----+----7----+----8
$                    (19) INITIAL CARDS
$---+----1----+----2----+----3----+----4----+----5----+----6----+----7----+----8
*INITIAL_VELOCITY
         0
 0.000E+00-1.668E+02 0.000E+00 0.000E+00 0.000E+00 0.000E+00
*INITIAL_VELOCITY_NODE
$       NID        VX         VY         VZ        VXR        VYR        VZR
          1 0.000E+00-5.275E+02 0.000E+00 0.000E+00 0.000E+00 0.000E+00
          2 0.000E+00-5.275E+02 0.000E+00 0.000E+00 0.000E+00 0.000E+00
          3 0.000E+00-5.275E+02 0.000E+00 0.000E+00 0.000E+00 0.000E+00
          .          .          .          .          .          .          .
          .          .          .          .          .          .          .
          .          .          .          .          .          .          .
      10319 0.000E+00-5.275E+02 0.000E+00 0.000E+00 0.000E+00 0.000E+00
      10320 0.000E+00-5.275E+02 0.000E+00 0.000E+00 0.000E+00 0.000E+00
      10321 0.000E+00-5.275E+02 0.000E+00 0.000E+00 0.000E+00 0.000E+00
$---+----1----+----2----+----3----+----4----+----5----+----6----+----7----+----8
$                    (22) DEFINE CONTACT SURFACE
$---+----1----+----2----+----3----+----4----+----5----+----6----+----7----+----8
*CONTACT_AUTOMATIC_SINGLE_SURFACE_TITLE
$       CID  IF. NAME
          2 ALL
$      SSID       MSID      SSTYP      MSTYP     SBOXID     MBOXID        SPR        MPR
          0          0          0          0          0          0          0          0
$        FS         FD         DC          V        VDC    PENCHK         BT         DT
 0.000E+00  0.000E+00  0.000E+00  0.000E+00         50          0  0.000E+00  1.000E+20
$       SFS        SFM        SST        MST       SFST       SFMT        FSF        VSF
   .100E+01   .100E+01                        .100E-04   .100E-04   .100E+01   .100E+01
$---+----1----+----2----+----3----+----4----+----5----+----6----+----7----+----8
$                    (23) DEFINE RIGID WALL
```

```
$---+----1----+----2----+----3----+----4----+----5----+----6----+----7----+----8
*RIGIDWALL_PLANAR
$         1           RIGIDWALL NAME:GROUND
$      NSID     NSIDEX      BOXID
           2          0          0
$        XT         YT         ZT         XH         YH         ZH       FRIC
  .000E+00 -.128E+02  .000E+00  .000E+00  .873E+02  .000E+00  .000E+00
*SET_NODE_LIST
$       SID        DA1        DA2        DA3        DA4
           2
$      NID1       NID2       NID3       NID4       NID5       NID6       NID7       NID8
      5077       5078       5079       5080       5081       5082       5083       5084
      5085       5086       5087       5088       5089       5090       5091       5092
      5093       5094       5095       5096       5097       5098       5099       5100
         .          .          .          .          .          .          .          .
         .          .          .          .          .          .          .          .
         .          .          .          .          .          .          .          .
     10051      10052      10053      10054      10055      10056      10057      10058
     10059      10060      10061      10062      10063      10064      10065      10066
     10067      10068
$---+----1----+----2----+----3----+----4----+----5----+----6----+----7----+----8
*END
```

2.10.4 Closure Bolt Design Evaluation

The SEC closure bolts are designed for the normal conditions of transport (NCT) and hypothetical accident condition (HAC) package tests specified in 10 CFR §71.71 [1] and §71.73, respectively, and the following analyses demonstrate the ability of the closure bolts to meet the performance requirements specified in NUREG/CR-6007 [7]. Both NCT and HAC load combinations are evaluated in accordance with Regulatory Guide 7.8 [3], as delineated in Section 2.1.2.2. All nomenclature herein is consistent with the definitions of NUREG/CR-6007.

2.10.4.1 Geometric and Material Properties

The closure lid is secured using 12, 3/4-10UNC-2A closure bolts fabricated of ASTM A320, Grade L43, alloy steel bolting material. The material properties are given in Section 2.3, and relevant geometric properties are listed in Table 2.10.4-5.

2.10.4.2 Loading

2.10.4.2.1 Closure Bolt Forces/Moments Characteristics

The closure bolts are loaded by operational loads, such as pretorque tension, residual torsion from bolt tightening, cask internal pressure, and differential thermal expansion, as well as NCT and HAC free drop impact loads. As shown in Tables 2.10.4-7 to 2.10.4-9, 18 different load combinations are analyzed. Input loads for each load combination are developed in the subsections that follow. In each case, the formula used to develop the bolt load (consistent with NUREG/CR-6007) is reviewed. Input bolt force values are given in Table 2.10.4-6, and resulting combined loads are given in Table 2.10.4-7.

Prying forces from load cases involving internal forces on the closure lid are eliminated through tapering the outside of the lid, as shown in Figure 2.10.4-1. The taper originates at the bolt circle, and relieves the material outboard of the bolt circle so that prying cannot occur. Prying from the puncture load, which is an external load on the closure lid, is still possible and this load is considered.

2.10.4.2.2 Closure Bolt Forces/Moments Generated by Preload

The closure bolts are preloaded to 90 ± 10 ft-lb torque, resulting in a minimum and maximum preload torque of 80 ft-lb and 100 ft-lb, respectively.

From Subsection 4.2 of NUREG/CR-6007, the maximum non-prying tensile force per bolt, Fa_{max}, is found from

$$Fa_{max} = \frac{Q_{max}}{(K)(Db)}$$

where Q_{max} is the maximum applied closure bolt preload, K is the nut factor, and Db is the closure bolt nominal diameter. The minimum preload force is computed in the same way except for the use of Q_{min} in the place of Q_{max}.

The maximum residual torsion is 50% of the applied torsion:

$$Mtr = 0.5(Q_{max})$$

Preload forces on the bolts under each loading condition are given in Table 2.10.4-6.

2.10.4.2.3 Closure Bolt Forces/Moments Generated by Gasket Loads

From Subsection 4.3 of NUREG/CR-6007, some gasket types can produce loads in the closure bolts. The SEC uses one elastomeric O-ring seal between the closure lid and the cask. Due to the relatively small size of the seal (0.275 inch diameter) and modest compressive forces, closure bolt load due to O-ring seal compression is very small, and is therefore ignored.

2.10.4.2.4 Closure Bolt Forces/Moments Generated by Pressure Loads

From Subsection 4.4 of NUREG/CR-6007, utilizing appropriate temperature dependent material properties from Section 2.3, the maximum non-prying tensile force per bolt, Fa, due to pressure loads are based on the following formulae:

$$Fa = \frac{\pi(Dlg)^2(Pli - Plo)}{4(Nb)}$$

$$Mbb = \left(\frac{\pi(Dlb)}{Nb}\right)\left(\frac{Kb}{Kb + Kl}\right)\left(\frac{(Dlb)^2(Pli - Plo)}{32}\right)$$

where Dlg is the closure lid diameter at the location of gasket load reaction (i.e., the O-ring seal diameter), Pli is the pressure inside the closure lid, Plo is the pressure outside the closure lid, Nb is the total number of closure bolts, Dlb is the closure lid diameter at the closure bolt circle, and the formulas for the bolt and lid stiffnesses, Kb and Kl, respectively, are:

$$Kb = \left(\frac{Nb}{Lb}\right)\left(\frac{Eb}{Dlb}\right)\left(\frac{Db^4}{64}\right)$$

$$Kl = \frac{(El)(tl)^3}{3\left[\left(1-(Nul)^2\right)+\left(1-Nul\right)^2\left(\frac{Dlb}{Dlo}\right)^2\right](Dlb)}$$

where Lb is the shank length of the closure bolts, Eb is the elastic modulus of the closure bolt material, Nul is Poisson's ratio of the closure lid material, Db is the bolt diameter, and Dlo is the closure lid outer edge diameter.

Subsection 4.4 of NUREG/CR-6007 indicates that some shear forces could arise in the bolts due to pressure-related expansion of the cask wall relative to the lid, and from a difference in temperature between the cask and the lid. Since the upper casting and the closure lid have essentially the same temperature, no shear due to a temperature difference can arise. Further, due

to the thick wall construction of the cask (upper casting wall thickness of 11⅜ inches) relative to the small inner diameter (10¾ inches) and the low design pressure (50 psi), any expansion of the cask wall relative to the lid may be neglected. Therefore, shear forces in the bolts arising from pressure or temperature differences are ignored.

The pressures used to evaluate bolt loads in the above formulas are summarized in Table 2.10.4-1. Pressure forces on the bolts under each loading condition are given in Table 2.10.4-6.

Table 2.10.4-1 - Pressures (psia) for Evaluation of Bolt Pressure Loading

	NCT Cold (Including Cold Free Drops)	NCT Reduced External Pressure	NCT Warm Free Drops	HAC Free Drops	HAC Fire Event
Pli (Cask Internal)	14.7①	64.7②	64.7	64.7	64.7
Plo (Cask External)	14.7	3.5③	14.7	14.7	14.7

Notes:

① Per Regulatory Guide 7.8, the pressure inside the cask for NCT cold conditions is taken as atmospheric.

② This value is the sum of the design pressure of 50 psi and ambient of 14.7 psia.

③ The reduced external pressure case corresponds to 10 CFR §71.71(c)(3) as discussed in Section 2.6.3.

2.10.4.2.5 Closure Bolt Forces/Moments Generated by Temperature Loads

While the temperature of the closure bolts and of the closure lid are essentially identical in all cases, a thermally induced load is applied to the bolts since the thermal expansion coefficient of the ASTM A320, Grade L43, alloy steel closure bolts and Type 304 stainless steel closure lid differ. NCT cold (-40 °F case), NCT cold (free drop case), NCT warm, HAC cold, and HAC warm (fire) conditions are analyzed.

From Subsection 4.5 of NUREG/CR-6007, utilizing appropriate temperature dependent material properties from Section 2.3, the maximum non-prying tensile force per bolt due to thermal differential expansion of the closure bolt and the closure lid is based on the following formula:

$$Fa = \left(\frac{\pi}{4}\right)(Db)^2(Eb)[(al)(Tl) - (ab)(Tb)]$$

where Db is the bolt diameter, Eb is the elastic modulus of the closure bolt material, al is the thermal expansion coefficient of the closure lid material, ab is the thermal expansion coefficient of the closure bolt material, Tl is the temperature change of the closure lid from a reference temperature of 70 °F, and Tb is the temperature change of the closure bolt from a reference

temperature of 70 °F. The temperature changes used in the above equation are summarized in Table 2.10.4-2.

Table 2.10.4-2 - Bolt Temperature Changes for Evaluation of Bolt Thermal Loading

	NCT Cold (-40 °F)	NCT/HAC Cold Free Drops (-20 °F)	NCT/HAC Warm Free Drops (350 °F)	HAC Fire Event
Tl	-110	-90	280	460
Tb	-110	-90	280	460

Under NCT cold, -40 °F conditions, the temperature of the closure bolt and lid material decreases from 70 °F to -40 °F. The change in tensile force for each closure bolt (i.e., reduction in preload force) is

$$Fa = \left(\frac{\pi}{4}\right)(Db)^2(Eb)[(al)(Tl) - (ab)(Tb)] = 3{,}191\,lb$$

where Db = 0.75 inch, Eb = $28.3(10)^6$ psi, al = $8.21(10)^{-6}$ in/in/°F, ab = $5.89(10)^{-6}$ in/in/°F, Tl = -110 °F, and Tb = -110 °F. The minimum preload force is found from

$$Fa_{max} = \frac{Q_{min}}{(K)(Db)} = 6{,}882\,lb$$

where Q_{min} = 960 in-lb and K = 0.186 from Table 2.10.4-5. Therefore, the minimum remaining clamping force per bolt under NCT Cold, -40 °F conditions is 6,882 - 3,191 = 3,691 lb. Thus, the closure lid bolts do not loosen under the worst case temperature conditions.

Thermally induced forces on the bolts under each loading condition are given in Table 2.10.4-6.

2.10.4.2.6 Closure Bolt Forces/Moments Generated by Impact Loads

Impact loads arise from the NCT, three ft and HAC, 30 ft free drop events per 10 CFR §71.71(c)(7) and §71.73(c)(1), respectively. The impact loads are computed for the SEC in end (vertical), side (horizontal), and slapdown orientations as discussed in Section 2.7.1. The loads on the lid closure bolts are evaluated for both NCT and HAC in these three orientations, and is dependent on the inertia loading at the center of gravity of the closure lid. In the first two orientations (end and side), the cask is stable (i.e., does not rotate on impact) and the relevant inertia load on the closure lid is the same as that on the c.g. of the cask. In the case of the slapdown free drops, the cask obtains an angular acceleration, and in such a case the impact level at the closure lid is not the same as for the c.g. of the cask. The closure lid acceleration loads used for the slapdown event are evaluated in Section 2.6.7.2 for NCT and Section 2.7.1.4 for HAC. The accelerations used for the bolt load analysis are shown in Table 2.10.4-3, which are conservatively rounded up from the values determined in the drop analysis in Section 2.7.1.

Note that, in the end drop event, any support of the closure lid which might occur due to contact with the impact limiter is conservatively ignored. Also, in the slapdown event, only the governing, secondary impact is evaluated, with the closure lid located at the secondary end. In the secondary event, the cask orientation is assumed to be horizontal to the ground.

Table 2.10.4-3 - Impact Accelerations From Free Drop Events

Drop Orientation and Temperature	Acceleration at Cask c.g., g①	Acceleration at Closure Lid c.g., g
NCT		
Cold, End	78/80	80
Cold, Side	43/50	50
Cold, Slapdown②	24/25	49
Warm, End	57/60	60
Warm, Side	30/35	35
Warm, Slapdown②	17/20	39
HAC		
Cold, End	166/175	175
Cold, Side	135/145	145
Cold, Slapdown②	70/75	147
Warm, End	100/105	105
Warm, Side	81/85	85
Warm, Slapdown②	42/45	88

Notes:

① The acceleration data is given as: actual calculated impact/upper-bound impact. The upper-bound value is conservatively used for analysis.

② The governing, secondary slapdown is listed.

From Subsection 4.6 of NUREG/CR-6007, the maximum non-prying tensile force, Fa, and maximum shear forces per bolt due to the impact, for the cask with an inset closure lid and no opportunity for prying to occur, are calculated based on the following formulas:

$$Fa = \frac{(1.34)(\sin xi)(DLF)(ai)(Wl + Wc)}{Nb}$$

$$Fs = \frac{(\cos xi)(ai)(Wl)}{Nb}$$

where xi is the impact angle between the cask axis and the target surface, DLF is the dynamic load factor to account for any difference between the rigid body acceleration and the acceleration of the contents and closure lid, ai is the maximum rigid-body impact acceleration (g) of the closure lid c.g., Wl is the weight of the closure lid, Wc the weight of the cask content, and Nb is the total number of closure bolts.

The DLF is a function of the weight of the cask and the closure lid, accounting for the stiffness of the closure lid. Due to the rigidity of the SEC closure lid, the resulting closure lid frequency is very high, considerably higher than the input impact pulse frequency, and a DLF of 1.0 is therefore used.

Forces on the bolts as a result of free drop impacts, under each loading condition, are given in Table 2.10.4-6.

2.10.4.2.7 Closure Bolt Forces/Moments Generated by Puncture Loads

From Subsection 4.7 of NUREG/CR-6007, utilizing appropriate temperature dependent material properties from Section 2.3, the maximum non-prying tensile force, Fa, shear force, Fs, fixed-edge force, Ff, and fixed-edge moment, Mf, per bolt due to puncture are based on the following formulae:

$$Fa = \frac{-(\sin xi)(Pun)}{Nb}$$

$$Fs = \frac{(\cos xi)(Pun)}{Nb}$$

$$Ff = 0 \quad \text{(see footnote [1])}$$

$$Mf = \frac{(\sin xi)(Pun)}{4\pi}$$

where xi = 90° is the impact angle between the cask axis and the target surface, Nb is the total number of closure bolts, and Pun = $1.42(10)^6$ pounds, the flow load of the mild steel puncture bar, as discussed in Section 2.7.3.

Because the equation calculating the prying force, Fap, is written for an outward pressure, the sign of the fixed edge-moment, Mf, is not consistent with NUREG/CR-6007. As indicated in the NUREG/CR-6007 text, the negative sign identifies the load as an inward load. If used as negative in the Fap equation, the fixed-edge moment causes a compressive bolt force. Since this could obviously not occur from a closure lid center puncture, the sign has been reversed to indicate a positive moment. The prying force, Fap, is calculated from the following formula:

[1] Per Figure III.10 of NUREG/CR-6007 for an inward-directed puncture loading.

$$Fap = \left(\frac{\pi(Dlb)}{Nb}\right)\left[\frac{\frac{2(Mf)}{Dlb - Dli} - (C1)(B - Ff) - (C2)(B - P)}{C1 + C2}\right]$$

where Dlb is the closure lid diameter at the bolt circle, Dli is the closure lid diameter at the inner edge, P is the bolt preload per unit length of the bolt circle, B = P (per Table 2.1 of NUREG/CR-6007), C1 = 1, and P and C2 are based on the following formulae:

$$P = \frac{(Fa_{max})(Nb)}{\pi(Dlb)}$$

$$C2 = \left(\frac{8}{3(Dlb - Dli)^2}\right)\left[\frac{(El)(tl)^3}{1 - Nul} + \frac{(Dlb - Dli)(Elf)(tlf)^3}{Dlb}\right]\left(\frac{Lb}{(Nb)(Db)^2(Eb)}\right)$$

where El is the elastic modulus of the closure lid material, tl is the thickness of the closure lid, Nul is Poisson's ratio of the closure lid material, Elf is the elastic modulus of the closure lid flange material, tlf is the thickness of the closure lid flange, Lb is the grip length of the bolt, Db is the nominal bolt diameter, and Eb is the elastic modulus of the closure bolt material.

Prying forces on the bolts as a result of puncture impacts are given in Table 2.10.4-6.

2.10.4.2.8 Closure Bolt Forces/Moments Generated by Vibration Loads

From Subsection 4.8 of NUREG/CR-6007, resonant vibrations can produce loads in the closure bolts. As described in Section 2.6.5, the vibration normally incident to transport is 2g in the vertical direction, and 0.1g in the lateral and longitudinal directions. When the cask is in the transport mode, it is oriented vertically. The vertical force on the lid is 2g in magnitude. The longitudinal force on the lid is only 0.1g in magnitude, a modest inertia load relative to the other loads on the bolts, such as free drop impact loads, and is therefore ignored.

Utilizing appropriate temperature dependent material properties from Section 2.3, the maximum non-prying tensile force per bolt, Fa, due to vibration loads is based on the following formula:

$$Fa = \frac{(VTR)(ava)(Wl)}{Nb} = 150\ lb$$

where VTR = 1.0 is the vibration transmissibility of acceleration between the cask support and the closure lid, ava = 2 is the maximum vertical vibration acceleration (g), Wl = 900 lb is the weight of the closure lid, and Nb = 12 is the total number of closure bolts.

Forces on the bolts as a result of NCT vibration loading are given in Table 2.10.4-6.

2.10.4.3 Combination of Closure Bolt Forces/Moments from Different Loads

Per Subsection 4.9 of NUREG/CR-6007, the load combinations for normal and hypothetical accident conditions are presented in Table 2.10.4-7. The types of loads which are considered for each load combination case are designated in brackets (e.g., {}) in the first column of Table 2.10.4-7. The following abbreviations are used: L = preload force, P = pressure force, T = temperature force, I = impact force, U = puncture prying force, and V = vibration force.

2.10.4.4 Closure Bolt Stress Analysis

Per Section 5.0, Table 5.1, of NUREG/CR-6007, the calculation of the closure bolt tensile, shear, bending, and torsional stresses, and stress intensity for combined stresses, are based on the load combinations presented in Section 2.10.4.2. The bolt diameter used for stress calculations is based on the stress diameter of the closure bolts, i.e., 0.653 inches.

The closure bolt tensile stress, Sba, is defined as:

$$Sba = (1.2732)\frac{Fa}{Dba^2}$$

The closure bolt shear stress, Sbs, is defined as:

$$Sbs = (1.2732)\frac{Fs}{Dbs^2}$$

The closure bolt bending stress, Sbb, is defined as:

$$Sbb = (10.186)\frac{Mbb}{Dbb^3}$$

The closure bolt torsional stress, Sbt, is defined as:

$$Sbt = (5.093)\frac{Mtr}{Dbt^3}$$

Finally, the closure bolt stress intensity, Sbi, is defined as:

$$Sbi = \sqrt{(Sba + Sbb)^2 + 4(Sbs + Sbt)^2}$$

The calculated stresses are summarized in Table 2.10.4-8 and their resulting stress ratios are summarized in Table 2.10.4-9.

From Table 2.1-1, for NCT the allowable average tensile stress is S_m, and the allowable average shear stress is $0.6S_m$, where S_m is 2/3 of the yield stress, S_y, at temperature. For the NCT cold condition, the allowable tensile stress is $(2/3)S_y$ = 70,000 psi, and the allowable shear stress is $(0.6)(2/3)S_y$ = 42,000 psi, at a temperature of -20 °F. For the NCT warm condition, the allowable tensile stress is $(2/3)S_y$ = 62,500 psi, and allowable shear stress is $(0.6)(2/3)S_y$ = 37,500 psi, at a temperature of 350 °F.

For tension plus shear plus bending plus residual torsion, and closure bolts having a minimum ultimate stress, S_u, greater than 100,000 psi, the maximum stress intensity is $1.35S_m$ = $(1.35)(2/3)S_y$. Thus, for the NCT cold condition, the allowable stress intensity is 94,500 psi, and for the NCT warm condition, the allowable stress intensity is 84,375 psi.

For HAC, the allowable average tensile stress is the lesser of $0.7S_u$ or S_y, and the allowable average shear stress is the lesser of $0.42S_u$ or $0.6S_y$ at temperature. For the HAC cold condition, the allowable tensile stress is $0.7S_u$ = 87,500 psi, and the allowable shear stress is $0.42S_u$ = 52,500 psi, at a temperature of -20 °F. For the HAC warm condition, the allowable tensile stress S_y = 87,240 psi, and allowable shear stress is 0.6Sy = 52,344 psi, at a temperature of 530 °F.

Combining tension plus shear plus bending plus residual torsion is not applicable for HAC.

2.10.4.5 Closure Bolt Thread Engagement Length and Stress Area

The closure bolt holes in the cask body are fitted with Tridair® thread inserts made from 303 CRES steel. In order for the bolts, not the inserts, to govern stress analysis of the bolts, the pull-out yield and ultimate strengths of the insert should be greater than the tensile yield and ultimate strengths of the bolts. These relationships are expressed by the following formulae:

$$\frac{(A_{ins})(0.6S_{yp})}{(A_{tb})(S_{yb})} > 1.0 \qquad \text{eq. (1)}$$

$$\frac{(A_{ins})(0.6S_{up})}{(A_{tb})(S_{ub})} > 1.0 \qquad \text{eq. (2)}$$

where A_{ins} is the insert minimum engagement, $0.6S_{yp}$ is the yield shear strength of the parent material, A_{tb} is the tensile stress area of the bolt, S_{yb} is the yield strength of the bolt, $0.6S_{up}$ is the ultimate strength of the parent material, and S_{ub} is the ultimate strength of the bolt material. If these ratios are greater than unity, the bolt is the critical member.

According to the Tridair® catalog [23], the minimum shear area of the insert is A_{ins} = 2.4901 in^2. The tensile stress area of a standard 3/4-10UNC-2A bolt is A_{tb} = 0.3266 in^2. Table 2.10.4-4 gives the ratio of parent material pull-out load to bolt failure load for both yield (equation (1) above) and ultimate strengths (equation (2) above) for both NCT warm (350 °F) and cold (-20 °F) conditions. Since all of the ratios are greater than unity, the bolt is the critical member in all cases, and the parent material need not be further considered.

Table 2.10.4-4 - Bolt Parent Material vs. Bolt Strength

	S_{yp}, psi	S_{up}, psi	S_{yb}, psi	S_{ub}, psi	Yield Ratio using eq. (1)	Ultimate Ratio using eq. (2)
Cold (-20 °F)	30,000	75,000	105,000	125,000	1.31	2.74
Warm (350 °F)	21,650	65,200	93,750	125,000	1.06	2.39

2.10.4.6 Summary

As shown in Table 2.10.4-9, the largest tensile stress ratio, Rt, is 0.76, the largest shear stress ratio, Rs, is 0.63, the largest combined stress ratio is 0.79, and the largest stress intensity ratio is 0.73. In each case, the largest ratio is well less than unity in accordance with the recommendations of NUREG/CR-6007, and therefore, the SEC closure lid bolts are not of concern for all normal conditions of transport and all hypothetical accident conditions.

Table 2.10.4-5 - Geometric Parameters Used in Bolt Evaluations

Property	Description	Dimension
Db	Closure bolt nominal diameter, inches	0.75
Dba	Closure bolt diameter for tensile stress calculation, inches	0.653
Dbs	Closure bolt diameter for shear stress calculation, inches	0.653
Dbb	Closure bolt diameter for bending stress calculation, inches	0.653
Dbt	Closure bolt diameter for torsional stress calculation, inches	0.653
Lb	Bolt length between the top and bottom surfaces of the closure lid at the bolt circle, inches	4.4375
Nb	Number of closure bolts	12
K	Nut factor	0.186①
Q_{max}	Maximum applied preload torque, in-lb	1,200
Q_{min}	Minimum applied preload torque, in-lb	960
Dlb	Closure lid diameter at the bolt circle, inches	18.50
Dli	Closure lid diameter at the inner edge, inches	11.478
Dlo	Closure lid diameter at the outer edge, inches	19.75
Dlg	Face seal diameter, inches	13.25
tc	Cask wall thickness, inches	11.375
tl	Closure lid thickness, inches	16.875
tlf	Lid flange thickness, inches	5.25
Wl	Weight of closure lid, lb	900
Wc	Weight of cask contents, lb	50

Notes:

① For cadmium plated bolts.

Table 2.10.4-6 - Closure Bolt Forces

Force	NCT				HAC		Force Parameter
	Cold (-40)	Drops (-20)	Warm	Warm (drops)	Cold	Hot (Fire)	
Preload							
Far{L}	8602.2	8602.2	8602.2	8602.2	8602.2	8602.2	Non-prying tensile force (lb)
Mtr{L}	600.0	600.0	600.0	600.0	0	0	Residual torsional moment (lb-inch)
Pressure							
Fa{P}	0	0	703.2	574.5	0.0	574.5	Non-prying tensile force (lbs.)
Fs{P}	0	0	0.0	0.0	0.0	0.0	Shear force (lb)
Temperature							
Fa{T}	-3204.4	-2590.1	7233.5	7233.5	-2590.1	11475.0	Non-prying tensile force (lb)
Fs{T}	0	0	0	0	0	0	Shear force (lb)
Impact (End)							
Fa{I}	0	8486.7	0	6365.0	18564.6	11138.8	Non-prying tensile force (lb)
Fs{I}	0	0	0	0	0	0	Shear force (lb)
Mf{I}	0	4052.1	0	3039.1	8863.9	5318.4	Fixed-edge moment (lb-inch/inch)
Mbb{I}	0	0.216	0	0.162	0.472	0.287	Bending Moment (lb-inch)
Impact (Side)							
Fa{I}	0	0	0	0	0	0	Non-prying tensile force (lb)
Fs{I}	0	3750.0	0	2625.0	10875.0	6375.0	Shear force (lb)
Impact (Slapdown)							
Fa{I}	0	0	0	0	0	0	Non-prying tensile force (lb)
Fs{I}	0	3675.0	0	2925.0	11025.0	6600.0	Shear force (lb)
Puncture							
Fa{U}	0	0	0	0	-118333.3	-118333.3	Non-prying tensile force (lb)
Fs{U}	0	0	0	0	0.0	0.0	Shear force (lb)
Ff{U}	0	0	0	0	-24432.4	-24432.4	Fixed-edge force (lb/inch)
Mf{U}	0	0	0	0	-113000.0	-113000.0	Fixed-edge moment (lb-inch/inch)
Fap{U}	0	0	0	0	94.6	95.1	Prying Force (lb)
Vibration							
Fa{V}	0.0	150.0	150.0	0.0	0	0	Non-prying tensile force (lb)

Notes:

① Results of calculations are based on loads, geometric properties, and mechanical properties per NUREG/CR-6007.

Table 2.10.4-7 - Normal and Hypothetical Accident Conditions Load Combinations

Load Combination	Identification per Table 4.9 of NUREG/CR-6007							
	① Fa_pt (lbs.)	② Fa_al (lbs.)	③ Fa_c (lbs.)	④ Fap_c (lbs.)	Fa (lbs.)	Fs (lbs.)	Mbb (lb-in)	⑤ Mtr (lb-in)
1. NCT Cold Operating (-20) {L}, {P}, {T}, {V}	6,012	150	6,012	0	6,012	0	0	600
2. NCT Hot Operating {L}, {P}, {T}, {V}	15,836	853	15,836	0	15,836	0	0	600
3. NCT Cold Impact (End) {L}, {P}, {T}, {I}	6,012	8,487	8,487	0	8,487	0	0	600
4. NCT Hot Impact (End) {L}, {P}, {T}, {I}	15,836	6,940	15,836	0	15,836	0	0	600
5. NCT Cold Impact (Side) {L}, {P}, {T}, {I}	6,012	0	6,012	0	6,012	3,750	0	600
6. NCT Hot Impact (Side) {L}, {P}, {T}, {I}	15,836	575	15,836	0	15,836	2,625	0	600
7. NCT Cold Impact (Slapdown) (L}, {P}, {T}, {I}	6,012	0	6,012	0	6,012	3,675	0	600
8. NCT Hot Impact (Slapdown) {L}, {P}, {T}, {I}	15,836	575	15,836	0	15,836	2,925	0	600
9. HAC Cold Pressure {L}, {P}, {T}	6,012	0	6,012	0	6,012	0	0	0
10. HAC Hot (Fire) Pressure {L}, {P}, {T}	20,077	575	20,077	0	20,077	0	0	0
11. HAC Cold Impact (End) {L}, {P}, {I}	8,602	18,565	18,565	0	18,565	0	0	0
12. HAC Hot Impact (End) {L}, {P}, {I}	8,602	11,713	11,713	0	11,713	0	0	0
13. HAC Cold Impact (Side) {L}, {P}, {I}	8,602	0	8,602	0	8,602	10,875	0	0
14. HAC Hot Impact (Side) {L}, {P}, {I}	8,602	575	8,602	0	8,602	6,375	0	0
15. HAC Cold Impact (Slapdown) (L}, {P}, {I)	8,602	0	8,602	0	8,602	11,025	0	0
16. HAC Hot Impact (Slapdown) {L}, {P}, {I}	8,602	575	8,602	0	8,602	6,600	0	0
17. HAC Cold Puncture (L}, {P}, {U}	8,602	-118,333	8,602	95	8,697	0	0	0
18. HAC Hot Puncture {L}, {P}, {U}	8,602	-117,759	8,602	95	8,697	0	0	0

Notes (continued on next page):

① Fa_pt is the summation of Fa{L} + Fa{T} for NCT, or Fa{L} for HAC, from Table 2.10.4-6.

Notes (continued from previous page):

② Fa_al is the summation of Fa{P} + Fa{I} or Fa{P} + Fa{U}, from Table 2.10.4-6, whichever is the application load combination.

③ Fa_c is the greater of Fa_pt or Fa_al.

④ Fap_c is Fap{U}, from Table 2.10.4-6.

⑤ Mtr, the closure bolt residual torsional moment, is not used for HAC evaluations.

Table 2.10.4-8 - Closure Bolt Stress Analysis Results

Load Combination	Tensile Stress, Sba (psi)	Shear Stress, Sbs (psi)	Bending Stress, Sbb (psi)	Torsional Stress, Sbt (psi)	Stress Intensity, Sbi (psi)
1. NCT Cold Operating {L}, {P}, {T}, {V}	17,951	0	0	10,975	28,355
2. NCT Warm Operating {L}, {P}, {T}, {V}	47,283	0	0	10,975	52,129
3. NCT Cold Impact (End) {L}, {P}, {T}, {I}	25,340	0	0	10,975	33,524
4. NCT Warm Impact (End) {L}, {P}, {T}, {I}	47,283	0	0	10,975	52,129
5. NCT Cold Impact (Side) {L}, {P}, {T}, {I}	17,951	11,197	0	10,975	47,839
6. NCT Warm Impact (Side) {L}, {P}, {T}, {I}	47,283	7,838	0	10,975	60,426
7. NCT Cold Impact (Slapdown) (L}, {P}, {T}, {I}	17,951	10,973	0	10,975	47,424
8. NCT Warm Impact (Slapdown) {L}, {P}, {T}, {I}	47,283	8,734	0	10,975	61,558
9. HAC Cold Pressure {L}, {P}, {T}	17,951	0	0	0	17,951
10. HAC Warm (Fire) Pressure {L}, {P}, {T}	59,948	0	0	0	59,948
11. HAC Cold Impact (End) {L}, {P}, {I}	55,431	0	0	0	55,431
12. HAC Warm Impact (End) {L}, {P}, {I}	34,974	0	0	0	34,974
13. HAC Cold Impact (Side) {L}, {P}, {I}	25,685	32,471	0	0	69,837
14. HAC Warm Impact (Side) {L}, {P}, {I}	25,685	19,035	0	0	45,924
15. HAC Cold Impact (Slapdown) (L}, {P}, {I)	25,685	32,919	0	0	70,671
16. HAC Warm Impact (Slapdown) {L}, {P}, {I}	25,685	19,707	0	0	47,044
17. HAC Cold Puncture {L}, {P}, {U}	25,967	0	0	0	25,967
18. HAC Warm Puncture {L}, {P}, {U}	25,969	0	0	0	25,969

Table 2.10.4-9 - Summary of Stress Ratios

Load Combination	Applied Tensile Stress	Allowable Tensile Stress	Tensile Stress Ratio, Rt	Applied Shear Stress	Allowable Shear Stress	Shear Stress Ratio, Rs	Combined Stress Ratio<1	Applied Stress Intensity	Allowable Stress Intensity	Stress Intensity Ratio<1
1. NCT Cold Operating {L}, {P}, {T}, {V}	17,951	70,000	0.26	0	42,000	0.00	0.26	28,355	94,500	0.30
2. NCT Warm Operating {L}, {P}, {T}, {V}	47,283	62,500	0.76	0	37,500	0.00	0.76	52,129	84,375	0.62
3. NCT Cold Impact (End) {L}, {P}, {T}, {I}	25,340	70,000	0.36	0	42,000	0.00	0.36	33,524	94,500	0.35
4. NCT Warm Impact (End) {L}, {P}, {T}, {I}	47,283	62,500	0.76	0	37,500	0.00	0.76	52,129	84,375	0.62
5. NCT Cold Impact (Side) {L}, {P}, {T}, {I}	17,951	70,000	0.26	11,197	42,000	0.27	0.37	47,839	94,500	0.51
6. NCT Warm Impact (Side) {L}, {P}, {T}, {I}	47,283	62,500	0.76	7,838	37,500	0.21	0.78	60,426	84,375	0.72
7. NCT Cold Impact (Slapdown) (L}, {P}, {T}, {I}	17,951	70,000	0.26	10,973	42,000	0.26	0.37	47,424	94,500	0.50
8. NCT Warm Impact (Slapdown) {L}, {P}, {T}, {I}	47,283	62,500	0.76	8,734	37,500	0.23	0.79	61,558	84,375	0.73
9. HAC Cold Pressure {L}, {P}, {T}	17,951	87,500	0.21	0	52,500	0.00	0.21	17,951	N/A	N/A
10. HAC Warm (Fire) Pressure {L}, {P}, {T}	59,948	87,240	0.69	0	52,344	0.00	0.69	59,948	N/A	N/A
11. HAC Cold Impact (End) {L}, {P}, {I}	55,431	87,500	0.63	0	52,500	0.00	0.63	55,431	N/A	N/A

Table 2.10.4-9 - Summary of Stress Ratios

Load Combination	Applied Tensile Stress	Allowable Tensile Stress	Tensile Stress Ratio, Rt	Applied Shear Stress	Allowable Shear Stress	Shear Stress Ratio, Rs	Combined Stress Ratio<1	Applied Stress Intensity	Allowable Stress Intensity	Stress Intensity Ratio<1
12. HAC Warm Impact (End) {L}, {P}, {I}	34,974	87,240	0.40	0	52,344	0.00	0.40	34,974	N/A	N/A
13. HAC Cold Impact (Side) {L}, {P}, {I}	25,685	87,500	0.29	32,471	52,500	0.62	0.68	69,837	N/A	N/A
14. HAC Warm Impact (Side) {L}, {P}, {I}	25,685	87,240	0.29	19,035	52,344	0.36	0.47	45,924	N/A	N/A
15. HAC Cold Impact (Slapdown) (L}, {P}, {I)	25,685	87,500	0.29	32,919	52,500	0.63	0.69	70,671	N/A	N/A
16. HAC Warm Impact (Slapdown) {L}, {P}, {I}	25,685	87,240	0.29	19,707	52,344	0.38	0.48	47,044	N/A	N/A
17. HAC Cold Puncture {L}, {P}, {U}	25,967	87,500	0.30	0	52,500	0.00	0.30	25,967	N/A	N/A
18. HAC Warm Puncture {L}, {P}, {U}	25,969	87,240	0.30	0	52,344	0.00	0.30	25,969	N/A	N/A

Notes:

① Applied Tensile Stress, Sba; Applied Shear Stress, Sbs, Applied Stress Intensity, Sbi, all taken from Table 2.10.4-8.

② NCT and HAC allowable stresses at temperature are defined in Section 2.10.4.4.

③ $\sqrt{(Rt)^2 + (Rs)^2} \leq 1$

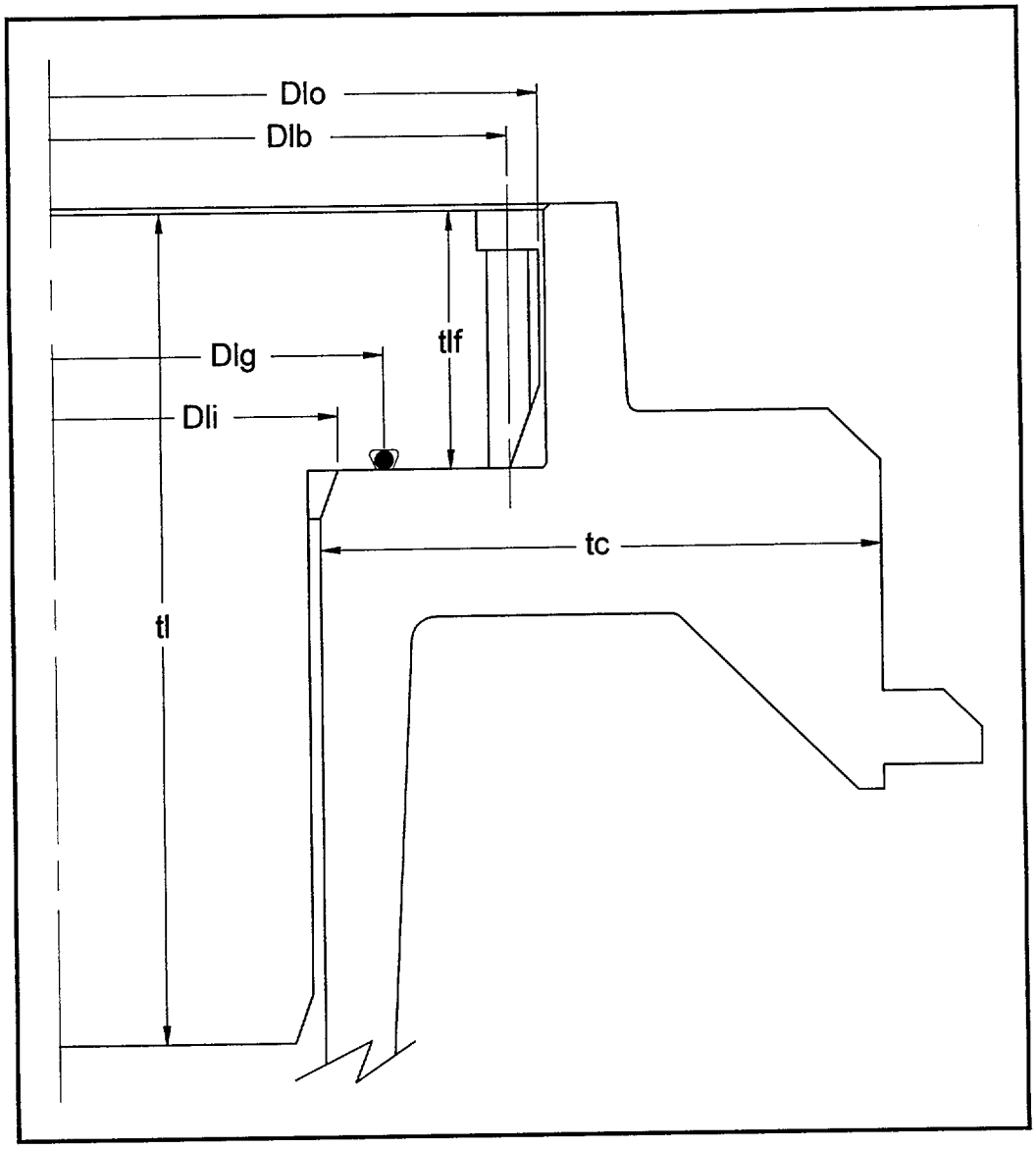

Figure 2.10.4-1 - Closure Bolt Analysis Configuration

2.10.5 Dynamic Test Results

This section describes the quarter scale dynamic test of the SEC impact limiters. Four quarter scale, prototypic impact limiter specimens were tested using a test cask. The test cask was made of solid steel, and simulated the weight of the prototypic cask. Three HAC, 30 ft free drop tests and three, HAC puncture tests were performed. The test was conducted in accordance with PacTec document TP-007, *Test Plan for the SteriGenics Isotope Cask.* The 30 ft free drop test orientations consisted of end (vertical), side (horizontal), and c.g.-over-corner (54.5° to the horizontal). The puncture test orientations consisted of side, c.g.-over-bar axis, and an orientation in which the bar axis was chosen to place the maximum separation loads on the impact limiter attachments. Testing was performed in Tacoma, Washington on October 22, 1998.

Dynamic testing had a twofold purpose:

- To confirm that the dynamic finite element modeling of the impact limiter behavior is capable of accurate predictions of impact accelerations and deformations. This confirmation is primarily accomplished by comparisons between test and predicted impact limiter deformations. The dynamic finite element impact model is described in detail in Section 2.10.3, and results of the modeling, including predicted impact accelerations and deformations, are discussed in Section 2.7.1.
- To ensure that impact limiter damage is of an acceptable magnitude. This is accomplished by demonstrating that an impact limiter cannot be dislodged by a HAC event, that the impact limiters do not "bottom out", and that impact and puncture damage is consistent with thermal analysis assumptions.

2.10.5.1 Test Article Configuration

The test was conducted with quarter scale components. Therefore, all dimensions of the test articles were ¼ that of the full size, prototypic cask. It follows that the volume, and thus the weight, of the test package must be $(1/4^3) = 1/64$ that of the full size package. The weight of the test package, including the test cask and two impact limiters, was 307 lb, or within 1.8% of the value of W/64 = 312.5 lb, where W = 20,000 lb from Table 2.2-1.

The configuration of the test package is shown in Figure 2.10.5-1. As shown, the test cask is solid steel, including threaded lift provisions to facilitate rigging at the required orientations. The upper and lower impact limiters, the cask-to-impact limiter interface configuration, and the impact limiter attachments are prototypic based on the drawings given in Apendix 1.3.2 *Packaging General Arrangement Drawings*, with exceptions noted below.

1. The circumferential welds attaching the toroids to the impact limiter cap structures were welded oversize. The prototypic welds are full penetration groove welds with a ⅛ inch (quarter scale) fillet reinforcement, whereas the test article welds had up to ⅜ inches of reinforcement (quarter scale). This difference (¼ inches) is insignificant, since added reinforcement of a full penetration groove weld adds no extra strength. The minimum

section is the same, which is the thickness of the basic shell of the toroid at the edge of the weld.

A very small amount of added stiffness is also a possible result of the extra reinforcement. However, this is also negligible, since the observed deformation in the dynamic test occurred at the contact with the ground, which was relatively far from the noted oversized welds. Therefore, the weld stiffness could have had very little effect on the stiffness and deformation of the test articles.

2. The test package used a quantity of eight, evenly spaced attachment pins between an impact limiter and the test cask, whereas the prototypic package has a quantity of 12, evenly spaced pins. As will be noted in the discussion of results, the test impact limiters did not become dislodged by any of the impact or puncture tests, therefore demonstrating the adequacy of the original, eight pin design. The addition of four more pins (an increase in quantity of 50%) for the final, prototypic design is conservatively chosen based on results of testing (further discussed in Section 2.10.5.3.6).
3. The diameter of the hole in the impact limiter cap through which the attachment pins pass was up to 0.030 inches oversize on the test articles. The maximum quarter scale dimension for the holes is 0.282 inches, and the actual hole size was 0.313 inches. This difference is also conservative, since the result is to reduce the material resisting tearout of the pins and increase the likelihood of loss of the impact limiter. However, as noted in Section 2.10.5.3.6, no tearout of the holes was noted following testing. Therefore, the increased hole size is not significant.
4. The distance from the attachment pin hole center to the edge of the cap section was smaller in the test articles than in the prototypic design. The test article distance was nominally 0.38 inches, whereas the prototypic design distance (in quarter scale) is 0.43 inches. This difference represents added material to resist tearout of the attachment pins, and is conservative.
5. The test impact limiters had one inch diameter holes in the center of the cap section, instead of a threaded lifting provision. This difference had no effect on test results.
6. The test impact limiters had no tamper indicating tabs or wires. This difference had no effect on test results.

The material used to fabricate the impact limiter toroidal shells underwent static tensile testing to establish its stress-strain properties. The material properties used for the analytical comparison to dynamic test results is discussed in Section 2.10.5.4. The temperature of the toroidal shells was approximately 60 - 70 °F during all testing.

2.10.5.2 Test Facilities

The drop testing was performed using a horizontal concrete slab which was approximately 20 inches thick × 4 feet × 8 feet. A 2 inch thick × 46 inch × 60 inch steel plate was placed on top of the concrete slab and welded to two 8-inch wide steel channels embedded in the concrete. The estimated weight of the drop pad is 9,295 lb, which is more than 30 times the weight of the assembled cask and limiters, and therefore well within the IAEA recommendation that the

impacted weight be at least ten times that of the test package. Based on these characteristics, the drop pad satisfies the requirement of 10 CFR §71.73 for an essentially unyielding, horizontal surface.

The bar for the puncture tests was a 1.5 inch diameter, solid, mild steel bar which was orthogonally socket welded through a 1 inch × 12 inch × 12 inch steel plate. The top circumferential edge of the bar has a 1/16-inch radius. The bar dimensions are reduced by a factor of 4 from those specified in 10 CFR §71.73(c)(3), consistent with a quarter scale test. Two bars were used in the testing. The first, used for tests 4 and 5, extended 8 inches above the plate. The second bar extended 24 inches above the plate so that it could strike the underside of the upper impact limiter before the lower impact limiter struck the ground. The lengths were sufficient to cause maximum damage to the SEC as required by 10 CFR §71.73(c)(3). The plate supporting the puncture bars was firmly welded to the steel plate covering the drop pad during puncture testing.

The free drop height of all HAC free drops was 30 ft, +3/-0 inches, as verified using a measured length of twine and a plumb bob. The height of all HAC puncture drops was 40 inches, +3/-0 inches, verified in a similar manner. The orientation of drops was measured using an inclinometer. A visual record was made of the drop events using a standard video camera, and still photographs made of the test articles both before and after test. The electrically actuated release hook used to suspend and release the cask provided a clean release with no initial disturbance, and all drops were completely free from the specified height.

2.10.5.3 Test Sequence and Results

Four different, prototypic test articles were used for all of the testing, designated by number as IL1, IL2, IL3, and IL4. Each of the three free drops (end, side, and c.g.-over-corner) was performed with an undamaged specimen. All of the drop orientations were stable, i.e., did not induce significant cask rotation upon impact. The side drop, shown in Figure 2.10.5-2, used IL1 and IL2. The end drop, shown in Figure 2.10.5-3, used IL3 on the impacting end. The c.g.-over-corner drop, shown in Figure 2.10.5-4, used IL4 on the impacting end. (IL1 remained in place on the upper end of the cask during the second and third free drops, but did not suffer any additional damage.)

The first two puncture drops (the side orientation, shown in Figure 2.10.5-5, and c.g.-over-puncture bar axis orientation, shown in Figure 2.10.5-6) used undamaged portions of IL4, separating the free and puncture drop impacts by approximately 120° of circumference. The damage inflicted by these two puncture events on IL4 did not overlap, either with each other, or with the prior free drop damage. The final puncture drop, shown in Figure 2.10.5-7, impacted IL1 in an area not affected by prior free drop damage.

Post-test measurements were taken of the impact limiter configuration to determine the impact deformations. This was accomplished by sawing the impact limiter in half, with the saw cut axis running through the approximate center of the damaged area, and subsequently making paper tracings of the deformed shape. Comparisons made between the deformed shape and the shape of an undamaged region of the impact limiter allowed calculation of the impact deformation. Since the damage to the limiters was in general not severe, relatively large undamaged regions

existed for this purpose. For each 30 ft free drop, a figure was prepared showing an overlay of three impact limiter outlines; first, the undamaged shape; second, the post-test deformed shape; and third, the analytical prediction using the LS-DYNA [16] dynamic finite element code. The analytical prediction is discussed in Section 2.10.5.4. Since the finite element model is constructed using shell elements located on the meridian of the toroids, an appropriate half-thickness offset is used to facilitate direct comparison to the traces of actual articles.

The test orientations are summarized in Table 2.10.5-1. Test results are summarized in Table 2.10.5-2, and are now discussed in detail. In Table 2.10.5-2, all deformations are defined along the axis of cask travel during impact, i.e., normal to the ground.

Table 2.10.5-1 - Summary of Drop Test Orientations

Test No.	Test Description	Limiter Designation	Test Unit Axis Orientation①
1	30 ft Side Drop	IL1, IL2	0°
2	30 ft End Drop	IL1, IL3	90°
3	30 ft C.G.-Over-Corner Drop	IL1, IL4	54.5°
4	40 in. Side Puncture	IL1, IL4	0°
5	40 in. C.G.-Over-Corner Puncture	IL1, IL4	54.5°
6	40 in. Puncture Below Upper Limiter	IL1, IL4	12°

Notes:

① Orientation angle with respect to the horizontal plane.

2.10.5.3.1 HAC 30 ft Side Drop

This test was a free drop from a height of 30 ft in the side (horizontal) orientation on IL1 and IL2, shown in Figure 2.10.5-2. This test produced side drop damage for comparison with analytical predictions, and also applied the greatest forces to the impact limiter attachment pins of any free drop orientation, as discussed in Section 2.7.1.5. The rebound after impact was relatively small. The resulting deformation, measured normal to the cask axis, was 1.06 inches on IL1 and 1.14 inches on IL2, for an average of 1.10 inches. Photographs of the deformation are shown in Figures 2.10.5-8 and -9, and a graphical comparison of the deformed shape and the analytical prediction is given in Figure 2.10.5-10.

None of the impact limiter attachment pins failed in the drop. Some pins became slightly bent as a result of contact between the exposed pin handles and the deformation bulge of the toroid. Significantly, the attachment pins showed essentially no shear deformation from the drop, and the material resisting tearout of the pins showed almost no plastic deformation. The overall

deformation of the test articles was modest, and no impending failure of any structural welds was noted. The analytical model deformation prediction was 1.29 inches, or within 17.3% of the test deformation. Therefore, the side drop analysis successfully predicted the empirical results.

Table 2.10.5-2 - Summary of Drop Test Results

Test No.	Test Description	Measured Deformation, inches	Remarks
1	30 ft Side Drop	1.10	Worst-case 30 ft free drop attachment loads: no pins sheared
2	30 ft End Drop	0.82	Orientation for maximum impact loading of cask
3	30 ft C.G.-Over-Corner Drop	1.92	Orientation for maximum deformation of impact limiter
4	40 in. Side Puncture	0.15	---
5	40 in. C.G.-Over-Corner Puncture	0.6	Orientation for maximum puncture damage to toroid: damage minimal
6	40 in. Puncture Below Upper Limiter	negligible	Worst-case puncture drop attachment loads: limiter remained attached (4 pins sheared)

2.10.5.3.2 HAC 30 ft End Drop

This test was a free drop from a height of 30 ft in the end (vertical) orientation on IL3, shown in Figure 2.10.5-3. This test produced end drop damage for comparison with analytical predictions. This test did not place significant shear loads on the impact limiter attachment pins, although several pins again experienced slight bending due to contact between the handles and the toroid deformation. Again, the rebound after impact was small, just enough to tip the cask on its side. The resulting deformation, measured parallel to the cask axis, was 0.82 inches. Photographs of the deformation are shown in Figures 2.10.5-11 and -12, and a graphical comparison of the deformed shape and the analytical prediction is given in Figure 2.10.5-13. Again, the overall deformation of the test article was modest, and no impending failure of any structural welds was noted. The analytical model deformation prediction was 0.90 inches, or within 9.8% of the test deformation. Therefore, the end drop analysis successfully predicted the empirical results.

2.10.5.3.3 HAC 30 ft C.G.-Over-Corner Drop

This test was a free drop from a height of 30 ft in the c.g.-over-corner (54.5° to the horizontal plane) orientation on IL4, shown in Figure 2.10.5-4. The actual angle achieved was 55.5°, which

was within an acceptable variation. The test produced c.g.-over-corner drop damage for comparison with analytical predictions. The test did not place significant shear loads on the impact limiter attachment pins. Slight bending of a few of the pins occurred for the same reasons stated above. Again, the rebound after impact was small. The resulting deformation, measured along a line parallel to the cask travel during impact, was 1.92 inches. Photographs of the deformation are shown in Figures 2.10.5-14 and -15, and a graphical comparison of the deformed shape and the analytical prediction is given in Figure 2.10.5-16. Again, the overall deformation of the test article was modest, and "bottom-out" of the impact limiter was not approached. The analytical model deformation prediction was 2.20 inches, or within 14.6% of the test deformation. Therefore, the c.g.-over-corner drop analysis successfully predicted the empirical results.

2.10.5.3.4 HAC Puncture Drop in the Side Orientation

This test was a free drop of IL4 from a height of 40 inches onto the 8 inch long puncture bar. The cask was in the horizontal orientation, and the bar axis was normal to the cask axis. The bar struck the limiter at its center, as shown in Figure 2.10.5-5. Since the bar axis did not pass through the cask c.g., upon impact with the bar, the cask quickly rotated away from the bar, and damage to the impact limiter was minimal. The depth of indentation was approximately 0.15 inches. There was no evidence of cracking of the toroidal shell as a result of this deformation. A photograph of the deformation is shown in Figure 2.10.5-17. Since the deformation was very slight, the side puncture drop test was successful.

2.10.5.3.5 HAC Puncture Drop in the C.G.-Over-Bar Axis Orientation

This test was a free drop of IL4 from a height of 40 inches onto the 8 inch long puncture bar. The cask was oriented such that the axis of the bar passed through the c.g. of the cask, and therefore represented the worst-case damage to the impact limiter toroidal shell. The drop orientation is shown in Figure 2.10.5-6. The depth of the indentation was approximately 0.6 inches. There was no evidence of cracking of the toroidal shell as a result of this deformation. A photograph of the deformation is shown in Figure 2.10.5-18. Since the worst-case damage was very modest and would have no effect on thermal analysis assumptions, the c.g. over bar axis test was successful.

2.10.5.3.6 HAC Puncture Drop on the Upper Impact Limiter from Beneath

This test was a free drop of the cask from a height of 40 inches onto the 24 inch long puncture bar. The cask was oriented such that the impact with the bar occurred beneath the upper impact limiter (IL1), as shown in Figure 2.10.5-7. The cask was inclined approximately 12° away from the bar axis. This angle was made as small as possible, such that the puncture bar would not strike the lower limiter (IL4), and yet strike the upper limiter in a manner to place the largest possible shear loads on the attachment pins. There was essentially no resulting deformation of the upper limiter at the impact point, but four of the eight attachment pins were sheared off. Other pins showed some shear deformation. As a consequence of this, however, the impact limiter did not become dislodged from the cask. The resulting misalignment of the limiter was very modest, characterized by a gap between the cask mounting surface and mating impact

limiter cap structure of less than ½ inches. A photograph of the sheared pins, along with an intact pin for comparison, is shown in Figure 2.10.5-19. As noted above, however, the actual quantity of attachment pins on the prototypic cask is 12, a conservative increase of 50%. Since the worst-case loading of a puncture bar did not dislodge the impact limiter from the cask, the puncture on the upper limiter from beneath was successful.

2.10.5.4 Analytical Predictions

Analytical predictions of the three 30 ft free drop tests are performed using the LS-DYNA dynamic finite element models described in Section 2.10.3. A description of the use of these models in evaluating cask impact accelerations and maximum deformations is given in Section 2.7.1. The analytical predictions were based on the material properties of the plates used to fabricate the toroids used in the dynamic drop tests. The material properties were determined by a tensile test performed on material from the same heat, subject to the same thermal treatment, as the material used to fabricate the dynamic test article toroids. The engineering yield stress (0.2% offset) and ultimate stress of the material was 38,000 psi and 92,650 psi, respectively, at 70 °F. The stress-strain curve used in the analytical prediction was generated as follows.

First, based on the discussion given in Section 2.3.2, the engineering stress-strain data was converted to true stress-strain data, using the relation

$$\sigma_{true} = \sigma_{eng}\left(1+\varepsilon_{eng}\right)$$

If the value of engineering yield strength of 38,000 psi is substituted for σ_{eng}, along with the 0.2% offset strain ($\varepsilon_{eng} = 0.002$), the resulting true yield strength is 38,076 psi. If the value of engineering ultimate strength of $S_y = 92,650$ psi is substituted for σ_{eng}, along with the ultimate strain of $\varepsilon_{eng} = 0.547$ (54.7% elongation), the true ultimate strength is $S_u = 143,330$ psi. These values are used to create a bi-linear true stress strain curve having a tangent modulus found from

$$E_t = \frac{S_u - S_y}{\varepsilon_u - 0.002} = 242{,}520 \text{ psi}$$

where ε_u is the true ultimate strain, found from

$$\varepsilon_u = \ln\left(1+e_{eng}\right) = 0.436$$

In the analysis, a rounded value of 240,000 psi was used. Next, the bi-linear stress-strain curve was modified by transforming it into a multi-linear, convex-upward curve as discussed in Section 2.3.2. The amount of modification was determined by comparing the results of static crush tests with finite element model predictions. The modification was performed by multiplying the stress values on the bi-linear curve by factors greater than or equal to unity. The static crush test articles were prototypic, fabricated using the same material, and tested at room temperature (i.e., 70 °F) in the same end, side, and c.g.-over-corner orientations. The resulting multi-linear stress-strain curve produced good agreement between the static tests and static test predictions, (as shown in Figures 2.3-2 to 2.3-4) and was therefore used to generate the dynamic test predictions presented in this section. The multi-linear stress-strain points are given in Table 2.10.5-3.

To obtain the analytical prediction of impact limiter deformation, the analytical impact sequence is carried through the impact, rebound, and elastic springback phases. The resulting deformation is therefore comparable to the post-test deformation of the test articles.

Table 2.10.5-3 - Bi-Linear and Multi-Linear Stress-Strain Curves Used for Dynamic Test Analytical Predictions

Strain (in/in) ①	Bi-linear Stress (psi)	Multi-linear Stress (psi)	Multiplying Factor
0.001343	38,000	38,000	1.0
0.051343	50,000	57,000	1.140
0.101343	62,000	73,000	1.177
0.301343	110,000	125,000	1.136
0.601343	182,000	182,000	1.0

Notes:

① Using an elastic modulus of $28.3(10^6)$ psi at 70 °F and a yield stress of 38,000 psi, the calculated strain at yield is 0.001343 in/in.

2.10.5.5 Summary

The purposes of the dynamic testing, discussed in the introduction to this Section, were accomplished. The comparisons made between impact limiter deformations from the dynamic test and the analytical prediction based on finite element modeling demonstrated that the analytical approach and method of obtaining material properties is adequate for use in evaluating bounding impact accelerations and deformations in Section 2.7.1. Further, the integrity of the impact limiter structure and its attachment to the cask is confirmed under dynamic conditions. Deformations under all conditions were modest and do not differ from thermal analysis assumptions.

FIGURE WITHHELD UNDER 10 CFR 2.390

Figure **2.10.5-1** - Test Article Configuration

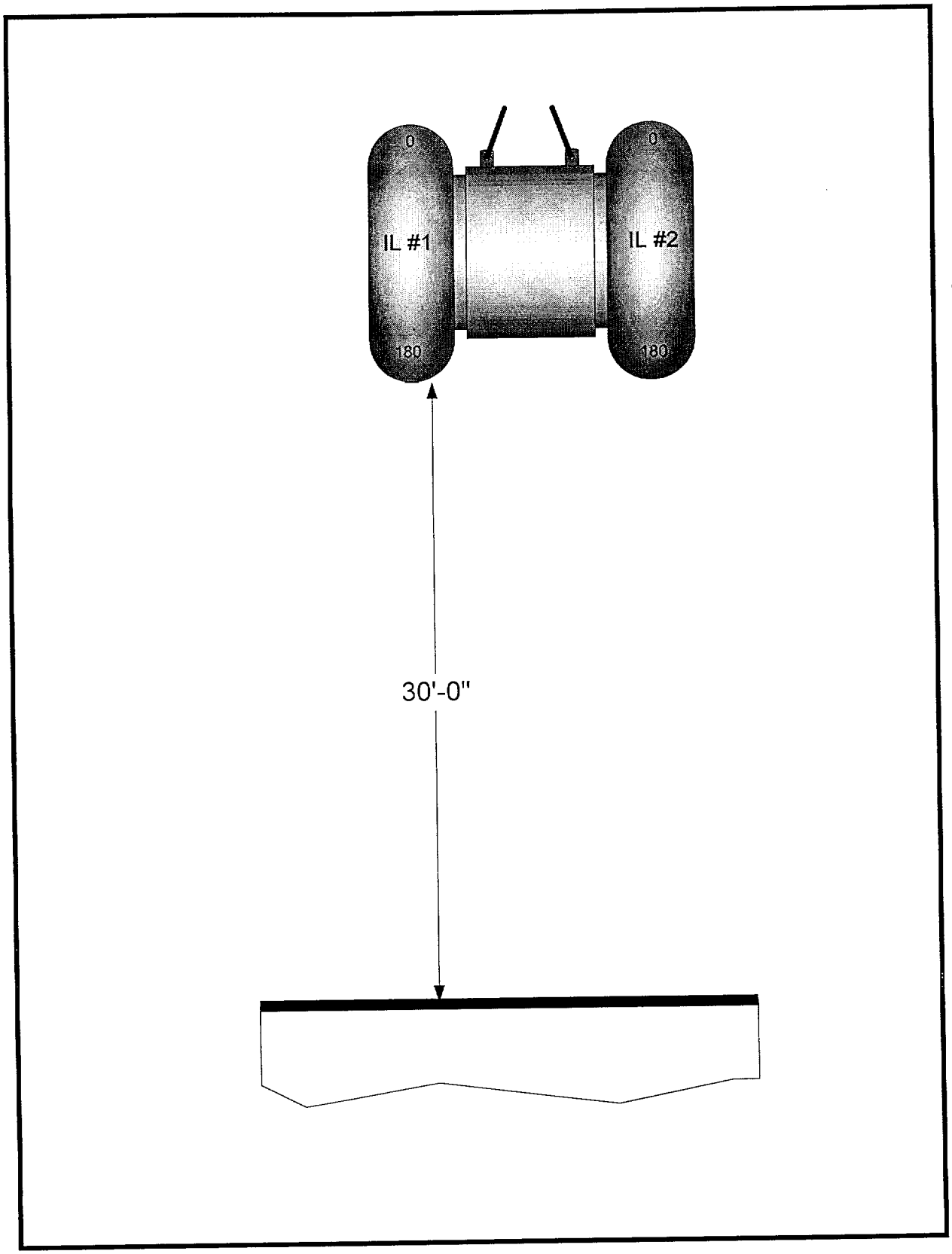

Figure 2.10.5-2 - HAC 30 ft Side Drop Configuration

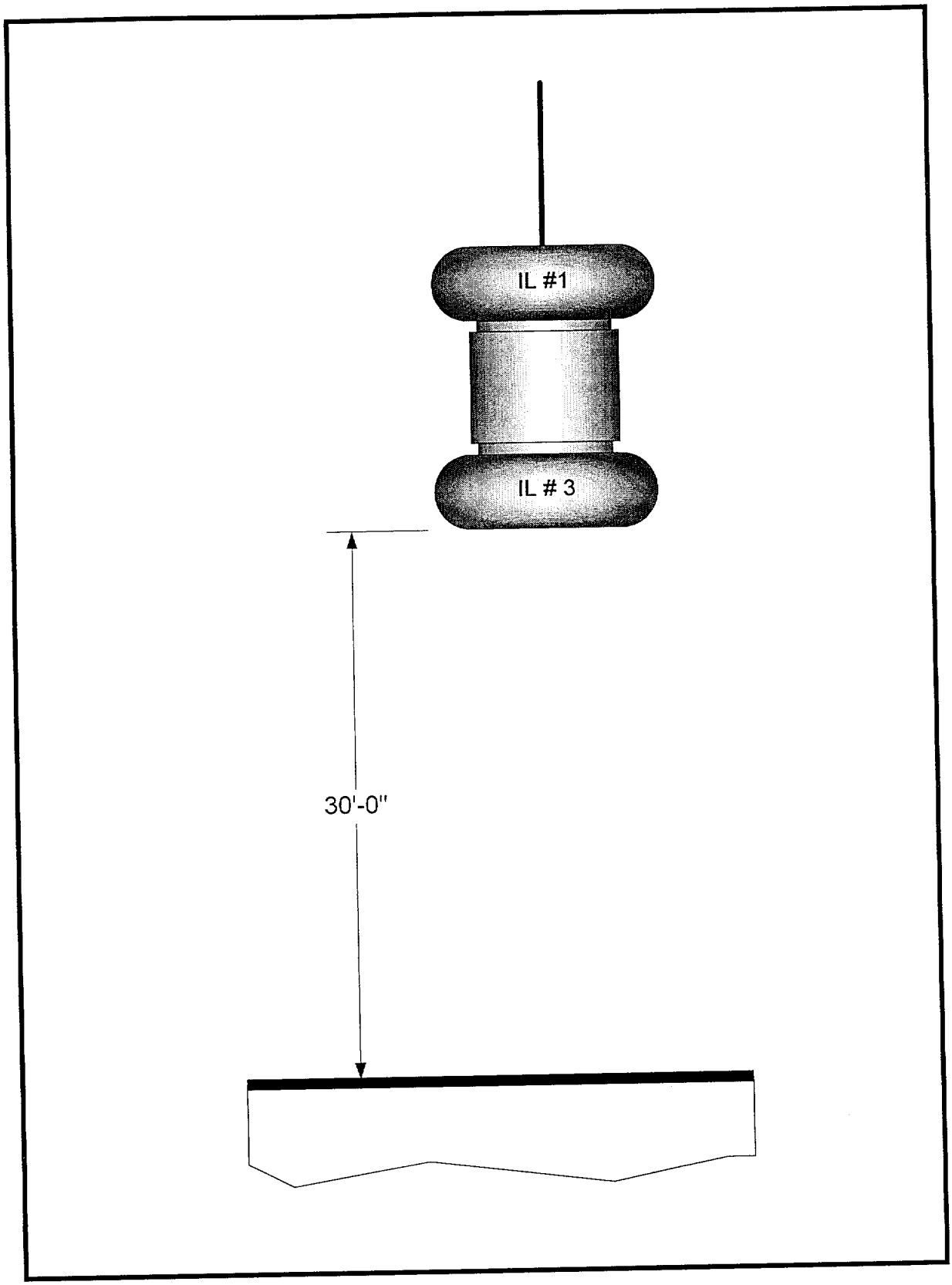

Figure 2.10.5-3 - HAC 30 ft End Drop Configuration

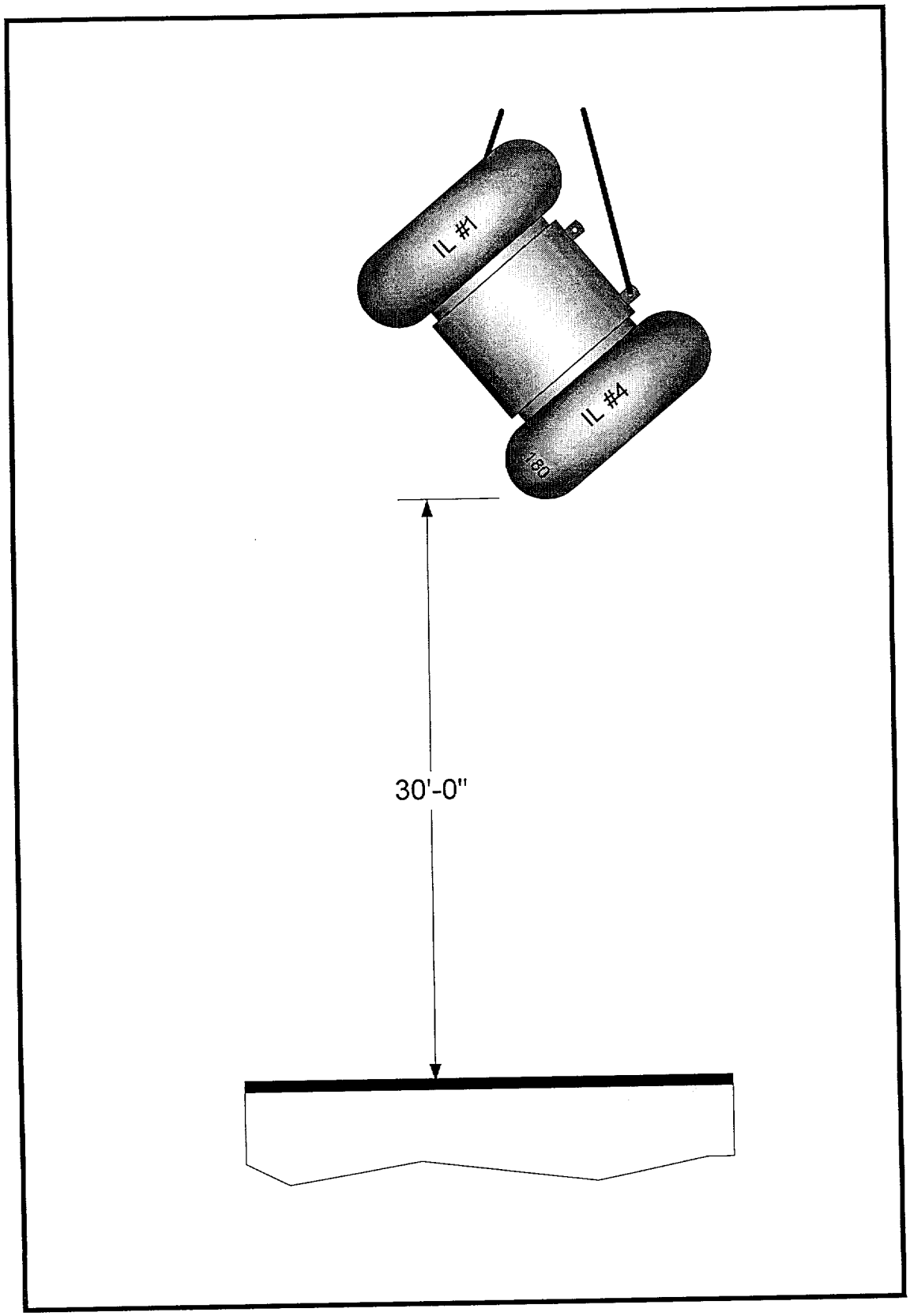

Figure 2.10.5-4 - HAC 30 ft C.G.-Over-Corner Drop Configuration

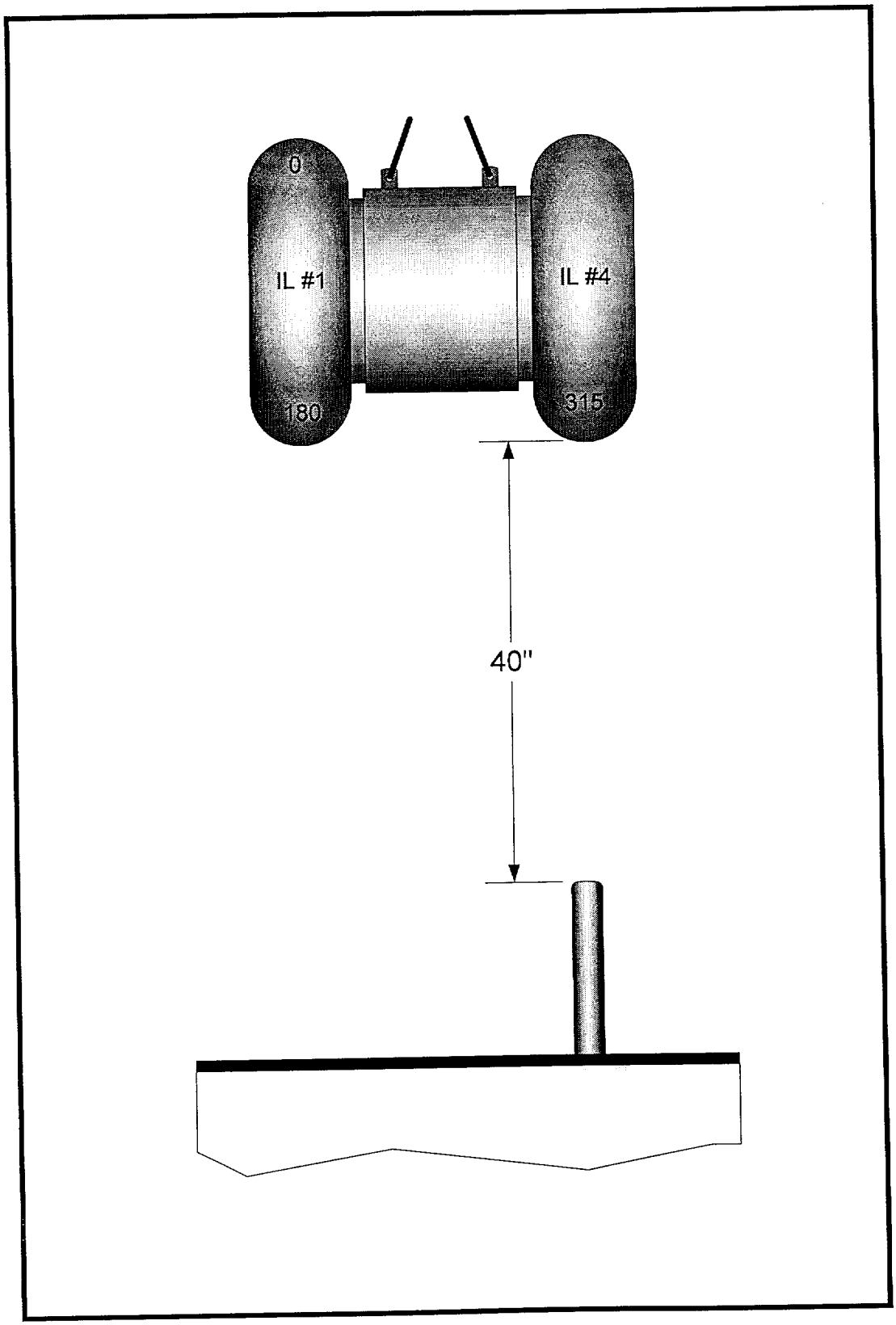

Figure 2.10.5-5 - HAC Side Puncture Drop Configuration

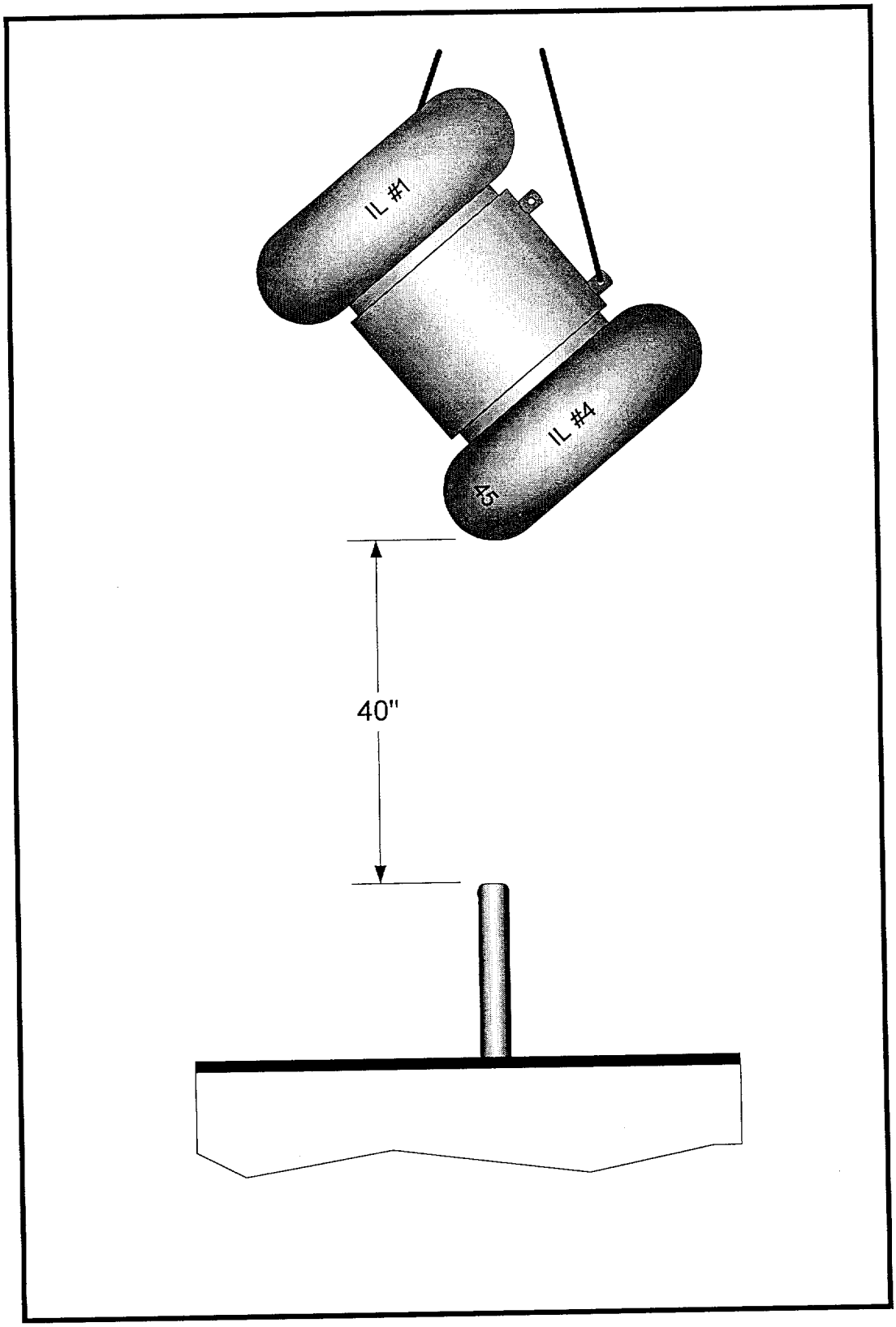

Figure 2.10.5-6 - HAC C.G.-Over-Corner Puncture Drop Configuration

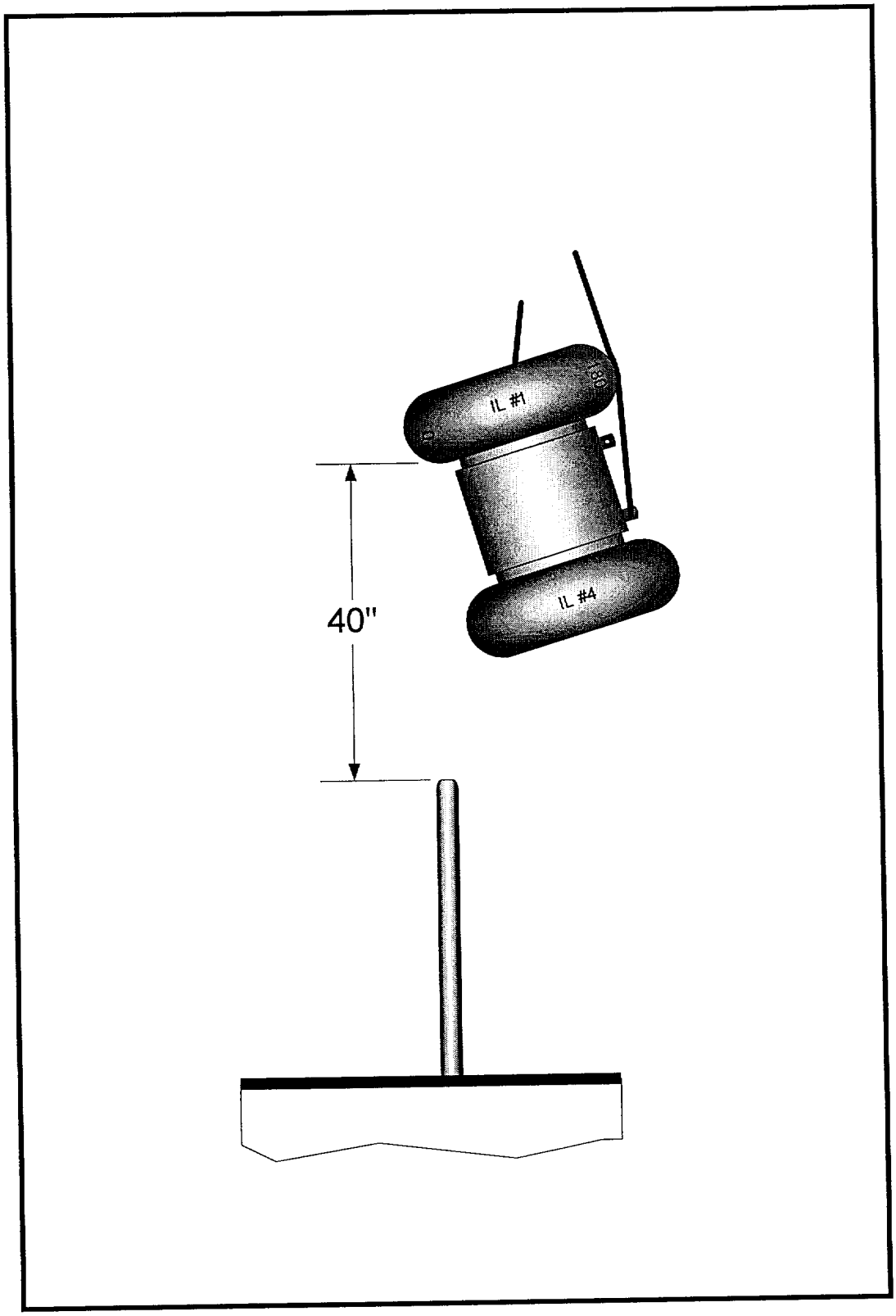

Figure 2.10.5-7 - HAC Puncture Drop Configuration, on Upper Limiter From Beneath

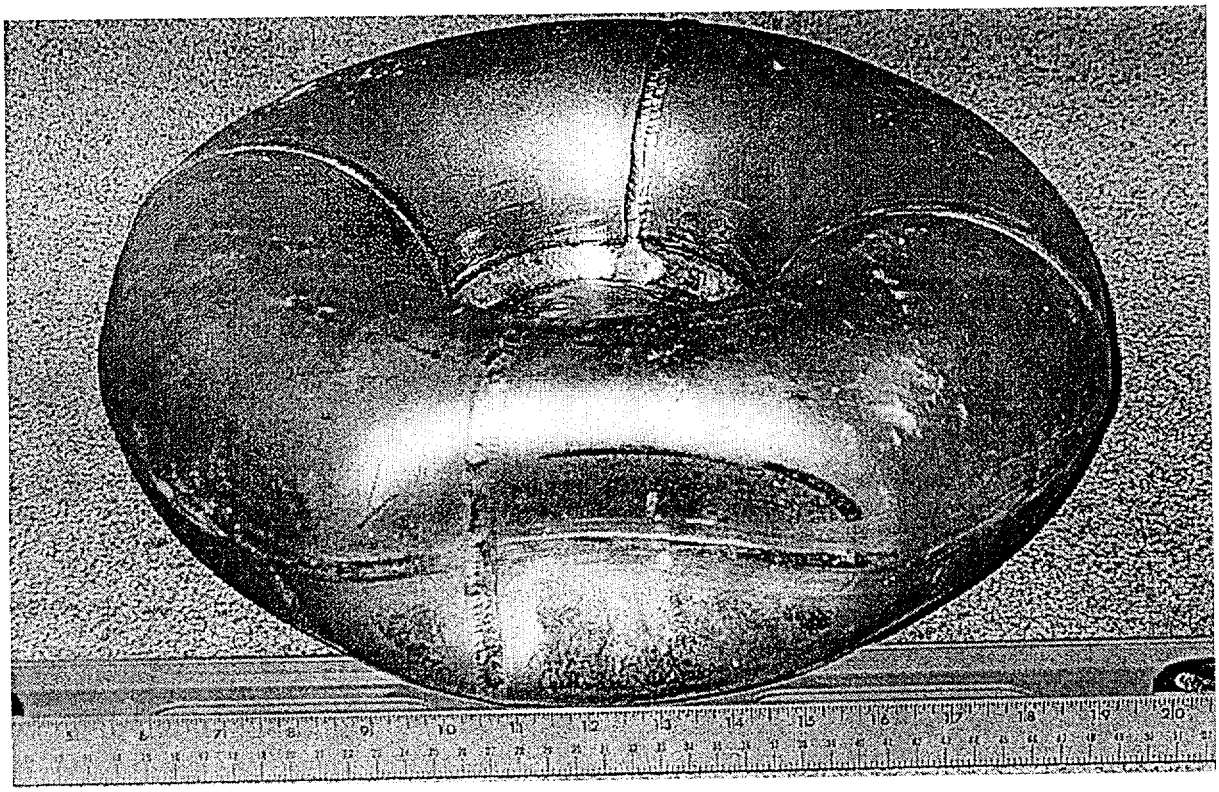

Figure 2.10.5-8 - HAC 30 ft Side Drop Damage, External View

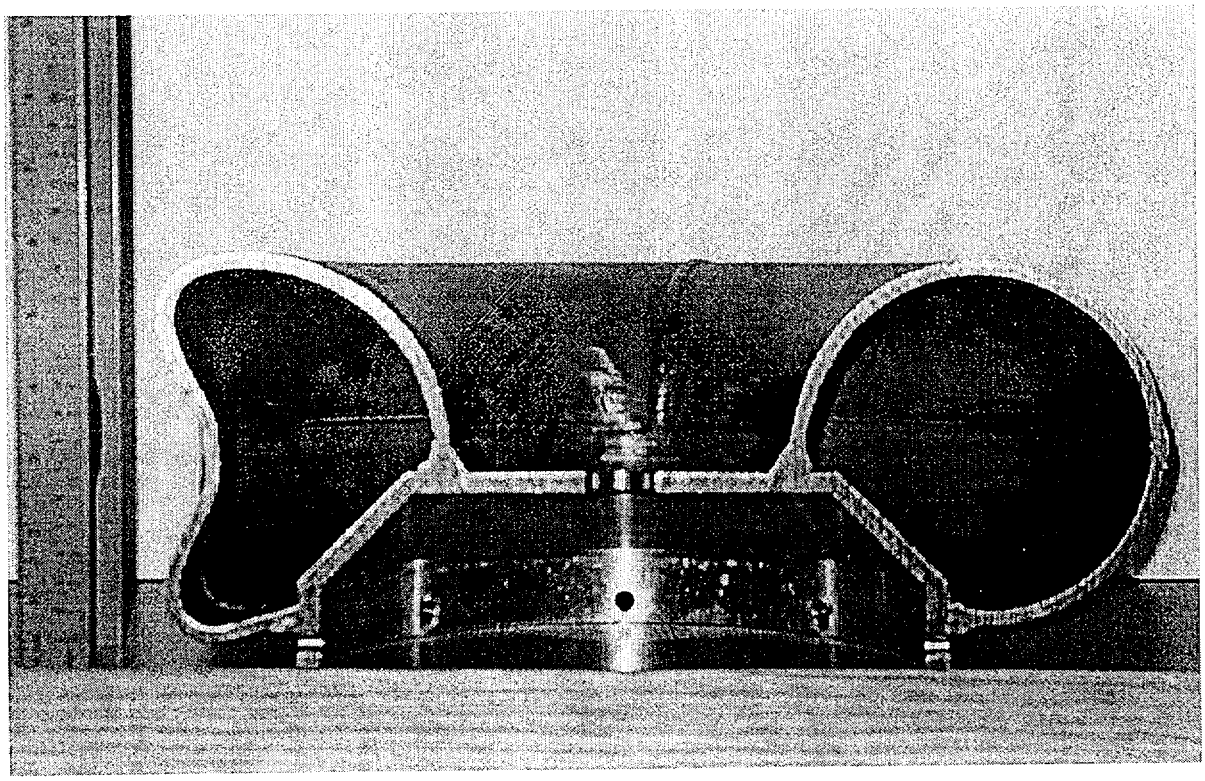

Figure 2.10.5-9 - HAC 30 ft Side Drop Damage, Section View

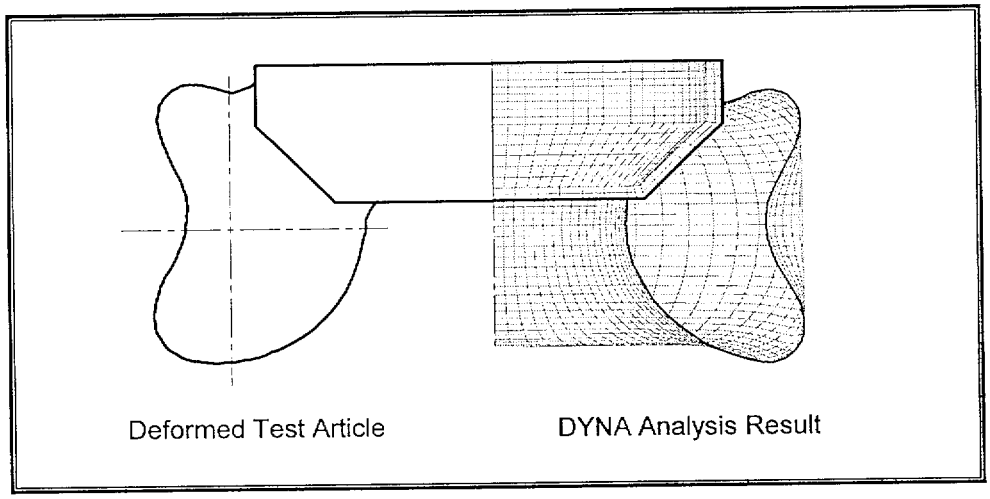

Figure 2.10.5-10 - HAC 30 ft Side Drop Damage, Trace Comparisons

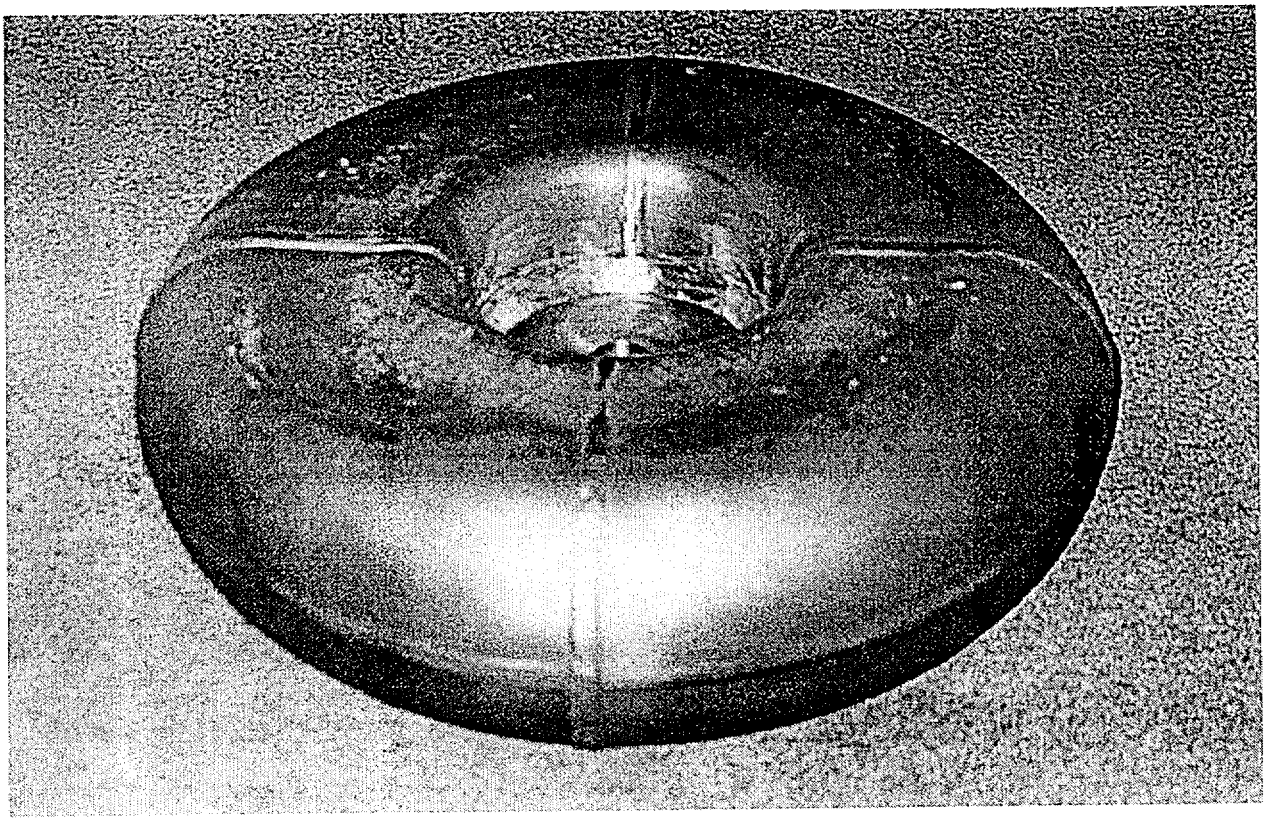

Figure 2.10.5-11 - HAC 30 ft End Drop Damage, External View

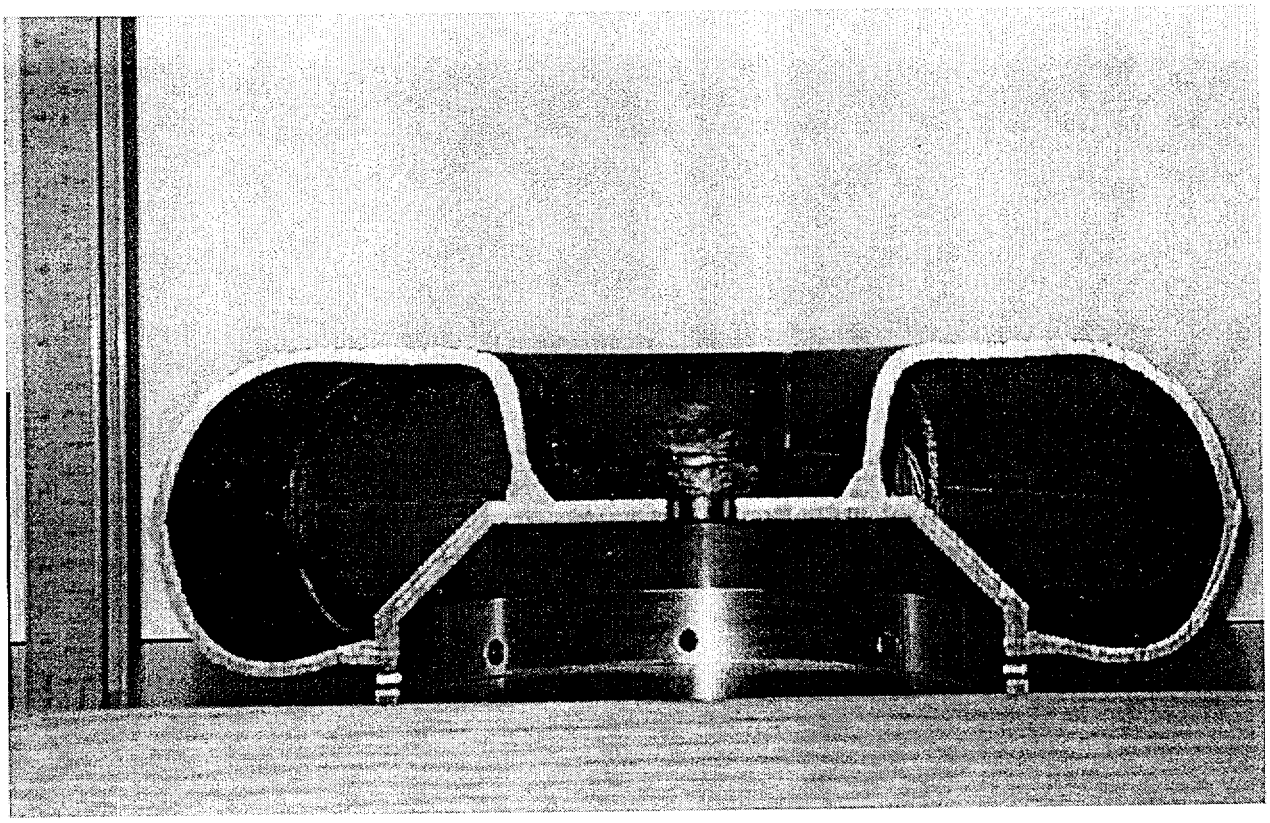

Figure 2.10.5-12 - HAC 30 ft End Drop Damage, Section View

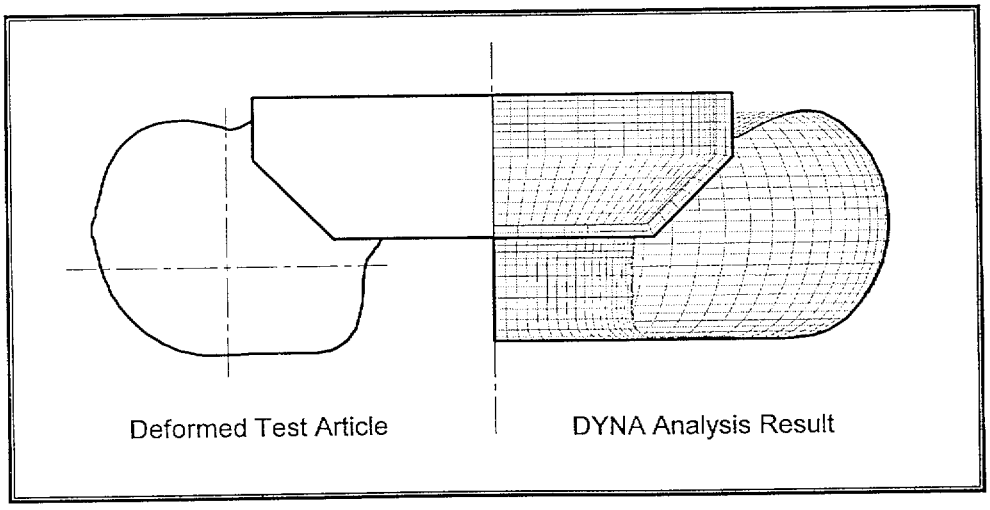

Figure 2.10.5-13 - HAC 30 ft End Drop Damage, Trace Comparisons

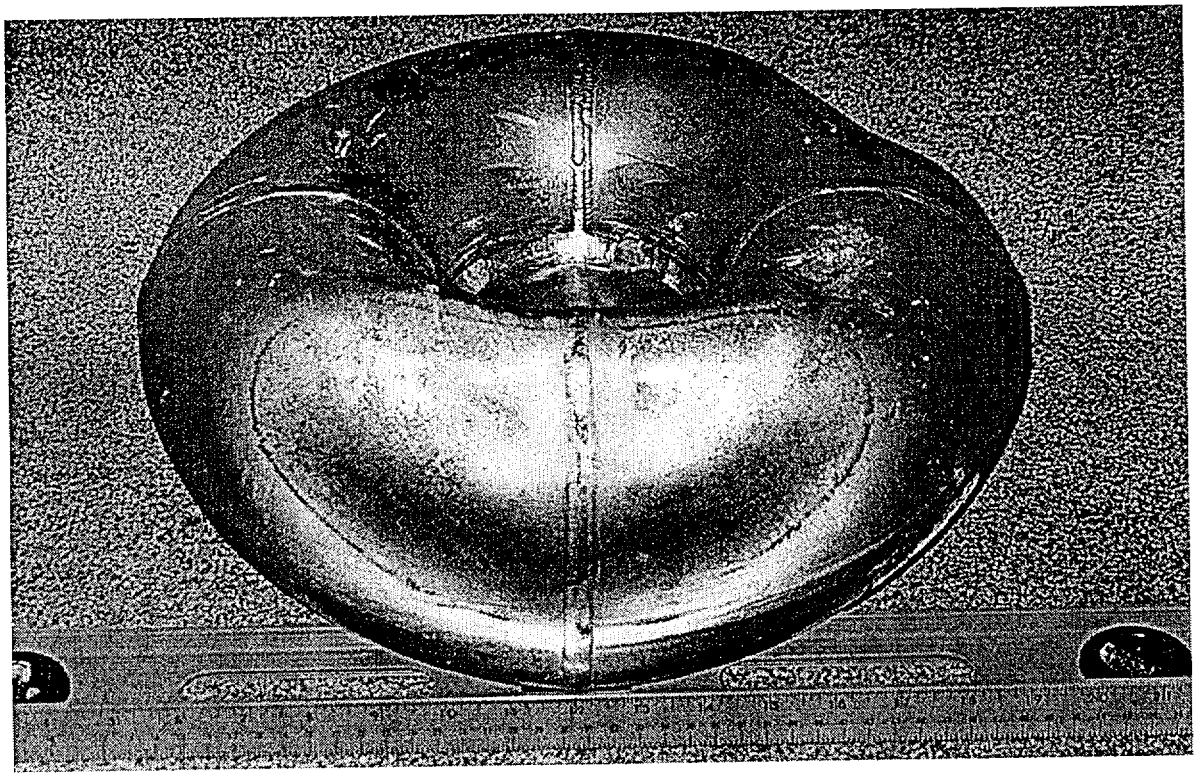

Figure 2.10.5-14 - HAC 30 ft C.G.-Over-Corner Drop Damage, External View

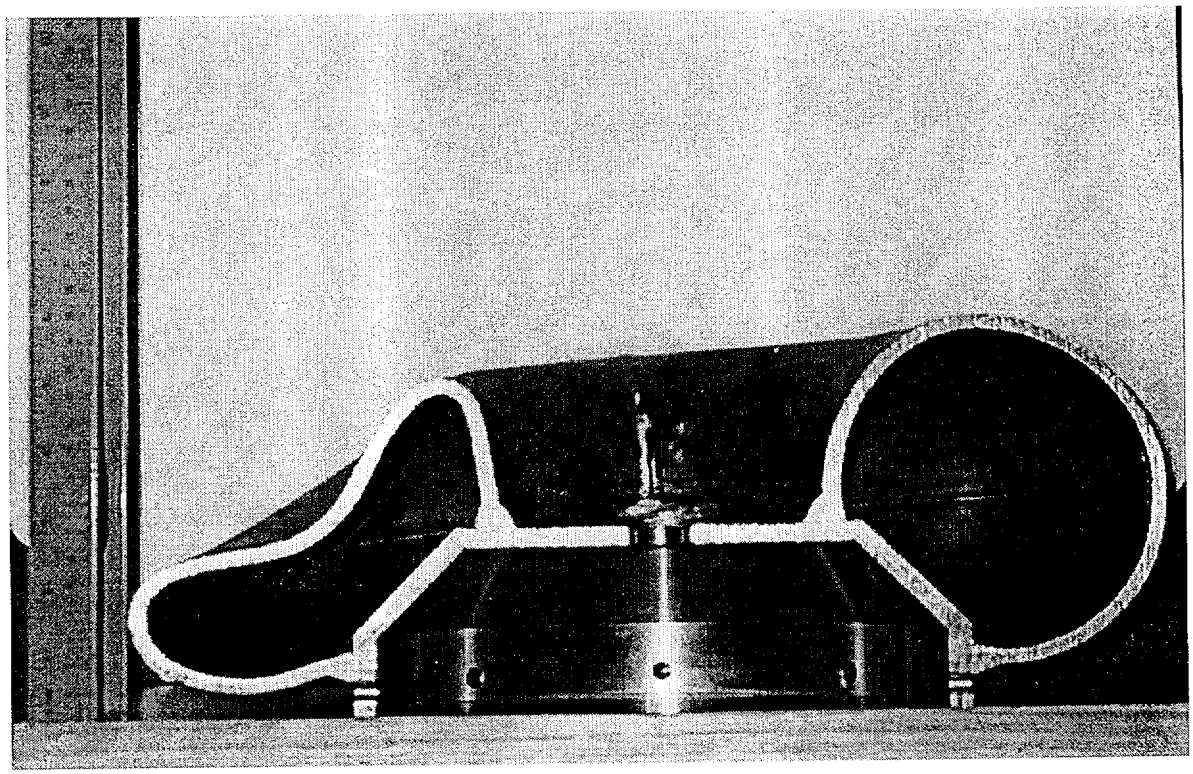

Figure 2.10.5-15 - HAC 30 ft C.G.-Over-Corner Drop Damage, Section View

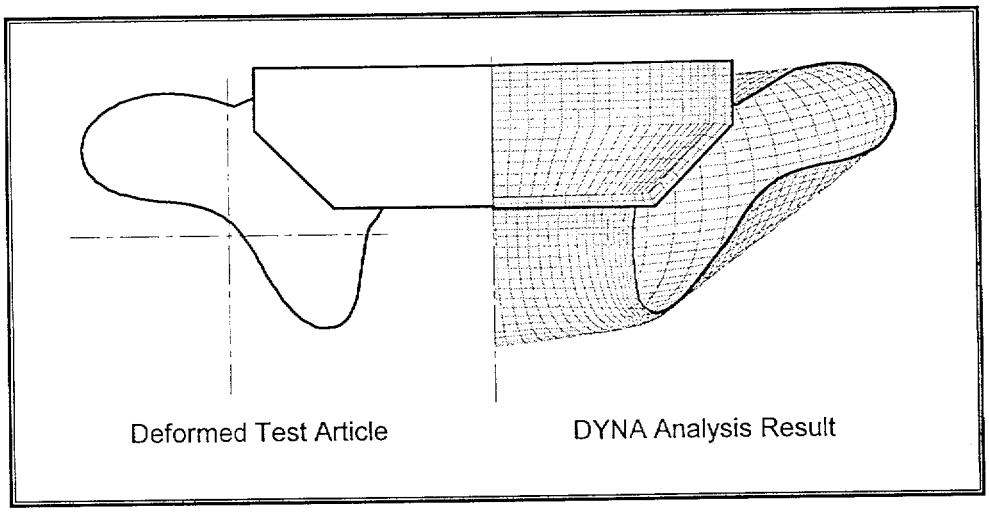

Figure 2.10.5-16 - HAC 30 ft C.G.-Over-Corner Drop Damage, Trace Comparisons

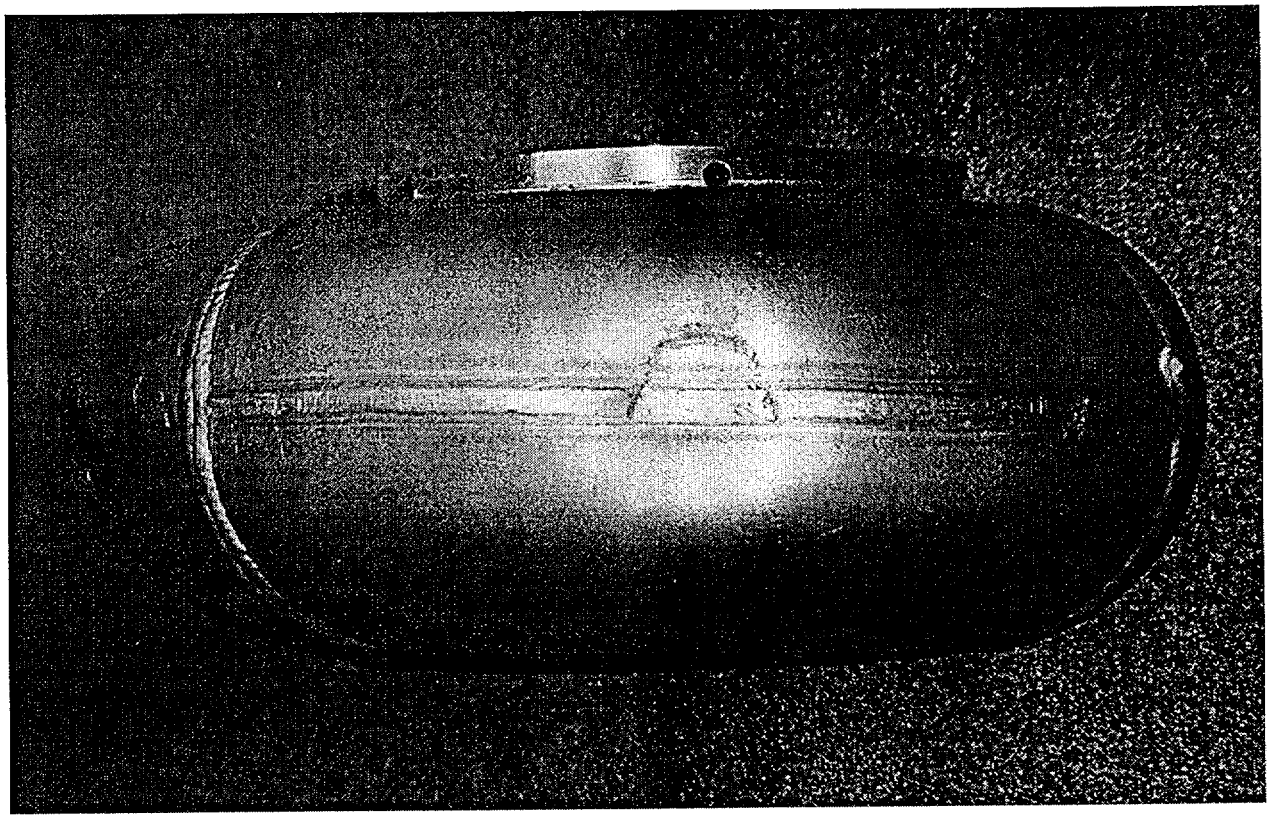

Figure 2.10.5-17 - HAC Side Drop Puncture Damage, External View

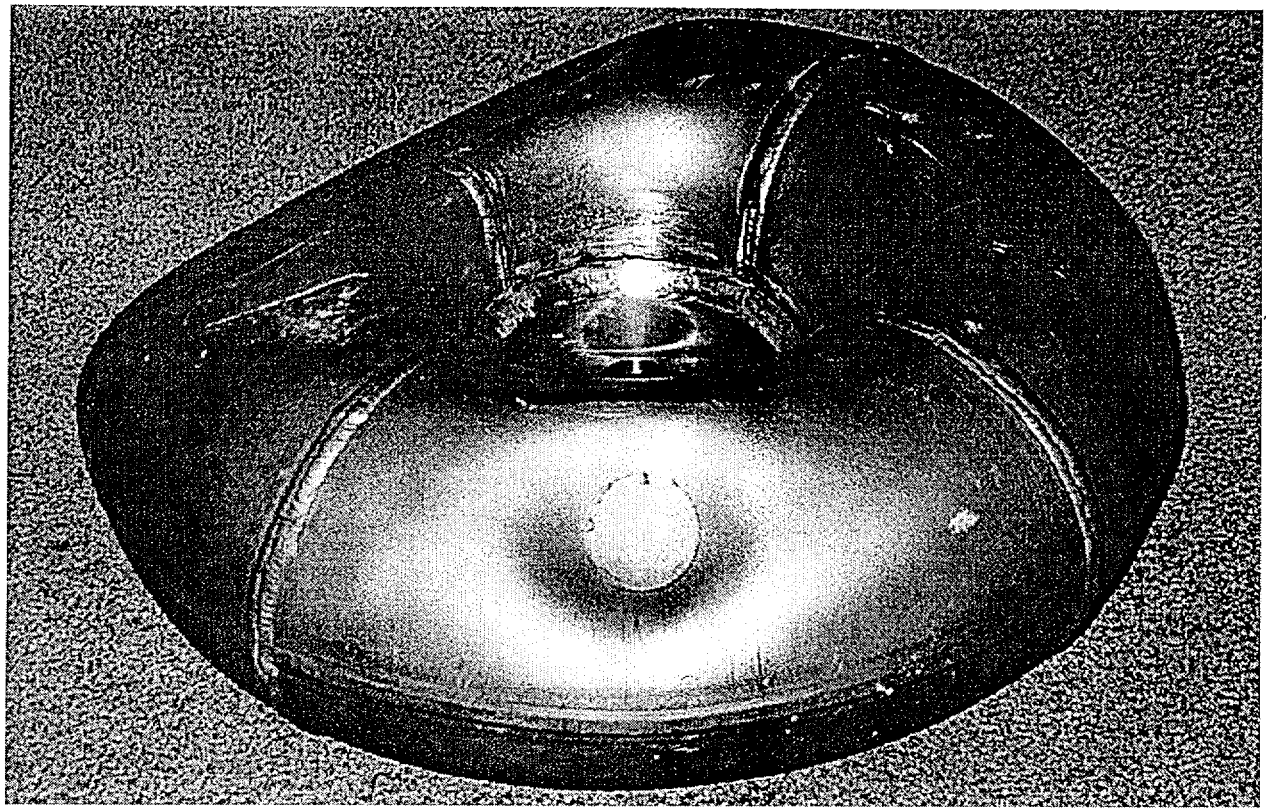

Figure 2.10.5-18 - HAC C.G.-Over-Corner Puncture Drop Damage, External View

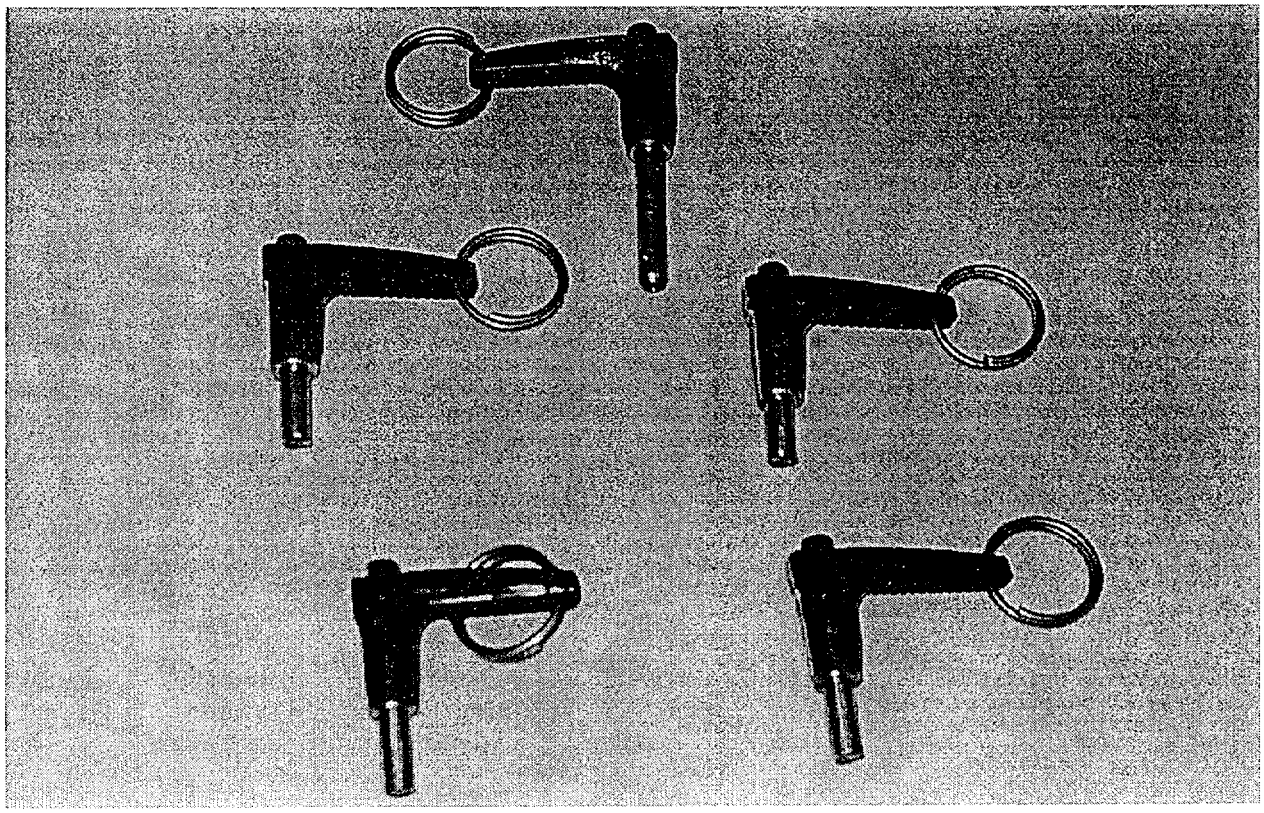

Figure 2.10.5-19 - HAC Puncture Drop on Upper Limiter From Beneath, Sheared Attachment Pins